Master's thesis

NTNU
Norwegian University of Science and Technology
Faculty of Natural Sciences
Department of Chemistry

Hanne Brigtsen Olsen

Monitoring of Natural Waters and Sediments and Treatment by Electrochemistry and Activated Carbon of Trace Elements in Acid Mine Drainage at the Location of a Former Ore Processing Facility in Trondheim

Master's thesis in MSENVITOX
Supervisor: Øyvind Mikkelsen
May 2020

NTNU
Norwegian University of
Science and Technology

Hanne Brigtsen Olsen

Monitoring of Natural Waters and Sediments and Treatment by Electrochemistry and Activated Carbon of Trace Elements in Acid Mine Drainage at the Location of a Former Ore Processing Facility in Trondheim

Master's thesis in MSENVITOX
Supervisor: Øyvind Mikkelsen
May 2020

Norwegian University of Science and Technology
Faculty of Natural Sciences
Department of Chemistry

NTNU
Norwegian University of
Science and Technology

Abstract

The Killingdal area in Trondheim was subject to extensive ore processing and shipping activities for many years, until 1986. This lead to a comprehensive contamination of the soil and sediments in the area. Clean-up projects both on land and in the Trondheimsfjord were conducted in the time period 2009 to 2016, but water containing high concentrations of potentially toxic trace elements continue to escape this area and flow into the fjord, posing a great threat to the biological diversity. This thesis is part of a project dedicated to treat the contaminated water in a tunnel at the Killingdal area, and was initiated in 2018.

Eight trace elements were in focus both during the monitoring and in the treatment experiments; iron, chromium, nickel, copper, zinc, arsenic, cadmium, and lead. All these elements can be toxic to organisms in high doses, and their concentrations in the tunnel at Killingdal were categorised in class III to V in the classification of conditions formulated by the Norwegian Environment Agency. This indicates potentially chronic effects to extensive acute toxic effects. In addition, aluminium was investigated, due to the potential release from aluminium electrodes during electrolysis. All samples were analysed by ICP-MS at the laboratories at NTNU.

The conditions in the Killingdal stream and the effluent from the Killingdal area into the Trondheimsfjord were monitored over the period of one year. Results from the monitoring program showed that the Killingdal stream was not heavily contaminated with trace elements, as close to all concentrations were within or below class II. The effluent results revealed high concentrations of copper and zinc (class V), and elevated concentrations of arsenic and cadmium (class III and IV). Sediments in the Trondheimsfjord were sampled once and compared to previous reports. The analyses indicate that even though the concentrations have been reduced since 1972, the sediments are still polluted by mainly copper (class V), zinc (class IV), and arsenic (class IV), and to some extent cadmium and lead (some locations with class III and IV). From trace element concentrations measured in the effluent from Killingdal and observed trends, correlation analysis, and analysis of trace element/lithium relationships in the sediments, it can be concluded that the contamination originates from Killingdal.

Testing of two potential polishing steps for removal of trace elements, not sufficiently treated during a main treatment step, were conducted. These two methods were electrochemical treatment with a combination of aluminium and graphite electrodes, and activated carbon treatment. The electrochemical treatment exhibited some removal capacity. Treatment with aluminium electrodes showed maximum removal efficiencies of 40.2 % (Fe), 39.2 % (Cu), 21.4 % (Zn), 69.5 % (As), 12.9 % (Cd), and 41.0 % (Pb). Chromium and aluminium were most efficiently removed when solely graphite electrodes were used (6.61 % to 7.30 % and 18.6 % respectively). Activated carbon treatment had more promising results. During the experiment, maximum removal efficiencies of 99.3 % (Fe), 46.7 % (Cr), 93.2 % (Cu), 84.8 % (As), and 98.5 % (As) were observed. Increase of Ni (44.4 %), Zn (16.4 %), and Cd (11.3 %) in the end of the experiment was observed, but could potentially be improved by modifications of the system, such as increasing the low pH of the water. These results indicate that there is a potential for activated carbon as a polishing step, and that it should be investigated further for large-scale water treatment at Killingdal.

Sammendrag

Killingdal er et område i Trondheim hvor det inntil 1986 foregikk prosessering og skipstransport av malm. Dette førte til omfattende forurensning av jord og sedimenter i nærområdet. Det har vært oppryddingsprosjekter både på land og i Trondheimsfjorden i tidsperioden 2009 til 2016, men vann med høye konsentrasjoner av potensielt giftige sporelementer fortsetter å renne fra Killingdal og ut i fjorden, noe som utgjør en trussel mot det biologiske mangfoldet i området. Denne masteroppgaven er en del av et prosjekt som ble igangsatt i 2018 og har som mål å rense forurenset vann som befinner seg i en tunnel i Killingdalområdet.

Åtte sporelementer har fått hovedfokus i løpet av overvåkningsprosjekter og eksperimenter i denne masteroppgaven; jern, krom, nikkel, kobber, sink, arsen, kadmium, og bly. Alle disse sporelementene kan være giftige for organismer i store mengder og konsentrasjoner av dem ble funnet til å være i klasse III til V i tilstandsklassifiseringen utarbeidet av Miljødirektoratet. Dette kan føre til alt fra kroniske effekter til omfattende akutte effekter som følge av eksponering. I noen tilfeller ble også aluminium studert, da det potensielt kan lekke ut fra aluminiumelektrodene under elektrolyse. Alle prøvene ble analysert med ICP-MS ved laboratoriene på NTNU.

Forholdene i Killingdalbekken og området i Tronsheimsfjorden, hvor vann lekker ut fra Killingdal, ble overvåket i ett år. Resultater fra dette viser at Killingdalbekken ikke er forurenset av sporelementer, ettersom tilnærmet alle konsentrasjonene som ble målt var i eller mindre enn tilstandsklasse II. Resultatene fra utslippet til fjorden avdekket høye konsentrasjoner av kobber og sink (tilstandsklasse V), og forhøyede konsentrasjoner av arsen og kadmium (tilstandsklasse III og IV). Sedimentene i Trondheimsfjorden ble samlet inn én gang og sammenlignet med tidligere rapporter. Analysene tyder på at selv om mengdene har blitt redusert siden 1972, så er sedimentene fortsatt forurenset av hovedsakelig kobber (klasse V), sink (klasse IV) og arsen (klasse IV) og delvis av kadmium og bly (noen lokasjoner med konsentrasjoner i klasse III og IV). Ut i fra konsentrasjoner målt i utslippet fra Killingdal og observerte trender, korrelasjonsanalyser og analyse av forhold mellom sporelementer og litium i sedimentene ble det konkludert med at forurensningen mest sannsynlig stammer fra Killingdal.

Forsøk med to potensielle poleringstrinn, for fjerning av sporelementer som ikke fjernes effektivt av et hovedrensetrinn, ble utført. Disse metodene var elektrokjemisk rensing, med ulike kombinasjoner av aluminiumelektroder og grafittelektroder, og rensing med aktivt kull. Forsøkene som omhandlet elektrokjemisk rensing fjernet en del av sporelementene. Best effekt hadde kun aluminiumelektroder, som ga maksimale observerte rensekapasiteter på 40.2 % (Fe), 39.2 % (Cu), 21.4 % (Zn), 69.5 % (As), 12.9 % (Cd) og 41.0 % (Pb). Krom og aluminium ble mest effektivt fjernet da kun grafittelektroder ble brukt (6.61 % to 7.30 % og 18.6 %). Rensing med aktivt kull viste mer lovende resultater. I løpet av eksperimentet ble følgende renseprosenter observert; 99.3 % (Fe), 46.7 % (Cr), 93.2 % (Cu), 84.8 % (As) og 98.5 % (As). Økning av Ni (44.4 %), Zn (16.4 %) og Cd (11.3 %) ble observert ved slutten av eksperimentet, men dette kan potensielt forbedres ved å øke pH i vannet, som under forsøkene var relativt lav. Disse resultatene gir en indikasjon på at det er potensiale for å bruke aktivt kull som et poleringstrinn og at det bør testes videre for bruk i vannrensing i større skala på Killingdal.

Acknowledgment

This master thesis has been a great experience. I was very lucky to start my master thesis when Trondheim Municipality started their project. Through this project I have had the possibility to increase my knowledge concerning water treatment, monitoring programs, and project planning, among others, which are interesting subjects relevant in later research and employments.

First, I would like to thank my supervisor Prof. Øyvind Mikkelsen from the Department of Chemistry at the Norwegian University of Science and Technology (NTNU) for suggesting this project as my master thesis. In addition, I am grateful for all the support, both during field work and when writing, and interesting discussions concerning the content of the thesis. A big thank you to Syverin Lierhagen at NTNU for running all the ICP-MS analyses on my samples, and for explaining the results afterwards. Also a big thank you to Anica Simic whi stepped in and analysed my samples during the quarantine period. I would also like to thank the crew in the workshop at the Faculty of Natural Sciences at NTNU for making the setup we used for some of my experiments.

I also want to thank Trondheim Municipality, and Kyrre Halvorsen and Anette Fenstad in particular. Without them this thesis would not have existed, and they have contributed with many great inputs and ideas during these two years. I am excited to follow this water treatment project the next few years. The crew at Tromek, and especially Eirik Hindseth, also deserves a big thanks for lending a hand every time it was needed and helping adjusting the experiment setup at Killingdal. In addition, I want to thank the crew at the Gunnerus Research Vessel for the exciting trip we had and the great effort done for me to get the sediment samples.

I would also like to thank my partner in crime (and studies) Stine Steen. All the trips back and forth to the Killingdal area and long days in the laboratory would not have been the same without you. And all my friends, thank you for the support you showed me and all the fun we have had through the years. To my family, thank you for reading through the thesis and giving me a lot of great feedback and supporting me all the way. Finally, I am very greatful for my fiancé Matias, who stuck by my side the whole time, supported me in ups and downs, helping me doing whatever was needed, and motivated me to reach the finish line.

Contents

List of Figures

List of Tables

Nomenclature

AC	Activated carbon
ACF	Fibrous activated carbon
AMD	Acid mine drainage
ATP	Adenosine triphosphate
CTD	Conductivity, Temperature and Depth sensor
DNA	Deoxyribonucleic acid
DNV GL	Det Norske Veritas and Germanischer Lloyd
emf	Electromotive force
Exp.	Experiment
GAC	Granular activated carbon
ICP-MS	Inductively Coupled Plasma Mass Spectrometry
ISO	International Organization for Standardization
NGI	Norwegian Geotechnical Institute
NIVA	The Norwegian Institute for Water Research
NTNU	Norwegian University of Science and Technology
PAC	Powdered activated carbon
PAHs	Polycyclic aromatic hydrocarbons
RSD	Relative standard deviation
SPSS	Statistical Product and Service Solutions
TGD	Technical Guidance Document for Deriving Environmental Quality Standards

1 Introduction

Killingdal in Trondheim is an area along the coast in Ilsvika. In the present it is characterised by a park, but ten years ago it was the location of an abandoned ore processing facility. This facility was operated by *Killingdal Grubeselskap* from 1891 to 1986, where sphalerite, pyrite, and chalcopyrite were processed to extract elements such as copper, lead, sulphur, and zinc. *Killingdal Grubeselskap* went bankrupt in 1986, and the area was left to deteriorate. This caused water enriched by elements present in the residues to accumulate in the remnants of the buildings and structures. Investigations of the sediments outside of this area revealed high concentrations of among others cadmium, lead, zinc, copper, and iron, and the conclusions were that they originated from the Killingdal residues. These elements are known to be harmful to aquatic organisms, and it is potentially detrimental that they leak into the Trondheimsfjord and sediments.

Between 2009 and 2016 the area was completely transformed, the processing facility was removed and great efforts were made to avoid continuous spread of contamination from the area. However a tunnel in the ground was kept to monitor a remaining land fill, and it was discovered that the tunnel became an accumulation point for highly contaminated water even after all the effort to avoid this. Several toxic elements were measured in class of conditions III or higher, which can cause chronic effects or more severe effects in aquatic organisms. This water was leaking out into the fjord, contaminating the water and the sediments. The sediments in the Trondheim Harbour, including Ilsvika, were exchanged with or covered by new sediments in the project *Cleaner Harbour*. This was an effort to reduce the potential leakage of pollution from the sediments to the overlaying water. The Norwegian Geotechnical Institute (NGI) investigated the sediments outside the Killingdal area in 2019 to see the status after three years, and they found elevated concentrations of several toxic trace elements. Their conclusion was that the contamination originated from Killingdal.

As a response to all the contamination from Killingdal, a project intended to clean the water in the tunnel was initiated in 2018. The concentrations released into the fjord in 2018 were not acceptable, and a proper treatment facility that could stop this pollution was necessary. This thesis is a part of that project, aiming to find new treatment methods to remove trace elements from the water. The current deadline for reduced release into the fjord is by the end of 2021. While Trondheim Municipality was developing the treatment facility, it would be helpful to have someone that could test different treatment methods in small-scale experiments to see if they had potential to later be used in a large-scale water treatment.

The result was two master projects, one focusing on the removal of the majority of contaminants from the water in a main treatment step, and one focusing on the elements that escape the main treatment step in a polishing step. In this thesis the focus is on the polishing step, and methods that were tested were electrochemical treatment with different combinations of aluminium and graphite electrodes, and activated carbon. A choice was made to mainly focus on the trace elements iron, chromium, nickel, copper, zinc, arsenic, cadmium, and lead. This was based on their high presence in the Killingdal water, high potential toxicity to aquatic organisms in the Trondheimsfjord, and these are the elements Trondheim Municipality have focused on in their analyses.

There are two aims in this thesis. The first is to monitor the natural waters in close proximity to the Killingdal tunnel, to analyse the amount of contamination present and investigate if there are any

trends in trace element concentrations during a year. This includes the Killingdal stream and the Trondheimsfjord. In addition the sediments outside the Killingdal area were analysed to compare with previous reports to see the impact of the release from the Killingdal tunnel. The second aim of this thesis was to test and assess the ability of electrochemical treatment and activated carbon to remove trace elements from the water at Killingdal.

2 Theory

2.1 The Killingdal area

Killingdal is originally a mining area in Ålen in Holtålen Municipality, 134 km south of Trondheim (40 km north of Røros). The ore deposit was discovered as early as in 1674, and in 1677 the first mining operations were initiated. At first, *Røros Kobberverk* with other companies operated the mines, but in 1891 *Killingdal Grubeselskap* became the owner. Quartz (SiO_2), sphalerite ((Zn, Fe)S), and pyrite (FeS_2) are listed as major minerals in these mines, and chalcopyrite ($CuFeS_2$) is listed as a subordinate mineral. Main products from these minerals were copper (Cu), lead (Pb), sulphur (S), and zinc (Zn). The raw ore was transported to Trondheim by train along the *Røros Line* to a processing and shipping facility operated by *Killingdal Grubeselskap*. [1] Both the location of the Killingdal mines and the transportation route for the ore are shown in figure 2.1.

Killingdal in Trondheim is an area in Ilsvika, right outside of the centre of Trondheim. The exact location of the Killingdal area is shown in figure 2.2. Today it is a park area. It used to be the location of the shipping facility for the ore from the Killingdal mines from 1891 and from 1953 it was also the location of their processing facility. In 1986 *Killingdal Grubesekslap* was declared bankrupt, and the facility in Ilsvika was left to deteriorate, with residues of ore and trace elements remaining. Pictures of how the area looked before the cleanup are presented in figures 2.3a and 2.3b.

In the last decades, several studies have been carried out and reports have been published regarding

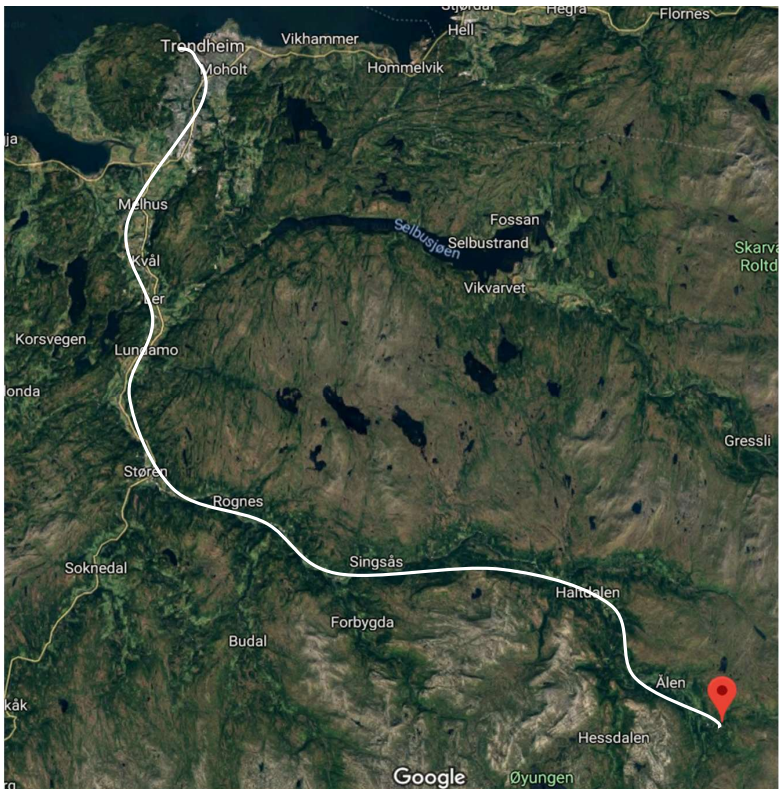

Figure 2.1: Map over the route the ore was transported from the Killingdal mines to the Killingdal area in Trondheim. The Killingdal mines are indicated by a red marker in the bottom right corner, while Trondheim is located at the top of the map. The route is indicated by a white line. (Map from Google Maps a white line added afterwards.) [2]

Figure 2.2: Trondheim seen from above. The tunnel in the Killingdal area is located in the top left corner, indicated by a blue marker.

pollution in the Killingdal area in Trondheim. In 1972 to 1975, the University of Trondheim carried out a recipient study on behalf of the Trondheimsfjord committee, a committee from Norwegian ornithological association of Nord- and Sør-Trøndelag. They investigated blue mussels, common limpet, and knotted wrack, among others, in 27 different locations in the Trondheimsfjord. The results showed that organisms living in Ilsvika, where the processing plant was located, had elevated levels of zinc and copper compared to many of the other locations that were investigated. [5]

A few years later, in 1981, a new investigation was conducted as a part of a monitoring program [6]. This time the investigation was performed by NIVA on behalf of the Norwegian Pollution Control Authority. Both the fauna and the sediments outside *Killingdal Gruber* processing facility were analysed. In the sediments, high concentrations of mercury (Hg), cadmium (Cd), lead (Pb), zinc (Zn), copper (Cu), and iron (Fe) were detected. zinc and copper were also detected in high concentrations in knotted wrack at the biological station in Fagervika this year [7]. Later analyses performed in 1987, 1991 [8], 1994 [9], and 2000 [10] detected elevated concentrations of many or all of the elements mentioned above.

In 2009 it was decided that a major cleanup and transformation was needed. Multiconsult, a projecting and consultancy company, was assigned the task to remove the old buildings and make the area into the park area it is today. In 2010 the process was initiated, and in 2011 the park area was finished. According to Multiconsult, more than 10 000 tons highly contaminated soil was removed from the Killingdal area. [11] How parts of the Killingdal area looks in 2020 is shown in figure 2.4.

Most of the infrastructure was removed during the cleanup, but a tunnel was kept in the ground, beneath the bicycle lane in figure 2.4b. A special land fill was positioned over this tunnel. Subsequently,

(a) PHOTO: HANS H. BJØRSTAD [3]

(b) PHOTO: TRONDHEIM HAVN [4].

Figure 2.3: Part of the processing facility at Killingdal.

a bentonite membrane was positioned to cover this land fill, and a coverage of new soil was placed on top. The tunnel made it possible to investigate the land fill from beneath. [12] The assumption was that by removing the contaminated soil and infrastructure, the release of contaminants into the Trondheimsfjord would stop. Unfortunately, the tunnel started to fill up with water, and discharge of contaminated water into the Trondheimsfjord continued from a diffuse leakage from the tunnel. An attempt was done to try and stop water from seeping into the tunnel. It was assumed that the Killingdal stream was a big water source, running through contaminated soil and into the tunnel. The stream was therefore guided through rigid concrete tubes and directly out into the fjord in 2016.

Even though this initiative reduced the amount of water seeping in, small amounts of water are still entering the tunnel, filling it up with highly contaminated water. In December 2018 the first analysis of the Killingdal water was conducted for this thesis. The concentrations measured of different contaminants in the tunnel water are shown in table 2.1. All the elements are in class III or above. Based on the findings it was decided that the most suitable next step was to clean the water in the tunnel.

(a) Parts of the new Killingdal Park.

(b) Parts of the new bicycle lane in the Killingdal Park.

Figure 2.4: How the Killingdal area looked in 2020.

Table 2.1: Results from analysis of the water from the Killingdal tunnel in December 2018 and which condition category they fall into. There is no classification for iron (Fe), and therefore this cell is empty.

Element	Concentration (µg/L)	Classification [limits] (µg/L)
Fe	15200	None
Cr	6.74	III [3.4 – 36]
Ni	36.1	IV [34 – 67]
Cu	16300	V [>5.2]
Zn	11200	V [>60]
As	3.28	III [0.6 – 8.5]
Cd	35.6	V [>9]
Pb	47.6	IV [14 – 57]

In 2018 Trondheim Municipality built a small treatment plant in the tunnel. Figure 2.5 shows how the first setup was in 2018, and how it is in 2020. As the pictures show, the facility has been modified several times the last 1.5 years, but the main principal is still the same. Water from inside the tunnel is pumped up into the tank closest to the door, the closest tank in figure 2.5b. From here the water flows into a second tank containing a treatment medium, and in the newest facility there are several tanks with different treatment mediums. After the treatment the water flows into a final tank where contaminants can sediment, as the closest tank in figure 2.5a. Theory says that surface water in these sedimentation tanks has the lowest amount of particles. At Killingdal, this water flows down from the tank and back into the tunnel again. In the latest development of the treatment plant, the water is released directly into the fjord from the final tank.

(a) Setup used in the beginning of the project.

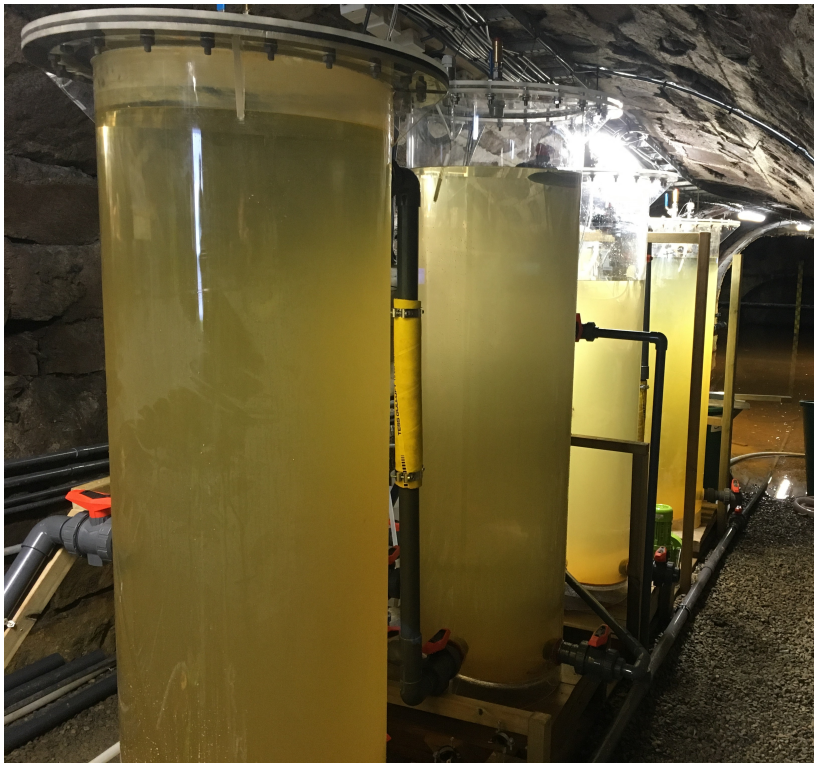

(b) Setup in 2020.

Figure 2.5: How the treatment plant was in the beginning and how it was in 2020. The appearance has changed, but the principle is still the same.

2.2 Cleaner Harbour

Due to extensive discharges of municipal waste and waste from the different industries along the harbour over the years, and the results from the different reports presented above in section 2.1, Trondheim Municipality decided that action must be taken. In addition to the cleanup on land, Trondheim Municipality initiated a cleanup project in the Trondheimsfjord. As early as in 1999 Trondheim Harbour got a warning about the possibilities of getting a decree if efforts were not made to improve the conditions in the fjord [13].

The project called *Cleaner Harbour* was initiated in 2008. The goals were to prevent environmental or health risks associated with dispersion of environmental pollutants, to remove the polluted sediments, and to restore the biological diversity in the area. This was accomplished by dredging and covering the sediments. [13] Dredging is a process where parts of the seafloor is removed and disposed somewhere else [14]. The plan was to remove the contaminated sediments and replace them with new, clean sediments. In some areas this worked well, while in other areas dredging was not possible and covering was the only action used. The project was completed in 2014. [13]

One of the areas included in the project *Cleaner Harbour* was the Ilsvika harbour outside the Killingdal area. Due to a very steep seafloor and instability caused by high amounts of (quick) clay in this area, and the absence of shipping traffic to whirl up the masses, it was decided that a thin-layer covering was enough to reduce the potential leakage of contaminants into the seawater. Limestone was used as the covering material, and it was placed on the seafloor as a 10 cm thin layer. Amounts of contaminants in dispersed particles were measured before, during, and after covering. These measurements showed that the dispersed particles were contaminated before the covering, indicating their potential role as a medium for contamination spreading. After the covering, on the other hand, the dispersed particles from the covered areas were clean. [13]

In 2019 NGI completed a monitoring project where they among others checked the seawater outside the Killingdal area to see how much trace elements it contained. They found that the trace element concentrations have increased during the past 3 years. The conclusion is that the source must be the Killingdal tunnel as the concentrations of zinc, copper and cadmium in the tunnel match the concentrations released into the fjord. It is therefore necessary to stop the run-off from Killingdal as soon as possible. [15]

2.3 Trace elements

In nature, the amount of elements that can be found in the different compartments varies greatly. While the four dominant elements in the Earth's crust are oxygen, silicon, aluminium, and iron, the four most common elements in the human body are hydrogen, oxygen, carbon, and nitrogen. How the elements are distributed depends on physical and chemical factors such as weathering, the pH in the surroundings, what redox properties they have, their solubility, and so on. [16]

Usually, the elements that take part in biological systems are divided into three groups; major, minor, and trace. Major elements account for 96 % of the organism, and are the components of the organism's structural parts. They are the same as the four most common in the human body, that is hydrogen, oxygen, carbon, and nitrogen. Elements classified as minor are important to sustain the electrolyte balance processes, and constitute 3.6 % of the organism. Calcium, chlorine, magnesium, sodium, potassium, and phosphorus are all classified as minor elements. The last category, trace elements, are usually only representing 1 % of an organism. A number of them play important roles in growth, development, and general health of the organism. Trace elements usually occur in concentrations less than 100 µg/g [17]. This group consists of all the elements that are not mentioned in the two other groups. Metals, transition metals, and semi-metals are therefore all classified as trace elements. [16] Elements that are categorised as trace elements in organisms, do not have to occur in trace amounts in other compartments, but for simplicity when the term *trace element* is used in this thesis it refers to the definition above.

The major source of all trace elements is the Earth's crust. Starting from there, trace elements can travel many routes that may lead to incorporation in animals or humans. Erosion of natural rocks creates sediments and soil. From these compartments, plants can easily absorb the elements through their roots. The edible parts of the plants will then provide a route to animals or humans that eat them. Water is also an important route for elements. It can take part in the erosion of rocks, and transport and distribute elements to areas where they can be absorbed by plants or animals. Trace elements can also travel directly to living organisms through drinking water. Winds and volcanic activity may distribute trace elements by air. Humans may inhale these elements, or they may land on soil or in water, where they may take the same routes as mentioned above. [16]

The speciation of the elements, or the physio-chemical form an element exists as, can change drastically between compartments. Trace elements seldom exist as free ions or elements in the Earth's crust. Instead they are found as soluble salts, insoluble carbonates, oxides, organic and inorganic complexes, or in many cases as sulphides, among others. In water trace elements are commonly found as colloids, organic, or mineral substances, and only rarely and at specific conditions as soluble forms. Sediments and soil contain trace elements mainly as oxides and hydroxides of iron and manganese, attached to clays, or as parts of organic substances. pH and redox conditions are important factors playing a role in the speciation of trace elements. [16]

2.3.1 Biological effect of trace elements

When it comes to effects in organisms, trace elements can be divided into two categories; essential and non-essential. Essential elements are crucial for organisms to survive. They often take part in enzymatic reactions as cofactors or as parts of important molecules. The optimal concentration of a

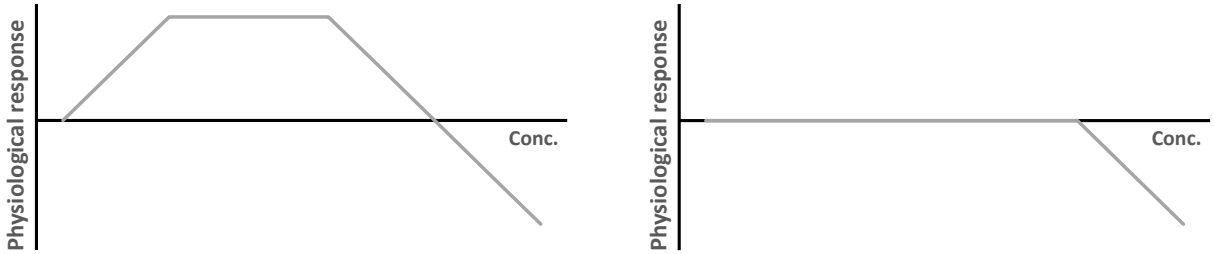

(a) Essential trace elements.

(b) Non-essential trace elements.

Figure 2.6: The relationship between the concentration of a trace element in an organism and the expected response of the same organism. Figure 2.6a: Dose-response graph for essential trace elements. At first the graph increases, this is the deficiency area. When the graph is flat the corresponding trace element is in its optimal concentration. In the end the graph starts to descend, this is the toxicity area. Figure 2.6b: Dose-response graph for non-essential trace elements. At first there is no response, and the graph stays flat. When the concentration reaches a threshold value it starts to decrease, this is when the element concentration becomes toxic to the organism.

trace element is the concentration interval that matches the requirement of the organism to sustain vital processes in the body. Usually there is a defined range of concentrations where the effects in the organism are most favorable. An optimal concentration is indicated by the flat top part of the graph in figure 2.6a. This varies from element to element, and can be very different between organisms. Examples of trace elements that are important in humans and animals are arsenic, chromium, iron, nickel, copper, and zinc. [16]

Non-essential elements are not involved in any processes in organisms. Often they pose a threat to organisms by inhibition or induction of vital reactions, which causes toxic effects. Figure 2.6b shows the relationship between non-essential elements and the physiological response. In many cases, it is possible for an organism to survive after exposure to low concentrations of a non-essential element. However, when the concentration reaches a threshold level the effects will become toxic. The threshold concentration varies greatly between elements. Some non-essential elements can stay in an organism without causing harm, and are often found in biology even though there has not been established a reason. Examples of such elements are lithium and boron. Other elements are not usually found in an organism, and can cause problems even at very small doses. These are often termed toxic, and include cadmium, lead, and mercury. [16]

As mentioned above, there are many ways the trace elements can find their way into living organisms. It can be through the lungs, gills, skin, or with the food ingested. Many animals have the ability to excrete the elements they have consumed. However, if the intake is higher than the rate of excretion, or if the element is not so easily removed, it can accumulate in the tissues of an organism. This is known as bioaccumulation. In addition, many trace elements can transfer from one trophic level in the food chain to the next. This can in many cases cause a build-up in the higher trophic levels, to many times the amount found in the environment. When this occurs, it is called biomagnification. This increase in concentration can lead to detrimental effect in the organism if critical levels are reached, or it can be harmful to ingest by consumers. [16]

2.3.2 Copper (Cu)

Copper is an essential trace element and is after zinc and iron the third most common trace element in the human body [18]. The most common oxidation states are the cuprous ion (Cu^{+}) and cupric (Cu^{2+}) ion. In the aquatic environment, copper is also an essential element to many organisms such as different mollusc and crustacean species [19], as well as fish [20]. However, in too high concentrations, copper can be toxic. Microbes like algae and plankton are the most sensitive species to copper contamination, while bivalves and some aquatic plants have shown higher resistance to copper [21]. Copper has been linked to among others reduced fertilization capacity in blue mussel [22] and coral gamete [23], and can affect the calcium homeostasis in sea urchin eggs [24].

In nature, copper in soil generally occurs as sulphides, and the most common type is chalcopyrite ($CuFeS_2$). [25] In this combination, most studies have found that copper is in the form of Cu^{+}. When this mineral is exposed to air, species like Cu^{2+} and Fe^{3+} sulphate, Cu_2O and Cu_2S might form [26]. Other common types are chalcocite (Cu_2S) and bornite (Cu_5FeS_4). [16] Chalcopyrite in the rocks are often accompanied by iron sulphides pyrite (FeS_2) and pyrrhotite (FeS). Other common sulphide minerals in copper ores are molybdenite (MoS_2), sphalerite (ZnS), and galena (PbS). [25] In addition, there are some trace elements that are commonly found in association with copper minerals. Examples are zinc, lead, cadmium, arsenic and nickel [27]. During weathering of the minerals mentioned above, copper can be released as e.g. Cu^{2+}, $CuOH^{+}$, $CuOH_2$, and $CuCO_3$ into the interstitial soin solution [16]. Copper can also attach to clay, oxides of iron and manganese, or organic material, depending on what the soil consists of. In natural waters, copper can be found as Cu^{2+}, $Cu(OH)^{+}$, $CuSO_4$, and $CuCO_3$ [16], or as organic complexes, as copper has a tendency to complex strongly with organic compounds such as humic substances, stronger than other divalent metals [28]. Further, it can move to the sediments, which functions as big sinks for copper. Iron oxides and organic material bind copper strongly, in principal causing the biological effects to become very low where concentrations of these substances are high. [18] It has generally been reported that copper do not biomagnify [19, 29, 30], but there might be indications that copper can biomagnify in some very specific food chains [29].

2.3.3 Zinc (Zn)

Zinc is another metal that is common to mine for. As copper, is is an essential trace element, and it is the second most abundant trace element in the human body. Main oxidation states are Zn^{+} and Zn^{2+}, with the latter being the most common. [31] Zinc can be found in many different industries, such as metallurgy, construction, and batteries [32]. The role of zinc in many aquatic organisms, e.g. fish, is as an essential nutrient, and it is important in several metabolic processes and as cofactor for enzymes [29]. However, high concentrations of zinc have been proven to decrease the amount of motile sperm of mud crab [33], and it has been shown that zinc can cause malformations of fish embryos.

In nature, deposits where zinc can be found often also contain lead, and their production are closely linked. The most important mineral retrieved from zinc ores is sphalerite (ZnS). [32] This is used to produce metallic Zn that further can be used for galvanization of steel and iron as a protection against corrosion, or to make brasses and alloys. Trace elements that are commonly found in association with zinc minerals are cadmium, copper, lead, and arsenic [27]. Weathering of zinc-containing minerals

cause the release of e.g. Zn^{2+}, $ZnCl^{+}$, $ZnOH^{+}$, and $ZnCO_3$ in soil solutioon [16]. In the ocean, zinc can exist as Zn^{2+}, hydroxides ($ZnOH^{+}$, $Zn(OH)_2$), carbonates ($ZnCO_3$), and also bind to different organic materials [16]. The bioavailability of zinc is strongly dependant on the complexation, but most ligands decrease the availability due to reduced activity of the free zinc ion. [34] As with copper, there are some conflicting views on the biomagnification of zinc [19, 29, 30], but zinc has been proven to biomagnify in a Arctic food web [30]. The concentrations of zinc are often enriched in fine-grained, organic-rich sediments.

2.3.4 Lead (Pb)

Lead is generally considered as a non-essential metal. It has no established essential effects, neither in humans nor animals. The main oxidation state of lead is 2+. It used to be added to petrol to avoid knocking, but this is now banned. Lead has been shown to accumulate in tissues of fish and other aquatic organisms, and it can cause harm to the neural network, affect the development at embryonic and larval stage, and cause behavioural changes. [35]

The main mineral containing lead is galena (PbS). This is a mineral that has been found to be closely linked to zinc minerals, and their processing is therefore related. [32] In addition, lead may exist in association with chalcopyrite. Galena may contain other elements like zinc, copper, and cadmium [27]. When the lead-containing rocks are weathered, Pb^{2+} is released into the environment where it can be incorporated into clays, iron and manganese oxides, and organic matter. It can also form $PbOH^{+}$ and $Pb_4(OH)_4{}^{4+}$ when weathered. In water, lead is usually associated with carbonate ($PbCO_3$), chloride ($PbCl^{+}$, $PbCl_2$), and hydroxide ($Pb(OH)^{+}$ to $Pb(OH)_3{}^{-}$), but it can also be attached to inorganic colloids. Sediments acts as a sink for lead. Here, it can be stored, but there is also recent evidence that lead can be involved in biomethylation, a process where toxic lead species such as $(CH_3)_3Pb^{+}$ and $(CH_3)_4Pb$ are produced. [16]

2.3.5 Iron (Fe)

Iron is an essential trace element and transition metal that is used in, among others, steel production and constructions. It is involved in a lot of different functions in an organism, such as the role as a cofactor in the transport of oxygen, and as an electron donor/acceptor in many proteins involved in ATP synthesis and DNA synthesis. The oxidation states that normally occur in nature are Fe^{2+} and Fe^{3+}. [31] Although iron is an essential element, elevated concentrations can have severe effects to aquatic organisms. It has been discovered that exposure to high concentrations can produce reactive oxygen species that can damage lipids, disrupt cell membranes, and may impair the DNA. In addition, the precipitation of iron hydroxides on top of the sediments could affect the food quality and availability, and alter the habitat structure. [36]

In the Earth's crust, iron is one of the main constituents. Here, it is mostly found as sulphides, but in many variations. The most common iron sulphide mineral is pyrite (FeS_2). Iron is a major constituent in a considerable amount of minerals, with examples such as arsenopyrite (FeAsS), shpalerite, and chalcopyrite. Associated elements in pyrite are arsenic, cadmium, copper, mercury, nickel, lead, and zinc, among others. [37] When these minerals are exposed to air and water, the iron may be released and oxidised from Fe^{2+} to Fe^{3+}, which will induce the acidification of soil and water nearby. This is discussed more in detail in section 2.9. Common species found in natural waters

are $Fe(OH)_2^+$, $Fe(OH)_4^-$, while precipitated $Fe(OH)_3$ and Fe^{2+}/Fe^{3+} attached to e.g. organic and inorganic particles are more commonly found in the sediments. [16]

2.3.6 Chromium (Cr)

Chromium is a transition metal can exist as oxidation states Cr^{2+}, Cr^{3+} and Cr^{6+}, with the two latter being the most common. A common use is in stainless steel alloys, as it prevents oxidation from occurring. It is not proven to have any essential functions in the human body. There are also some discussions around the essentiality of chromium (III) essentiality in vertebrates, but it has been discovered to improve the growth of fish. The hexavalent form is the most toxic form, and has been proven to be carcinogenic. It is also the most bioavailable form, and poses a threat to aquatic organisms if it ends up in the ocean. The trivalent form is less toxic to e.g. fish, and in some cases the hexavalent form can be reduced down to this in nature. [38]

Rocks and minerals with chromium can be found in the Earth's crust. Chromite (Fe, Cr_2O_4) in a chromium-containing mineral that be mined and transformed into the applicable chromium metal. A common associated trace element of chromite is nickel [27]. When chromium-containing rocks and soils are weathered, it can release the species $Cr(OH)^{2+}$, CrO_4^{2-}, and CrO_3^{3-} into the surrounding soil solution [16]. In natural waters, common chromium species are $Cr(OH)_2(H_2O)_4^+$ and CrO_4^{2-}. These are both including hexavalent chromium, as this is the most soluble oxidation state. This is also what makes this the most toxic oxidation state, as it is able to cross membranes due to the polar properties. Trivalent chromium, on the other hand, is less soluble, and From here, sediments are sinks to chromium, where it is stored as attached to clay, iron and manganese oxides, and insoluble organic complexes. [16]

2.3.7 Nickel (Ni)

Nickel is an essential trace element, that commonly has the oxidation state Ni^{2+} in natural water systems. It is a transition metal widely used in industry, as for example in the production of stainless steel. The essentiality of nickel is well established for plants and terrestrial animals, but not for aquatic organisms. There are some recent studies indicating that it is essential to fish, but this is not well investigated [39]. However, if the concentration of nickel gets too high, it can have negative impacts on aquatic organisms by disrupting homeostasis of Ca^{2+}, Mg^{2+}, and $Fe^{2+/3+}$, it can cause allergic reactions in the respiratory track, or it can generate reactive oxygen species that can damage cells and tissues [40]. Research may also indicate that nickel can biomagnify through some specific food chains [29].

In ores nickel can be found in the mineral garnierite ($(FeNi)_9S_8$), but it also often exist as an elemental impurity in other minerals. It is commonly found incorporated in or in association with minerals such as chalcopyrite, chromite, and pyrolusite (MnO_2) [27]. The presence of nickel is usually high in sulphide ores, or in iron and aluminium rich ores called laterite [41]. When these types of rocks are weathered, it can cause the release of Ni^{2+}, $NiOH^+$, NiO_2^-, and $Ni(OH)_3^-$ into interstitial soil water [16]. In oxic water conditions, nickel is commonly bound to dissolved organic material or insoluble iron or manganese oxyhydroxides. In anoxic conditions, on the other hand, it occurs as insoluble sulphides [39]. It can therefore easily be transported with water, but will also be sedimented with the particles it is attached to.

2.3.8 Arsenic (As)

Arsenic is a metalloid which can exist in the oxidation states 0, 3+ and 5+ [31]. It is considered as an essential element, but the mechanisms and processes it is essential in/for have not been established. However, a majority of the compounds arsenic form are harmful, and the trivalent arsenic ion has been found to be more toxic than the pentavalent ion. Arsenic accumulation in fish tissues can cause damage to the liver, gallbladder, and kidneys [42].

Relatively high amounts of arsenic can be found in the environment, as it is the twentieth most abundant element in the Earth's crust. It is often found as arsenopyrite (FeAsS) [27], and smelting of copper, nickel, lead, and zinc ores is the mots important anthropogenic source [43]. Other minerals that include arsenic in their structure or where arsenic is associated are chalcopyrite, galena, and sphalerite [27]. Weathering of soils and rocks could release arsenic in the form of AsO_4^{3-}, AsO_2^- and $H_2AsO_3^-$ in soil solutions [16]. In natural waters, the oxidation states As^{3+} and As^{5+} are the most common. Under aerobic conditions arsenic often exists as AsO_4^{3-}, while AsO_3^{3-} is the main species in anaerobic conditions. Microbial methylation can change these species into $CH_3AsO_3^{2-}$ and $(CH_3)_2AsO_2^-$, which again can be transformed into toxic volatile arsenic species, such as AsH_3. One feature with both the arsenic oxidation states is that they will attach to the surface of iron(III) oxides and hydroxides. Adsorption and co-precipitation with $Fe(OH)_3$ is a route of arsenic out of water, and into sediments. [43] Both Adra et al. [44] and Espana et al. [45] have investigated the scavenging abilities of precipitation of iron secondary minerals and both found that iron precipitation and arsenic removal are closely linked. Therefore, addition of iron hydroxides is a common method to remove arsenic from drinking water and wastewater [46].

2.3.9 Cadmium (Cd)

Similar to lead, cadmium is considered a non-essential element to all living organisms. It is a transition metal with the possible oxidation states Cd^0 and Cd^{2+}, and due to its non-corrosive nature, it has been a common element to use in electroplating and galvanizing. When high concentrations of cadmium is ingested, it can lead to deficiency of the essential elements copper and zinc. Calcium deficiency in aquatic organisms has also been reported due to cadmium intake, and other sub-lethal effects in fish and invertebrates are lower reproduction and growth, and structural changes of the gills. [47]

Cadmium exists naturally in the Earth's crust, present as CdS. Here it can also be found as an impurity in zinc minerals such as sphalerite and smithsonite ($ZnCO_3$), and it occurs in association with minerals such as chalcopyrite and galena. [27] Weathering of these soils and rocks can produce the free cadmium ion, together with chloride, hydroxide, and carbonate species, in soil solutions [16]. Major species found in natural waters are $CdCl^+$, $CdCl_2$, $CdCl_3^-$, and Cd^{2+} [16], but the persistence in water is dependent on the adsorption on and desorption from e.g. clay particles and humic substances. In sediments, cadmium has been discovered as $CdCO_3$ [29].

2.4 Trace element analysis with ICP-MS

There are many ways to analyse trace elements in the environment. One method that has shown itself as a reliable and versatile technique is the inductively coupled plasma mass spectrometry, or ICP-MS. The method is a combination of the ICP part, which is a plasma ion source where the elements in the sample are transformed to ions, combined with a mass spectrometer that detects the ions. Results delivered from the ICP-MS show the total concentrations of the different preselected elements that are in the sample. [48]

In the ICP part, an argon plasma is produced by exposing argon gas to an ignition source which ionize the argon atom. Oscillating electric and magnetic fields will then trap the argon cations causing them to collide and plasma is formed. The sample is then introduced to the ICP part as an aerosol, vapour, or fine powder. This happens at atmospheric pressure. When moving through the ICP part, the sample transforms from an aerosol, through an atomic gas, to atomic ions in the end. The argon plasma is well suited at producing cations, while elements that normally turn into anions, such as chlorine, bromine, and iodine, are often harder to detect. [49]

After moving through the ICP part, the ionized sample moves toward the MS part. The interface between the two parts consists of two cone-shaped metal plates with small holes (1 mm) in the middle, which are intended to congregate the sample ions. Here, the atmosphere goes from atmospheric pressure, through low pressure, all the way to vacuum. The ions then move through lenses which are positively charged, causing the cations to cluster together in a beam in the middle of the tube focused on the MS opening. The interface also includes a photon stop, which prevents photons from reaching the MS part. [49]

When the ions reach the MS part, they are separated based on their mass-to-charge ratio. The quadrupole, which is the most common MS type, is subject to an alternating voltage. As a result, an electrostatic filter is established, which only allows ions with a certain mass-to-charge ratio pass through at a specific moment. The detector identifies the number of ions that appear and changes it into a signal that can be measured and related to a concentration of a specific element. [49]

A great advantage with the ICP-MS instrument is the low detection limits, and they vary between the different elements. Table 2.2 shows the detection limits for the trace elements in focus in this thesis. Another benefit with this instrument is that it needs small amounts of material to make an analysis, which increases the number of samples that can be analysed drastically. Because of the high temperatures in the plasma, it can handle both simple and complex matrices, often without significant matrix effects. If concentrations of matrix elements get too high, their signals can mask the signal of the analyte. Diluting the sample, separation of the matrix and the analyte, or the use of an internal standard can minimise these effects. [49] However, to know the specific species existing in the sample, for example the concentrations of soluble and insoluble fractions, a pre-treatment step has to be performed.

To assure that only the correct ion is let through, it is important to have an appropriate resolution, or mass-to-charge interval. If this is too high, interferences can cause problems. Some interferences that can appear are small molecular ions or isotopes that have approximately the same mass-to-charge ratio as one of the sample analytes. Background ions that often are present include Ar^+, ArO^+, ArH^+, H_2O^+, O^+, $O_2{}^+$, and $Ar_2{}^+$. These ions can interfere with the true signals. [49] An example

Table 2.2: ICP-MS detection limits [49] and some common interferences [50] for the trace elements in focus. Unit is µg/L for the detection limits.

Element	Detection limit	Analyte	Interferences
Al	0.06		
Fe	0.45	$^{56}Fe^{+}$	$^{40}Ar^{16}O^{+}$, $^{40}Ca^{16}O^{+}$
Cr	0.02	$^{52}Cr^{+}$	$^{40}Ar^{12}C^{+}$, $^{35}Cl^{16}OH^{+}$, $^{34}S^{18}O^{+}$
Ni	0.005	$^{58}Ni^{+}$	$^{42}Ca^{16}O^{+}$
Cu	0.003	$^{63}Cu^{+}$	$^{31}P^{16}O_2{}^{+}$, $^{46}Ca^{16}OH^{+}$
Zn	0.008	$^{64}Zn^{+}$	$^{32}S^{16}O_2{}^{+}$, $^{31}P^{16}O_2H^{+}$, $^{32}S_2{}^{+}$, $^{48}Ca^{16}O^{+}$
Cd	0.003		
Pb	0.007		
Ca	2.0		
As	-	$^{75}As^{+}$	$^{40}Ar^{35}Cl^{+}$, $^{40}Ar^{19}F^{16}O^{+}$

is $^{40}Ca^{2+}$, which overlap with the $^{40}Ar^{+}$. To avoid this, the isotope $^{44}Ca^{2+}$ is measured instead. Calcium itself could be an interference for nickel, when it forms the compound CaO. By measuring the isotope ^{62}Ni instead of ^{60}Ni, this problem could be avoided. Same solution is used for the interferences of MoO to cadmium signals. Common interferences for the elements in focus in this thesis are presented in table 2.2. In addition, the ICP-MS instrument does not tolerate organic solvents well. Carbon can accumulate and cause clogging or cross-interferences between samples. [50]

Not all samples can be run directly with ICP-MS. In many cases, the samples have to be processed in some way before they enter the instrument. Water samples often contain particles, and these have to be filtered out before the sample is analysed. If the concentrations of analytes are high, the sample may be diluted before analysis. Solid samples, such as sediment samples, have to be decomposed and dissolved. To begin with, the sediment samples has to be freeze dried. This is a process where the water is first frozen into ice in a freezer. Then the samples are transferred to the freeze dryer, and the pressure is lowered to below 6.11 mbar. The reason why 6.11 mbar is the limit is because it is at this pressure the triple point of water is located, as shown in figure 2.7. At the triple point the boundaries of the three phases *solid*, *liquid*, and *vapour* meet. When the pressure is below 6.11 mbar, the frozen water can be converted directly to vapour when the appropriate temperature is reached. The process where water moves directly from solid phase to gaseous phase is called sublimation. By using this method, what is left is the dry sediment sample.

Further, the solids have to be dissolved. This procedure is called digestion, and proceeds by adding concentrated nitric acid (HNO_3) to the sample and insert them into e.g. an Ultraclave. This is a machine that can expose the samples to high pressure and temperature, causing the materials in the sample to break down and dissolve into the acid. After dilution with pure water, the sample is ready to be analysed.

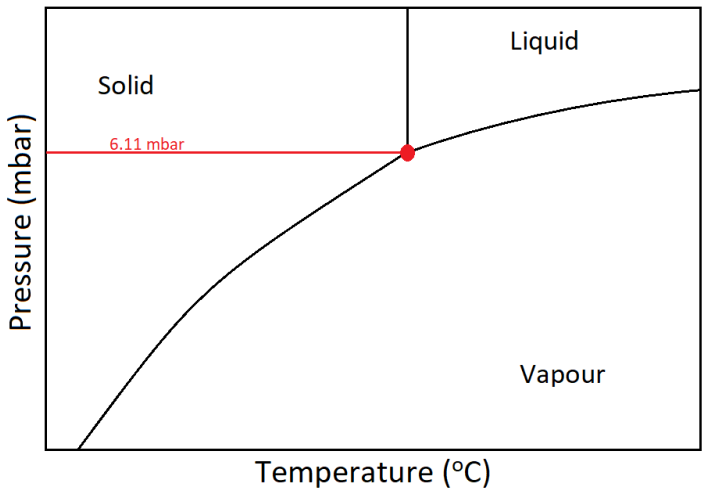

Figure 2.7: Phase diagram for water loosely based on the phase diagrams in Atkins' Physical Chemistry [51] and the operating manual for Freeze Dryer APLHA 1-4 LDplus/ALPHA 2-4 LDplus [52]. The different phases are separated by the melting pressure curve (between solid and liquid), vapour pressure curve (between liquid and vapour), and the sublimation pressure curve (between solid and vapour).

2.5 Water and its role as a matrix

Many trace elements act as acids when they are introduced to water. Because most trace elements occur as cations, they will have a positive charge. The water molecule is on the other side a neutral molecule, but the oxygen represents a negative part of the molecule and the two hydrogen atoms represent a positive part. Together they form a so-called dipole. The positively charged trace element will attract the oxygen in the water molecules and repel the hydrogen atoms, which will become more available for other compounds. The illustration in figure 2.8 shows how water molecules can be arranged around the trace element cation. As a result of this, the trace element addition will cause the pH in solution to decrease. [53]

In water, all trace element cations will be hydrated, i.e. associated with water molecules. The

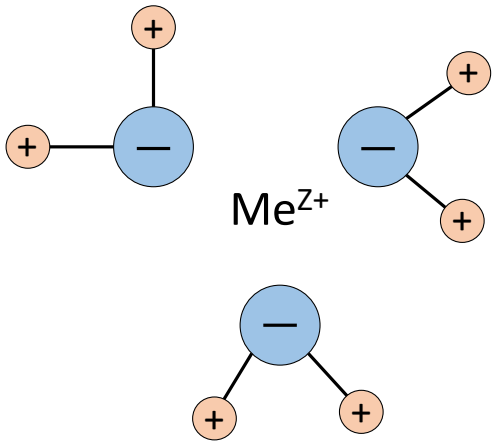

Figure 2.8: Illustration of how water molecules are arranged around trace element cations when these ions are hydrated. The blue balls are representing oxygen atoms, while the orange balls represent hydrogen atoms. Me^{Z+} represents an arbitrary trace element with a charge of Z+, where Z is an integer above zero.

combination of a trace element cation and water molecules is an example of a complex. Trace elements usually take the role as central atom, while the water molecules act as ligands, which are atoms, molecules or ions that are bound to the central atom. Most trace elements with charge from 2+ and up usually stay as complex with water molecules only at lower pH. When pH increase, trace element cations form complexes with hydroxide (OH) molecules. The trace elements may also react with other compounds, where they exchange the water molecules with the preferred ligands, and in many cases two or more central atoms converge and become one larger multinuclear complex. This is especially common when the trace element concentration is high. At very high pH, they may exist as oxo-complexes which include O^{2-}. These distribution of water hydrolysis products dependant of pH and charge of trace elements are shown in figure 2.9a. The bond between the trace element and the water molecules are not very strong, and the cation is usually regarded as a *free ion*. This is the reason why the elements in the upper left corner in figure 2.9a are not paired with H_2O groups. When the pH increases, more OH groups become available to react with the *free ion* creating the hydroxo complexes. [53]

Dissolution and precipitation of trace elements in water depends on the element speciation, the pH of the water and the concentration of the element. To illustrate this, the ferric and ferrous ions can be used. The ferrous ion is a relatively soluble species, that can remain as a dissolved in water when pH is below 7. This is illustrated in figure 2.9b by the line named Fe^{2+}. When the pH is above 7, $Fe(OH)_2$ will start to precipitate. Ferric ions, on the other side, are precipitated at a much lower pH value, which is illustrated by the line labeled Fe^{3+} in figure 2.9b. Already at pH 3 the solution will contain only a very low amount of *free* ferric ions. The rest will precipitate as $Fe(OH)_3$. Between these two stages, several species of ferric and ferrous ions can exist. The mononuclear species are $Fe(OH)^+$, $Fe(OH)^{2+}$, and $Fe(OH)_2{}^+$, and multinuclear species can be e.g. $Fe_2(OH)_2{}^{4+}$ and $Fe_3(OH)_4{}^{5+}$. The slope of the lines in figure 2.9b are equal to the negative version of the charge. A larger positive charge will have a higher repulsive force towards the protons in the water molecules, causing them to be removed easier from the complex. [53]

There are many ways to sample water to analyse trace element concentrations. In many cases, a clean container in an inert material submerged into the water that is going to be sampled is the easiest and best way. However, when water right above the sediments in the ocean is supposed to be sampled, the method above is not adequate. According to the standard NS-ISO 5667-9:1992, a closed-pipe sampler is suitable for this task. An example of such a device is a rosette sampler. It consists of a hollow tube with lids in both ends. When sampling, it is lowered down from a vessel to the planned depth while remaining open. At the planned depth, a mechanism closes the lids in both ends, and the closed tube with the water is lifted up to the surface where samples can be taken. The inner sides of the tube are usually made of an inert plastic material, to avoid contamination of the sample. [54]

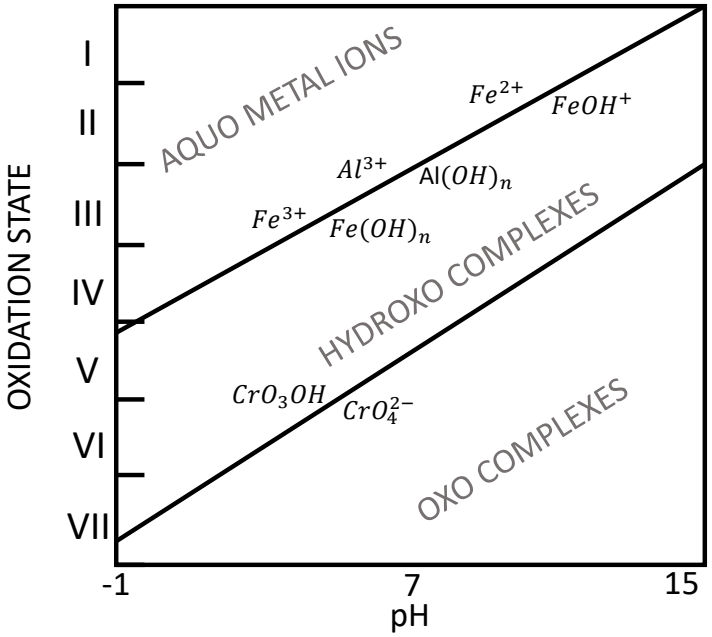

(a) Illustration of which hydrolysis complexes different common trace elements take part in when dissolved in water. Low oxidation state trace elements stay in complex with H_2O as aquo complexes. When oxidation state and/or pH increases, hydroxo and oxo complexes become more dominant.

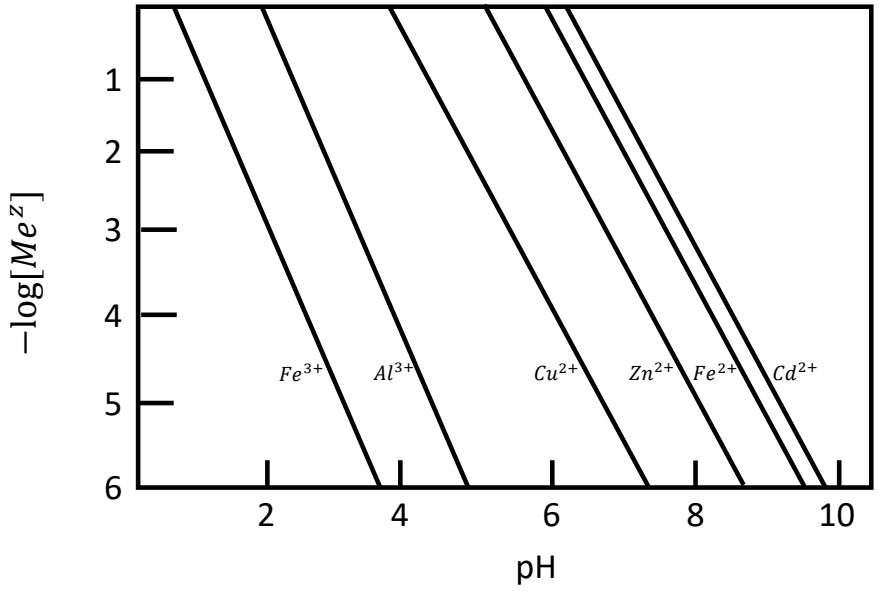

(b) Solubility of oxides and hydroxides for different trace elements. When the pH increases, a lower concentration of the trace elements can stay as *free ions* in a given solution.

Figure 2.9: Illustrations of how trace elements behave in different conditions in water. Both figures are modified versions inspired by Stumm and Morgan's Aquatic Chemistry [53].

2.6 Soils and their role as a matrix

Soil is the result of weathering, or breakdown, of rock minerals by wind, rain, and biological reactions, which results in dissolution of species and formation of new secondary minerals. It generally consists of clays, carbonates, iron and manganese hydroxides, and organic components, but the specific composition varies from place to place depending on the rock composition and the activity of soil-living animals and plants. The original parent mineral also decides the texture of the soil, i.e. the amount of different sized particles, and affect the physical and chemical properties of the soil. [27] The form a trace element exist on in soil can be divided into three categories. *Inert* forms of elements are resistant to changes in solution, will respond to changes in a period of years. An example of this are elements incorporated in the structure of minerals. The *non-labile* form is kinetically constrained and change slowly, i.e. in a matter of days to months. Strongly surface-adsorbed elements are an example of this. *Labile* forms are reversibly bound in the soil, and react to changes in the solution almost instantly. Electrostatically bound hydrated trace elements in clay and humic acids are labile forms.

pH is probably the most important factor controlling the solubility of trace elements in soil. The lower the pH of the soil and the interstitial water is, the more soluble most trace elements are. Dissolution of solids can be exemplified by

$$MCO_{3(s)} + 2\,H^+ \longrightarrow M^{2+} + CO_{2(g)} + H_2O \tag{2.1}$$

where M represents an arbitrary trace element with the oxidation state 2+. When the pH decreases, increased proton concentration in the soil will push the reaction to the right, causing the trace element to dissolve. In polluted land sites, e.g. areas affected by mining processes, rain and river water can dissolve the most labile bound trace elements in the soil. This will cause the pH in the water and soil to decrease, and less labile trace elements can be dissolved. Other effects of the lower pH is more positive charge of the iron and manganese hydroxide surfaces which will repel cation trace elements, and a higher competition with protons for available sites. [27]

Another factor influencing the release of trace elements from soil is the redox potential, i.e. the activity of electrons. The electron activity is highest when the redox potential is low, or even negative, indicating reducing conditions. This is typical further down in the soil. In the surface layers where oxygen cause oxidising conditions, the redox potential is high, while further down in the soil reducing conditions are dominant . In many reduction reactions in soil, protons play a role. One example is the reaction

$$Fe(OH)_{3(s)} + 3\,H^+ + 2\,e^- \longrightarrow Fe^{2+} + 3\,H_2O \tag{2.2}$$

where Fe^{3+} is reduced to Fe^{2+}. This reaction has a tendency to occur when the redox potential is low, and shows how the pH can be increased in reducing conditions. Low reduction potential can also cause iron and manganese hydroxides to dissolve, releasing all trace elements attached to it, reduction of the trace element itself can occur, or new complexes can form. [27]

Temperature may also play a role in the trace element mobility in soil. Higher temperatures can help a reaction happen, as the excess energy it provides may be what is needed to overcome the energy barrier of that particular reaction. Both adsorption and desorption reactions can be affected. The temperature of the surroundings can also alter the equilibrium of a reaction, affecting the final

endpoint of the reaction. [27] In addition, high concentrations of trace elements in the soil will lead to more leakage. When more elements are present than what the binding sites can hold, the excess elements are free to be transported away by water.

2.7 Marine sediments and their role as a matrix

Sediments are a combination of many different components, with different sizes, shapes and origins, that accumulates at the bottom of the sea. Particles weathered from different kinds of rocks, residues from calcifying organisms and other types of organic matter, or precipitation of minerals directly from the water are all common constituents of sediments. [55] Many trace elements in the ocean tend to attach onto clays or Mn/Fe oxides or form organic complexes that are not very soluble [16], which are all normal constituents of sediments. This attachment happens through cation exchange, which is a process where the positively charged trace elements in the ocean take the seats of positively charged elements in the sediments, or chemisorption, a process where the trace elements are attached to the sediments through electrostatic attractions.

There are many ways in which sediments can be formed. One way the material is brought to the accumulation area is by sinking down from the surface water, or transport by waves, currents, winds, ice or movement of masses. It is also possible that the sediment material is produced at the accumulation site by chemical reactions or biological processes. [55]

In an accumulation area where the conditions for sedimentation are ideal, the deposits will lie in a chronological order, meaning that old deposits will be buried by new deposits [56]. If the deposition rate is the same through time it is possible to estimate the time period when a specific layer was formed, and to gain knowledge about the biological, chemical and physical situation in this specific area. The sediments become a reflection of the water and environment at a given time. Because of this, a concentration of a contaminant found in a specific layer can be correlated to an event that happened when the sediments were deposited. [55] Also, the environmental pollutants that are the biggest threats tend to attach to particles that becomes part of the sediments. It is therefore practical to investigate the sediments to check the spreading of these environmental pollutants in an area. [57]

Sediments are home to a wide variety of life, and the organisms that lives here can strongly affect the composition of the sediments. Among others, bacteria that lives at the top of the sediments have the ability to change the chemistry and toxicity of the trace elements in the sediments by changing the complexes they take part in, or by altering the oxidation state of given elements. [16] A classic example is biomethylation of mercury (Hg). In this process, bacteria convert inorganic mercury (Hg^{2+}) to the methylated form CH_3Hg^+ or $(CH_3)_2Hg$. [16, 58] These forms of mercury are very toxic as they act as neurotoxins, causing neurological disturbances in the organism exposed. They are also lipid soluble which makes it possible for mercury to bioaccumulate in organisms [58].

Organisms that live deeper down in the sediments may also affect the structure of the sediments. Bioturbation is a phenomenon of biological mixing of sediments and solutes, and biological mixing of gradients in the sediments. Macrofauna feeding, production of burrows and movement between the surface and deeper parts of the sediments can influence which diagenetic processes that takes place by introducing oxygen to the deep. Usually there is not a lot of oxygen in the deeper parts of the sediments, and other organic matter decomposition reactions such as denitrification, manganese reduction and sulfate reduction are dominant. However, when the macrofauna dig into the sediments new, oxygen-rich water enters the deep and oxic remineralization becomes the dominant decomposition reaction. This will cause the conditions in the sediments to go from anaerobic to aerobic, which

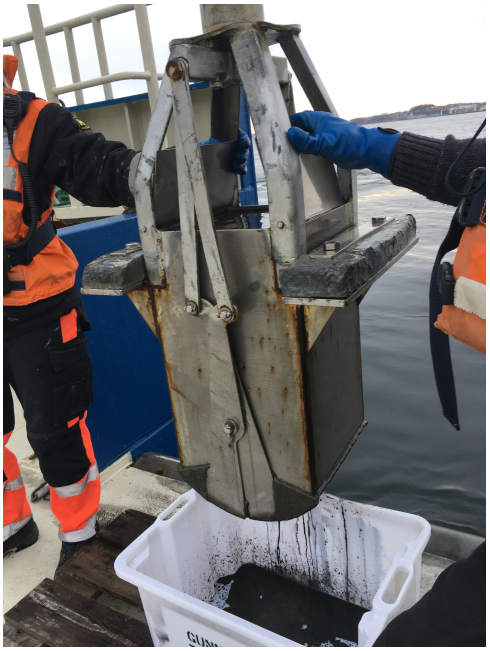

Figure 2.10: Example of a box corer used to collect sediment cores from the Trondheimsfjord sediments.

can change the oxidation state of polluting elements and potentially making them more bioavailable. This may also cause some pollutants to leak back into the water above, where it can be taken up by organisms, and affect the composition of sediments that finally are preserved. [59]

Sampling of sediments can be done by the help of a box corer. This is a device that grabs a relatively large portion of the sediments and brings it to a vessel, with the sediment surface intact. Two shovels connected to each other as figure 2.10 shows stays open on the way down, and close when they come in contact with the sediments. Then they are closed and stay this way until they are manually opened again on deck. By using a box corer, a large amount of surface sediments and deeper sediments are collected. This enables the collection of subsamples from many different layers of the core. In addition, both the fauna in the sediment-water interface and the water directly above the sediments are brought to the surface, making it possible to sample that as well. [57].

2.8 Classification of trace elements in water and sediments

To establish the health and environmental condition of a body of water, and to be able to estimate the potential threat to organisms living in that water, a classification system is needed. The Norwegian Environment Agency, in collaboration with The Norwegian Institute for Water Research (NIVA) and Norwegian Geotechnical Institute (NGI), have made a set of guidelines, or classifications, ranging from class I which indicates background levels of the contaminant, to class V which indicates very bad conditions.These classifications are made in accordance with Technical Guidance Document for Deriving Environmental Quality Standards (TGD. No. 27). [60] Table 2.3 explains the five different categories.

The categories depend on the concentrations of specific elements, and upper limits for the different classes can vary greatly between elements. As an example, arsenic is in class I if the concentration in freshwater is less than 0.15 µg/L, while the concentration of lead must be less than 0.02 µg/L to be in class I. [60] Water with concentrations of an element in class IV will potentially cause more harm to organisms than water with concentrations of the same element in class II.

Class I, also often referred to as *background level* is defined as the state of a body of water with little or no anthropogenic influence.The upper limit for this class is therefore dependant of what can be found in the environment naturally. For man-made chemicals, the upper limit for class I will be zero, because it is not a substance that should exist naturally in the environment. Trace elements on the other hand exist in the Earth's crust naturally, and the limits for class I are higher than zero. The limits between the other classes/categories are extracted from the responses of a given quality parameter, to a specific dose in a dose-response curve. Countries with similar water types intercalibrate the class boundaries between each other, so that it is possible to compare water conditions. To decide the condition of a body of water the quality parameter with the worst classification of condition is often used. This is to ensure that even the most sensitive quality parameters are not affected. Examples of quality parameters used to establish classification of conditions are phytoplankton, aquatic flora, soft-sediment macrofauna, and fish. [61]

Table 2.3: Explanation of the different categories within the classification of trace elements and organic environmental toxicants in water and sediments.

Background (I)	Good (II)	Moderate (III)	Bad (IV)	Very bad (V)
Background level	No toxic effects	Chronic effects due to long-term exposure	Acute toxic effects due to short-term exposure	Extensive acute toxic effects

2.9 Acid mine drainage (AMD)

For the past centuries there has been a high demand for different trace elements to be used in e.g. industry and, more recently, consumer products. Both copper and zinc are examples of metals the market is in need of, and is extensively mined for. However, there are some drawbacks in relation to mining. The mine itself and the accompanying buildings and transport routes are massive interruptions of the nature, and the mining industry is associated with waste consisting of the gangue minerals in the ore and leftover minerals from the extraction processes. One of the most serious problems connected to mining is however acid mine drainage (AMD) [62] .

When water runs through e.g. active or abandoned mines, spoil pits or treatment sludge pounds, the oxygen-rich water comes in contact with sulphide-containing material, causing the sulphide mineral to oxidize. This happens naturally but is drastically enhanced by mining activities. The result is a run-off characterized by a low pH and high concentrations of sulphate, trace elements, and other potentially toxic elements and substances, called acid mine drainage. How much contamination the AMD contains depends on the amount of different elements in the oxidized sulphide mineral and in the gangue minerals. [62]

There are many trace element sulphide minerals that may cause AMD, but the most common ones are those that contain iron. To illustrate the processes that occur, it is common to use pyrite (FeS_2), as this is the sulphide mineral that occurs most often, and the reaction mechanisms are thoroughly investigated. The first step that takes place is the oxidation of pyrite by oxygen, where dissolved iron, sulphate and protons are produced, as shown in equation 2.3. [62]

$$FeS_2 + \frac{7}{2}O_2 + H_2O \longrightarrow Fe^{2+} + 2\,{SO_4}^{2-} + 2\,H^+ \tag{2.3}$$

This reaction causes an increase in dissolved solids in the water, and it also lowers the pH due to the added protons. The second step of the process is dependent of oxidizing conditions, and O_2 concentrations, pH and bacterial activity plays important roles. If the conditions are sufficient, most of the Fe^{2+} will be oxidized to Fe^{3+}, as equation 2.4 shows. [62]

$$Fe^{2+} + \frac{1}{4}O_2 + H^+ \longrightarrow Fe^{3+} + \frac{1}{2}H_2O \tag{2.4}$$

This second step is often the rate-limiting step of the process. The reason is that the conversion of Fe^{2+} to Fe^{3+} is very slow at pH below 5. Reaction rates can be significantly increased by the catalytic help of acidophilic bacteria, i.e. bacteria that can live in very acidic environments. [63]

The third step is also pH dependent, since Fe^{3+} will precipitate if the pH is between 2.3 and 3.5 as a hydroxide. Equation 2.5 shows this reaction. [62]

$$Fe^{3+} + 3\,H_2O \longrightarrow Fe(OH)_{3(s)} + 3\,H^+ \tag{2.5}$$

Residual Fe^{3+} that does not precipitate may take part in oxidation of pyrite through the following equation.

$$FeS_2 + 14\,Fe^{3+} + 8\,H_2O \longrightarrow 15\,Fe^{2+} + 2\,{SO_4}^{2-} + 16\,H^+ \tag{2.6}$$

The total reaction for dissolution of FeS_2 into Fe^{2+}, oxidation to Fe^{3+} and precipitation to $Fe(OH)_3$ is shown in equation 2.7. This is a combination of equations 2.3, 2.4, and 2.5. [62]

$$FeS_2 + \frac{15}{4}O_2 + \frac{7}{2}H_2O \longrightarrow Fe(OH)_3 + 2\,{SO_4}^{2-} + 4\,H^+ \tag{2.7}$$

There is also a total reaction equation for the stable Fe^{3+} used to further oxidize pyrite, which is a combination of equation 2.3, 2.4, and 2.6. This overall equation is shown in equation 2.8. [62]

$$FeS_2 + \frac{15}{8}O_2 + \frac{13}{2}Fe^{3+} + \frac{17}{4}H_2O \longrightarrow \frac{15}{2}Fe^{2+} + 2\,{SO_4}^{2-} + \frac{17}{2}\,H^+ \tag{2.8}$$

Equations 2.3 to 2.8 present how FeS_2 will behave in water. When examining these equations it is evident that they all release protons into the solution. This causes the pH to decrease, and the mine drainage to become acidic. This allows the trace elements in the solution to become soluble and be transported easily with the flow of the solution. In addition, there are many other types of sulphide minerals that can be oxidized by the water and affect the AMD. The stoichiometry and elements involved will then be different. [62] AMD is therefore a complex mixture depending on the geology of the mining area, whether there are bacteria present, temperature, and if there are water and oxygen available [64]. Figure 2.11 presents the water at Killingdal, which can be characterized as AMD water.

As equations 2.7 and 2.8 show, AMD often contains high amounts of sulphate, due to the presence of sulphur in many of the most common ore minerals. Sphalerite, pyrite, and chalcopyrite all contain sulphur. Due to this the speciation of e.g. iron and aluminium is strongly influenced, causing these elements to be present as sulphate complexes such as ${FeSO_4}^+$, ${Fe(SO_4)_2}^-$, ${AlSO_4}^+$, and ${Al(SO_4)_2}^+$. The oxo and hydroxy complexes only exists in small amounts at low pH, but becomes more dominant from pH between 5 and 6. Depending on the composition of the AMD and the pH, many different secondary minerals (i.e. minerals formed by precipitation from the AMD) may precipitate. These minerals often contain iron and aluminium in combination with oxy, hydroxy and sulphate groups, such as schwertmannite ($Fe_8O_8(SO_4)(OH)_6$) and basaluminite ($Al_4(SO_4)(OH)_{10} \cdot 12 - 36H_2O$). These minerals often have small particle size and high surface area, which makes them suitable to scavenge and attract other trace elements. Secondary iron minerals are known to attract arsenic, while aluminium have been proven to attract chromium. [65] They are both known to scavenge lead, cadmium, copper, zinc, and cobalt [65, 66].

2.9.1 Treatment of AMD

Because of the high amounts of harmful elements that exists in the AMD, the water must be treated, preferably before it comes in contact with nature. This can be accomplished in many ways. To mention some, trace elements can be removed from water by chemical precipitation, ion exchange, adsorption, coagulation and flocculation, sedimentation, electrochemical treatment, or biological mediation [67, 68, 69]. Treatment methods of AMD can be divided into two categories: *passive*

Figure 2.11: A picture taken of the water in the Killingdal tunnel, that can be described as acid mine drainage (AMD) water.

and *active*. Both categories may include physical, chemical, and biological methods, but as *active* treatment require regular input of reagents and operation by staff members, *passive* treatments only need maintenance occasionally and often utilize natural chemical or biological processes for AMD treatment. In addition, *passive* methods are best suited in the treatment of AMD with low acidity, i.e. a low hydrogen ion concentration and low potential for release of protons due to precipitation of trace element hydroxides, while *active* methods can be used in almost all types of AMD. [69]

The most common treatment method for AMD treatment is chemical precipitation through the increase in pH, which is used in both *passive* and *active* systems. Since AMDs are acidic, adding a neutralising agent such as limestone ($CaCO_3$), hydrated lime ($Ca(OH)_2$), magnesite ($MgCO_3$), or sodium hydroxide (NaOH) can increase the pH in the water. This will affect the solubility of many of the trace elements in the AMD, causing them to precipitate (as hydroxides, sulphides and carbonates [70]). Examples of trace elements that can be removed are copper, lead, zinc, nickel, cadmium, iron, chromium (III), and arsenic (V), while mercury, chromium (VI), and arsenic (III) are usually unaffected by the addition of a neutralising agent. [69] This method is effective and can be applied to AMD in any form, but it produces a large amount of sludge that needs to be handled and the trace elements in this sludge can be remobilised if the pH changes [70].

Passive treatment methods such as oxic/open limestone drains, anoxic limestone drains, and limestone diversion wells are all based on the AMD flowing over or through limestone aggregates. The limestone will increase the pH and cause trace element precipitation, as described above. All these methods have proven to be effective for AMD treatment, but they require maintenance to remove the produced sludge or avoid blockage of the limestone. These methods will also have a hard time removing all

the trace elements in the AMD, as limestone only increase pH to 7.5-8.0. [69, 71]

Active treatment methods are based on adding reagents regularly. Pulsed carbonate reactors add CO_2 to the AMD before neutralising it with $CaCO_3$ to increase dissolution and chemical precipitation. This is an effective and low-cost method, but it may require a second treatment step to increase the pH. Another method, biological redox control, utilizes bacteria to reduce sulphate to soluble H_2S and HS^-, which can further react with and precipitate the trace elements in the AMD. This creates a more stable sludge than with trace element hydroxides, but it requires specific conditions, such as temperatures between 5 °C to 40 °C and pH levels above 5.5, for the bacteria to thrive. Adding synthetic resins to the AMD is also an active treatment method. The toxic trace elements in the AMD are replaced by non-toxic ions and are immobilised. Adding resins is effective, but only a few are regarded commercially viable. [69] Adsorption materials remove trace elements from the AMD by adsorption, which is a phenomenon where a substance is attached to the surface of another substance, and in many cases, they can release oxides and/or hydroxides to increase the pH (olivine). This is an efficient method that produce little sludge and do not require chemical addition, but in many cases the adsorption capacity is low and the materials are expensive. [70]

When treating AMD with high element concentrations, the treatment methods mentioned above may in many cases let through water containing higher concentrations of harmful elements than what is allowed to release into the environment. This could happen when only parts of the water is in contact with the treatment material, or if the treatment material is blocked by other contaminants. In some cases, toxic trace elements are released from the treatment material through different chemical reactions. This was seen in the projects conducted by Steen [72], where chromium was released during treatment with olivine. A second treatment step, called a polishing step, can be used to remove the residues from the main treatment steps described above. The following sections describes some alternatives that can be used as polishing steps.

2.9.2 Electrochemical treatment

A method that has been used for a long time to extract trace elements from water is electrochemical treatment. Electrochemical reactions are based on the transfer of electrons between two species, also known as reduction-oxidation (or redox) reactions. Whenever such a reaction happens one species is oxidised, which means that it gives up one or several of its electrons, while the other species gain these electrons, causing it to be reduced. [16] One example of a redox reaction is shown in equation 2.9.

$$\frac{1}{2}H_{2(g)} + AgCl_{(s)} \longrightarrow H^+_{(aq)} + Cl^-_{(aq)} + Ag_{(s)} \tag{2.9}$$

Here, electrons are removed from the hydrogen atoms, and their oxidation number change from 0 to I+. Copper on the other hand gains electrons, and the oxidation number change from II+ to 0. The reactions that happen in equation 2.9 can be divided into two reactions, as shown in equations 2.10 and 2.11. In electrochemistry they are called *half-cell reactions*, and they happen at separate electrodes.

$$2\,H^+_{(aq)} + 2\,e^- \longrightarrow H_{2(g)} \tag{2.10}$$

$$AgCl_{(s)} + e^- \longrightarrow Ag_{(s)} + Cl^-_{(ag)} \tag{2.11}$$

Each of these reactions, written as reduction reactions, have a specific *standard electrode potential* or *standard reduction potential*. This is defined as the standard potential of a reaction where hydrogen gas (H_2) is oxidised [53] and describes the difference in potential between the electrode and the solution. By convention, the potential of the hydrogen reduction reaction is zero, so the reaction in equation 2.10 will have a standard reduction potential of 0 V. The standard electrode potential of equation 2.11 however is not zero, but equal to the potential difference between the electrodes, also called the electromotive force (emf). In the case of AgCl reduction, the standard electrode potential is 0.222 V. [16]

If the electrochemical cell consists of a redox reaction that does not include the oxidation of $H_{2(g)}$, the emf can be found by adding together the half-cell electrode potentials as equation 2.12 shows.

$$E_{cell} = E_{reduction} - E_{oxidation} \tag{2.12}$$

The strongest oxidants, which themselves are easily reduced, have high and positive electrode potentials. Reducing agents on the other hand have less positive or negative electrode potentials, as they are not so easily reduced themselves. The list that include the most common half-cell reactions and their standard electrode potentials is called the *electrochemical series*. A selection of this series is shown in table 2.4.

Electrolysis is a process where electricity is used to drive a redox reaction that otherwise is regarded unfavourable. A power source is connected to electrodes, which again are placed into a solution containing ionic species. The ions that exist in the solution can move freely. However, if a potential difference is applied though the addition of electricity from the power source, the ions close to the electrodes may be affected. Ions that are negatively charged or neutral species that readily give away their electrons may be oxidised at the anode, while the positively charged ions or neutral species that readily gain electrons may be reduced at the cathode. A current will move through the ions in the solution from one electrode to the other. [16] An example of a setup for electrolysis is presented in figure 2.12. If the electrodes that are used are inert, it means that they themselves are not affected by the redox reactions, but they transfer the electrons to the reactions in the solution. In some cases, the electrodes are affected by the redox reactions, causing them to dissolve into the solution. These types of electrodes are called *sacrificial* electrodes.

In the electrochemical treatment of AMD the intention is to have cations plate out onto the cathode in the elemental state or to precipitate, either by themselves or by attachment to other precipitates. Technologies that have been used to successfully treat wastewater, and have been tested for AMD as well, are electrocoagulation, electroflotation, and electrodeposition. These methods are categorised as fast, they require less or no addition of chemicals, and produce less sludge. On the other hand, they involve high initial investments to build the setup and need electricity, which can be expensive. [67]

Electrocoagulation use the concept of a sacrificial anode to produce coagulation ions. The most common anode materials are iron and aluminium, as they release multivalent ions as poly-oxyhydroxide complexes and oxides favouring electrocoagulation process. The coagulants will destabilise the contaminants in the solution by neutralising the repulsive forces, causing them to interact with each other to form larger flocs. At the cathode hydrogen gas is produced, which can transport

Table 2.4: Selected half-cell reactions from the electrochemical series. [53, 16]

Half-cell reaction	E° (V)
$HCrO_4^- + 7\,H^+ + 3\,e^- \longrightarrow Cr^{3+} + 4\,H_2O_{(l)}$	+1.37
$Cl_{2(g)} + 2\,e^- \longrightarrow 2\,Cl^-_{(aq)}$	+1.36
$Cr_2O_{7(aq)}^{2-} + 14\,H^+_{(aq)} + 6\,e^- \longrightarrow 2\,Cr^{3+}_{(aq)} + 7\,H_2O_{(l)}$	+1.36
$MnO_{2(s)} + 4\,H^+_{(aq)} + 2\,e^- \longrightarrow Mn^{2+}_{(aq)} + 2\,H_2O_{(l)}$	+1.23
$O_{2(g)} + 4\,H^+_{(aq)} + 4\,e^- \longrightarrow 2\,H_2O_{(l)}$	+1.23
$Br_{2(l)} + 2\,e^- \longrightarrow 2\,Br^-_{(aq)}$	+1.08
$NO_3^-{}_{(aq)} + 4\,H^+_{(aq)} + 3\,e^- \longrightarrow NO_{(g)} + 2\,H_2O_{(l)}$	+0.96
$Fe(OH)_{3(s)} + 3\,H^+_{(aq)} + e^- \longrightarrow Fe^{2+}_{(aq)} + 3\,H_2O_{(l)}$	+0.95
$2\,Hg^{2+}_{(aq)} + 2\,e^- \longrightarrow Hg_2^{2+}{}_{(aq)}$	+0.91
$Hg_2^{2+}{}_{(aq)} + 2\,e^- \longrightarrow 2\,Hg_{(l)}$	+0.80
$Fe^{3+}_{(aq)} + e^- \longrightarrow Fe^{2+}_{(aq)}$	+0.77
$O_{2(g)} + 2\,H^+_{(aq)} + 2\,e^- \longrightarrow H_2O_{2(aq)}$	+0.70
$MnO_4^-{}_{(aq)} + 2\,H_2O_{(l)} + 3\,e^- \longrightarrow MnO_{2(s)} + 4\,OH^-_{(aq)}$	+0.59
$O_{2(g)} + 2\,H_2O_{(l)} + 4\,e^- \longrightarrow 4\,OH^-_{(aq)}$	+0.40
$Cu^{2+}_{(aq)} + 2\,e^- \longrightarrow Cu_{(s)}$	+0.34
$AgCl_{(s)} + e^- \longrightarrow Ag_{(s)} + Cl^-_{(ag)}$	+0.22
$SO_4^{2-}{}_{(aq)} + 4\,H^+_{(aq)} + 2\,e^- \longrightarrow SO_{2(g)} + 2\,H_2O_{(l)}$	+0.16
$Cu^{2+}_{(aq)} + e^- \longrightarrow Cu^+_{(aq)}$	+0.16
$2\,H^+_{(aq)} + 2\,e^- \longrightarrow H_{2(g)}$	0.00
$Pb^{2+}_{(aq)} + 2\,e^- \longrightarrow Pb_{(s)}$	-0.13
$Ni^{2+}_{(aq)} + 2\,e^- \longrightarrow Ni_{(s)}$	-0.24
$PbSO_{4(s)} + 2\,e^- \longrightarrow Pb_{(s)} + SO_4^{2-}{}_{(aq)}$	-0.36
$Cd^{2+}_{(aq)} + 2\,e^- \longrightarrow Cd_{(s)}$	-0.40
$Fe^{2+}_{(aq)} + 2\,e^- \longrightarrow Fe_{(s)}$	-0.44
$Cr^{3+}_{(aq)} + 3\,e^- \longrightarrow Cr_{(s)}$	-0.74
$Zn^{2+}_{(aq)} + 2\,e^- \longrightarrow Zn_{(s)}$	-0.76
$2\,H_2O_{(l)} + 2\,e^- \longrightarrow H_{2(g)} + 2\,OH^-_{(aq)}$	-0.83
$Mn^{2+}_{(aq)} + 2\,e^- \longrightarrow Mn_{(s)}$	-1.18
$Al^{3+}_{(aq)} + 3\,e^- \longrightarrow Al_{(s)}$	-1.68

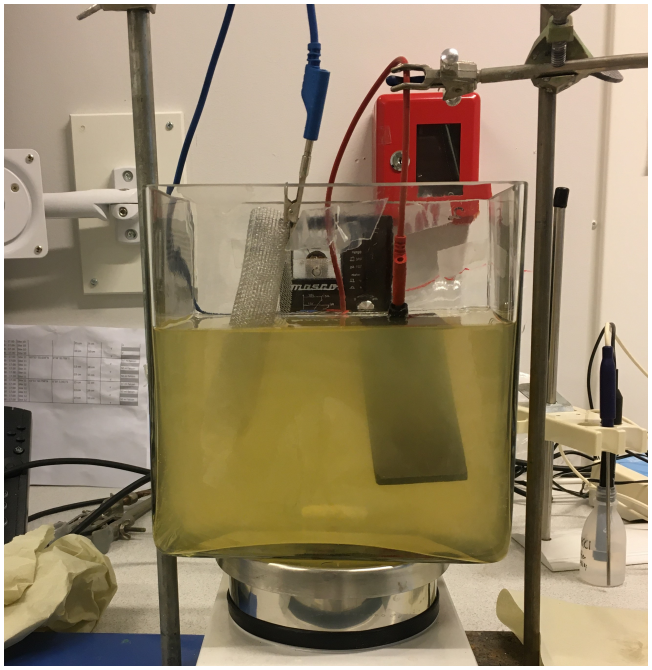

Figure 2.12: Example of setup for electrolysis. The left electrode works as the cathode where the reduction reactions happen, while the anode to the right is where the oxidation reactions takes place. The orange water contains a large amount of ions. In the back there is a power source (black box behind the electrolysis container)

the contamination-containing flocs to the surface where it can be collected and discharged, or the flocs can be removed by sedimentation. Both trace elements and sulphate can be removed by the electrocoagulation process. The concentration of coagulating ions depends on the current density, and the longer the process runs the more ions will be released into the water and the removal efficiency will increase. The removal efficiency is also determined by the affinity of the contaminants to the coagulant. [73]

The second method, electroflotation, is a process based on the electrolysis of water. The water is converted into hydrogen gas and oxygen gas as shown in equation 2.13, which will rise to the surface of the solution. The suspended contaminants in the water will float to the surface due to the rise of the bubbles, causing them to be separated from the water phase. [74]

$$2\,H_2O_{(l)} \longrightarrow 2\,H_{2(g)} + O_{2(g)} \tag{2.13}$$

Inert electrodes are normally used in electroflotation. Common anode materials are graphite and lead oxide (PbO_2) as they are cheap and easily attainable, but have limited lifetime. Over time carbon in the graphite anode is converted to CO_2, and the lead is reduced to Pb^{2+}. Platinum is a much more stable anode material, but it is very expensive to use in larger scales. The separation efficiency depends on several factors, such as bubble size, properties of the suspended contaminants, the volume ratio between bubbles and contaminants, and the retention time. Smaller bubbles have been proven to give a higher separation and flotation efficiency, as they provide a larger area for particles to attach to. [74]

Electrodeposition is a method commonly used in the industry to retrieve metals from wastewater.

Trace element cations in the solution are in this process attached to the cathode due to the reduction to their elemental form. Copper is a trace element that can be deposited to the cathode. This happens through the reaction in equation 2.14.

$$Cu^{2+}_{aq} + 2\,e^{-} \longrightarrow Cu_{(s)} \tag{2.14}$$

The deposited elements form a layer on the surface of the cathode. Here they are immobilised and that way they are extracted from the AMD. The deposition process occurs between the surface of the electrode and the solution, so the efficiency of the deposition depends strongly on the mass transfer of the solution.

Due to the limited surface area of the electrodes for attachment and expensive electrode materials, electrochemical treatment methods are not optimal for large-scale removal of high concentrations of e.g. copper, zinc, and iron. However, to treat solutions with a broad range of trace elements in lower concentrations as a polishing step electrochemical methods have in many cases proven itself ideal.

2.9.3 Adsorption on activated carbon

Activated carbon, or activated charcoal, is another cleaning medium that can be used to remove many different elements from water. It represents the treatment category *adsorption*, which is as mentioned previously a phenomenon where a substance is attached to the surface of another, usually much bigger, system. This causes a higher concentration of the given substance on the surface of the system compared to the inside, which is probably the broadest definition of what adsorption is [75, 76].

Adsorption of substances in liquids or gases onto solid surfaces happens as a result of unbalanced forces on the surface due to force fields around the ions, atoms or molecules the solid consists of. These forces can reach out into the liquid or gas and retain the ions or molecules it comes into contact with. [77] Generally, these forces are labelled *colloid interactions* or *surface interactions*. [76] The attached molecules or ions will then to a certain extent restore the balance of forces. Adsorbate is the name of the ions or molecules from the gas or liquid that is attached to the surface, while the substance they attach to is called the adsorbent. [77]

Looking at the interactions themselves, adsorption can be divided into two types; physical adsorption and chemical adsorption. Interactions due to physical adsorption depend on weak van der Walls forces. They are nonspecific which means that they can occur between any substance and solid surface, and the layer of adsorbed phase can be several molecules thick. Chemical adsorption on the other hand is interactions caused by the adsorbent surface and adsorbate exchanging or sharing electrons, which makes them a lot stronger. In addition, the interactions are more specific, and the adsorbed phase is usually only one molecule in thickness. [77]

Activated carbon (AC) is an adsorption medium that mainly consists of carbon, together with small amounts of hydrogen (H), nitrogen (N), sulphur (S) and oxygen (O). To make AC, two steps are required. In the first step, called the carbonization process, a carbon rich material is broken down through pyrolytic decomposition in an inert atmosphere. [77] Because the main requirement for the material is a high carbon content, many different precursor materials can be utilized. Traditionally coal, lignite or wood were used [78, 68]. These days researchers are testing many other materials,

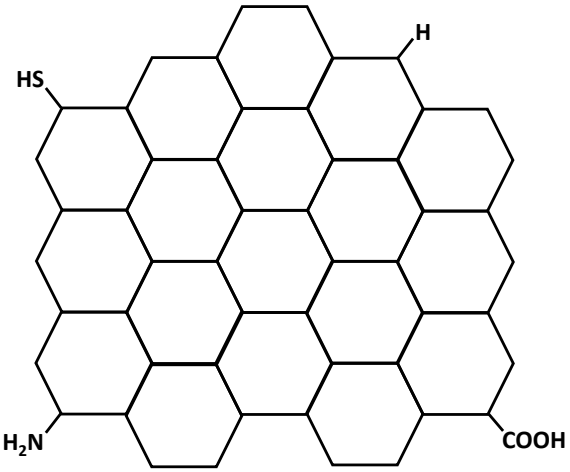

Figure 2.13: Examples of possible functional groups on activated carbon.

such as Jackfruit peel waste [78], seeds from Black Sapote [68], residues from the plant Agave Tequilana [79], and coconut shells [80]. Stacks of flat, aromatic carbon sheets that make up the AC structure are formed during the carbonization step, and because of irregularity of the sheet stacking pores appear all over in the structure. A problem is that these pores often are clogged by e.g. dust. Therefore, the second step is the activation of the carbon material, where the goal is to produce AC with as many free pores as possible. This gives rise to an extremely high surface area of the AC. [77]

The porosity and the high surface area are the two properties that influences the adsorption capacity of AC the most. However, it can also be influenced by the chemical structure of the surface. On the edges of the aromatic sheets, the valency of the carbon atoms may be unbalanced, which gives rise to interactions between the carbon atom and other atoms such as O, H, N, and S. These interactions create surface groups that can react with other substances. The oxygen, hydrogen and nitrogen that already exists in the AC can also produce surface groups that can interact with substances they come in contact with. Surface groups with oxygen are often regarded as the most important groups, as they influence the polarity, acidity, and chemical reactivity of the surface. Carbon-oxygen surface groups are produced through the oxidation of unsaturated carbon double bonds by oxygen. These groups can be either acidic or nonacidic, where the acidic ones are polar and may be carboxylic groups or lactones. In water, these acidic groups will be ionized through the reaction

$$\mathrm{C{-}COOH} \longrightarrow \mathrm{C{-}COO^- + H^+} \tag{2.15}$$

as the proton is released into solution. By releasing protons from these groups, they obtain a negative charge. The protons and cations in the solution will compete for these negative sites for adsorption. When pH is low, there is a large amount of protons in the solution, making the sites less available for other cations. However, when pH increases there are less protons in the water, and the negative sites become more available to adsorption by other cations. [77]

Due to the high porosity, high surface area, fast adsorption kinetics [80], and many different functional groups on the surface, AC is an ideal and very versatile adsorbent, with a wide range of target

compounds. Among others, it is used in the purification of air, in pharmaceuticals, and to remove contaminants from wastewater [77]. It is also possible to modify the AC to target specific pollutants. Different modification methods may be acid treatment, base treatment, impregnation treatment, treatment with ozone, surfactant treatment, plasma treatment, and treatment with microwaves [81, 77]. When modifying activated carbon, it is possible to add or remove functional groups, which will change the chemistry of the surface drastically [82]. Also the precursor material may decide which contaminants the AC is most effective on [81]. But, the choice of precursor material is often largely dependant on availability, cost, and purity [78], and AC may be very expensive alternative, especially as a main treatment step in the treatment of heavily contaminated water. However, in a polishing step much lower concentrations are required to be removed, which lowers the amount of AC needed and prolongs its lifetime.

Granular activated carbon (GAC) is a common variant of activated carbon. As the name suggests, the material is on the form of granulates, which are relatively large grains of a few mm. By using GAC instead of e.g. powdered activated carbon (PAC), a lower hydrodynamic resistant is observed, and it is easier to regenerate. When it is saturated, it can be treated with steam and reused. It is more expensive than the powdered type, but is much more suitable for water treatment. Fibrous activated carbon (ACF) is also suitable for water treatment, but is a much more expensive alternative than GAC. [77]

3 Materials and methods

Absolutely all the water samples in this thesis, both from the natural waters (the Killingdal stream, the tunnel, the Trondheimsfjord) and from the experiments at the laboratory have been filtered with a 0.45 µm *polyethersulfone membrane* filter. In addition, all the samples described, both water samples and sediment samples, were analysed with either an *ELEMENT 2* from Thermo Fisher or an *Agilent - 8800 ICP-MS Triple Quad* at NTNU, either by or with the help of Syverin Lierhagen. In total, 37 elements were analysed for in freshwater samples, i.e. samples from the Killingdal stream, inside the tunnel, and experiments from the laboratory. 28 elements were analysed for in seawater samples, i.e. seawater samples taken from land, sediment samples, and water samples from 1 m above the sediments. Which elements were analysed for in the different categories are shown in table 3.1. All the results were reported with corresponding RSD values. The RSD value represents the uncertainty in the value it corresponds to, and represents how closely repeated measurements agree with each other, based on three scans, and it counts for approximately 90 % of the total uncertainty of the ICP-MS analyses.

3.1 Monitoring of the Killingdal stream and coastal water, and sediments in the Trondheimsfjord

3.1.1 Water from the Killingdal stream

The Killingdal stream is a small stream that runs from the woods in the left part of the picture in figure 3.2. From the woods, it is guided under a car road, approximately two meters under the ground through pipes. On the other side of the road, the stream exits the pipes and runs down to the fjord, down a man made path of concrete. The samples taken in the Killingdal stream were collected in a point where two smaller streams met, right before the stream entered the pipes below the road. A picture of this location is presented in figure 3.1. The location of this sampling point in comparison to the Killingdal tunnel and the fjord can be seen in figure 3.2, where the Killingdal stream sampling point is indicated by the red ring furthest to the left. The frequency of how often the samples were taken varied, depending on the weather and season, but there were usually not

Table 3.1: Elements that were analysed for at the NTNU laboratory. The x in a cell means that this element was analysed for in the given category.

	Al	As	Ba	Ca	Cd	Ce	Co	Cr	Cu	Dy	Er	Eu	Fe
Freshwater	x	x	x	x	x	x	x	x	x	x	x	x	x
Seawater	x	x	x	x	x	x	x	x	x	x	x	x	x
	Gd	Hg	Ho	K	La	Li	Mg	Mn	Mo	Na	Nd	Ni	P
Freshwater	x	x	x	x	x	x	x	x	x	x	x	x	x
Seawater	x	x	x		x			x	x		x	x	x
	Pb	Rb	S	Si	Sn	Sr	Ti	V	Zn	Br	Cl		
Freshwater	x	x	x	x	x	x	x	x	x	x	x		
Seawater	x			x	x		x	x	x				

Figure 3.1: Picture of the location where the samples were taken from the Killingdal stream. One of the two smaller parts of the stream can be seen running down from the upper left corner of this picture. The point where the two streams meet and where the samples are taken is in the bottom left corner. In the right part of the picture, the road the river flows beneath is shown.

Figure 3.2: The Killingdal area seen from above. The sample points of the Killingdal stream and the Trondheimsfjord are marked with red circles. The entrance to the tunnel is marked with a blue circle. The map was found at NVE Atlas' web page [83].

(a) **(b)**

Figure 3.3: Pictures of where the coastal water samples were taken. Figure 3.3a show how the wall looks like, and figure 3.3b show the effluent from the Killingdal tunnel seeping out into the fjord.

more than 1-2 weeks between each sampling. Sampling was carried out according to the standard NS-EN ISO 5667-6:2016 [84], and preservation and handling was in accordance with the standards ISO 5667-3:2018 [85] and NS 4784 [86]. In short, the samples were extracted from the stream with a polypropylene syringe. First the syringe was conditioned to the water by rinsing three times with the stream water, and then the syringe was filled with the sample. Then, a filter was placed on the tip of the syringe, and a part of the sample was filtered and used to rinse the polypropylene ICP-MS tube three times before a 10 mL filtered sample was added. For preservation, the samples were added ultrapure nitric acid (HNO_3) and kept either in a stand in the Killingdal tunnel or at the NTNU laboratory in a refrigerator at 4.6 °C. Comments were also made if there were low or no water flow in the stream.

3.1.2 Coastal water from the Trondheimsfjord

The sea samples were taken at a point with diffuse leakage of tunnel water into the fjord, marked with the bottom red ring in figure 3.2, approximately 30 m from the entrance to the Killingdal tunnel. Here, the border between land and water is a sloping wall of big rocks, as can be seen in figure 3.3a. During the winter these rocks are slippery, but during the summer they are dry and safe to climb on. The sampling point was recognised by the relatively low growth of seaweed and the orange colour of the rocks. In addition, when the water levels were high enough, there was a visible effluent of tunnel water into the fjord, as figure 3.3b shows. Samples were taken from land, and sampling usually happened when the sea level was approximately in the middle of high tide and low tide. This location could be recognised by the level where there was larger amounts of seaweed and where there was an effluent seeping into the fjord, as shown in figure 3.3b. The frequency of sampling varied, depending on weather, season and sea level. Exactly the same sampling and preservation methods were used as described in section 3.1.1. This was in accordance with the standard ISO 5667-9:1992 [54] which covers the sampling of marine waters, and standards ISO 5667-3:2018 [85] and NS 4784

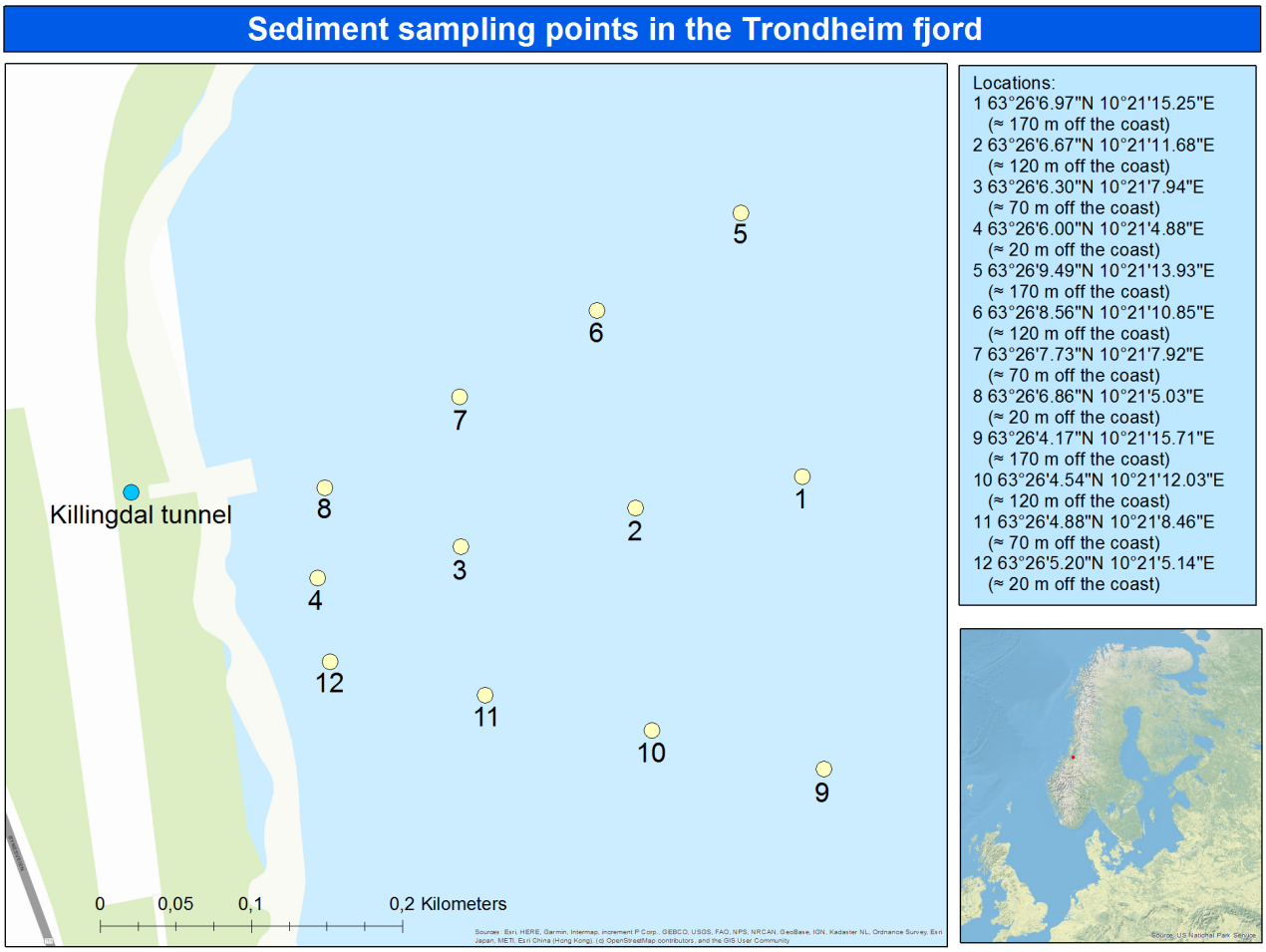

Figure 3.4: Overview picture of the locations where the sediment samples were taken. The blue marker furthest to the left indicates the entrance to the Killingdal tunnel, the rest are the sediment sample points (1-12). The exact sample coordinated are presented in table B.1 in appendix. This map is created in the GIS program ArcGlobe [87].

[86] which covers the preservation and handling of water samples.

3.1.3 Sediments in the Trondheimsfjord

The sediments from which the samples were extracted were brought to the surface from the bottom of the Trondheimsfjord by a box corer at the NTNU research vessel Gunnerus. Two samples were taken at each sample point, shown in figure 3.4, and the sampling was carried out according to the standard NS-EN ISO 5667-19:2004 [56]. In short, the content of the box corer was released into a plastic box. From this sediment pile, the two samples were taken by scraping the top part of the sediment into plastic containers. As far as possible, only the parts of the sediments that had not been in contact with the box corer were sampled, to avoid contamination from the interior of the metallic box corer. The sediment samples were kept in a freezer at $-27\,^{\circ}\mathrm{C}$ until analysis.

To be able to analyse the sediment samples with ICP-MS, they first had to be freeze dried and decomposed. Freeze drying was carried out with the frozen sediment samples to remove the water. The samples were placed inside a Freeze Dryer ALPHA 1-4 LDplus/ALPHA 2-4 LDplus, and dried for approximately 24 hours at 0.92 mbar and $-21\,^{\circ}\mathrm{C}$. The digestion procedure was initiated by

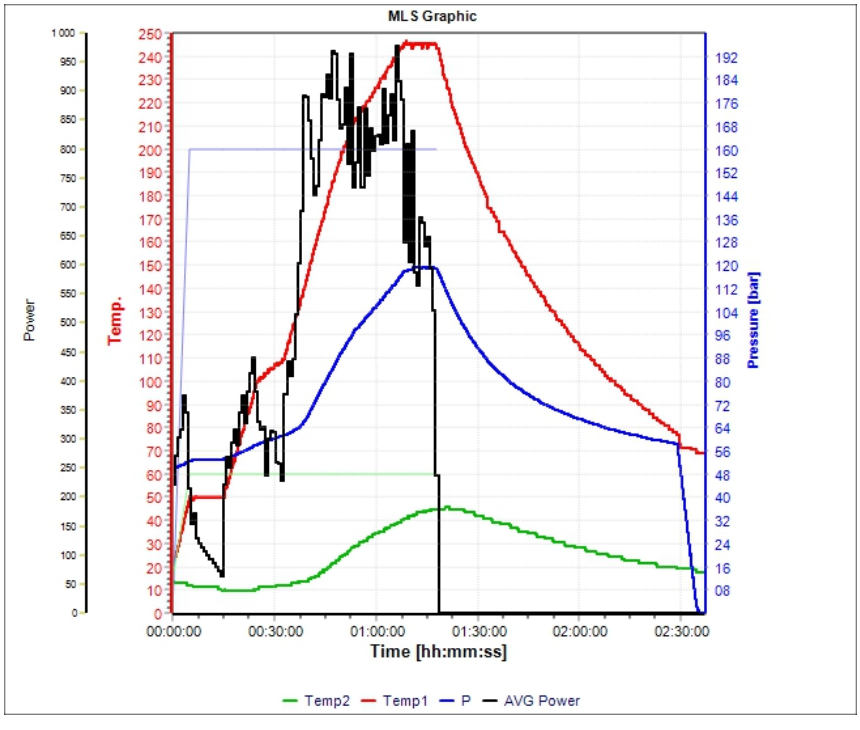

Parameter

```
Signature name  :
Signature date  :
Signature func. :
Operator        :Administrator
Date            :17.01.2020
15:37:58
Method filename
:Stand-profile-245C-10-min-oper
Create run      :Administrator
Microwave Power :pulse
Load pressure   :50.0 bar
Release temp.   :78.0 °C
Release pressure:10.0 bar/min
Cooling         :ON
Auto open       :OFF
Cooling on Temp.:40.0 °C
Ground load     :300 30 2
Ventilation time:01:18:52
Rotor           :40 positions
Vessel-Type     :18ml teflon and
quarts
```

Figure 3.5: Procedure used for operating the MLS Microwave to break down the different compounds in the sediment samples. The exact pogram used is shown in appendix B.3.

transferring a subsample of 250-350 mg sediment from each sediment sample to a teflon digestion tube. Two different reference materials were also used, one for seawater sediments and one for freshwater sediments. Three parallels of approximately 100 mg each from both references were transferred to digestion tubes. The exact weight of each subsample and reference sample is presented in table B.2 in appendix. Each digestion tube was then added 9 mL 50 % HNO_3. Three extra blanks, i.e. tubes with only 9 mL HNO_3, was added to the batch. The sediment samples, reference material and blanks were then placed into a an UltraCLAVE from Milestone, following the specifics displayed in figure 3.5. After the ultraclave, the samples were diluted to between 107 and 112 g with Milli-Q water and transferred to polypropylene ICP-MS tubes, to be analysed by ICP-MS at NTNU. The exact weight of the diluted samples is presented in table B.2 in appendix.

3.1.4 Bottom water from the Trondheimsfjord

Together with the sampling of sediments, in every other sediment sampling point two deep-water samples were taken, one unfiltered and one filtered. A rosette sampler with CTD was lowered down to approximately 1 m above the sediment surface, closed to contain the water, and brought to the surface, while the CTD measurd the conductivity, temperature and depth. From the water in the Rosett sampler, water samples were extracted according to the standard ISO 5667-9:1992, and the same methods for sampling and preservation as descibed in section 3.1.2 were used. The addition of nitric acid was carried out at the laboratory at NTNU, not at the vessel.

Before delivering these samples for analysis, the unfiltered samples were filtered. The procedure was initiated by emptying the polypropylene ICP-MS tube into a clean glass container. Afterwards, the sample was transferred into a polypropylene syringe and a filter was put at the tip. The filter was

then rinsed with the sample by squeezing through 15 droplets two times. These 15 droplets were also used to wash a new polypropylene ICP-MS tube. In the end, the remaining sample was transferred through the filter and into the new ICP-MS tube.

A summary of all the monitoring samples are presented in table D.1 in appendix.

3.2 Setup for electrochemical treatment of water in the lab

The setup used in the laboratory to treat the water from the tunnel at Killingdal is illustrated in figure 3.6. This is a general setup that was used for all the experiments in the lab, in different variations.

The same procedure was used for all the experiments, except the test of the setup with two aluminium electrodes. 3 L of the water that is supposed to be treated is poured into the glass container. A first sample is extracted with a polypropylene syringe before the experiment is started. Then, the magnetic stirrer is turned on at 400 rounds per minute (rpm) and the voltage is applied. A sample is extracted every 20 minutes until the experiment has been running for 80 minutes, i.e. at 20 minutes, 40 minutes, 60 minutes and 80 minutes, to check for potential changes in the composition of the water. Between each time new water is tested, new aluminium electrodes are made and carbon electrodes are rinsed with Milli-Q water.

Water from Killingdal is brought to the laboratory at NTNU in closed 10 L polyethylene containers the same day as the experiment is carried out. Two types of water are collected from Killingdal; *Cleansed* water which means that it has recently been transported through the treatment facility Trondheim Municipality has in the tunnel, and *Not cleansed* water which means that it has not been transported through this facility recently but is collected from approximately 20 m inside the tunnel.

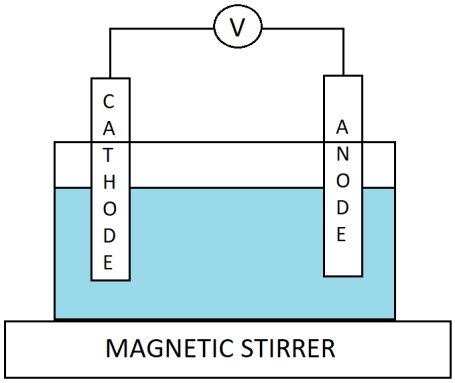

Figure 3.6: Graphical representation of the setup for electrolysis of water from Killingdal. The electrodes are connected to a voltage source (V), and the blue area is the water that is being treated.

3.3 Preliminary test of setup with two aluminium electrodes

The setup for the electrochemical treatment with aluminium electrodes was built according to figure 3.6. The aluminium electrodes were made by cutting out smaller pieces of approximately 200 mm × 15 mm from a large aluminium wire fence. For this, a steel scissor was used. The anode was placed in the bottom of a glass container as a flat rectangle. As the cathode, a piece of the aluminium wire fence was shaped into a 200 mm long cylinder, and placed vertically down into the glass container. Figure 3.7 shows the finished setup.

Electrochemical treatment with aluminium electrodes was tested two times on *artificial* water in the laboratory before water from the tunnel at Killingdal was tested. The first test was performed with a 0.07 M NaCl solution. During this test, the solution was stirred for 30 minutes before the electrodes were examined. The second test was performed with a 0.01 M $ZnCl_2$ solution. This time the solution was stirred for 1 hour before the electrodes were examined. pH was measured before the electrolysis was started, and right after the electrolysis was stopped. The pH meter was calibrated with pH solutions of pH 4 and pH 7.

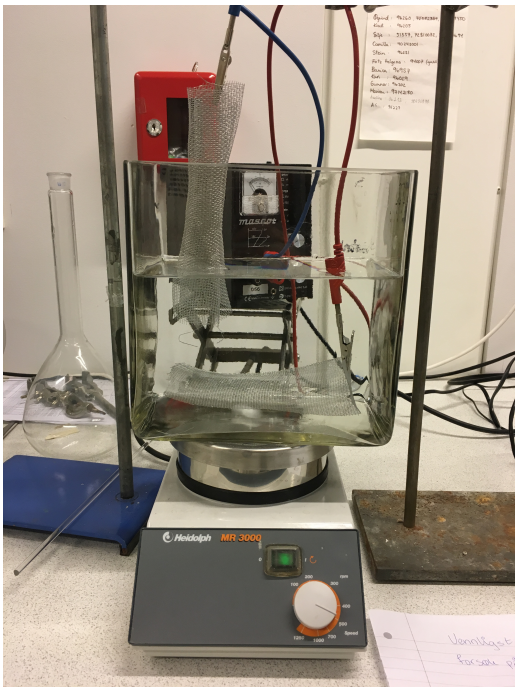

Figure 3.7: Finished setup used to test how the aluminium electrodes work. Here, the flat electrode in the bottom is the anode, and the cylindrical electrode is the cathode.

3.4 Electrochemical treatment of water from Killingdal in the lab

After testing that the setup function as planned, the treatment of water from Killingdal could start.

3.4.1 Aluminium electrodes

In the laboratory, the same setup was used as described in section 3.2. The finished setup is shown in figure 3.8a.

Three different experiments were run with the water from Killingdal with the same setup as described in 3.3 and procedure that was followed is the same as described in section 3.2. The first experiment used the *Cleansed* water with a voltage of 1 V. Also the second experiment used the *Cleansed* water, this time with a voltage of 1.5 V. In the third experiment, the *Not cleansed* water was used, with a voltage of 1.5 V.

3.4.2 Blank with aluminium electrodes

A blank experiment, i.e. an experiment with exactly the same setup as used for the water from Killingdal in section 3.4.1 but with a known solution, was performed to test the release of aluminium ions into the solution from the electrodes (specifically the anode). The known solution used was 0.0001 M (10^{-4} M) NaSO4. Two experiments were run, one with 1.5 V voltage applied and one without. The same procedure as in section 3.2 was used. The setup is shown in figure 3.8b.

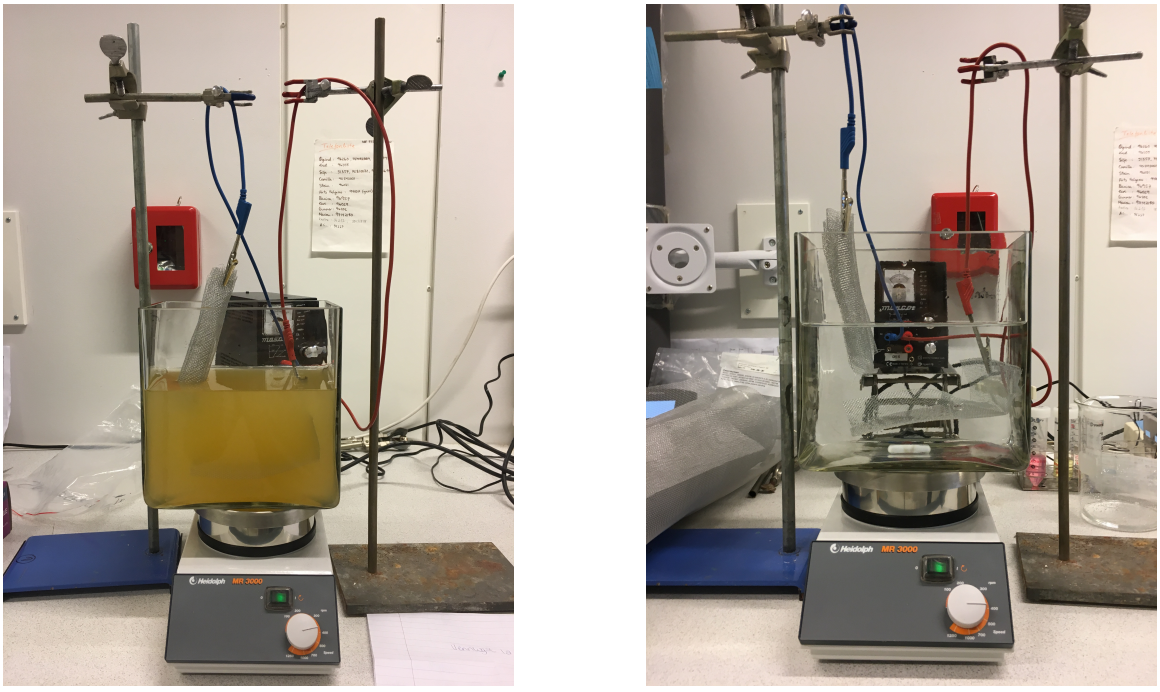

(a) **(b)**

Figure 3.8: Finished setup used for electrolysis of water from Killingdal. In figure 3.8a the cylindrical electrode to the left is the cathode, while the flat electrode in the bottom right is the anode and in figure 3.8b is the setup for blank test of aluminium electrodes.

(a)

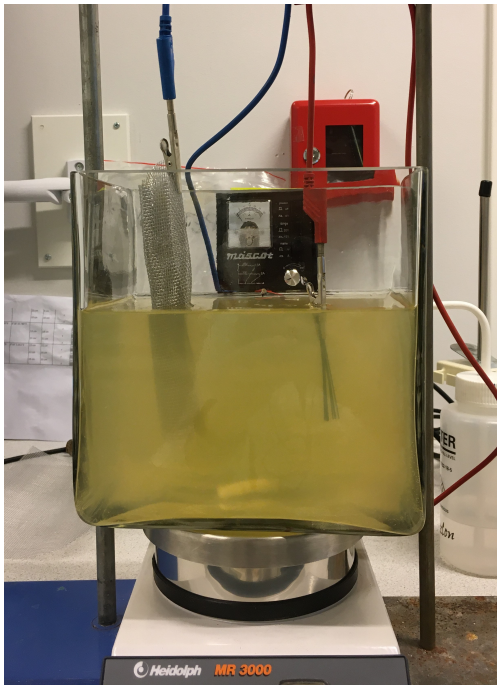

(b)

Figure 3.9: Experiment with aluminium cathode and graphite from a mechanical pencil anode. Figure 3.9a show the attachment of graphite to the alligator clip. Figure 3.9b shows the setup.

3.4.3 Aluminium cathode and mechanical pencil graphite anode

A test was performed on graphite from a mechanical pencil (STAEDTLER Mars micro carbon 0.7 HB) to see if the setup could work with a graphite anode. *Not cleansed* water from Killingdal was used in this test. *Cleansed* water was not used, as the treatment facility operated by Trondheim Municipality was not running at the time the water was collected. The nine graphite sticks were attached to the alligator clip as shown in figure 3.9a, and connected as the anode. In figure 3.9 both the graphite sticks electrode and the setup are depicted. The cathode was still a cylindrical shaped piece of aluminium wire fence, as in the previous experiments. The experiment was carried out as explained in section 3.2 with a voltage of 1.5 V. Only 1.5 V was used in this and the following experiments, as there was not observed any significant changes in the trace element removal during the experiments with aluminium electrodes at 1.0 V and 1.5 V. In addition, the pH of the water was measured before the experiment was started and right after the experiment was finished. The pH meter was calibrated with pH solutions of pH 4 and pH 7.

3.4.4 Aluminium cathode and cylindrical carbon anode

For these experiments, the same equipment setup was used as in figure 3.7. A cylindrical shaped piece of aluminium wire fence was still used as the cathode. The anode was a longer cylindrical carbon stick with a piece of metal on top. This particular electrode was bought at www.fybikon.no, it is 90 mm long and 6 mm in diameter. In figure 3.10 both the round carbon electrode and the setup are depicted. For this setup, the effect on both *Cleansed* and *Not cleansed* water from Killingdal was tested. The experiment was carried out as described in section 3.2, and pH was measured before and after the electrolysis. The pH meter was calibrated with pH solutions of pH 4 and pH 7. After

(a)

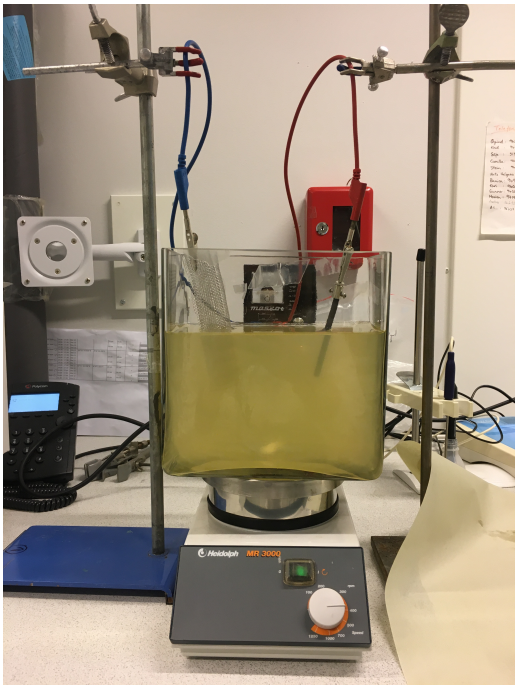

(b)

Figure 3.10: Experiment with aluminium cathode and cylindrical carbon anode. Figure 3.10a shows the cylindrical carbon electrode. Figure 3.10b shows the setup.

being used, the carbon electrode was rinsed with Milli-Q water and stored in the plastic bag it was delivered in.

3.4.5 Aluminium cathode and flat carbon anode

To perform this experiment, the setup from figure 3.7 was used. Instead of the flat aluminium anode, a flat carbon electrode from www.lekolar.no with the measurements 125 mm × 50 mm × 6 mm was used. The flat carbon electrode and the complete setup are shown in figure 3.11. Also here, both *Cleansed* and *Not cleansed* water from Killingdal were tested. The procedure was the same as described in section 3.2, and the pH of the water was measured both before and after the experiment. The pH meter was calibrated with pH solutions of pH 4 and pH 7.

3.4.6 Cylindrical carbon cathode and flat carbon anode

The experiments with the carbon electrodes were conducted with the same setup as the electrolysis with aluminium electrodes in figure 3.7, except that the electrodes were changed from aluminium to carbon. As the carbon electrodes, the cylindrical electrode from section 3.4.4 and the flat electrode from section 3.4.5 were used. The cylindrical carbon electrode was connected as the cathode and the flat carbon electrode as the anode, similar to the original setup for the aluminium electrodes. The complete setup is shown in figure 3.12. As the previous experiments, the procedure was carried out as described in section 3.2, and the pH was measured before and after the experiment was conducted. The pH meter was calibrated with pH solutions of pH 4 and pH 7.

A summary of all the experiments with electrochemical treatment are presented in table D.2 in appendix.

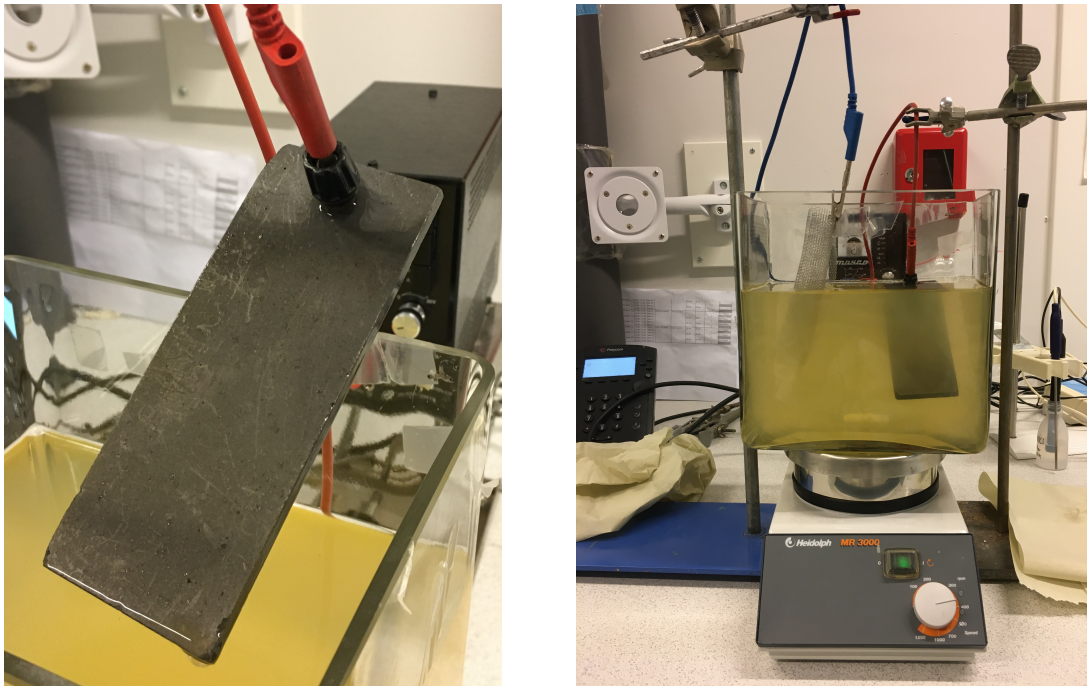

(a) **(b)**

Figure 3.11: Experiment with aluminium cathode and flat carbon anode. Figure 3.11a shows the flat carbon electrode. Figure 3.11b shows the setup.

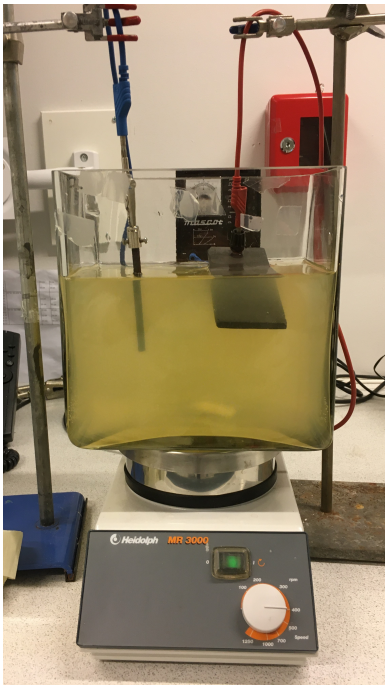

Figure 3.12: Setup for electrochemical treatment with two carbon electrodes.

3.5 Treatment of water from Killingdal with activated carbon

Activated carbon was also tested for its abilities to remove the contaminations from the water at Killingdal. The method was tested on site in the tunnel at Killingdal in a setup made by the workshop at NTNU. Figure 3.13 shows both the graphical setup (3.13a) and the actual setup used on site (3.13b).

The experiment was initiated by filling the bottom of the test pipes with gravel to avoid the escape of activated carbon out of the pipe or blockage of the valve. This gravel was rinsed three times, with 7 L *Not cleansed* water each round (in total 21 L of water). A sample was then taken of the *Not cleansed* water to know what is in the water the gravel is rinsed with. Another sample was taken of the last water to flow through the pipe after three rounds of rinsing, i.e. after approximately 21 L, to see if the gravel released any elements into the water or removed any elements from the water. After this, 4 scoops of activated carbon of the brand *SUPER KULL Chemviron* 0.4 mm to 1.4 mm was added to the test pipe. Each scoop contained approximately 55 g of activated carbon, which gives a total of 220 g of activated carbon. Further, approximately 7.6 L *Not cleansed* water was poured into the pipe. The pipe was left alone for a few minutes to let the activated carbon sink to the bottom before continuing with the rest of the experiment. The complete setup with gravel, activated carbon and water is shown in figure 3.14.

The valve was then opened to let water flow through the treatment agent and out of the pipe. One sample was taken of the water exiting the valve when approximately 3.8 L had flown out of the pipe and one was taken when all of the water had flown out of the pipe, which is equal to a volume of 7.6 L. When the pipe was empty, the valve was closed and approximately 7.6 L of new *Not cleansed*

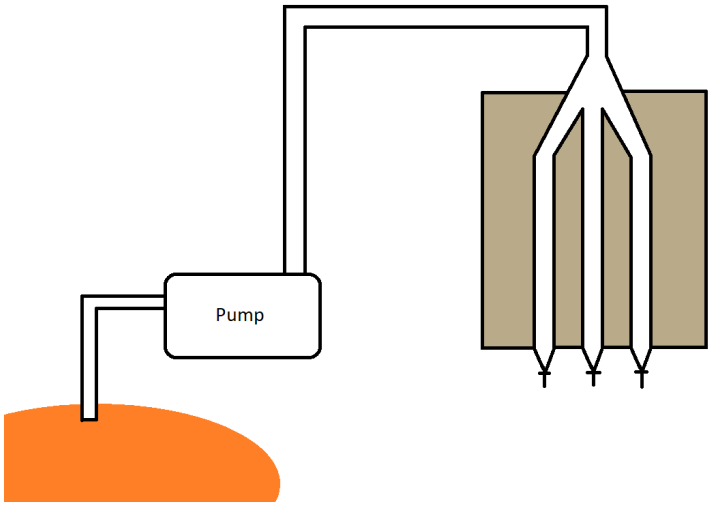

(a)

(b)

Figure 3.13: Removal efficiency of the trace elements in focus by activated carbon was tested on site at Killingdal. Figure 3.13a shows how the setup was initially planned to be. Figure 3.13b shows what the actual setup used at Killingdal looks like.

Figure 3.14: Activated carbon on top of gravel in the pipe setup at Killingdal.

water was used to refill the pipe. The pipe was again left alone for a few minutes to let the activated carbon sink, then the valve was opened to again let water flow through the treatment material. When all of this volume had flown through the pipe, a third sample was taken of the last water escaping the valve.

A summary of all the equipment used in both the monitoring program and the treatment experiments is presented in table D.3 in appendix.

3.6 Statistical analysis

In some cases it was necessary to perform some statistical analyses of the result concentrations. When investigating the trends of the sediment samples or the impact of the gravel on the activated carbon adsorption results, means of different groups were to be compared. At first, it is necessary to check the normality of the data set, to see how the distribution of the concentrations is and to be able to determine which statistical analysis method to use. For this, a Shapiro-Wilk analysis was performed, and the result whether a data set was normally distributed or not was obtained. A simple diagram that can be used to choose the appropriate statistical analysis to use further is presented in table 3.2.

In the case of gravel rinsing, it was necessary to check if the element concentrations before and after rinsing were significantly different and therefore could impact the further results. Since the data set had a non-normal distribution, it was decided to use the Mann Whitney-U test. The null-hypothesis defines the relationship between the two groups, and is that they are not different. A Mann Whitney-U test will then provide a number indicating the probability of this statement, which is the p-value. If the p-value is bigger than 0.05, which is a conventional limit, then the probability that the null-hypothesis is true is high enough for it to remain. However, if the p-value is below 0.05, the null-hypothesis is rejected, and the probability that these two groups are different is significant. When comparing sediment concentrations in different distances from shore, a Kruskal-Wallis H test was used, as there were four different distances involved and the concentrations had a non-normal distribution. As for the Mann Whitney-U test, the means for each group are compared, to see if they are significantly different or not. The null-hypothesis is that they are not different, and if $p > 0.05$ the probability of this being true is high, but if $p < 0.05$, the null-hypothesis must be rejected.

In some cases it was also interesting to do a correlation analysis, to see if there were any relationship between the different elements. From this, a number between 1 and -1 is obtained for each pair of elements investigated. If the number is 1 or close to this, it indicates a high positive correlation between the elements, i.e. when one of them increases in concentration, so does the other one. When -1 or close to it is obtained, it indicates a negative correlation between the elements, which tells us that when one element increases in concentration, the other one decreases. A number of around zero indicates no correlation. The closer to 1 or -1 the correlation value is, the stronger the correlation is. A larger data set will give a more accurate representation of the true correlations than a small data set, as it will even out variations and outliers.

Table 3.2: Overview of statistical methods used to compare means, and the different requirements that must be met to use them.

	Normal distribution	Non-normal distribution
Compare 2 groups	Student's t-test	Mann Whitney-U test
Compare 3 groups or more	ANOVA	Kruskal-Wallis H test

4 Results and discussion

In total, the freshwater samples were scanned for 37 elements and seawater samples were scanned for 28 elements. Out of these, eight trace elements were selected to be the main focus of the following discussion. These eight elements are iron, chromium, nickel, copper, zinc, arsenic, cadmium, and lead. They were chosen due to their abundance in the water at Killingdal and their potential heath risk for aquatic organisms when released into the Trondheimsfjord. In addition, in some parts of the discussion, aluminium, calcium, sulphur and lithium concentration have been investigated. Some of these elements are essential to life, but can be toxic in high concentrations. Others are non-essential, and can be toxic even in very small concentrations. Investigation of iron was based on the considerable amounts and the potential clogging it can cause in a treatment plant. A decision was made to not include mercury in the focus of this thesis. It has not been a major focus for Trondheim Municipality as previous monitoring of the area has shown that the mercury concentrations are low [88]. In addition, is has been hard to analyse, especially in the fjord, so the data may not be reliable and in some cases it was not possible to get results at all. All results are reported with three significant digits, and all the raw data from ICP-MS are presented in appendix O.

4.1 Monitoring of the Killingdal stream

In total, the Killingdal stream was sampled 18 times from 11.10.2018 until 12.11.2019. The results from the analyses of these samples are presented in table 4.1, with the date they were sampled and cells coloured according to the corresponding class of conditions from table A.1 in appendix. The concentrations with the RSD values are presented in table E.1 in appendix.

When processing the results from the Killingdal stream it became visible that one sample had extremely high concentrations compared to the other samples. This particular sample was taken on 31.01.2019 and showed between a 200 % (As) and 190 000 % (Cd) increase in concentration compared to the second highest value for seven out of the eight trace elements focused on. As table 4.1 shows, in the case of copper, zinc and cadmium this sample contained concentrations far above the lower limit for class V, and for nickel and lead the concentrations were well within the limits of class III. It is hard to conclude why this sample had so high concentrations. It could be due to a specific pollution incident shortly before sampling, or contamination of the sample from the syringe, filter or other equipment. All potential contamination sources and efforts made to avoid them are discussed later, in section 4.7. The week prior to this sampling the temperature had consistently been below $-4\,^{\circ}\mathrm{C}$, and there had not been any precipitation or massive snow melt to transport these contaminants to the stream. Comments made during the sampling mention that the water flow in the stream was very low this day. The syringe could have come in contact with sedimented contaminants, that were resuspended and possibly dissolved, causing the high concentrations measured. Another explanation could be that snow from the road had recently ended up in the stream and contaminating it. As this sample would not prevent a good representation of the data, it was decided to exclude this sample from graphs presenting the trends over the year.

By investigating table 4.1 it is evident that the Killingdal stream is not heavily contaminated by the trace elements in focus. This conclusion is based on the large amount of class I (*Background*) and class II (*Good*). However, only arsenic had the majority of its concentrations in the *Background* class

Table 4.1: Concentrations of the trace elements in focus in the Killingdal stream from 11.10.2018 until 12.11.2019. The unit is µg/L for all the concentrations. The colours are based on the classifications in table A.1 in appendix. Iron does not have any classifications.

Date	Fe	Cr	Ni	Cu	Zn	As	Cd	Pb
11.10.2018	33.6	0.209	0.639	3.34	8.07	0.0783	0.0102	0.0231
12.12.2018	54.7	0.456	1.22	4.36	13.3	0.0876	0.0181	0.103
17.12.2018	18.0	0.261	0.558	2.32	4.34	0.0673	0.00704	0.0292
18.01.2019	21.6	0.336	0.580	2.54	4.39	0.0546	0.00965	0.0315
31.01.2019	2250	0.262	29.9	6710	9650	0.314	34.3	4.36
07.02.2019	24.0	0.221	4.59	2.46	5.24	0.0433	0.00785	0.0386
02.03.2019	57.3	0.317	0.591	3.32	9.43	0.0657	0.0139	0.0757
05.03.2019	18.9	0.232	0.553	2.35	5.48	0.0449	0.00973	0.0219
22.03.2019	38.1	0.328	0.503	2.40	7.87	0.0294	0.00897	0.0555
24.05.2019	7.22	0.138	0.480	2.17	2.51	0.129	0.00292	0.00632
28.05.2019	11.4	0.219	0.552	2.38	4.48	0.0687	0.00796	0.0175
03.06.2019	20.8	0.273	0.521	2.51	4.43	0.0902	0.0107	0.0280
09.06.2019	26.7	0.291	0.512	4.13	5.52	0.0371	0.0111	0.0435
12.09.2019	9.70	0.193	0.481	2.62	2.32	0.0471	0.00818	0.00675
19.09.2019	77.2	0.418	0.652	3.76	6.64	0.0795	0.0159	0.0860
02.10.2019	119	0.409	0.647	4.43	8.79	0.103	0.0148	0.139
18.10.2019	11.8	0.180	0.646	2.56	2.55	0.0489	0.00811	0.0177
12.11.2019	16.9	0.203	0.665	2.88	3.61	0.0528	0.00951	0.0227

I. The rest had concentrations in class II, which may indicate that there is a small contamination of trace elements, but in such a small extent that it will not cause any harm to the living organisms. It also appears that due to the low concentrations in the Killingdal stream, this is not a major source of contamination into the Killingdal tunnel on its own. But, when leaking through the soil above and into the tunnel, it might mobilise the trace elements present, causing them to be transported into the tunnel water.

To check if there were any trends for the element concentrations in the stream, the concentrations in table 4.1 were normalised for each element based on the average concentration of that particular element. The graphs in figure 4.1 show the trends for the normalised trace elements concentrations. From this figure it appears that the trends of several elements are similar to each other. For most elements the first sampling point, 11.10.2018, is close to the average concentration. Then the second sample taken two months later shows a higher concentration than in October. After this the concentrations go down and stay around the average, from 17.12.2018 to 07.02.2019. A peak is then observed during the early spring of 2019. Arsenic, represented by the green line, peaks during the early summer. A new increase of concentration between 12.09.2019 and 02.10.2019 is observed, before it decreases again the 18.10.2019.

It appears as the highest concentrations are measured during the winter and fall, as concentrations measured 12.12.2018 and 02.10.2019 are among the highest and the ones in between are lower. These are periods where the water flow in the river is most likely high due to precipitation of rain and

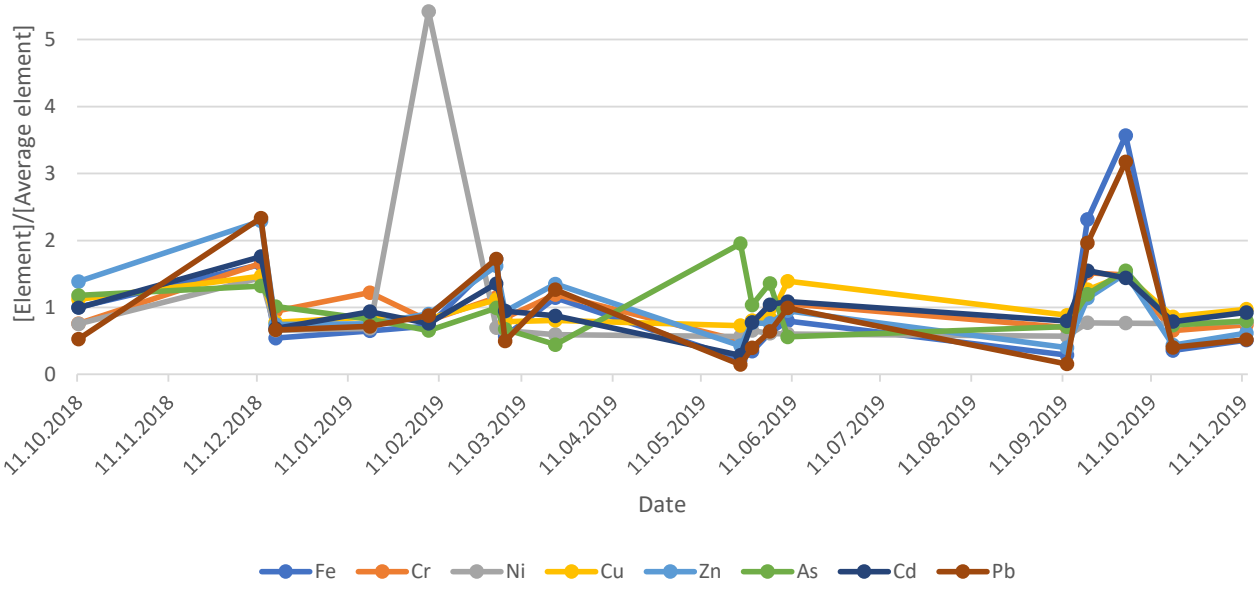

Figure 4.1: Trends for the trace elements in focus in the Killingdal stream. The graphs are made by normalising the measured concentrations by the average concentration for each trace element.

wet snow. Weather data collected from 01.10.2018 to 04.02.2020 at Sverresborg weather station are presented in appendix N. The week before the sampling 12.12.2018, the snow depth had been up to 18 cm at the Sverresborg weather station, but decreased down to 13 cm the last two to four days before due to temperatures above 0 °C. There is also a small peak for several of the elements in the beginning of March. During the second half of February the temperatures fluctuated between below the freezing point during night and above the freezing point during the day, and the snow depth decreased from 52 cm down to 4 cm. An increasing trend from lower than average to above average was observed in the beginning of June for many of the trace elements. This could be related to the heavy rainfall that was experienced during the week before sampling. Two days before the sampling on 03.06.2019 there had been a rainfall of 33.5 mm, and the day before the sampling on 09.06.2019, 21.4 mm of rain had been registered. A heavy rainfall was also experienced before and on the same day as the samplings on 19.09.2019 and 02.10.2019. In addition, comments about high water flow in the stream were noted on 09.06.2019, 19.09.2019, and 02.10.2019. The lowest concentrations were measured in May and September. When comparing this to weather in April/May and August/September, the weather in these two periods were relatively warm, especially in August, and included very little precipitation. The water flow in the stream has potentially been low during sampling and has not carried with it a lot of contamination. From these trends, it can be concluded that the Killingdal stream carries more trace elements when there is more water flowing.

The concentrations in table 4.1 and trends in figure 4.1 indicate that the forest above the Killingdal area might be affected by the ore transport and processing during the decades when the *Killingdal Gruber* company was active. Dust and residues might have found its way into the woods, without being removed during the later clean-up processes. By the levels in the stream it does not seem to be large amounts of contamination, or it is existing in a very stable form. However, as the trends show, when there is heavy rainfall or snow melting, more elements are mobilised and transported by the stream. According to Espana [65] evaporative salts from AMD waters are produced during dry

Table 4.2: Results from sampling of the Killingdal stream where it flows into the Trondheimsfjord, in µg/L. The colours are based on the classifications in table A.1 in appendix. Iron does not have any classifications.

Date	Fe	Cr	Ni	Cu	Zn	As	Cd	Pb
09.06.2019	30.7	0.259	0.756	5.89	7.05	0.169	0.00927	0.945
12.09.2019	13.4	0.207	0.778	4.34	5.50	0.190	0.0177	0.0665
19.09.2019	85.7	0.389	0.693	5.12	7.17	0.0769	0.0189	0.965
02.10.2019	105	0.470	0.752	5.00	8.64	0.0740	0.0168	0.465
18.10.2019	21.4	0.232	0.770	4.99	5.10	0.113	0.0161	0.180

seasons and dissolved during periods with a lot of rain. If the Killingdal stream dries out during the summer, there might be precipitation of trace element sulphate salts on the edges of the stream, and when the rain season starts in the autumn more trace elements will be measured in the stream as seen above.

Another explanation could be that the soil in these woods naturally contain higher concentration of the elements in focus than what is common in the rest of Norway and similar areas. The classifications used are based on averages from many areas with similar topography. There is a possibility that the minerals the soil is produced from has a naturally higher content of chromium, nickel, copper, zinc, cadmium, and lead.

In addition, trace element concentrations were measured in the end of the Killingdal stream, where it flows into the fjord, on five occasions. This was to see if the journey through the pipes below the road and down the man-made stream was contaminating the water. The results are presented in table 4.2, and show no significant difference in the concentrations compared to the sampling point of the Killingdal stream further up. All elements were in class II for freshwater, except for arsenic which had three out of five concentrations in class I, as the elements in table 4.1. This is a clear indication that the Killingdal stream is not contaminated on its path down the new Killingdal area.

4.2 Monitoring of the Trondheimsfjord

For the monitoring of the release point of the effluent from Killingdal, a total of ten samples were collected. Nine samples were analysed, while the tenth sample was not analysed due to the Covid-19 situation. The choice of sampling location was due to the clearly visible release of effluent. During the first visit at the Killingdal tunnel, a tour of the insides of the tunnel was conducted. Because of the movement of the water, a lot of the precipitated sludge was resuspended into the water in the tunnel. Afterwards, when the fjord right outside the entrance to the tunnel was inspected, there was a clear release of orange particles from the rocks right below the water surface, which had the same colour as the water inside the tunnel. The exact point where the effluent was released from was noted, and this became the location of the fjord sampling. The results from the analyses are presented in table 4.3, coloured depending on the classification of conditions it belongs to in accordance with table A.2 in appendix.

The results show a substantial release of copper, zinc, arsenic, and cadmium into the fjord through the effluent. The release of copper and zinc are mostly in class V, arsenic is mostly in class III, and cadmium fluctuates between class III and IV. This corresponds well to the high amounts of copper, zinc, arsenic and cadmium that are found in the tunnel water. Chromium, nickel and lead, along with iron, are released in lower amounts, class I and class II (iron does not have any classifications).

When comparing the concentrations in table 4.3 to the concentrations in the tunnel (Steen [72]) it becomes evident that the tunnel water contains far higher concentrations of all the elements. Copper and zinc are in class V in both sample types, but the concentrations are usually ten times lower in the samples from the fjord compared to the tunnel. Chromium, nickel, cadmium, and lead are generally one class of conditions higher inside the tunnel than in the samples measured in the fjord. Also iron exists in concentrations many times lower in the fjord samples compared to the tunnel. In the end, arsenic has approximately the same concentrations in the tunnel as the fjord.

The decrease in concentrations could be a result of dilution of the effluent when released into the fjord. Waves and currents mix the effluent into the fjord water. Another possibility is that the

Table 4.3: Results from analysis of water samples collected between 12.12.2018 and 19.09.2019 from the Trondheimsfjord where the effluent from Killingdal is released. All concentrations are listed in µg/L. The cells are coloured depending on the corresponding class of conditions they belong to, according to the classes in table A.2 in appendix. Iron does not have any classifications.

Dato	Fe	Cr	Ni	Cu	Zn	As	Cd	Pb
12.12.2018	37.5	0.0707	5.36	830	1610	0.679	6.17	0.172
02.03.2019	65.0	0.204	4.38	512	1510	0.418	5.93	0.132
05.03.2019	18.2	-0.0640	0.788	56.9	174	1.29	0.699	0.0524
11.03.2019	5.35	0.0210	0.425	27.5	82.8	1.22	0.346	0.0362
22.03.2019	15.4	0.0550	1.81	142	390	1.01	1.72	0.0983
28.05.2019	7.62	0.0496	0.489	4.92	7.23	0.519	0.0325	0.0210
03.06.2019	2.95	0.0365	0.297	14.2	61.4	1.08	0.294	0.00937
09.06.2019	10.4	0.0550	1.37	114	428	0.706	1.51	0.0346
19.09.2019	37.2	1.58	2.63	141	510	1.45	2.08	0.154

Figure 4.2: Accumulation of effluent released into the Trondheimsfjord.

elements precipitate when coming into contact with the more alkaline ocean water as hydroxides, oxides, sulphates, carbonates, or mixed complexes, depending on the available anions. Since the samples collected were all filtered, the fraction of precipitated elements was not measured, only the fraction that stayed dissolved. However, when the concentrations of dissolved copper and zinc, and to some extent arsenic and cadmium, are still in high classes of conditions, the effluent is a problem.

One day during sampling, an accumulation of effluent was observed between some rocks that are part of the sloping wall. This is depicted in figure 4.2, showing that at certain times of the day, when the water level is at the right height, the effluent is not efficiently diluted. The description for class V is *Extensive acute toxic effects*, which means that even after a brief visit into the effluent from Killingdal, aquatic organisms could get permanent disabilities or die.

To see if there were any trends for when the element concentrations were high and low, the concentrations in table 4.3 were normalised for each element based on the average concentration of that particular element. The graphs in figure 4.3 show the trends for the normalised trace elements concentrations. From this graph it appears that the release into the fjord varies over the year. In 12.12.2018 the concentrations released were above average for six out of the eight elements in focus, with only arsenic and lead having concentrations lower than average. For iron and chromium there were an increase in concentration released the 02.03.2019 compared to the last sample, while nickel, copper, arsenic, and lead decreased. In this period both limestone and olivine were tested as treatment materials, which may have impacted the composition of the water. General for all the trace elements, except arsenic, is that they all decreased after 02.03.2019, and stayed around or below average concentrations the next sampling dates. The 11.03.2019, 28.05.2019, and 03.06.2019, all had low release of contaminants. The last sampling in September showed an increase in released concentration. For most elements this increase was not that severe, but for chromium there was a substantial increase compared to the average release concentration. Fortunately, as table 4.3 shows,

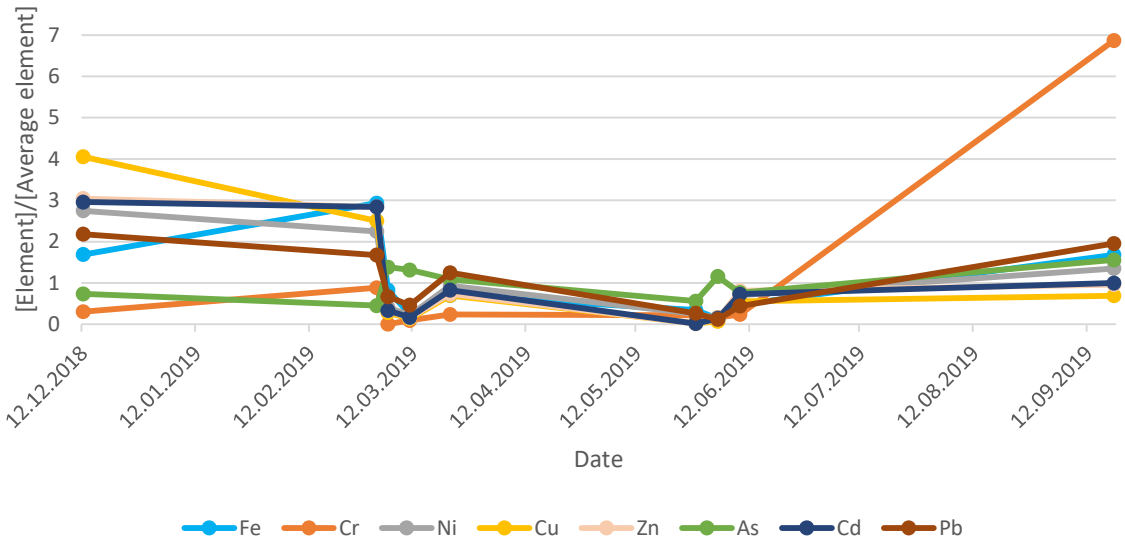

Figure 4.3: Trends for the trace elements in focus in the Killingdal effluent in the Trondheimsfjord. The graphs are made by normalising the measured concentrations by the average concentration for each trace element.

the concentration of chromium was only in class II, which indicates that it will not cause any toxic effects in the aquatic organisms coming in contact with the water.

Over the period when the the monitoring of the release location was conducted, the concentrations of nickel, copper, zinc, and cadmium in the effluent were significantly decreased. This could indicate that the treatment methods used by Trondheim Municipality works for these trace elements. Iron and lead concentrations fluctuate considerably during the monitoring period, but the last sample show approximately the same as the first. And as mentioned, chromium increases drastically in the last sampling. The trends that are visible in table 4.3 and figure 4.3 could be influenced by several factors. As mentioned above, there could be a bigger concentration released of trace elements than these results show, but due to filtration of the samples only the dissolved fraction is measured. However, the filtrated samples will give a relatively accurate description of the conditions in the effluent, as the free dissolved ions in most cases pose the biggest risk for the health of aquatic organisms.

A big problem with the monitoring throughout the project was the fact that after it had rained or snowed, or when the temperature was below 0 °C outside, the rocks that made up the sloping wall down to the sampling location were extremely slippery. In addition, a lot of times the water was moving vigorously back and forth along this wall due to natural waves or waves from shipping traffic, making it hard to get out of if one were to fall into the water. Low tide made it hard to reach down to the water, and the rocks closest to the water were slippery due to seaweed and other growths. The amount of samples taken from the fjord was therefore drastically reduced due to the risk of falling into the water. Another factor was that the release of effluent from the tunnel was only observed when the water level was above a particular height. During low tide, the fjord showed less impact by the effluent. This is exemplified by the sample collected 28.05.2019 in table 4.3. According to notes taken that day, the fjord did not have any visible release of effluent into the fjord and there was a low tide. This day was the day with the lowest copper, zinc, and cadmium concentrations, in addition to low concentrations of iron, chromium, nickel, arsenic, and lead. The concentrations of

copper and zinc are still too high, but they are a lot better than during higher water levels.

4.3 Investigation of sediment samples

As expected, the analysed samples showed clear contamination of the sediments in the Trondheimsfjord. Since the samples were taken only of the uppermost part of the sediments, the contamination has happened after *Cleaner Harbour* was conducted. The averages of the two samples taken in each sample location for this study in 2019 are shown in table 4.4. Each cell is colour coded based on which class of conditions the concentration correlates to, according to table A.3 in appendix.

From the results it is evident that there is a significant contamination of copper in the surface sediments, based on the classifications of conditions. In fact, the lower limit for class V for copper in sediments is 147 µg/g, and 8 out of 12 sample locations had higher concentrations than this limit. Additionally, zinc and arsenic exist in substantial amounts in most of the sample locations, as they both have a lot of concentrations in class IV. Cadmium and lead occur in elevated concentrations in many of the sample locations, but not as severely as for copper, zinc and arsenic.

Iron was also detected in substantial amounts. Because there does not exist any classifications of conditions for iron, it is not coloured in table 4.4. Without these classifications it is difficult to say anything about the severity of these concentrations. However, it is possible to calculate the percentage of iron in the sediments in Ilsvika. It then becomes evident that iron is a huge constituent, with eleven out of the twelve sample locations containing more than 1 % iron and four sample locations having more than 15 % of iron in their sediments. In 2014 DNV GL performed an environmental study of Nordgulen, a fjord in Sogn og Fjordane in Norway. Here they, among other things, investigated the trace element concentrations in the fjord. The results showed that iron constituted between 1.77 % and 16.8 % of the sediments, approximately the same as in Ilsvika.

Table 4.4: Concentrations of trace elements in focus in samples collected in 2019 in µg/g at sampling locations 1-12, in addition to a sample (25) taken of the deeper sediments in location 9 from 2019 and a sample of the upper 2 cm of the sediments in the Korsfjord in 2013 (Kf). The concentrations are coloured according to table A.3 in appendix. Iron does not have any classifications.

Location	Fe	Cr	Ni	Cu	Zn	As	Cd	Pb
1	173000	61.6	30.1	1740	4180	455	9.51	791
2	175000	57.6	17.3	1310	4270	495	9.69	1010
3	10400	12.4	5.0	51.1	102	22.3	0.15	29.3
4	38200	35.3	15.0	287	649	82.8	1.45	101
5	168000	84.5	31.2	1160	2610	414	4.73	612
6	83100	57.9	21.0	481	895	218	1.03	277
7	23900	19.4	7.47	138	251	63.0	0.358	80.5
8	167000	38.9	20.9	2070	8430	457	22.9	1090
9	32900	25.4	8.93	162	353	89.3	0.394	113
10	7940	11.5	4.99	32.9	69.2	16.5	0.118	18.3
11	42200	25.2	9.43	280	724	113	1.33	166
12	18700	31.0	8.13	110	385	29.5	1.01	41.0
25	234000	121	32.1	2270	7460	754	17.8	1650
Kf	41300	116	63.1	36.1	129	5.62	0.232	23.3

Table 4.5: Summary of the results from six studies of the Trondheimsfjord conducted between 1981 and 2010, together with the average of the sampling locations closest to shore that were analysed in this thesis (2019). For 2000 the samples were taken at two depths, 2 cm (137 cm). The unit is µg/g. The cells are coloured based on the current classification of conditions from table A.3 in appendix.

	1981 [6]	1987 [8]	1991 [8]	1994 [9]	2000 [10]	2010 [90]	2019
Hg	0.56	-	-	2.87	0.38 (6.00)	0.279	0.431
Cr	42	-	-	152	152 (13.40)	69	46.8
Ni	-	-	-	44.50	135 (16.90)	35	19.7
Cu	1800	1738	2400	192	2050 (10300)	970	917
Zn	7878	6017	7000	520	4320 (<2)	1500	3370
As	-	-	-	-	49 (1100)	320	217
Cd	18.70	14.80	7.20	1.29	20 (210)	11	8.94
Pb	1704	1263	1500	160	209 (2965)	490	444

DNV GL described this as high iron concentrations [89]. It is therefore reasonable to address the concentrations of iron in Ilsvika as high.

4.3.1 Contamination levels over the years

Most of the recipient studies conducted through the years have sampled in Ilsvika or in its proximity. A summary of the results from these reports are shown in table 4.5. The same locations are not sampled from year to year, and different factors have played in when deciding sampling locations in these reports. The report from 1981 sampled in Ilsvika, but it does not state exactly where, other than describing that the sediment was extracted from 60 m depth and the sample was taken at the top of the sediment pile [6]. According to the 1991 report, the sampling in 1987 happened at the same location as in 1981 [8]. In 1991, six locations were sampled ranging from 21 m depth to 72 m depth, and the sample was extracted from the sediment surface [8]. One of the locations from 1991, II.1, which is used in table 4.5 is close to location 5 in 2019. In 1994, sampling in Ilsvika was not prioritised, and Ilabassenget was the only location close by that was sampled. Therefore, the values in table 4.5 for 1994 is from Ilabassenget, which is east from Ilsvika. The report from 2000 used a sample location, 37, close to location 4 in 2019. Here both the sediment surface (0-2 cm) and what is assumed to be the layer right below the polluted sediments (below 137 cm), were sampled. The last report included in table 4.5 is from 2010. The sampling location, F2, is close to sampling location 37 from the 2000 report, and the sediment sample was taken from the upper 10 cm of the sediment pile. [90]

According to table 4.5, both zinc and lead have been significantly reduced since 1981. However, both have increased since 1994. Chromium, copper, and cadmium increased between 1981 and 2000, and nickel has increased between 1994 and 2000, but they have all decreased again in 2010 or 2019. High concentrations between 2000 and 2010 could be explained by increasing activity in this area due to the clean-up of the Killingdal area that was conducted in 2009 and the remediation of the contaminated sediments. Still there are elevated concentrations of all the trace elements except chromium and nickel. The high concentrations of iron, copper, zinc, arsenic, cadmium, and lead are a problem for Trondheim Municipality and the success of the *Cleaner Harbour* project. New

sediments were placed in the fjord to prevent the old sediments from contaminating the water above and the biota living close by. And they are preventing the old sediments from releasing contaminants, but they are themselves getting contaminated. This means that the new covering material may be a potential source of contamination of the fjord in the future.

Due to the Covid-19 situation, the samples of the seawater right above the sediments were not analysed in time to include in this thesis. However, there are two possible outcomes of the analysis of these samples. The first is that there is a low or no contamination of the water above the sediments. This would be in accordance with the general understanding that sediments usually contain a higher amount of contaminants than the water above [16], due to the affinity of the contaminants to the usually less polar clays, oxides and organic compounds that are often present in the sediments [55]. However, if the conditions in the fjord changes, it may cause the pollutants to be released into the fjord again. The second possible outcome of the analysis of the deep water samples could be that there are high levels of one or several of the trace elements in focus. This might be because of the release from Killingdal, but it could also be caused by the release from the underlying sediments. No matter the source, if the concentrations are in class III or above it is not ideal for the organisms living in these waters. At the sediments, low trophic level organisms such as molluscs, seaweed and crustaceans are often found. These form the foundation of the food web, and if they are contaminated, it can either lead to the pollutants moving up the food chain where humans in the end can be exposed, or if the food source for the higher trophic level organisms disappears ecosystems can collapse.

Another concern is the combination of trace elements and polycyclic aromatic hydrocarbons, or PAHs. PAHs are organic, lipophilic contaminants, consisting of two or more aromatic rings linked together with a pair of carbon atoms shared between them. They are released from human activities such as combustion of petroleum products. In 2014, Gauthier et. al. summarized several articles about the combined effects of trace elements and PAHs. Here they discovered that nickel, copper, zinc, and cadmium combined with different PAHs showed more-than-additive effects in 44.7 % of the studies. More-than-additive effects are when the toxicity of the mixture is greater than the sum of the toxicity of the separate constituents. Examples of these effects can be when the trace elements and PAHs interact directly with each other, or it can be that one of them have an effect on the transport, metabolism, and detoxification of the other. [91] In the Trondheimsfjord, many of the reports have investigated the amounts of PAHs. The reports from 1994 [9] and 2000 [10] both reported high concentrations of PAHs in Ilsvika, and the 2010 report [90] presented PAH concentrations in *Moderate* to *Bad* conditions. It is therefore reasonable to think that the aquatic organisms living in the Trondheimsfjord are subject to a mixture of PAHs and trace elements, which can have severe effects on their health.

4.3.2 Trends

To see if there were any trends in the sample locations and their distance from shore, the concentrations were divided into four groups; the locations 20 m from shore (4, 8, 12), the locations 70 m from shore (3, 7, 11), the locations 120 m from shore (2, 6, 10), and the locations 170 m from shore (1, 5, 9). The results for the trace elements iron, chromium, cadmium, nickel, zinc, copper, lead, and arsenic are presented in figure 4.4. The average concentrations and standard error the error bars in

figure 4.4 represents, are presented in appendix F. When studying the graphs in figure 4.4 it becomes visible that there are three main categories of trends. The first category contains the elements that have the same trend as iron in figure 4.4a. In the second category the elements that have a similar trend as copper in figure 4.4d is collected. The third category contains the trends that resembles zinc in figure 4.4e.

To check if the concentrations in the different locations are significantly different, the statistics analysis program SPSS was used. Most distributions of concentrations were normally distributed, but they did all have groups with non-normally distributed values, as table G.1 in appendix shows. In addition, the number of parallels were relatively low. Based on these factors, it was decided to use Kruskal-Wallis H Test to check if the distributions of the elements are the same or not across all the different distances from shore. From this test, elements with a p-value lower than 0.05 have concentrations that are significantly different between the location groups. Results from this test are presented in table G.2.

Trends of iron, chromium, arsenic, and lead

Even though they existed in different concentrations, iron, chromium, arsenic, and lead all had a similar trend when plotted. Trends of the four trace elements are presented in figures 4.4a, 4.4b, 4.4f, and 4.4h, respectively. This particular category of trends starts with group 1 showing relatively high concentrations, and group 2 is lower than group 1. The trend is then that group 3 is higher than group 1, and group 4 is the tallest of them all representing the locations furthest from shore. An explanation of this trend could be that the elements bound to particles in the effluent from the Killingdal tunnel sink to the bottom immediately after release into the fjord. The dissolved elements on the other hand may be precipitated or adsorb to particles in the fjord, but this takes longer time and they may be transported further out into the fjord before they reach the sediments. The fact that group 3 and 4 are the tallest ones can indicate that a large portion of the elements with this trend exist as dissolved species in the AMD at Killingdal.

The high concentrations of iron in the sediments is no surprise. Table 2.1 presented iron as one of the top three constituents of the water in the Killingdal tunnel by far, and an information sheet about occurrence of different minerals in the Killingdal mines states that the iron-containing minerals sphalerite and pyrite are major minerals in the mines [1]. One effect of a high precipitation rate of iron is that it can increase the sedimentation rate of other trace elements. Elements that may be affected are lead, cadmium, zinc, and nickel [89]. This is because when dissolved iron in the acidic AMD is introduced to the way more alkaline seawater in the fjord it forms oxides, oxyhydroxides and hydroxides. These particles become surfaces where other ions can adsorb to. Iron precipitation then becomes a possible route to long-term storage in the sediments for many polluting elements. One problem with this is that these oxides can be sensitive to changes in oxygen concentrations, as they are redox sensitive [92]. If the amount of oxygen changes in the environment around them, the iron oxides may dissolve or release the pollutants.

From table 4.4 it becomes evident that chromium is present in the sediments only in background levels. Ten out of twelve locations had concentration below the lower limit of class II. This corresponds well with the concentrations released into the fjord in the Killingdal effluent, which contains chromium in class I on most sampling days (see table 4.3 in section 4.2). The highest concentrations (class II) are

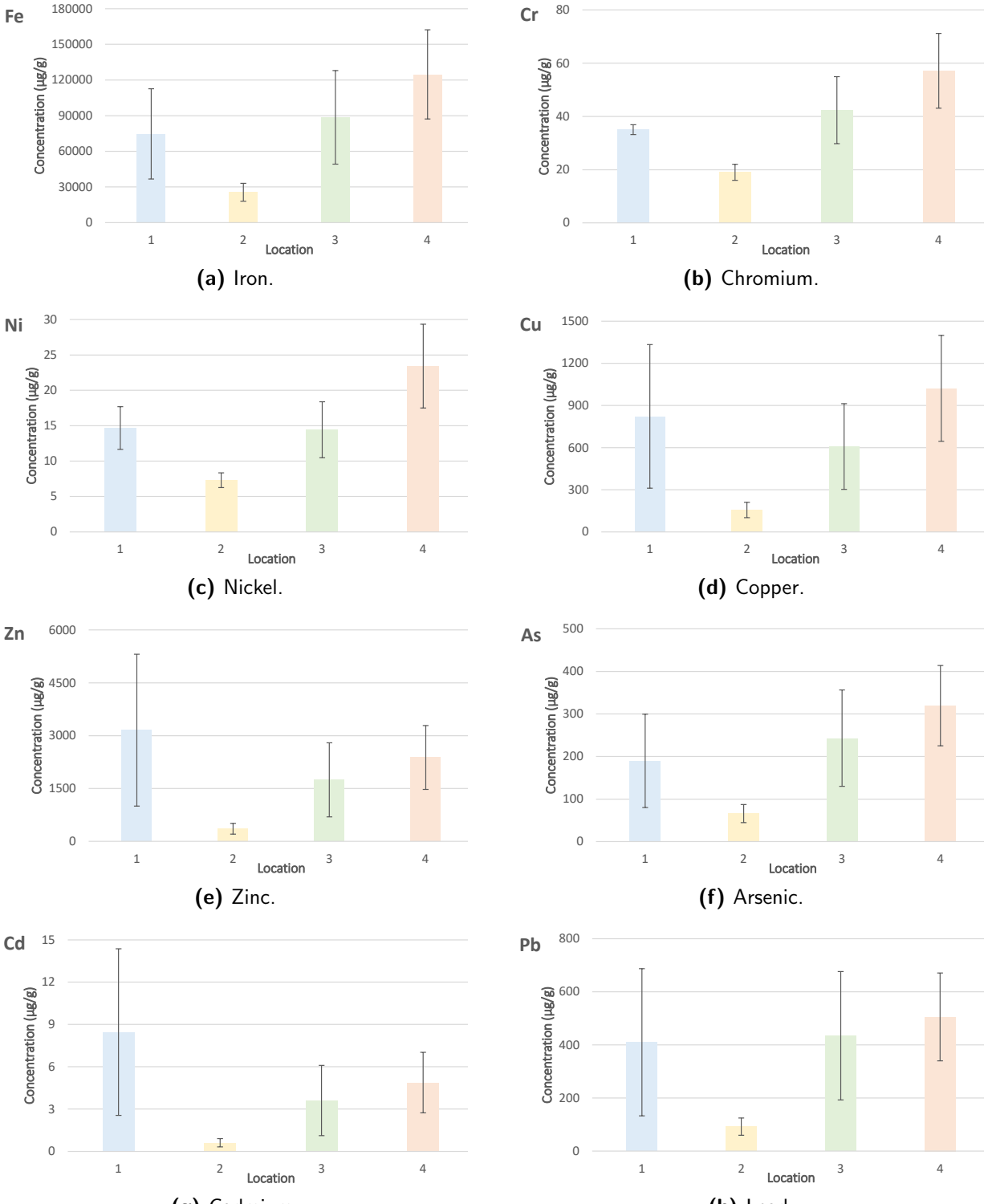

(a) Iron. **(b)** Chromium. **(c)** Nickel. **(d)** Copper. **(e)** Zinc. **(f)** Arsenic. **(g)** Cadmium. **(h)** Lead.

Figure 4.4: Trends of the trace elements in focus in the sediments in Ilsvika. The sample locations were grouped where 1 represents the locations closest to shore, and 4 represents the locations furthest from shore. The error bars represents the standard error for the mean of the sample concentrations in that particular group.

found in locations 1 and 5, which are the points furthest from the shore in the middle section and the north section. This may indicate that there is a source other than the Killingdal tunnel where chromium is released from. The values in class II could also be a result of an outlier that got to affect the average because of the low amount of parallels. In sampling point 1, one of the analysed parallels had a concentration slightly below the lower limit for class II, which is 60 µg/g. The other sample had a concentration of a few µg/g above this limit, making the average slightly above class I. A higher number of parallels may have evened this concentration out to class I, making it a background value as well. In location 5, on the other hand, both samples analysed had concentrations well above the lower limit of class II, making the possibility of them belonging to class II more reliable.

As table 4.4 shows, the arsenic concentrations in eight out of twelve sampling locations were categorized as class IV. These are very severe numbers, indicating possible acute toxic effects in aquatic organisms in the water column and sediments, due to short-term exposure. Locations both close to shore and further out showed high concentrations. Arsenic is one of the elements that has a strong adsorption affinity towards iron hydroxides. An explanation of the trend observed in the Trondheimsfjord for arsenic might include the adsorption or co-precipitations onto newly formed iron hydroxides, and the subsequent sedimentation to the bottom of the ocean.

The lead concentrations in the sediment samples were not alarmingly high, but they were still elevated compared to background. Six out of twelve sampling locations listed in table 4.4 had concentrations in class III, indicating an anthropogenic source. Lead is one of the three trace elements extracted as main products from the Killingdal ore [1]. However, the lead crude ore grade was only at 0.4 % and the mineral which contains lead, galena, is listed as an accessory mineral, constituting less than 1 % of the ore. It is therefore reasonable that lead is not present in extremely high concentrations, especially if the Killingdal tunnel is the only source. The historical trends in table 4.5 show that the amount of lead drastically decreased between 1981 and 1994. A reason for this decline could be the ban from adding lead to gasoline. When cars in Trondheim stopped releasing lead into the environment, a great source had been removed [93]. Lead could easily be transported from traffic and out into the fjord. When this was not an issue anymore, a clear decreasing trend could be observed. However, there has been an increase after 1994, and in 2010 levels were three times higher than what was reported in 1994. An obvious explanation to this could be that the sampling locations were most likely not the same these years. In addition, the *Cleaner Harbour* project started in 2009. The testing and clean-up work may have disturbed some of the older sediments, causing higher lead concentrations to be measured. No such increase have been observed for the other trace elements, indicating either that the other elements are better conserved in the sediments than lead, or this disturbance may have only played a small part in the increase of lead concentrations.

The trends shown in figures 4.4a, 4.4b, 4.4f, and 4.4h were tested by Kruskal-Wallis H Test in SPSS to see if the concentrations are changing between the different distances from shore. From this analysis, iron, arsenic, and lead showed no significant difference between the four distance groups (H_3=5.31 at p=0.150, H_3=5.77 at p=0.123, and H_3=5.53 at p=0.137). This means that even though they show a clear trend, there is a possibility that the concentrations are not significantly different from each other. A reason why the analysis came up with this conclusion may be that the values grouped together are collected from different sampling locations. As an example, group 1 represents all the locations that are 20 metres from shore, which means that it represents location 4, 8, and 12.

These locations are separated by several metres, and may have very different exposure to the effluent from the Killingdal tunnel. This is reflected in table 4.4, where if location 4, 8, and 12 are compared, the concentrations are 38 200 µg/g, 167 000 µg/g and 18 700 µg/g, respectively. The concentration in location 8 is four times as great as location 4 and almost nine times as great as location 12. The variations in concentrations in the same groups are also reflected by the error bars in figures 4.4a, 4.4f, 4.4h. Sampling location 4 is closest to the tunnel effluent source, but the fact that location 8 has the highest concentration can indicate that the currents move the contaminants northwards. In general, the middle section of locations (1-4) and the north section (5-8) have the highest concentrations of Fe, which could imply a general northwards current. For chromium however, the results from the statistical analysis showed a significant difference (H_3=9.29 at p=0.026 and $n = 28$). This is an indication that the concentrations are significantly different between the various distances from shore. It also strengthens the trend in figure 4.4b.

Trends of copper and nickel

The second category of trends consist of the trace elements copper and nickel. What separates them is that the trend for copper and nickel have a lower group 3 than group 1, where as the group 3 is the tallest of the two for iron. An explanation to why this trend appears could be the same as for the iron trend, but the transformation of the trace elements from dissolved to precipitated may take a longer time, giving the elements longer time to drift further from shore.

As mentioned previously, copper was the most severe pollutant in the case of classification of conditions, as presented in table 4.4. Eight out of twelve sampling locations had copper concentrations in class V, and five out of twelve locations had at least twice as high concentrations as the lower limit for class V, which is 147 µg/g. This can potentially cause extensive acute toxic effects in aquatic organisms living in the water column and the sediments. There are some conflicting views on whether copper biomagnifies or not. However, the concentrations of copper are so high in the Ilsvika sediments that the effect on aquatic organisms can be detrimental, with or without biomagnification.

Together with chromium, nickel mostly exists in the sediments in background levels. Only two of the sampling locations, locations 1 and 5, exhibited concentrations above class I. In addition, this limit is at 30 µg/g, which means that the concentrations in both location 1 ad 5 are only slightly above the limit, and could easily be rounded off towards class I if there had been more parallels. The theory that nickel and chromium only exists in background levels in Ilsvika is backed up by the report from 2000 [10]. Appendix 4.4 in this report presents the concentrations of copper, zinc, lead, nickel, chromium, cadmium, and arsenic, and how much they believe to be natural and contamination. Their analyses indicate that the concentrations of chromium and nickel mainly corresponds to natural levels, with a smaller portion being caused by contamination. [10] In addition, as presented in table 4.3 in section 4.2, the amount of nickel released in the Killingdal effluent into the fjord is mostly in class II, which should not cause any harm to aquatic organisms.

When analysed with SPSS the concentrations of copper in the locations 1 to 4 were not significantly different (H_3=4.94 at p=0.176). Still these results indicate that a portion of the copper in the Killingdal AMD exists as adsorbed to particles, while another portion occur as dissolved elements. The results from the Kruskal-Wallis H Test revealed that the concentrations of nickel were significantly different between the four distances off the shore (H_3=8.44 at p=0.038). This indicates low variance

between the concentrations in the same location, and larger variance between the distances. It also indicated that the trend shown in figure 4.4c is correct.

Trends of zinc and cadmium

The third type of trend observed from the graphs in figure 4.4 belong to zinc and cadmium. They are separated by the rest because group 3 and 4 are lower than group 1, as shown in figures 4.4e and 4.4g. Group 2 is still the lowest bar, indicating that not a lot of the elements sediment here. As for the two other categories, the trends can also say something about the distribution of zinc and cadmium between particulate and dissolved form. Due to the low bars furthest out, it can be assumed that a great portion of the released zinc and cadmium from Killingdal already exist as particles, which are relatively rapidly sedimented close to shore. Another possibility is that the dissolved ions are relatively soluble in the seawater, causing the dissolved ions to move to sediments further away from shore than what this thesis analysed.

Zinc was the element, except from iron, that existed in the highest concentrations in the sediments in Ilsvika. Because zinc was one of the main products retrieved from the Killingdal ore [1], the probability that the water from Killingdal tunnel is the source is very prominent. In addition, the effluent from the Killingdal tunnel releases zinc concentrations in class IV and V, according to table 4.3 in section 4.2. Even though the concentrations are high, they are classified as mainly condition class III and IV, with one location (location 8) in class V. This is because large amounts of zinc is needed before it can cause toxic effects. As with copper, there are some conflicting views on the biomagnification of zinc. In contrast to copper, zinc has been proven to biomagnify in an Arctic food web [30]. However, the zinc concentrations are still so high that they are a potential risk to the aquatic organisms.

Cadmium showed more varying concentrations in the different sampling locations in Ilsvika, ranging from class I in locations 3 and 10, to class IV in location 8. However, eight out of the twelve sample locations had concentrations in or below class II, indicating relatively low concentrations of cadmium. The release of cadmium from the Killingdal tunnel was relatively substantial, with five out of nine samples containing class IV concentrations and three out of nine containing class III concentrations. The trend in figure 4.4g may indicate that a lot of the released cadmium is located close to shore, but the concentrations are still low. Analyses of the cadmium concentrations in the deep-water samples could have said something about the possible release of cadmium from the sediments and into the overlying water. According to Alloway [27] and Okocha [47], cadmium is more soluble when complexing with chloride ions. In the tunnel water at Killingdal, high concentrations of chloride exist. This could imply that a major part of the cadmium released into the fjord is present in chloride complexes. Due to the fact that high cadmium concentrations are released into the fjord, and this is not reflected in the sediments in Ilsvika, it may appear as if most of the cadmium released into the fjord stays in the water column rather than sedimenting, and the fraction measured close to the shore could be explained by a few relatively insoluble cadmium compounds.

Neither zinc nor cadmium showed a significant difference in concentrations between the different distances from shore in SPSS ($H_3 = 4.19$ at $p = 0.242$ for zinc and $H_3 = 4.42$ at $p = 0.219$ for cadmium). It is therefore a possibility that the trends are not as clear as in figures 4.4e and 4.4g, but more evenly distributed between the locations. Nevertheless, zinc and cadmium exists in elevated concentrations

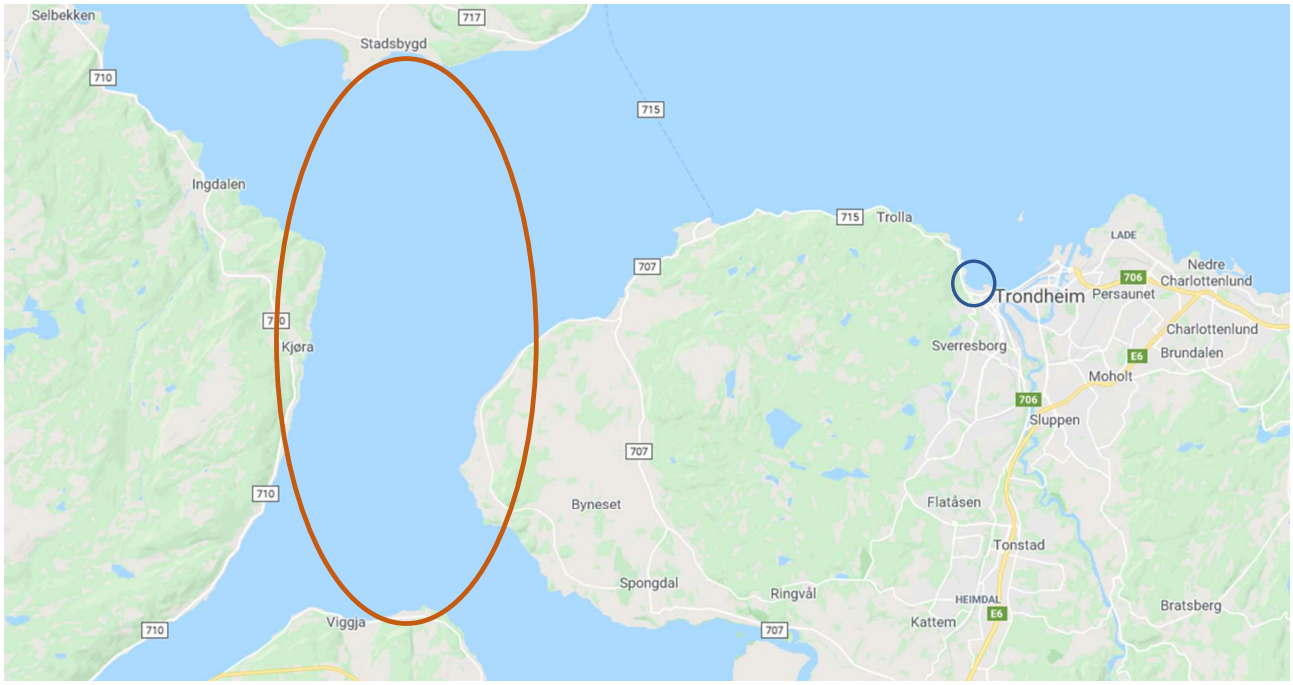

Figure 4.5: Location of the Korsfjord in relation to Trondheim [94]. The orange circle indicated the approximate location of Korsfjord, while the blue circle close to Trondheim indicates where the sediment samples in Ilsvika were collected.

in several locations, indicating that there exists an anthropogenic source.

4.3.3 Comparing sediment concentrations with sediments from the Korsfjord

In the original plan for the sediment sampling, two samples from the middle of the fjord were supposed to be collected. However, due to unforeseen incidents, these samples were not collected. Instead, the results from a previous sampling in the Korsfjord conducted by NTNU in 2013 were used.

The Korsfjord is the point where four fjords meet; Trondheimsfjord, Flakkfjord, Orkdalsfjord, and Gaulosen. Figure 4.5 gives an overview of the location. It is an area subject to, among others, the shipping traffic arriving or departing Trondheim, but it is not subject to the release of other anthropogenic discharges of trace elements, and do not have any specific point sources. In addition, the sedimentation rate in this area is relatively slow, compared to the sedimentation rate closer to Trondheim city. This sample can therefore be seen as a background sample representing relatively natural levels of trace elements. The results from this sampling are presented in table 4.4, indicated by *Kf*.

In the sample from Korsfjord, chromium, copper, zinc, and cadmium concentrations were all in class II, and arsenic and lead were in class I. All these seven elements are therefore not common to find in high concentrations in the sediments in this area. This implies that the high concentrations of copper, zinc, and arsenic, and elevated concentrations of cadmium and lead are introduced by anthropogenic release rather than natural occurrence. Since Killingdal is located close to the sampling points of the sediment samples, the tunnel effluent is a possible and probable source of trace elements.

Unlike the other elements, nickel was measured in relatively high concentrations, i.e. class III. This is higher than the concentrations measured in Ilsvika. During the sampling in the Korsfjord in 2013,

Table 4.6: Correlation coefficients from a Pearson correlation analysis conducted on all the concentrations of iron, chromium, nickel, copper, zinc, arsenic, cadmium, lead, sulphur, and calcium in all the samples analysed. No * indicates significance at the 0.01 level. * indicates significance at the 0.05 level. ** indicates low or no correlation.

	Fe	Cr	Ni	Cu	Zn	As	Cd	Pb	S	Ca
Fe	1									
Cr	0.827	1								
Ni	0.869	0.914	1							
Cu	0.928	0.635	0.798	1						
Zn	0.782	0.424*	0.623	0.941	1					
As	0.993	0.796	0.827	0.914	0.770	1				
Cd	0.711	0.334**	0.553	0.903	0.994	0.699	1			
Pb	0.921	0.614	0.726	0.969	0.945	0.917	0.906	1		
S	0.919	0.572	0.699	0.977	0.937	0.923	0.900	0.984	1	
Ca	-0.924	-0.913	-0.922	-0.815	-0.645	-0.898	-0.567	-0.805	-0.777	1

deeper sediment samples were also collected. When investigating these results it was discovered that the concentration of nickel did not change significantly with depth. Even at approximately 2 m depth nickel concentrations were measured to be 61.3 µg/g, and it did not vary considerably between the sediment samples. This could imply a naturally high amount of nickel in this area. Interestingly, the nickel concentrations in Ilsvika are mostly in background levels. It would have been interesting to compare these results to deep-water samples from Ilsvika to see if nickel is released into the fjord from the sediments.

4.3.4 Correlations

A Pearson correlation analysis was conducted on the sediment samples. The results are shown in table 4.6. These results were compared with the correlation values from the ICP-MS excel sheet with the analysis results constructed by Syverin Lierhagen, which are presented in appendix H. The correlation coefficients from the two analyses are in agreement with each other.

Looking at table 4.6 the vast majority of the correlation coefficients are significant, indicating high correlation between the trace elements. This supports the theory that there is contamination released from the same source. An explanation for these results is that they are all parts of the effluent from the Killingdal tunnel. When there is a large amount of AMD released into the Trondheimsfjord, the concentration of all the trace elements will increase. When less AMD is released into the fjord, the trace element concentrations in the sediments will be lower.

The only two exceptions from the strongest correlations involves chromium, zinc, and cadmium. Chromium has a low correlation coefficient together with cadmium, and a higher uncertainty in the coefficient with zinc. As previously stated, chromium and nickel exist in the sediments in background levels. Chromium and nickel generally also show the lowest correlation coefficients compared to all the other elements in table 4.6. Small amounts of the two trace elements may be released from the Killingdal tunnel, causing a correlation with the other elements released in high amounts from the tunnel. Nevertheless, the correlations may be weakened by the fact that most of their concentrations

found in the sediments are presumed to be there naturally.

In addition to the trace elements focused on in this thesis, sulphur and calcium was also included in this correlation analysis. Sulphur is an element that is a main constituent in the Killingdal ore. Two of the three minerals listed as major minerals in the ore, some of the subordinate minerals and the majority of the accessory minerals contain sulphur. In addition, sulphur was one of the main products from the ore. Early analysis taken in December 2018 showed high amounts of elemental sulphur in the Killingdal AMD. It was included in the correlation analysis to see if there was a correlation between it and all the other trace elements. If so, this result would support the theory that the correlating trace elements originate at the Killingdal tunnel. As table 4.6 shows, there is a strong correlation between sulphur and all the trace elements found in high concentration in the sediments. Iron, copper, zinc, arsenic, cadmium, and lead all have correlation coefficients above 0.9 when paired with sulphur. The lower correlation coefficient of chromium and nickel when paired with sulphur may support the theory that they mostly exist in the sediments as background levels.

Calcium shows a trend of being negatively correlated with all the other elements in the analysis. It was included in the correlation analysis because it is usually an easily dissolved element, especially in shallow waters. So when it is released into the fjord it will dissolve, and stay in the water column. The transport route of calcium into the sediments consists mainly of the production of calcium carbonate ($CaCO_3$). Many microorganisms and larger crustaceans need $CaCO_3$ to build their shells. In addition, $CaCO_3$ is an important building block in the creation of corals. The majority of $CaCO_3$ deposited in modern times is due to biological production [95]. When these organisms die, the $CaCO_3$ can sink to the sea floor and become a part of the sediments. Therefore, it can be assumed that high concentrations of Ca in the sediments are correlated with high amounts of organism activity in the area. However, what the results from the Pearson correlation analysis identify is that where there are high amounts of trace elements, there are low amounts of calcium, and the other way around when the trace element concentration are low. This may indicate that there is a low number of organisms living in the areas where trace concentrations are high. With the alarming concentrations of several of the analysed trace elements and the negative correlation between calcium and these elements, this may indicate that the release of Killingdal AMD into the fjord pose a risk to and may reduce the aquatic life in the Trondheimsfjord. No literature was found to back up this theory, and there might be other reasons for the negative correlations observed.

4.3.5 Trace elements/lithium relationship

According to a report by NIVA [57] and an article by Aloupi and Angelidis [96] the element lithium is normally not released into the water from anthropogenic sources. The relationship between trace elements and lithium in the sediments should therefore be relatively stable within the same area when there is no human influence, and it can reflect the composition of the minerals. If the relationships fluctuate between sediment samples from the same area, it can indicate that there is an anthropogenic source releasing trace elements into the water. The trace element-lithium relationship was therefore calculated for the different sample locations in Ilsvika. To do this, the average concentrations in the 12 sample locations were used. The results are presented in appendix I.

To check if some of these relationships were significantly different, SPSS was used. All the measured concentrations for aluminium, iron, chromium, nickel, copper, zinc, arsenic, cadmium, and lead

in all the locations were used. The concentrations were divided by the concentration of lithium from each sample location. Because there was collected only two parallels in all the sample locations, and only two samples were sub-sampled three times, it was not possible to check for normality in most of the sample locations, as table J.1 in appendix shows. And since the choice of statistical analytical method is based on the normality, the safest choice when not knowing the distribution of the values was to use the Kruskal-Wallis H test. The hypothesis the test is based on is that the element-lithium relationship is the same in all the locations. The results, which are presented in table J.2 in appendix, showed that this hypothesis could be retained for aluminium, chromium, and nickel ($H_{11}=13.62$ at $p=0.255$, $H_{11}=16.37$ at $p=0.128$, and $H_{11}=16.14$ at $p=0.136$ respectively). For the other six elements, the analysis indicates that the relationships between elements and lithium varies ($H_{11}=25.32$ at $p=0.008$ (Fe), $H_{11}=25.11$ at $p=0.009$ (Cu), $H_{11}=24.94$ at $p=0.009$ (Zn), $H_{11}=25.67$ at $p=0.007$ (As), $H_{11}=25.91$ at $p=0.007$ (Cd), and $H_{11}=25.66$ at $p=0.007$ (Pb)).

The element-lithium relationships overlap very well with the classes of conditions the different elements are in. Results from the element-lithium relationship analysis indicated that chromium and nickel are present in the sediments only in naturally occurring concentrations. This is the same as presented in table 4.4, where chromium and nickel are presented as being primarily present in background levels. Concentration of iron, copper, zinc, arsenic, cadmium, and lead on the other hand have in the same table elevated concentrations compared to background values. This correlates well with the element-lithium relationship analysis, where the fluctuations between relationships in different sampling locations were significant for these elements. Because of this, there is reason to believe that these elements have an anthropogenic source into Ilsvika, and that the source is the Killingdal tunnel.

4.3.6 Sample number 25

In addition to the in total 24 parallels taken in the twelve different sapling locations, a 25^{th} sample was collected in sampling location 9. Sample location 9 is part of the southern sample section (9-12), 170 m from shore. The sampling of this parallel varied slightly from the other parallels, in that it was taken 8 cm to 9 cm down into the sediment section that was bought up to the vessel instead of from the surface. A picture of this sediment stack is shown in figure 4.6. The decision to take a sample deeper down into the section was based on the clear layers. On the surface is a brown sediment layer, which is thought to be the sediments that have accumulated after the *Cleaner Harbour* project. Below this layer is a light grey layer. The looks of it corresponds well with the limestone covering deposited during the project. Beneath this again is the final layer which is almost black in colour, something that may indicate anoxic sediments. This is assumed to be the original sediments from before the *Cleaner Harbour* project. This sediment section was the most intact piece retrieved from the seafloor. It made it possible to take a sample from what was established to be before any measures had been performed.

The results for sample 25 showed quite prominent contamination. Of all the eight trace elements, sample 25 had the highest concentration for six of them, i.e. iron, chromium, nickel, copper, arsenic, and lead. For zinc and cadmium, sample 25 had the second highest concentrations. This, together with the recipient study from 1981, indicate that the sediments in Ilsvika have been exposed to contamination for decades. Comparing the results from sample 25 with the average results from

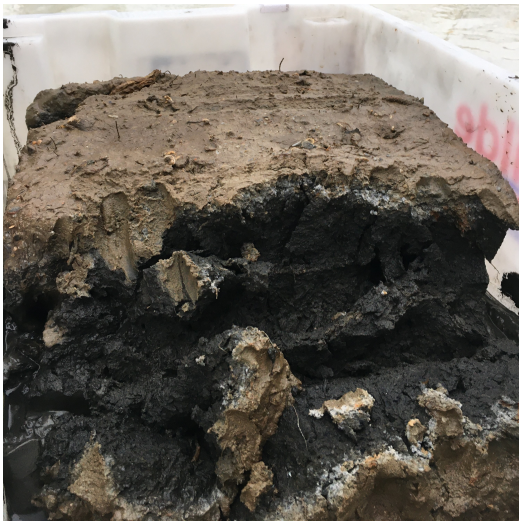

Figure 4.6: Picture of the sediment section brought up to the research vessel as sampling location 9.

the two parallels from location 9 in table 4.4, the concentrations are considerably lower at the surface. This may be a good indication that the amounts released from the Killingdal tunnel has been decreased the last years.

A problem, however, with having highly contaminated sediments relatively close to the sediment surface is possible effects of bioturbation. In the case of having large amounts of organisms living in the sediments, they can disturb the structure of the layers and cause the deeper sediments to be exposed to the water. This can cause the contaminants to come in contact with oxygen-rich water, which can induce a release of trace elements from their complexes and into the fjord. The elements will then be more available to other aquatic organisms, living above the sediments.

4.3.7 Issues with the sediments samples

A big problem with the sediment samples was that most of them were non-homogeneous. Because sediments consist of everything that falls down to the seafloor and stays there, fine grained sand may be mixed with larger grains, or even gravel-sized rocks. This complicates the task of finding representative samples, as trace elements may have higher affinity to some parts of the sediments compared to other parts. In addition, the classification of conditions are drawn based on fine-grained sediments, consisting of clay and/or silt, and they are therefore not intended to be used for sediments containing a large amount of larger particles [60]. Nevertheless, to be able to say anything about the severity of the contamination in the fjord, it is essential to have a classification system to use. The classifications used in this thesis are used by Trondheim Municipality and other institutions [15], and they still give an indication of how polluted the sediments are.

Another problem was that the box corer used in this project struggled from time to time to collect intact sediment sections like the one presented in figure 4.6. In many cases, it took a few attempts before the box corer managed to close and collect a sample. During these attempts, it may have cluttered up the sediment layers, making the sediment section less representative of how conditions actually are on the seafloor. Further, most of the retrieved sediment sections were small and wet, causing them to spread out in the plastic box. This made it hard to collect representative samples.

However, to try and cope with these challenges, it is important to collect several parallels from the same sediments. Two parallel samples were collected at each sampling location, and those samples that were particularly non-homogeneous were further sub-sampled in the laboratory prior to analysis. Unfortunately, the state of the sediment sections brought up from the seafloor were not recorded, so it is not possible to say which sections were intact and not. It is likely that these problems have occurred during earlier sampling of the sediments in Ilsvika. However, it is better to analyse and see what the results indicate, and then be careful with concluding rater than not knowing what the state of the sediments are.

When working with the samples in the laboratory, it became evident that some sediment samples were very discoloured. A strong orange colour, possibly indicating a high amount of iron in the sample, was present. However, a lot of this orange colour was associated with the larger rocks, and therefore excluded from the analysis. The reason is that it is not possible to break down large rocks during the pre-treatment before the ICP-MS analysis, and therefore only the fine-grained parts of the samples were used further. This may have caused some of the samples to present lower levels of contamination than actually present in the sediments. In other cases, there may have been more contamination in the finer parts of the sediment, causing the results to indicate higher concentrations than actually present. However, this is correct according to the ISO standard where larger rocks and other objects should be removed before analysis, so the results will most likely be comparable to other analyses.

4.4 Electrochemical treatment of water from Killingdal

4.4.1 Preliminary test of electrochemical cleaning

A preliminary testing of the setup described in methods section 3.3 and presented in figure 3.7 was performed to check that everything worked and that no toxic gases (like Cl_2 [97]) were released during the process. Both tests, with NaCl and $ZnCl_2$, worked as intended with no toxic gases. Examination of the electrodes after the electrolysis of the $ZnCl_2$ clearly showed deposition of $Zn_{(s)}$ on the cathode. This can be seen in figure 4.7.

During this testing, no ICP-MS samples were taken, but the pH was measured before and after the electrolysis of the $ZnCl_2$ solution. Prior to the experiment, the pH was measured to be 6.02, while after the electrolysis it was measured to be 4.79. This decrease in the pH indicated that one or more acidifying reactions have happened in the solution. The reason why pH is decreasing could be that there is aluminimum released from the anode, and the precipitation reaction between water and aluminium releases protons. Because the preliminary testing showed the potential for trace element removal through deposition and the construction of the electrodes and container was easy to mount, it was decided to continue to use the same setup for all the electrochemical experiments.

4.4.2 Electrochemical treatment of water from Killingdal

During the electrolysis of water from Killingdal, the colour of the water was observed. This was to see if the processes removed enough contaminants for the water to turn into a lighter colour than the orange tone it started with, which would indicate that a lot of the contaminants had attached to the electrodes. However, this did not happen. As far as what could be observed, the water did not change colour during the experiments. Additionally, the colour of the filters after filtering the

Figure 4.7: Zn deposits on the aluminium cathode after the preliminary tests.

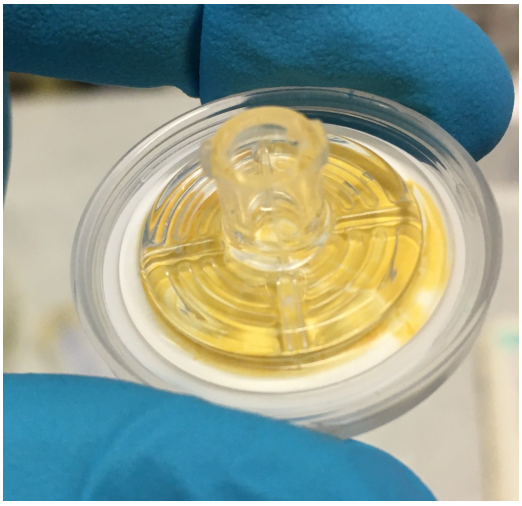

Figure 4.8: Example of a filter after use. The orange colour is caused by the particles the filter prevents from entering the ICP-MS tube.

samples did not change but continued to get an orange stain. The orange staining indicate a high content of iron, and it might also contain elements that are not soluble and rather stay adsorbed to larger particles. An example of how the filters looked after use is shown in figure 4.8.

Although there were no visual differences between the *not treated* and the *treated* water, the ICP-MS results showed that the elemental composition of the water was changing. Table 4.7 gives a summary of the percentage changes in concentrations for the eight trace elements in focus after these experiments, compared to the *not treated* water. In addition, figures 4.9a to 4.12b presents the plotted concentrations from the same experiments. The actual concentration measured are shown in tables K.1 to K.12 in appendix. In addition, aluminium has been included in the results for the electrochemical treatment in table 4.7 and as figure 4.13 due to it being the material of the electrodes in many of the experiments. To make it easier to refer to and follow in the text, the electrochemical treatment experiments were divided into six experiments, named *Experiment 1-6* as in table 4.7, depending on the types of electrodes used and voltage applied. As mentioned in the methods, *Cleansed* water refers to water that has recently been transported through the cleaning facility Trondheim Municipality has in the tunnel at Killingdal, and *Not cleansed* water refers to water that has not been transported through this facility recently but is collected from approximately 20 m inside the tunnel. In addition, *not treated* water refers to water that has not been subject to any of the treatment methods in this thesis, and can describe both *Cleansed* and *Not cleansed* water, while *treated* water refers to water that has been subject to either electrochemistry or activated carbon. These terms are used consistently throughout the thesis. As for the graphs, the concentrations measured are plotted against the time the samples were extracted. The results for one element from all experiments are plotted in one graph. Both in the graphs and in the rest of the section, the names of the experiments that are used in table 4.7 are shortened down to Exp. to make it easier to read. In the bottom of each graph is a description of each line explaining which experiment it belongs to and what type of water was used.

When studying table 4.7 and the graphs in figures 4.9a to 4.13, there are four main trends that can be observed. The first trend is the clear decrease in concentrations. Both iron and arsenic, in addition to copper and zinc in some experiments, decreased in concentrations during the 80 minutes

Table 4.7: Summary of all the percentages removed (green cells) or increased (orange cells) of trace elements in focus during the different electrolysis experiments of *Cleansed* and *Not cleansed* water from Killingdal. The results are divided into six different experiments, depending on the electrodes used and the voltage applied.

	Al	Fe	Cr	Ni	Cu	Zn	As	Cd	Pb
Experiment 1: Aluminium electrodes, 1.0 V									
Cleansed	206	36.2	2540	38.8	29.4	17.3	66.8	8.14	56.9
Experiment 2: Aluminium electrodes, 1.5 V									
Cleansed	246	40.2	6920	4.07	32.7	21.4	69.5	12.9	30.5
Not cleansed	51.1	24.1	1240	61.7	39.2	6.79	69.2	7.70	41.0
Experiment 3: Aluminium cathode and mechanical pencil graphite anode, 1.5 V									
Not cleansed	83.3	10.3	53.8	613	13.3	6.87	42.4	2.45	9.00
Experiment 4: Aluminium cathode and cylindrical graphite anode, 1.5 V									
Cleansed	4.20	10.1	40.3	4.11	6.21	1.92	51.6	1.63	0.720
Not Cleansed	37.6	13.3	45.4	1.94	6.21	1.60	11.9	1.15	35.7
Experiment 5: Aluminium cathode and flat graphite anode, 1.5 V									
Cleansed	10.0	20.2	5.22	92.0	0.325	5.26	41.2	1.44	390
Not Cleansed	35.0	19.5	33.2	268	0.739	13.1	59.1	3.36	306
Experiment 6: Cylindrical graphite cathode and flat graphite anode, 1.5 V									
Cleansed	18.6	8.93	7.30	22.5	3.10	0.356	2.38	1.15	114
Not Cleansed	0.409	8.53	6.61	80.5	12.2	7.34	17.0	0.752	137

Table 4.8: Summary of the measured initial and final pH values during the different electrolysis experiments.

	Initial pH	Final pH
Experiment 3		
Not cleansed 1.5 V	3.46	3.78
Experiment 4		
Cleansed 1.5 V	5.06	5.02
Not Cleansed 1.5 V	3.68	3.80
Experiment 5		
Cleansed 1.5 V	5.05	5.04
Not Cleansed 1.5 V	3.68	3.94
Experiment 6		
Cleansed 1.5 V	5.03	5.05
Not Cleansed 1.5 V	3.69	3.75

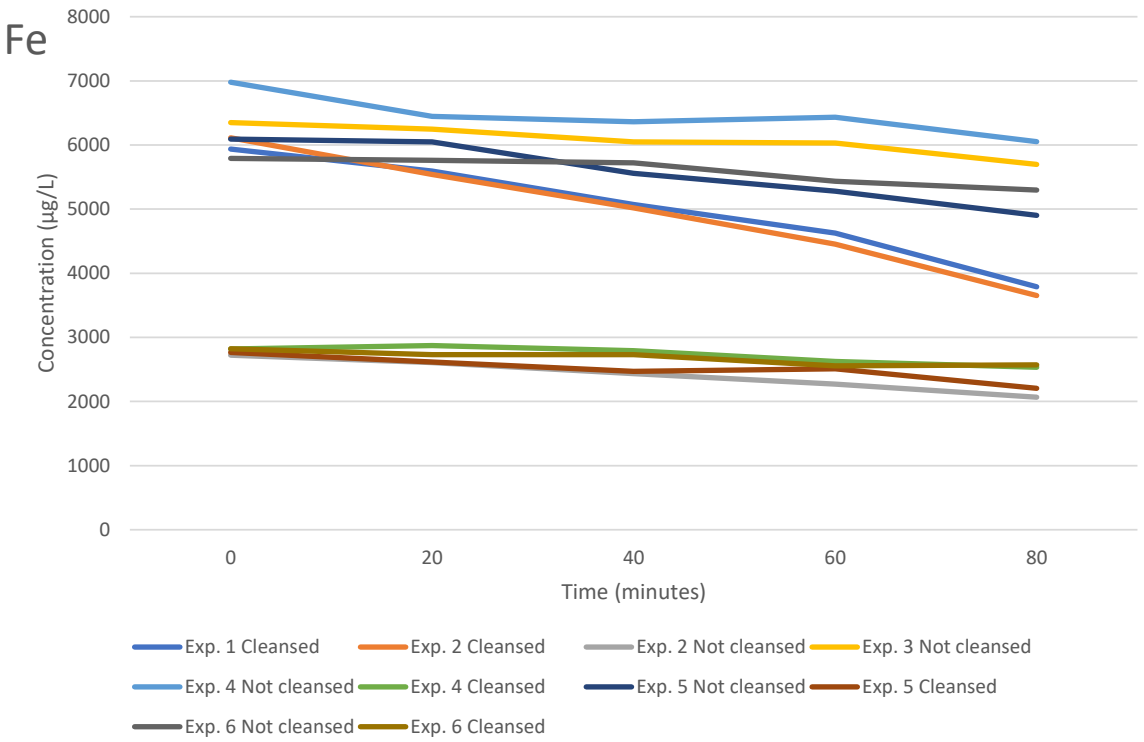

(a)

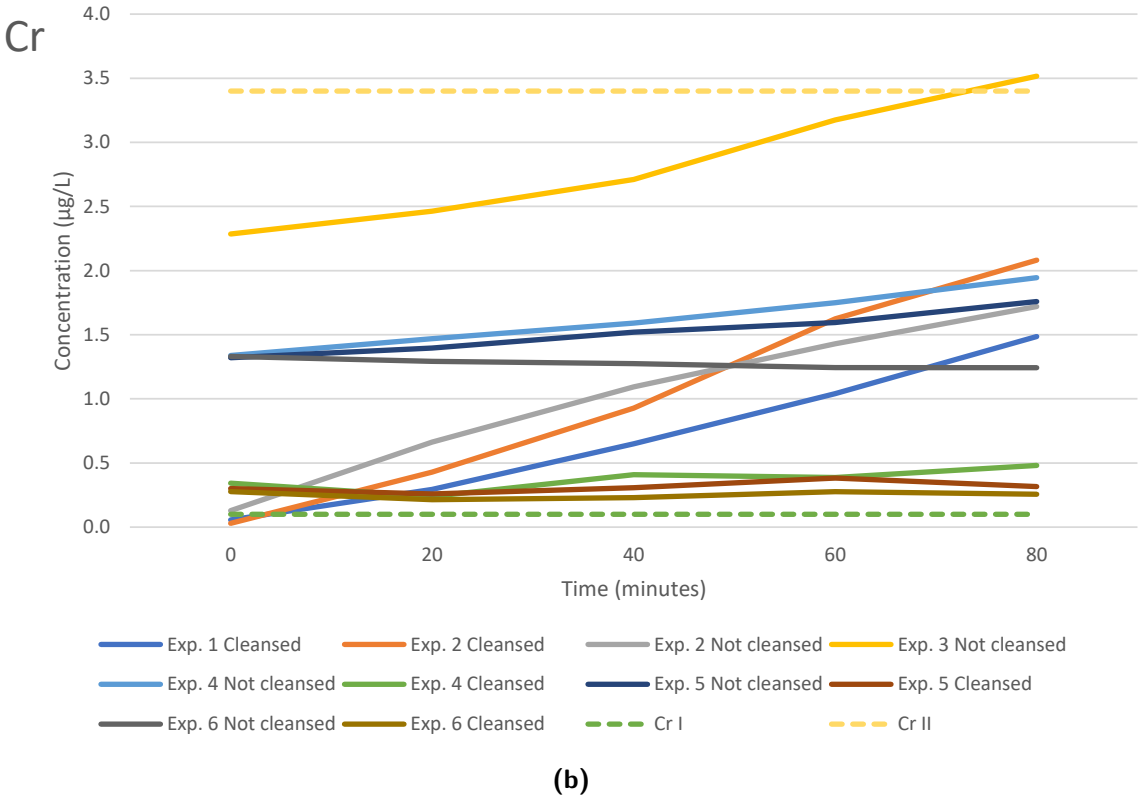

(b)

Figure 4.9: Results from *Experiment 1-6* in regards to 4.9a iron and 4.9b chromium. A line for the corresponding class of conditions is shown where applicable, according to table A.2 in appendix. The time of the sample extraction are on the x-axis.

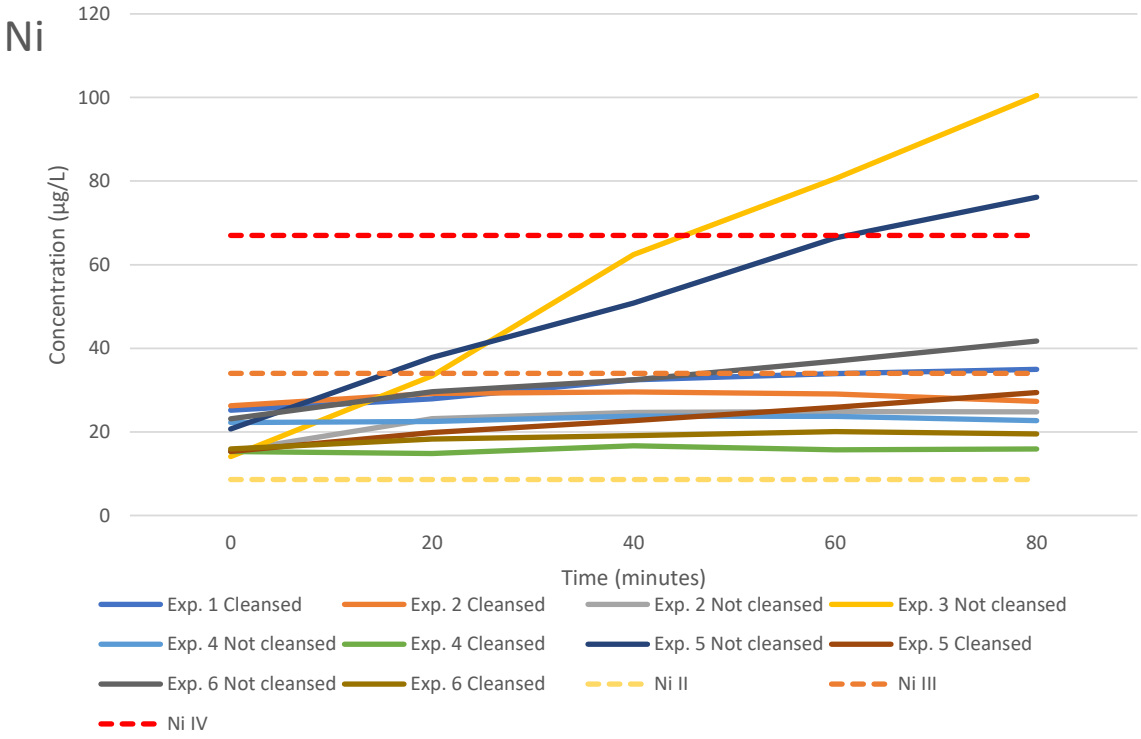

(a)

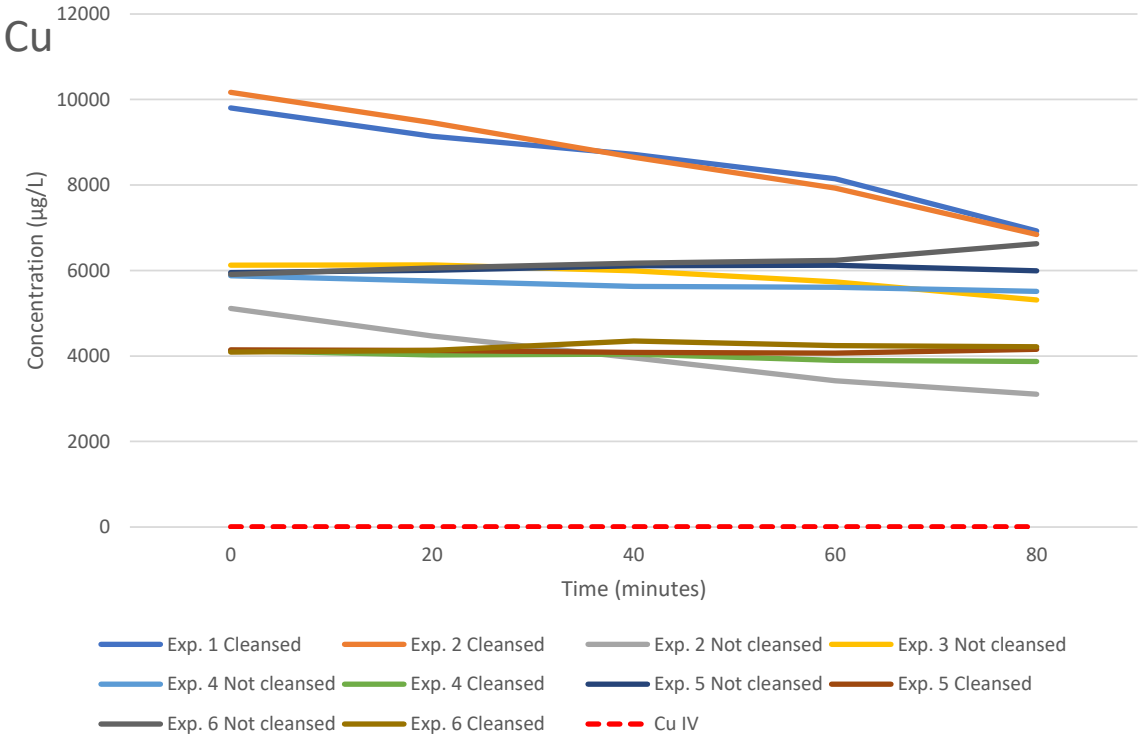

(b)

Figure 4.10: Results from *Experiment 1-6* in regards to 4.10a nickel and 4.10b copper. A line for the corresponding class of conditions is shown where applicable, according to table A.2 in appendix. The time of the sample extraction are on the x-axis.

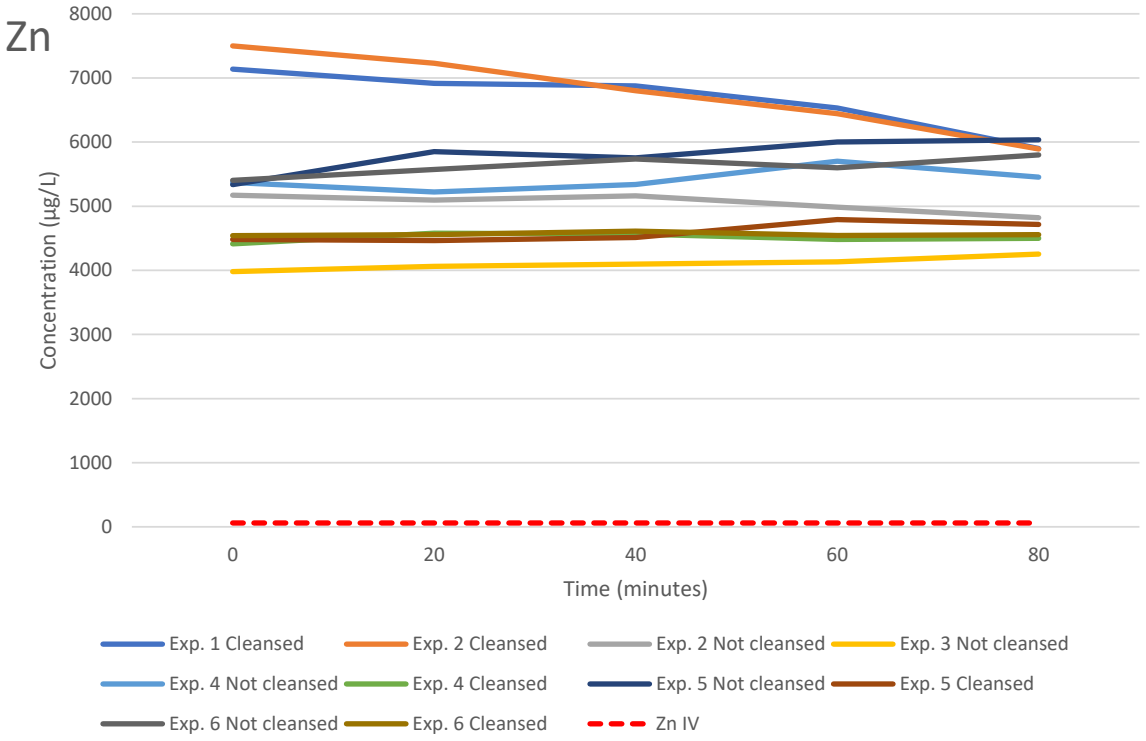

(a)

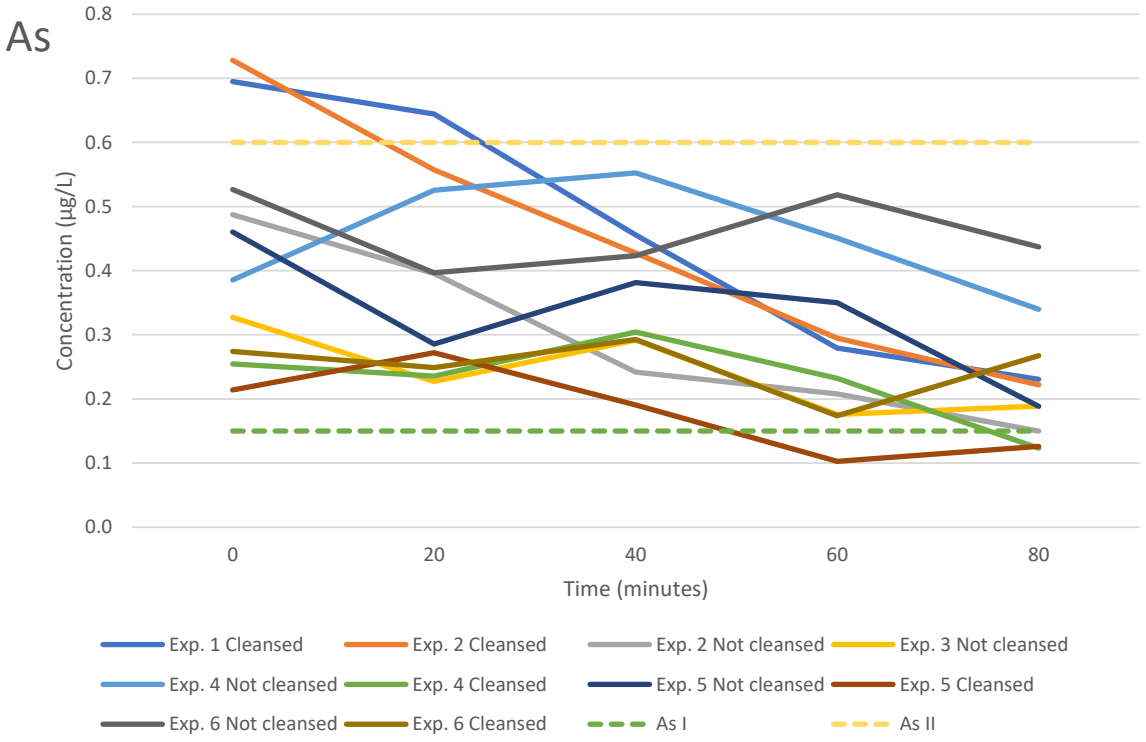

(b)

Figure 4.11: Results from *Experiment 1-6* in regards to 4.11a zinc and 4.11b arsenic. A line for the corresponding class of conditions is shown where applicable, according to table A.2 in appendix. The time of the sample extraction are on the x-axis.

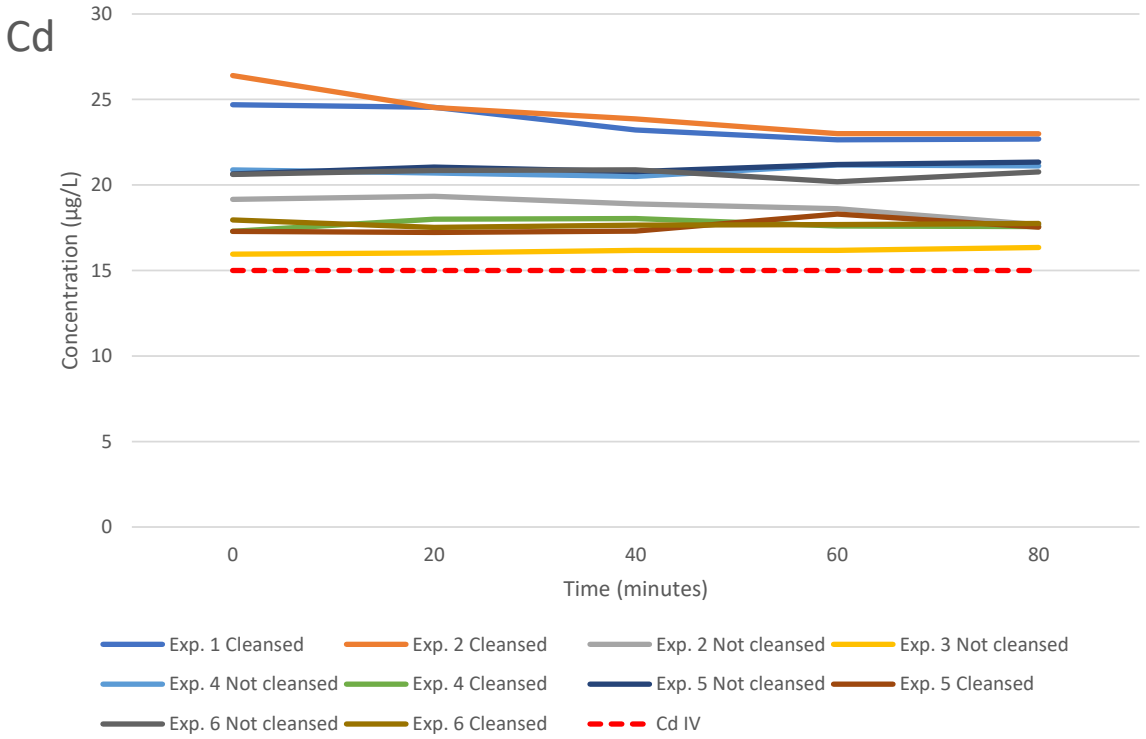

(a)

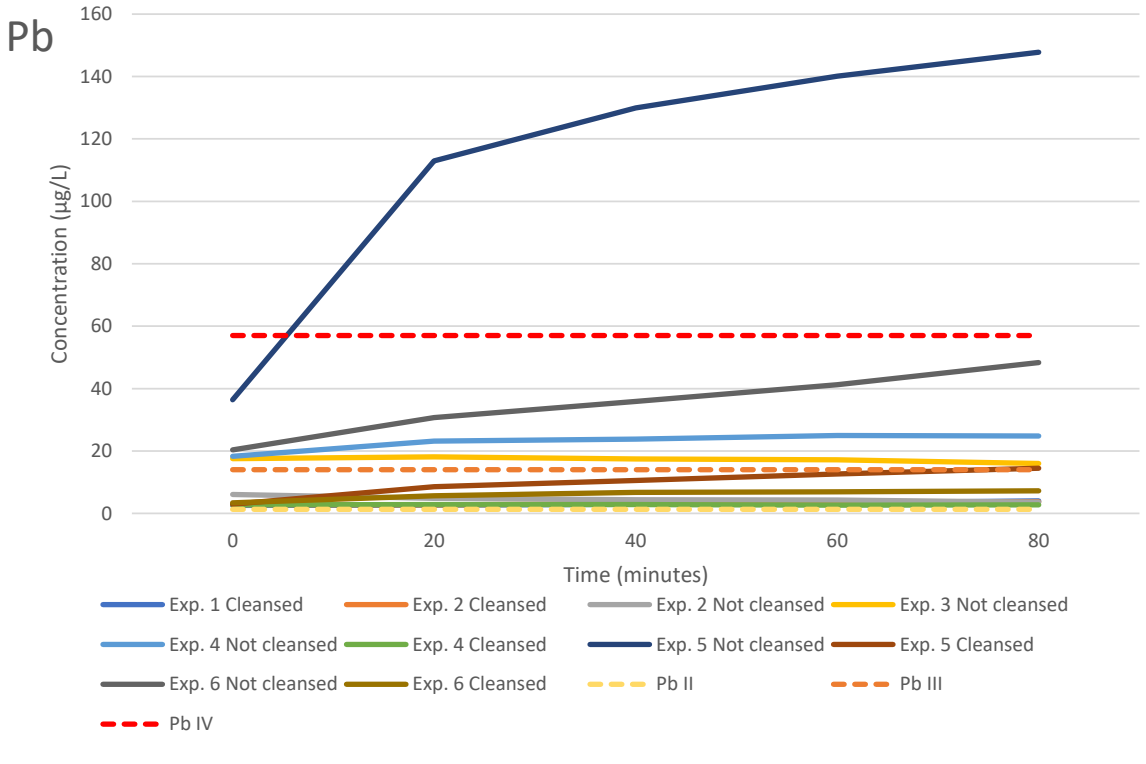

(b)

Figure 4.12: Results from *Experiment 1-6* in regards to 4.12a cadmium and 4.12b lead. A line for the corresponding class of conditions is shown where applicable, according to table A.2 in appendix. The time of the sample extraction are on the x-axis.

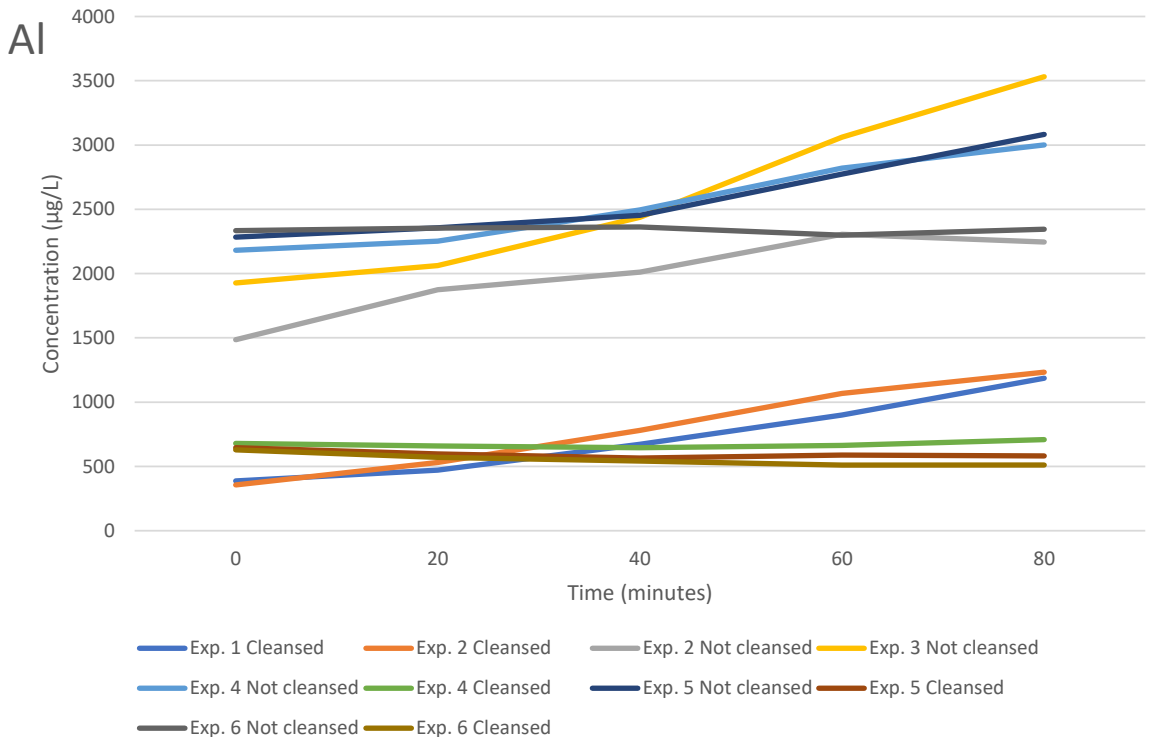

Figure 4.13: Results from *Experiment 1-6* in regards to aluminium. The time of the sample extraction are on the x-axis.

the electrolysis lasted, as indicated by the green cells in the respective columns. In an effort to try and eliminate the effect of interference and noise in the results, all changes larger than 10 % were regarded as a significant change, while all changes lower than this was regarded as no change. The second trend that was observed was the clearly increasing trends. Elements that showed this trend during the electrochemical treatment were aluminium, chromium, nickel, and lead. The third class of trends include the elements that did not show a significant increase or decrease at all, i.e. they are within ± 10 % from the initial concentration. Cadmium is an element that falls into this category, together with zinc and copper from Exp. 3 to Exp. 6. The last type of trends observed was a fluctuating trend. Even though the percentages in table 4.7 does not show it, some of the trends varied greatly throughout the experiments. Arsenic is an example of this, as figure 4.11b shows. Due to the large differences in results and trends, it is interesting to take a closer look at these four trends separately.

4.4.3 Decreasing trends

As described above, the first trend that was observed was the clearly decreasing trend. This is the result that is desired to see after these experiments, as it indicates that the experiments have been successful in removing the elements. The elements that were most successfully removed with the electrochemical treatments were iron and arsenic, both with mainly decreasing trends. For both, the highest removal efficiencies were seen during Exp. 1 and Exp. 2. In both these experiments, aluminium electrodes were used both as anode and cathode. As presented in table 4.7, the iron concentration is decreased by between 24.1 and 40.2 %, which is a substantial amount. There are extremely high concentrations of iron in the Killingdal water, which is the typical composition of

AMDs. This is one of the elements in the AMD that the main treatment step is supposed to remove. However, high amounts can still avoid being removed by this step, and it is therefore an advantage if the polishing step is able to remove more of it.

For arsenic, Exp. 1 and Exp. 2 were even more successful, with a removal of between 66.8 % to 69.5 %. Arsenic is one of the trace elements the polishing step is intended to remove, together with chromium and cadmium. It was therefore good to see that all the electrolysis experiments had an improvement in arsenic concentrations. Even though the initial concentrations are low, generally in class II, as can be seen from figure 4.11b, the results indicate that arsenic can be removed by electrochemical treatment.

In Exp. 5 significant decreases in concentrations for both iron and arsenic were observed again, although not as high as for Exp. 1 and Exp. 2. This was the experiment where a cylindrical shaped aluminium cathode was combined with a flat graphite anode. Iron was removed with approximately 20 %, while the removal of arsenic was 41.2 % and 59.1 % for *Cleansed* and *Not cleansed* water, respectively. Figure 4.9a shows that while the initial iron concentrations for Exp. 2 and Exp. 5 are approximately the same, the concentrations after the experiments are very different. One thing to notice in figure 4.9a is that for Exp. 1 and Exp. 2, the iron concentrations are higher in *Cleansed* water compared to *Not cleansed* water, which is opposite to the other experiments where the *Not cleansed* water usually has the highest concentration. This could be due to changes in the treatment facility operated by Trondheim Municipality at Killingdal. In this time period they tested addition of sodium hydroxides combined with polymers, which could have altered the composition of species in the *Cleansed* water. Regardless of the reason why the iron concentrations are high in the different types of water, the amount present is more efficiently removed by the electrolysis with only aluminium electrodes compared to all the other combinations of electrodes.

For arsenic the removal efficiencies in table 4.7 are relatively high for many electrode combinations. However, the RSD values, or uncertainty in the values, are very high for the experiments other than Exp. 1 and Exp. 2, causing the concentrations measured to potentially overlap. The experiments with aluminium electrodes were the only experiments where this was not the case, indicating that this method works for arsenic removal. In addition, as figure 4.11b shows, the electrolysis with aluminium electrodes has the potential to remove enough arsenic to move down from class III to almost class I.

The distribution of divalent and trivalent iron ions in the water from Killingdal was not investigated during this study. However, the pH of the water was always above 3.46 and as Fe^{3+} tend to precipitate as $Fe(OH)_3$ and other solids in the pH range 3.5-7.0 [98], it is reasonable to conclude that most of the dissolved iron in the Killingdal water is present as Fe^{2+}, which can stay dissolved in water at higher pH values. When the voltage is applied to a solution containing Fe^{2+} ions several reactions can take place. The Fe^{2+} ion can be reduced to its solid, elemental form by the cathode, through the addition of two electrons. Another option is that the Fe^{2+} ion is oxidised at the anode or by coming into contact with the oxygen mixed into the solution. The Fe^{2+} ion will then be transformed to the ($Fe_3{}^+$) ion, which can precipitate as $Fe(OH)_3$ or $Fe_3O_4(s)$ through

$$Fe_2{}^+ + 2\,Fe^{3+} + 8\,OH^- \longrightarrow Fe_3O_4(s) + 4\,H_2O \tag{4.1}$$

or

$$2\,Fe^{3+} + 3\,H_2O \longrightarrow Fe_3O_4(s) + 6\,H^+ \tag{4.2}$$

[99]. Iron may also transform into other secondary minerals.

As table 4.7 shows, the highest removal efficiencies of iron corresponds to the highest removal efficiencies of arsenic, and as mentioned in section 2.3.8 arsenic has a strong adsorption affinity towards iron hydroxides. During the precipitation of iron hydroxides in this electrochemical experiment, the pH remained between 3.4 and 5.1. In this pH range, the adsorption of arsenic (V) is the most efficient one, as $H_2AsO_4^-$ is the predominant As(V) species at pH 2-7 [100] and the iron hydroxide surface is positively charged [101]. For arsenic (III) on the other hand, H_3AsO_3 is the predominant species below pH 9, which is not as successfully adsorbed onto the iron hydroxides, as it lacks the negative charge that is attracted to the positive iron hydroxide surface. However, Kumar et al. [102] concluded in their study that during electrocoagulation arsenic (III) is oxidised to arsenic (V), and then adsorbed onto iron hydroxides. They tested both iron anodes and aluminium anodes, and found that the iron hydroxides produced from the iron anode had a greater capacity for arsenic removal compared to aluminium hydroxides. The experiments with aluminium electrodes in this thesis can be categorised as an electrocoagulation experiment. Even though aluminium is the element released form the anode, iron also exists in the solution and is precipitated during the process as discussed above. The electrolysis with aluminium electrodes, i.e. Exp. 1 and Exp. 2, are the experiments where most iron and arsenic were removed. This may indicate that iron hydroxide precipitation of arsenic (V) is the main route for arsenic removal. The produced particles can potentially be removed by sedimentation or flotation.

In addition to iron and arsenic, the removal of copper and zinc were also most successful in Exp. 1 and Exp. 2, as can be seen from table 4.7. Copper and zinc are found in extremely high concentrations in the Killingdal tunnel, similar to iron. In figure 4.10b and 4.11a, both copper and zinc are present in concentrations a great deal higher than the lower limit for class V. Even though a lot is removed, there is still a large amount of copper and zinc in the water that needs to be removed before releasing the effluent into the fjord. Nariyan et al. [73] found that copper is removed during the electrocoagulation with an aluminium anode, but the efficiency is lower than with an iron anode. Their conclusion is that the aluminum particles are smaller than the iron particles, causing the iron hydroxides to have a larger surface area where other elements can adsorb. However, AMD is a complex mixture of elements and their species, and copper and zinc have both been proven to adsorb to both aluminium and iron particles [73]. In this experiment, copper and zinc may have been removed by either adsorption or co-precipitation onto iron hydroxides or aluminium hydroxides, or by the deposition onto the cathode.

In the preliminary test of the setup described in section 4.4.1 it was obvious that zinc was deposited onto the cathode. However, this deposition was not as evident during the electrolysis with water from Killingdal. Several reasons could explain this. First, the amount of zinc was a lot higher in the test solution. While the concentration of zinc in the test solution was 0.65 g/L, the average concentration of zinc in the water from Killingdal was between 0.004 g/L and 0.0075 g/L. In addition, zinc has a relatively negative reduction potential compared to the other elements in the AMD solution, as table 2.4 in section 2.9.2 shows. During this experiment, the actual induced voltage on the electrodes was not measured, but it could be lower than the 1.5 V the voltage source was set to. This could make the reduction efficiency of zinc less during the experiments with the water from Killingdal.

Spatial decreasing trends were observed for aluminium and lead. As table 4.7 shows, aluminium is removed by 18.6 % for the *Cleansed* water in Exp. 6, when only graphite electrodes were used. Lead, on the other hand was removed by 41.0 % during Exp. 2 with *Not cleansed* water. This could be a coincident, or it could imply the potential for removal of these elements as well.

4.4.4 Increasing trends

The second trend observed in table 4.7 is a clear increasing trend of element concentrations. This was an undesired trend, which should be limited as much as possible. The elements that showed clear increasing trends were aluminium, chromium, nickel and lead.

In addition to the main eight trace elements in focus, aluminium was also investigated. The reason was that both the anode and the cathode in the first electrolysis experiment were made of aluminium. It was therefore necessary to check if the anode released any cations into the solution. The experiments with aluminium electrodes (Exp. 1 and Exp. 2) can be categorised as electrocoagulation experiments, as mentioned in the previous section. Aluminium is a common material for sacrificial electrodes. They are designed to dissolve into the solution during electrolysis through

$$Al_{(s)} \longrightarrow Al^{3+}_{(aq)} + 3\,e^- \tag{4.3}$$

So an increase in aluminium concentration is anticipated. These ions will produce hydroxides in the water, and precipitate.

To check the influence of the aluminium electrodes on the aluminium concentration, two blank experiments were run with a saline solution with known concentration (10^{-4} M $NaSO_4$) instead of water from Killingdal. The first experiment was run without any voltage applied. Results showed that the concentration of Al in the water increased from zero to a maximum of 0.805 µg/L during the first 40 minutes. After this, it decreased. In the second experiment, a voltage of 1.5 V was applied. This caused the release of aluminium to increase more than with no voltage, but only to a maximum of 12.4 µg/L after 40 minutes. An explanation could be that the high number of ions in the water from Killingdal is favouring the dissolution of the anode, while the lower concentration in the blank solution is not equally suited for the release of aluminium ions. In addition, reaction could happen in the complex water from Killingdal, which enhance the dissolution of aluminium ions, that will not take place during the blank electrolysis. A third explanation could be that some of the particulate aluminium species in the Killingdal water might be oxidised or reduced, causing dissolved aluminium to be released into the water.

The high release of aluminium during the electrolysis with only aluminium electrodes was the reason why it was decided to try other anode materials, to see if the removal of trace elements could be remained without increasing the aluminium concentration. And by looking at the removal percentages in table 4.7 the amount of aluminium released is decreased when graphite is used as the anode material instead of aluminium. And as mentioned before, in Exp. 6 *Cleansed* when only graphite electrodes are used, aluminum is removed from the solution after the electrolysis. The experiments with graphite anode, Exp. 3 to Exp. 6, can be described as a combination of electrocoagulation, electroflotation and electrodeposition. There was most likely a production of hydrogen gas at the cathode, as this is a favorable reaction, that could transport precipitated contaminants to the surface

of the water in the container. However, due to the stirring of the solution, this precipitation was not left to float, but might have been mixed into the water. No bubbles or floating sludge were observed, indicating that the electroflotation was not a big part of why trace elements were removed from the water. The graphite electrode was not dissolved during the electrolysis, but iron and aluminium already existing in the solution may have precipitated and adsorbed several of the other trace elements in the solution. Some electrodeposition may have happened with iron, copper and zinc.

As the graphs in figure 4.13 show, the initial aluminium concentration is relatively high, with the *Not cleansed* water holding at least 1490 µg/L aluminium before the experiment starts. Because the ICP-MS cannot analyse particles and the samples had to be filtered before analysis, the concentrations measured before the experiment are only representative of the dissolved fraction of the aluminium in the solution, while the total concentration is unknown. However, with such high dissolved concentrations, it is reasonable to think that there is aluminium in the particles removed by the filters. Aluminium is subject to hydrolysis, producing species such as $Al(H_2O)_5(OH)^{2+}$ and $Al(H_2O)_4(OH)_2{}^{+}$ at pH above 3, $Al(OH)_3$ at around pH 6.5, and $Al(OH)_4{}^{-}$ in more basic conditions. The water at Killingdal usually varies between a pH of 3 and 5, depending on the treatment. Due to this, it is reasonable to think that a large amount of the hydrolysed aluminium in the water exists as $Al(H_2O)_5(OH)^{2+}$ and $Al(H_2O)_4(OH)_2{}^{+}$, which can further interact with particles and ligands in the water. [16]

Chromium, nickel, and lead were all desired to be removed by electrochemical treatment, as they often are hard to remove during main treatment steps and chromium is even released when the water is treated by olivine, and adsorption material that has an efficient removal capacity for many of the other elements in the AMD [72]. As figure 4.9b shows, the chromium concentration is not extremely high in the AMD initially. However, after the electrochemical treatment, the concentrations increase greatly, and for Exp. 3 *Not cleansed* water, the concentration even exceeds the lower limit of class III. The highest percentage increase of chromium happened during Exp. 1 and Exp. 2, when only aluminium electrodes were used.

Chromium is an element that shows a strong affinity to the aluminium secondary mineral precipitates. In the typical AMD conditions, chromium is present as $HCrO_4{}^{-}$, and when positively charged aluminium compounds are formed at pH of approximately 4.5-5, the chromium ions will react with them [65]. In table 4.7 it is evident that Exp. 1 and Exp. 2 had the highest increase for both aluminium and for chromium. Even though the increase was expected for aluminium, it was not expected that chromium would increase from background levels to well into class II. No pH was measured during this experiment, but the other electrolysis experiments generally had an initial pH of 3.5-3.7 for *Not cleansed* water and approximately 5 for *Cleansed* water, as summarised in table 4.8. More chromium will potentially adsorb to the aluminium minerals in higher pH because there is a higher amount precipitating. This may explain why the chromium concentrations are lower in the *Cleansed* water.

In the blank experiments with aluminium electrodes the chromium concentration did not increase significantly. As table K.5 in appendix shows, the chromium concentration reached a maximum of 0.008 86 µg/L at 60 minutes, then it decreased again. This is a relatively low increase compared to what is released in most of the other experiments. No chromium should exist in the aluminium electrodes, which means that what is released presumably comes from particles in the solution.

For nickel, the most drastic increase in concentration takes place during Exp. 3 and Exp. 5, as illustrated by figure 4.10a. The nickel concentration increase from the lower parts of class III to far into class V during the 80 minutes the electrolysis lasted, and by looking at the trends it does not appear to flatten out any time soon. During the blank experiments there was a substantial release of nickel into the test solution. The nickel concentration increased by 52.7 µg/L and 12.7 µg/L without and with an applied voltage of 1.5 V respectively. Considering that the initial concentration of nickel was measured to be below 1 µg/L in these blank experiments, this is quite a lot, especially when the initial concentration in many of the other experiments were around 20 µg/L. Considering this, the large increase in nickel seen in figure 4.10a could be the result of a contamination from parts of the equipment, especially for Exp. 1 and Exp. 2 which had the same setup as the blank experiments. Some of the increase in nickel concentrations observed could also be attributed to the dissolution of relatively insoluble nickel complexes or release of nickel from particles during electrolysis.

In addition to the reduction of trace element ions to their elemental form on the cathode, the reduction of protons to hydrogen gas happens and compete with the other processes. As table 2.4 from section 2.9.2 shows, lead, nickel and chromium all have a lower reduction potential than the hydrogen gas-producing reaction. The reduction reactions of lead, nickel, and chromium are therefore not as electrolytically efficient as e.g. the removal of copper. One explanation to why these trace elements were not removed during the experiments could be that the voltage is not high enough to let all the reactions take place at once, and that the pH is too low for e.g. $Ni(OH)_2$ to precipitate [103]. However, when looking at the trends in table 4.7 it is evident that the highest increase for the different elements do not occur during the same experiments.

In the case of lead, the highest concentration increase happened during Exp. 5 and Exp. 6, as illustrated in figure 4.12b. In Exp. 5 *Not cleansed* water, the concentration increases by 306 %, ending up at more than twice the lower limit of class V. No lead was released from the blank experiments, indicating that the released lead is coming from the water itself. When examining the trends it appears that many of the curves are flattening out during the electrolysis. Since the results only represent the dissolved element fractions, it would be interesting to measure both the total lead concentrations in particulate form and dissolved form, to see if the trends flattening out is because approximately all the particulate lead is dissolved, or if there are any particles left. Or maybe the amount removed has caught up with the amount released from solution.

4.4.5 Flat trends

As mentioned previously, a change in concentration in this thesis is defined as above 10 % to minimise the influence of interference and noise. In addition, with the concentrations as those in the water from Killingdal, a 10 % will seldom have any large impacts on the removal of trace elements. Therefore, a third category of trends that could be observed in table 4.7 was those removal efficiencies within the ±10 % range. An element that shows this trend is mainly cadmium for all the experiments, in addition to copper and zinc from Exp. 3 to Exp. 6. All the other elements had at least one experiment showing no trend, but the majority of their results were either increasing or decreasing.

One experiment, Exp. 2 with *Not cleansed* water, had a decrease in cadmium concentration of 12.9 %. The rest were well within the ±10 % range, whether they were increasing or decreasing. As cadmium is one of the trace elements that the polishing step should take, because the main

treatment step appear to be insufficient in removing cadmium due to the small difference in *Cleansed* and *Not cleansed* water in figure 4.12a, this is a disappointing result. Figure 4.12a also illustrates that there are little or no changes in the cadmium concentrations during the electrolysis. Only Exp. 1 and Exp. 2 *Cleansed* show any significant changes. Still the concentrations continue to stay above the lower limit of class V, indicated by the red dotted line.

Neither in the blank experiment with applied voltage nor in the experiment without applied voltage was an increase in cadmium concentration observed, as the tables in appendix K.2 show. This is a positive result, as it indicates that the system does not supply the water with cadmium. In addition, the small amounts released during some of the electrolysis experiments may then come from particles in the water. According to Escobar et al. [104] the optimal conditions for removal of cadmium is at pH 7 and high concentrations. While cadmium is found in high concentrations in the Killingdal water, the pH is far from optimal, making the conditions less favourable for cadmium removal by electrocoagulation.

The low removal of zinc in these experiments was briefly discussed in section 4.4.3. According to Nariyan et al. [73] both copper and zinc removal are more efficient when iron anodes are used compared to aluminium electrodes. This was attributed to the larger sizes of the iron particles compared to the aluminium particles. They also observed that the iron anodes increased the pH and decreased the reduction potential of the solution more than the aluminium anodes. These factors could explain why the removal efficiency is low for zinc, and to some extent copper. An effect like this is probably not there in this extent when graphite anode is used, as this is inert to the electrolysis. However, other reaction can happen at the anode, causing e.g. already precipitated compounds to dissolve or induce the oxidation of Fe^{2+} to Fe^{3+}. As the solution was stirred during the experiments, the precipitates had nowhere to sediment, causing them to potentially come into contact with the opposite electrode of where they started, and be dissolved.

Copper has a reduction potential higher than the reaction for hydrogen gas production at the cathode. It was therefore assumed that there would be a high copper removal during these experiments. However, only Exp. 1 and Exp. 2 showed significantly decreasing copper concentrations, while the other experiments did not have any great effects, seen in figure 4.10b. According to Milchev and Zapryanova [105] copper deposition happens in a two-stage reaction.

$$Cu^{2+} + e^- \longrightarrow Cu^+ \quad \text{slow step} \tag{4.4}$$

$$Cu^+ + e^- \longrightarrow Cu_{(s)} \quad \text{fast step} \tag{4.5}$$

The slow reaction in equation 4.4 may have limited the deposition in the experiments in this thesis. It would be interesting to see if a higher potential or a longer retention time could increase the copper removal.

4.4.6 Non-linear trends

The last type of trends that was observed from the results was that some element concentrations varied greatly during the electrolysis. Instead of moving only downwards or upwards in an approximately linear manner, the concentrations were both higher and lower than the initial concentration in the time frame the experiments lasted, or they had a higher increasing or decreasing rate in some parts of

the experiment compared to others. This was called the non-linear trends, and is not easily detectable from table 4.7, as these percentages are calculated from the initial and final concentrations only. However, the graphs in figures 4.9a to 4.13 show these fluctuations.

The most prominent element in this category is arsenic. As figure 4.11b shows, the concentrations vary greatly during the different experiments. Exp. 4 *Not cleansed* can be used as an example. At first there is an increase of more than 0.15 µg/L during the first 40 minutes, then the concentration drops to approximately 0.5 µg/L lower than the initial concentration. In table 4.7 this looks like an 11.9 % decrease, but during the experiment there is actually first an increase of 43.3 %, something that makes it hard to predict the change of arsenic concentration in the water. However, all the RSD values for the arsenic concentrations in the electrochemical treatment experiments were high. This is most likely due to the low concentrations of arsenic in the Killingdal water. The large fluctuation could be a result of uncertain values and actually represent noise in the ICP-MS machine rather than real concentrations. Exp. 1 and Exp. 2 were the only experiments that had a significant change of arsenic concentrations even after the RSD values were accounted for. These are also the lines in figure 4.11b that show the least variations during the electrolysis, which supports that these results are reliable and that the electrolysis with aluminium electrodes were successful in the removal of arsenic with 66.8 % to 69.5 %.

Lead was another element that was observed having non-linear trends during Exp. 5. As the dark blue line in figure 4.12b shows, the concentration of dissolved lead increases with a relatively steep slope in the first 20 minutes of the experiment, then the curve flattens out more and more after this. As theorised in section 4.4.4 this might be due to the dissolution of the particulate lead fraction. It appears that these reactions happen relatively fast and more easily in the beginning, when a lot of lead particles are available to react. However, after a while there are less particulate lead that can react, and the dissolution declines.

4.4.7 General discussions

When examining the initial concentration of all the elements in Exp. 2, it is observed that the *Cleansed* water contain higher concentrations of iron, nickel, copper, zinc, arsenic, and cadmium compared to *Not cleansed* water. This indicates that the treatment method is changing the chemistry of the water into more dissolved elements when it flows through. Meanwhile, aluminium and lead have significantly higher concentrations in the *Not cleansed* water compared to the *Cleansed* water, which is the desired result. In this period, the treatment facility operated by the Municipality at Killingdal used sodium hydroxide (NaOH) to increase the pH of the water and polymers to increase the flocculation and sedimentation speed of the precipitated contaminants. This experiment was carried out on the 02.10.2019. pH measured in *Cleansed* water by Trondheim Municipality around this date are presented in table 4.9. When the pH is as high as shown in table 4.9 it is possible that several of the elements are hydrolysed to negative species, causing the sludge to be more unstable and the species to be more soluble in the water.

Fortunately, these elevated element concentrations in the *Cleansed* water compared to the *Not cleansed* does not continue. One feature that is visible from many of the graphs in figures 4.9a to 4.13 is that there is a difference in initial concentration in the *Cleansed* and *Not cleansed* water in Exp. 4 to Exp. 6, with *Not cleansed* having the highest concentrations. Elements for which this

Table 4.9: pH measured by Trondheim Municipality in the *Cleansed* water at Killingdal from 17.09.2019 to 04.10.2019.

Date	17.09	27.09	03.10 (10:22)	03.10 (14:45)	04.10
pH	6.20	8.50	8.60	7.00	9.90

is observed are aluminium, iron, chromium, nickel, and lead. Even though the *Cleansed* and *Not cleansed* water are collected at separate days, due to limited transportation options and time, they were collected four days apart, and there had not been any major changes in the treatment facility at Killingdal, so the differences observed are most likely caused by the removal of elements by the remediation methods. This could indicate that the procedure used in the treatment facility in the Killingdal tunnel made by Trondheim Municipality has started to work.

As mentioned above, *Not cleansed* water used in Exp. 4 to Exp. 6 is collected at the same day in the same container. They should therefore have the same initial concentration for all elements. However, while the concentrations are approximately the same throughout all the experiments for chromium, nickel, copper, zinc, and cadmium, it is varying for aluminium, iron, arsenic, and lead. For aluminium and arsenic the differences are small, which differ with 153 µg/L and 0.141 µg/L respectively. For iron and lead however, the changes are much bigger. As tables K.7, K.9 and K.11 in appendix show, iron varies in initial concentration by 1190 µg/L, and lead varies by 18.12 µg/L. None of the initial concentrations in the *Cleansed* water varied as much as this. Could it be that the water tanks were not mixed well enough? Would this cause iron to precipitate and lead to dissolve?

Due to the length of the experiments and convenience when it comes to bringing water from Killingdal to the laboratory at NTNU, it was decided to do Exp. 4, Exp. 5, and Exp. 6 with *Not cleansed* water one day, and *Cleansed* five days later. During this period Trondheim Municipality did not change their treatment facility or the treatment method used. The two days before the collection of *Cleansed* water a relatively high amount of snow has occurred, but no rain and snow melting had been detected. This indicates that there had not been any big changes of the conditions around the tunnel during the five days span, and that the input of new water probably had been low. It can therefore be assumed that the *Cleansed* water collected five days later is approximately the same in composition and pH as it was when the *Not cleansed* water was collected.

The total concentration of elements has not been analysed, only the dissolved concentrations. When concentrations of elements increase, we cannot be certain if the electrochemical treatment works or not. There are two possibilities when concentration increases:

1. The elements that increase in concentration are desorbed from the particles they are attached to, and in some cases they may be released from the electrodes (Al), and nothing is attached to the electrodes.

2. The elements that increase in concentration are desorbed from the particles they are attached to, and in some cases they may be released from the electrodes (Al), but some of it is attached to the electrodes. However, more is released from particles than attached to the electrodes, which causes an increase in concentration instead of a decrease.

How well the method would work had there been only dissolved elements and not particle bound

elements is hard to say for certain. It could be possible to gain more knowledge if total concentration of all fractions were measured before and after electrochemical treatment. If the total concentration was the same, we could say that nothing had been attached to the electrode, only desorbed from particles. If the total concentration had decreased, it could be concluded that some of the element concentration had been attached to the electrodes.

For the elements nickel, copper, zinc, arsenic, and cadmium, the initial concentrations are higher for the experiment with aluminium electrodes compared to the experiment with graphite electrodes. While nickel showed an increase during the electrolysis, the other elements decreased. It is therefore a possibility that a higher initial concentration have caused the greater removal efficiencies observed during the experiment with solely aluminium electrodes. In a study by Wang et al. [101] where they tested the removal efficiency of arsenic by electrochemical pH adjustment and precipitation with $Fe(OH)_3$, they had higher removal efficiencies (initial concentration was 8 mg/L to 60 mg/L, removed 99 %) compared to another experiment performed with much lower initial concentrations of arsenic (initial concentration was 0.05 mg/L to 1 mg/L, removed 53 %). Also the removal of copper and cadmium have been observed to decrease as initial concentration decrease during electrocoagulation experiments [104]. On the other hand, there appears to be no trend of the water with highest concentrations experiencing the highest removal efficiencies within experiments. And for copper in the electrolysis with only aluminum electrodes, as an example, table 4.7 shows that the *Not cleansed* water experiences the highest removal efficiency even though it has the lowest initial concentration. This might strengthen the theory that the experiment with solely aluminium electrodes is the best method to remove the elements, but to say anything for certain, an experiment with the same water would have been necessary.

When comparing all the different electrolysis experiments with each other form table 4.7, the electrolysis with aluminium electrodes (Exp. 1 and Exp. 2) appears to be the most efficient method to remove dissolved iron, copper, zinc, arsenic, and cadmium, and to some extent lead. On the other hand, Exp. 6 with only graphite electrodes worked best for aluminium and chromium. It might appear as the extra coagulants released from the aluminium anode are what is needed to make smaller suspended particles come together to either sediment or float, while the absence of the extra coagulants makes trace elements harder to remove. Nickel was released in all experiments, but was released in lowest amount in total during Exp. 4. It seems like the best electrochemical treatment would be a method where iron and aluminium in the solution are precipitating and scavenging all the other elements. Further work to improve this method could be to test water with elevated pH values higher than 5, to see if this could have any impact on the removal efficiency. In addition, it would be interesting to see if several aluminium wire fence pieces as used as the cathode in the experiments with graphite could be stacked in layers, to get a longer contact time and potentially more contact overall between the water and the cathode, and a larger area where trace elements could deposit onto.

4.5 Treatment of water from Killingdal with activated carbon

When activated carbon was tested as a polishing step for the AMD water at Killingdal, it was only possible to use *Not cleansed* water. This was due to the arrangement of the treatment facility operated by Trondheim Municipality. The ideal situation would have been to use the *Cleansed* water to see the polishing step ability, but the results will hopefully give an indication of the capacity and specific removal efficiency for each trace element. Due to this, *not treated* water refers to *Not cleansed* water only in this chapter.

Initially, the gravel used to avoid clogging of the bottom valve by activated carbon was rinsed with a total of 21 L *Not cleansed* water. This was carried out to rinse away potential contaminants and saturate the potential adsorption capacity of the gravel to avoid it affecting the results concerning the activated carbon. Table 4.10 presents the concentrations of the different trace elements in the *Not cleansed* water before use and in a sample taken when the last of the added water run through the gravel (when approximately 21 L have passed through). In addition it shows, in percentages, how much is found in the water after it has passed through the gravel compared to before.

As table 4.10 shows, the largest difference is in the copper concentration. It has been reduced by 10.7 %, which may indicate an adsorption or filtration capacity of the gravel towards copper. The significance of the difference was tested with a Mann-Whitney U test. It was conducted with the measured concentrations in water before and after gravel rinsing for each element separately. The results from table 4.10 were combined with results from two other gravel experiments to get enough parallels to test statistically. The normality of the groups were tested with a Shapiro-Wilk test, and it was found that no combination of concentrations in the water before rinsing and after were both normally distributed, which is presented in table L.1 in appendix. This is the reason why a Mann-Whitney U test was conducted, to check the significant difference between two groups without them being normally distributed. The results obtained from the the Mann-Whitney U test are presented in table L.2 in appendix and the p-values are included in table 4.10 for each element. From this, the conclusion was that there were statistically no significant difference between before and after rinsing, as all the p-values are above 0.05.

Table 4.10: Results from rinsing of gravel used to avoid activated carbon from clogging the valve in the setup at Killingdal. The RSD, i.e. uncertainty, is marked red when it was significant (above 10 %). P-values from the Mann-Whitney U test are also included.

	Not cleansed		After rinsing		Remaining	p-value
	Conc. (µg/L)	RSD (%)	Conc. (µg/L)	RSD (%)	(%)	
Fe	5700	1.9	5330	1.3	93.6	0.881
Cr	0.492	3.5	0.519	15.6	105	0.881
Ni	51.6	2.1	48.0	1.5	93.0	0.881
Cu	20500	0.9	18300	1.6	89.3	0.881
Zn	13200	1.6	12800	2.0	96.9	0.881
As	0.258	23.6	0.264	25.4	102	0.881
Cd	50.0	0.98	48.2	1.89	96.5	0.655
Pb	3.35	1.8	3.07	2.9	91.6	0.456

As mentioned in section 3.5, approximately 220 g of activated carbon was used in this treatment experiment. The amount used varies greatly between studies, dependent of which type of activated carbon that is used, and which element the method is supposed to remove. Eeshwarasinghe et al. [106] used a range of 0.05 to 0.8 grams of activated carbon per litre of water, while a review by Kurniawan et al. [107] reported as much as 20 grams activated carbon per litre of water. Due to the extremely high concentrations of different elements in the Killingdal tunnel, it was decided to use an amount that corresponded to the upper part of this range. Therefore, 220 g of activated carbon, or approximately 15 g/L, was used.

The results are presented in figure 4.14 and the actual concentrations are presented in table M.1 in appendix. The figures show four bars, each representing the volume when a sample was taken. The first sample was taken of *not treated* water, and represents the concentration at 0 L. Then a sample was extracted after 3 L, 6 L, and 12 L of water had passed through the activated carbon. Generally three types of trends can be identified. The first type of trend is similar to the trend of iron in figure 4.14a. A clear decrease in the iron concentration is observed during the experiment. Copper, arsenic and lead all have similar trends as iron. The second trend is exemplified by nickel in figure 4.14c. Here, there is first a small decrease in concentration, then in the end there is an increase in the concentration of nickel compared to the *not treated* water. Zinc and cadmium also have this type of trend. The last trend includes only chromium, as shown in figure 4.14b. First the trend increases, before there is a decrease to lower than the initial concentration. The trends will be discussed more in detail in the next sections.

4.5.1 Trends of iron, copper, arsenic, and lead

The first general trend observed was as mentioned a clear decrease in concentration during the experiment, exemplified by iron in figure 4.14a. It is recognised by the large removal efficiency of the activated carbon, and the difference between the bar at 0 L and the other bars is significant. For iron, copper and lead the lowest concentration is measured at 3 L, while the 6 L bar holds the lowest concentration of arsenic. From this it could be theorised that the maximum adsorption capacity is reached for iron, copper, and lead either right before or right after 3 L, while the maximum adsorption capacity for arsenic is reached right before or right after 6 L.

As discussed in previous chapters, the concentrations of iron and copper in the AMD are extremely high. This is due to the high content of iron and copper in the ore that was processed and shipped at Killingdal. The high concentrations in the residues from this time period are still contaminating the soil and water. Due to the amount of the two elements and the frequent precipitation of iron into secondary minerals it is a potential problem for treatment facilities, as the precipitates can coagulate and clog the system. It is therefore an element that is normally removed during a main treatment step or even before that if possible. Since *Not cleansed* water was the only type available, and the fact that relatively large amounts of iron and copper have been proven to escape the main treatment step, as seen by the differences between *Cleansed* and *Not cleansed* water in the section about electrochemical treatment, it was interesting to look at the removal efficiencies.

Figure 4.14a and table 4.11 show how the activated carbon removes iron with a great efficiency, especially in the beginning. During the first 3 L, a total of approximately 17 000 µg iron has been removed from the water and adsorbed or precipitated in the activated carbon. After 12 L of water

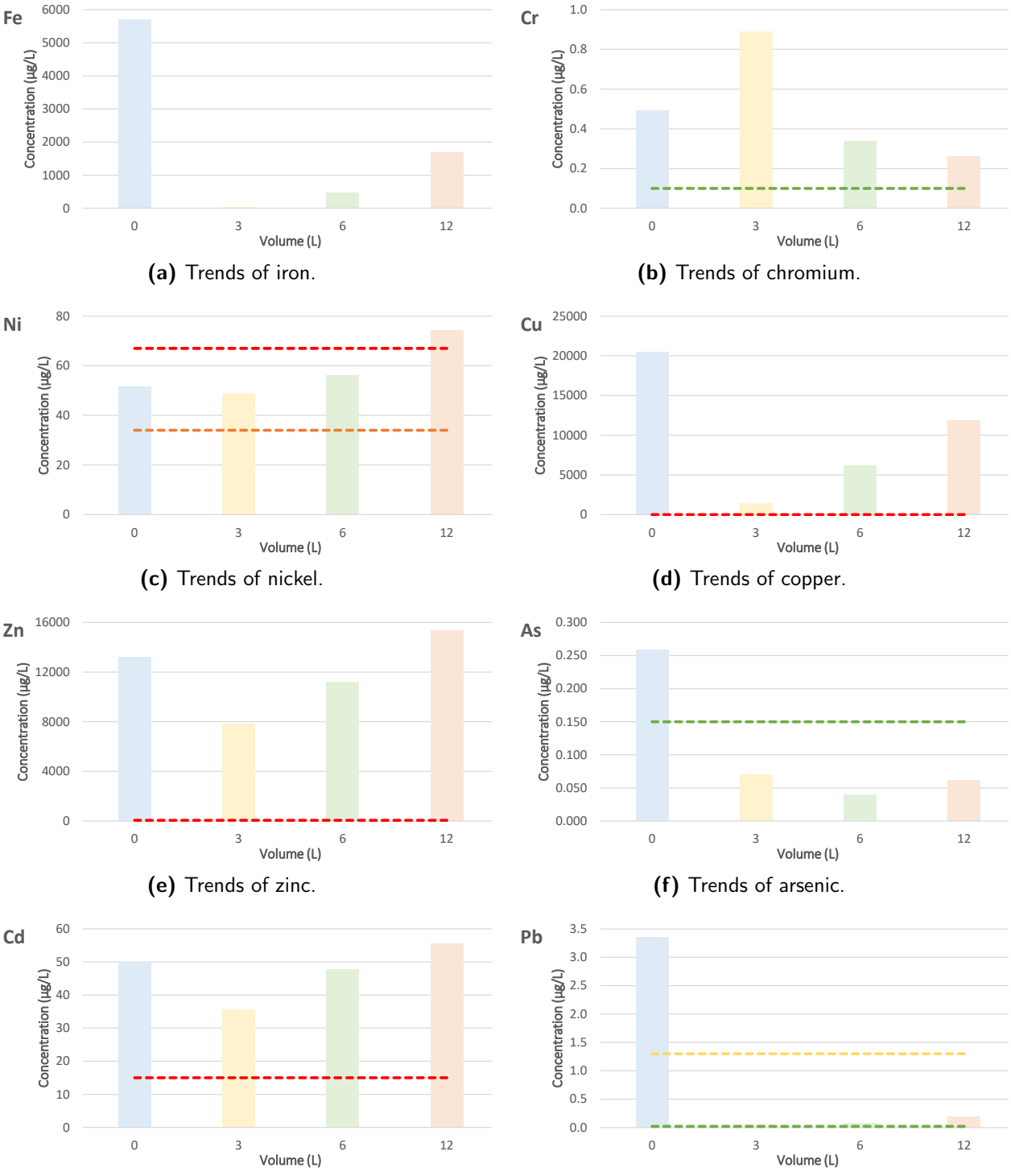

(a) Trends of iron.

(b) Trends of chromium.

(c) Trends of nickel.

(d) Trends of copper.

(e) Trends of zinc.

(f) Trends of arsenic.

(g) Trends of cadmium.

(h) Trends of lead.

Figure 4.14: Trends of the different trace elements in focus during treatment with activated carbon. The x-axis presents the volume of water that has passed through the activated carbon when a sample was collected. Dotted lines represents the lower limit of the corresponding class of condition, according to table A.2 in appendix.

Table 4.11: Amount of iron, copper, arsenic, and lead let through the activated carbon compared to *not treated* water.

Volume (L)	Fe (%)	Cu (%)	As (%)	Pb (%)
3	0.687	6.80	27.1	1.46
6	8.36	30.4	1.25	2.36
12	29.8	57.9	23.9	5.90

the amount removed has dropped to 70 % removed, which is still a significant improvement of the conditions in the water. The increase observed from 3 L to 12 L may indicate that the capacity is close to reached. If the experiment had continued for longer the concentrations let through may have increased to approximately the same as *not treated* water. However, the retention period through the activated carbon could have given the iron in the water time to precipitate and be filtered by the activated carbon granulates.

Figure 4.14d presents the results from the experiment with activated carbon in regards to copper. At 0 L copper exist in a concentration of above 20 000 µg/L, which is exceptionally high, even in this water. However, after 3 L only 6.80 % of the copper is let through, compared to the *not treated* water, as seen from table 4.11. After this the amount removed drops, and after 12 L 42.1 % of the copper is removed. Calculations using the 93.2 % removal efficiency for the first 3 L, 70 % for the next 3 L, and 42.1 % for the last 6 L, point to a removal of more than 196 000 µg copper per 220 g activated carbon, which corresponds to 0.89 mg copper per g activated carbon. This is most likely an underestimation of the concentrations removed, but it gives an idea of the amounts retained. If the main treatment step manages to remove large portions of the copper before it reaches the activated carbon, this method might be both highly effective and long-lasting for the treatment of copper contamination. One factor that might have increased the removal of copper from the water in addition to the activated carbon is the gravel in the bottom of the pipe. Table 4.10 shows a decrease of 10.7 % from the gravel. Although the statistical analyses showed that there was no significant difference between before and after rinsing, there could still be an impact of the gravel.

Lead can exist in high concentrations in AMD, and has been measured to as high as class IV in the water from the Killingdal tunnel. However, the mineral anglesite ($PbSO_4$) has a low solubility, causing it to easily precipitate in sulphate-rich water. The day of the activated carbon experiment the initial lead concentration was in the lower parts of class III. As the results for lead in figure 4.14h and removal efficiencies in table 4.11 show, lead is removed from the activated carbon with very high efficiencies. The highest percentage let through the activated carbon compared to *not treated* water is 5.90 % after 12 L. As the removal is so high, the bars representing 3 L and 6 L do not show. Therefore, a new graph with only the results from samples taken after activated carbon treatment are presented in figure 4.15, to show the trend is similar to that of iron and copper.

The iron and copper that exists in the water at Killingdal are probably present mainly as divalent cations, most commonly as free Fe^{2+} and Cu^{2+} at pH below 8 [108] for iron and 2.2 for copper [109], and $Fe(OH)^{+}$ and $Cu(OH)^{+}$ when the water becomes more alkaline. In addition, Kavand, Eslami, and Razeh [110] found that Pb^{2+} was the main lead species at pH values below 7 in water. These cations can adsorb to the negatively charged acidic surface groups on the activated carbon.

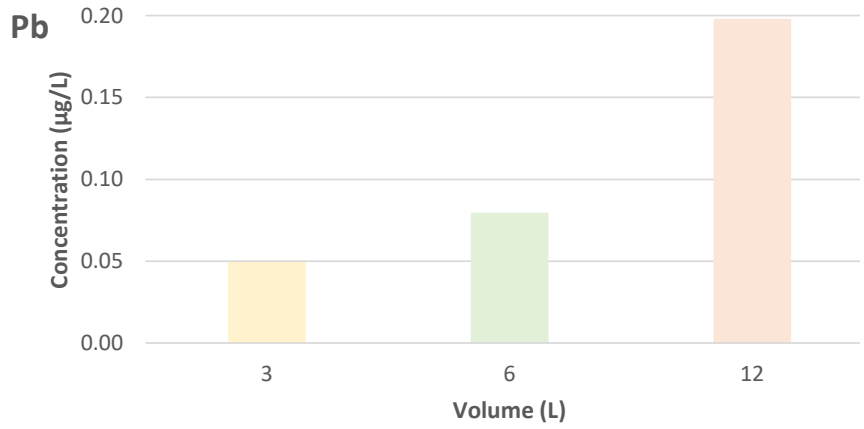

Figure 4.15: Trend of lead when the bar representing *not treated* water is excluded.

This happens through ion exchange reactions, where protons are exchanged with the cations. [77] However, it has been reported that the removal efficiency of elements usually present as cations is increasing when pH moves towards more neutral values. [111, 82] This has two explanations. At low pH values, there exist so much protons in the water that they will be adsorbed rather than any cations. This causes the surface of the activated carbon to be saturated with protons, making it positively charged and repelling the positively charged cations. Secondly, the non-polar characteristics of graphite in the activated carbon itself will repel the positively charged contaminants, which mainly exist as free ions in low pH conditions. When the pH is increased, however, there is less protons in the water, liberating more negatively charged sites where cations can more easily adsorb. In addition, as pH increases, many cations exist as hydroxide complexes, making them more easily adsorbed to the functional groups on the activated carbon surface.

The optimal pH for copper adsorption onto granulated carbon was found to be approximately 4 by Goyal et al. [112]. The pH of the water was not measured the day this experiment was performed, 18.12.2019. However, the pH was measured 12.09.2019 and 22.01.2020, and the pH was measured to be respectively 3.18 and 3.46. The pH in the water at Killingdal was therefore estimated to be in that range the day of the activated carbon experiments. As the free divalent copper ion was assumed to be predominant in the pH range below 2.2 by Kahn and Khattak [109], and above this the $Cu(OH)^+$ and $Cu(OH)_2$ start to become more dominant, it is reasonable to conclude that the water at Killingdal contain copper mostly in the form of $Cu(OH)^+$ and to some extent $Cu(OH)_2$. As these species are more desirable for copper adsorption to activated carbon, it could explain the large removal capacity of the treatment material. In addition, as the optimal pH is not yet reached, the adsorption capacity could increase even more if the pH was raised to above 4. If pH is increased above pH 6, $Cu(OH)_2$ precipitates. It would increase the amount of copper removed, but also increase the potential for clogging of the system.

The optimal pH range for lead adsorption is found to be between 5.5 and 6 [110]. Chen and Wang [111] state in their study that lead binds relatively well on activated carbon, at least compared to zinc, but not as well as copper. They also found that while copper was not affected by the presence of other elements in the water, lead was affected to a small extent. However, by the trends in our study, the lead removal seems more efficient than the copper removal, although both are quite

successful. This could be explained by the extremely high concentration of copper, and relatively low lead concentrations in the water from Killingdal. Due to the relatively low hydrated radius of lead compared to copper (0.401 nm and 0.419 nm respectively [113]), the lead ions may have reached into the smallest pores of the activated carbon, where the copper could not access. Lead did therefore not have to compete with copper for the active sites on the activated carbon, and was therefore successfully adsorbed. As the pH in the water at Killingdal is lower than the optimal pH for lead removal, a higher pH in the water that flow through the activated carbon could improve the capacity for lead ions even more. Lead can also combine with chlorine into anionic complexes [77]. These complexes can potentially adsorb onto the positively charged activated carbon surface. Due to the high concentration of dissolved chlorine in the water at Killingdal, the probability is high that some of the reason why the adsorption of lead to the activated carbon is so efficient is because of formation of such complexes.

Iron, copper and lead may also precipitate on the activated carbon surface even though the pH of the water has not reached the value where precipitation usually happens. In this case, activated carbon acts as a nucleus that can promote precipitation, which makes it easier for elements that easily form hydroxyl complexes, as iron, copper, and lead do, to form precipitates. [114]

One of the elements that the activated carbon as a polishing step is supposed to handle is arsenic. Generally, the arsenic concentration in the AMD at Killingdal is low. The day of the experiment, the arsenic concentration was measured at 0.258 µg/L, which is in the lower parts of condition class II. However, the results of the experiment could give an indication of the removal ability had there been more arsenic in the water that had to be removed. As figure 4.14f shows, arsenic had a slightly different trend compared to the other elements in this category. The lowest amount let through is 15 % after 6 L of water passed through, presented in table 4.11. After this the amount let through increases, but only to 23.9 %. All the concentrations after treatment with activated carbon are below the lower limit of class II.

Arsenic can potentially exist in the Killingdal water as both trivalent (As^{3+}) and pentavalent (As^{5+}) ion. Zhu et al. [115] did a study on the arsenic speciation distribution in AMD, where they found that arsenic is predominantly released from the ore as As^{3+} but is oxidised, mainly biologically, to As^{5+}. In addition, as figure 4.14f shows, arsenic is efficiently adsorbed to the activated carbon in the Killingdal conditions of pH 3.18-3.46. Several sources specify that As^{5+} is adsorbed most efficiently in the acidic pH range, with Gupta and Chen [116] and Hasim et al. [117] reporting a maximum of adsorption in the pH range 3-5, while As^{3+} is not readily adsorbed in these conditions. Since the different species of arsenic in the AMD at Killingdal was not analysed, only the total dissolved concentration, these factors could give an indication that the main oxidation state of arsenic at Killingdal is As^{5+}.

As mentioned in section 4.4.3 pentavalent arsenic exists mainly as $H_2AsO_4^-$ in the pH range at Killingdal, while trivalent arsenic exist predominantly as H_3AsO_3. The negative characteristics of the $H_2AsO_4^-$ ion is attracted by the positive sites on the activated carbon surface in the acidic pH range, while the neutral H_3AsO_3 is not. Another explanation to the high removal efficiency of arsenic could be that the activated carbon assist in the oxidation of trivalent arsenic to pentavalent arsenic. By itself, the oxidation of As^{3+} to As^{5+} is a slow reaction. Vega-Hernandez, Weijama and Buisman [118] did a study where they analysed the catalysing ability of granulated activated carbon

Table 4.12: Nickel, zinc, and cadmium let through the activated carbon compared to *not treated* water.

Volume (L)	Ni (%)	Zn (%)	Cd (%)
3	95.7	59.3	71.4
6	109	84.8	95.4
12	144	116	111

on the oxidation of As^{3+}. They showed that under aerobic conditions this process was very successful. During the experiments in this thesis, when the water from Killingdal was added the pipe which contained the activated carbon, the water was poured rather vigorously over, causing it to be mixed with the surrounding air. This would have assured oxidising conditions. When the arsenic in the water then came into contact with the activated carbon, it was transformed into pentavalent arsenic, which in its anionic form in water is readily adsorbed to the activated carbon surface functional groups.

4.5.2 Trends of nickel, zinc, and cadmium

The second general trend observed from the graphs in figure 4.14 is as exemplified by nickel in figure 4.14c. At first there is a decrease in concentration between 0 L and 3 L. Then, there is an increase of concentration at 6 L, and in the end 12 L has a higher concentration than the *not treated* water at 0 L. The fact that the concentrations are highest after 12 L indicates that there is a release of nickel, zinc, and cadmium into the water from the activated carbon, which is an undesirable result.

As figures 4.14c, 4.14e, and 4.14g show, nickel, zinc, and cadmium exist in high concentrations in the Killingdal AMD. While nickel is classified as class IV, both zinc and cadmium concentrations are all within class V. These figures might indicate that maximal saturation of nickel, zinc, and cadmium on the activated carbon may be reached either between 0 L and 3 L, or between 3 L and 6 L.

Similar to several of the elements in the previous category, nickel, zinc, and cadmium exist as divalent ions in the Killingdal water. In water, nickel can exist as Ni^{2+}, $Ni(OH)^{+}$, $Ni(OH)_4{}^{2-}$, and $Ni(OH)_{2(s)}$, depending on the pH [77]. At the pH in the Killingdal water (3.18-3.46), nickel most likely exist as Ni^{2+} or $Ni(OH)^{+}$. According to a study by Albrecht, Addai-Mensah and Fornasiero [119] the free divalent zinc ion is the dominant species up to pH 8.7, implying that this is the form zinc in the Killingdal water takes. Also, this study stated that the solid $Zn(OH)_2$ is dominant between pH 8.7 and 11.4. Leyva-Ramos et al. [120] state in their study that the main cadmium species in water below pH 8 is Cd^{2+}, and above pH 9 $Cd(OH)_2$ is precipitated. And similar to iron, copper, and lead, the adsorption capacity is increased as the pH increases, due to lower repulsion between the activated carbon surface and the cations, and more available negatively charged surface functional groups.

Several studies have been conducted on the removal of nickel, zinc, and cadmium by activated carbon. Optimal pH for removal have been discovered to be around 7 for nickel [121], and at approximately pH 8 [120] for cadmium. Above this, nickel will precipitate as $Ni(OH)_2$ and is therefore not available to adsorb to the activated carbon [121]. Optimal adsorption conditions for zinc were found to happen around pH 5 by Bhattacharya et al. [122], but it is largely dependant on the type of activated carbon and the other ions available in the solution [111]. Generally is seems like there is low adsorption

when pH is low. One reason to the relatively poor removal capacity for these trace elements by activated carbon could be that the pH is the water at Killingdal is too far away from the optimal pH for adsorption. However, a study by Sounthararajah et al. [114] tested the adsorption capacity of granulated activated carbon in a solution with pH 6.5 of the trace element copper, lead, cadmium, zinc, and nickel, and found a much lower adsorption capacity for cadmium, zinc, and nickel compared to copper and lead.

Another explanation of the trends in figures 4.14c, 4.14e, and 4.14g could be that nickel, zinc, and cadmium do not have a high affinity to the activated carbon functional groups, at least not as high as e.g. copper [123, 111]. At first, when there are many adsorption sites available, most cations are attached to the activated carbon surface. However, as the sites were increasingly occupied and new water with more cations with strong affinity to the surface groups came in contact with the activated carbon, the nickel, zinc, and cadmium ions lose the competition for the adsorption sites, and are released into the solution, as table 4.12 show. Chen and Wang [111] found that zinc adsorption was strongly affected by the presence of other elements in the water, due to the relatively low affinity to the activated carbon functional groups. The more ions with higher affinity than zinc, the less zinc is adsorbed. In addition, the non-modified activated carbon surface does not seem optimal for Cd^{2+} removal. Compared to other divalent cations, cadmium is larger when hydrated even though they are bound to the same amount of water molecules. The radius for e.g. copper and lead are 0.419 nm and 0.401 nm respectively, while it is 0.426 nm for cadmium, making it harder for the hydrated Cd^{2+} ion to access the smaller pores in the activated carbon [113]. The dominance of the Cd^{2+} and not the hydrated forms makes it harder to adsorb onto the nonpolar graphite layers. The positive charge will be repelled by the graphite and the positive surface functional groups, making adsorption difficult.

Chen and Wang [111] also looked at the effect of activated carbon on water pH. They did this by measuring the pH of the influent water and the effluent water, i.e. water before and after treatment with activated carbon. By doing this continuously, they observed how the effluent pH in the two experiments increased from 3.5 and 6.0 to 7.3 when the first water interacted with the activated carbon, and after a while it readjusted back to the influent pH when new water was added. This phenomenon was also observed by Sounthararajah et al. in their study [114]. It was concluded that the increase in effluent pH was due to adsorption of protons from the water onto the activated carbon. When the activated carbon surface was saturated with protons, and new water continued to flow through the material, no more protons were removed from the water and the pH stabilised at the influent pH. Unfortunately pH was not measured during the experiments at Killingdal, but it is assumed that the pH was between 3.18 and 3.46, which is close to the lowest pH value used in the experiment of Chen and Wang of 3.5. It could therefore be assumed that the same effect could have happened in the experiments with the Killingdal water. One effect observed by Chen and Wang during the change in pH in the experiment with water with pH 3.5 was that when the pH increased, there was a high adsorption capacity of copper, and potentially also precipitation of $Cu(OH)_2$. However, when the pH adjusted back to 3.5, there was an increase of copper in the effluent water compared to the influent water. This was attributed to the lower adsorption capacity of activated carbon when pH is low, and also the redissolution of the precipitated solids. More protons in the water will cause an exchange with, and desorption of, the adsorbed elements.

This could be an explanation to why the removal efficiency of copper was decreased during the

experiment, and might also reveal why the trends for zinc, cadmium, and to some extent nickel were observed. Since the experiment at Killingdal was designed in the way that two batches of water was added to the pipe with activated carbon separately, instead of a continuous flow, the first batch may have experienced an increase in pH as the water interacted with the activated carbon. Conditions were then more optimal for removal of most of the elements analysed in this study. However, when the new batch with low pH water was added to the pipe, the capacity of the activated carbon may have decreased, causing several of the pollutants to be desorbed into the water. When Chen and Wang used a solution with pH 6 instead of 3.5, they did not observe this desorption effect. A higher pH in the *not treated* water added to the pipe at Killingdal could have caused more optimal conditions for removal of all the contaminants, and it may have prevented desorption of contaminants into the water and prolonged the lifetime of the activated carbon.

A preferable method to remove nickel and cadmium from the water at Killingdal would therefore be to increase the pH of the water towards the optimal ranges before treatment with activated carbon. It is also possible to utilize activated carbon modified to target these trace elements. An example is the removal of cadmium. Activated carbon materials enhanced by magnesium [124] and sulphur [125] show a higher removal efficiency of cadmium compared to *not treated* granular activated carbon, as used in this study. Magnesium is easily exchanged with cadmium, giving it a site to adsorb to the activated carbon surface, and many cadmium species have shown high affinity towards sulphur. A type of activated carbon enhanced by certain groups that cadmium have a higher affinity to could be an option for the water at Killingdal. However, this might be a more costly option, as the modified activated carbon materials often are more expensive than the unmodified version.

4.5.3 Trends of chromium

Chromium is the only element in the third category of trends, due to its unique shape. As figure 4.14b shows, there is an 81.1 % increase of chromium in the solution after the first 3 L of water has passed the activated carbon. This is a quite large increase, however it only corresponds to about 0.40 µg/L. And, after 6 L and 12 L a decline down to 68.8 % and 53.3 % respectively of the concentration in the *not treated* water. This continuous decline might indicate that the adsorption capacity of activated carbon is not saturated yet. The chromium concentration is always above the line representing lower limit of class II during the experiments, but it is far below the lower limit of class III, indicating that the chromium contamination stays low during this experiment.

Chromium is an element that the polishing step is desired to remove from the water, and a lot of research has been conducted on the adsorption of chromium on activated carbon. Chromium (IV) has been observed to adsorb to positive functional groups on the activated carbon surface as the anionic species $HCrO_4^-$ or CrO_4^{2-} [126, 82]. These species are commonly found in pH conditions as found at Killingdal, as mentioned in section 4.4.4, and this could potentially explain some of the removal of chromium from the tunnel water. In a study by Valentín-Reyes et al. [82] it was suggested that this adsorption was due to anion-exchange between the hexavalent chromium complex and basic functional groups on the activated carbon. A problem with the adsorption of the anionic hexavalent chromium species is that they have been observed to compete with chlorine, causing the adsorption of chromium (VI) to be low when the chlorine concentration is high [82]. It may also compete with the anionic pentavalent arsenic species for the positive sites.

Another removal mechanism postulated by Valentín-Reyes et al., which is also investigated by several other research groups, is the reduction of hexavalent chromium to trivalent chromium followed by the adsorption of this new chromium species. The reduction happens as a result of contact between the hexavalent chromium ion and functional groups on the activated carbon surface that act as electron donors. These functional groups may be carboxylic, phenolic, and hydroxyl groups. [82] Further, since the sites where hexavalent chromium species were attached are positively charged, and so is the trivalent chromium ion, the reduction process will cause trivalent chromium ions to be released into the water through repulsion. This could explain the increase observed during the first 3 L of water passing through. However, if there are any negatively charged sites on the activated carbon surface, the trivalent chromium ion might re-attach and be removed from the water. These sites are often acidic carbon oxygen groups that loose an H^+ when placed in water. It is also possible that $Cr_3{}^+$ precipitates into solution as chromium hydroxide ($Cr(OH)_3$), but it requires a pH of higher than 5.

A second explanation to why the chromium concentration increases in the beginning of the experiment could be a release from the gravel used in the bottom of the pipe to avoid clogging of the valve. Table 4.10 shows an approximately 5 % increase of chromium in the water that has been in contact with the gravel compared to the initial concentration. There is some uncertainty in these numbers, and the Mann-Whitney U test showed no significant impact. If there still was some chromium left on the gravel after the rinsing, this could have been released during the experiment. When all the chromium from the gravel had been washed out, the adsorption to the activated carbon started to show. It is most likely not the explanation for all the chromium released, but might account for a small part.

4.5.4 General discussion for method

There are several factors that can affect the adsorption of trace elements onto activated carbon. Contact time between the contaminants in the water and the surface of the activated carbon plays a key role in the amount of trace elements that get to reach equilibrium. The longer time the contaminants have to get in contact with the functional groups and react with them, the more will be adsorbed. [127] This again will also be affected by the reaction rate of the different trace elements and the surface groups. A study by Bhattacharya et al. [122] found that the adsorption of zinc was significantly increased when the contact time was prolonged from half an hour to two hours. The solution for removing more zinc from the water at Killingdal could therefore be to decrease the rate of water flow through the activated carbon.

Initial concentration is another factor that can affect the adsorption capacity of the activated carbon. Usually, when the initial concentration of trace elements are high it results in a higher adsorption capacity of the adsorption material. This could be explained by the fact that higher concentrations makes transfer of trace elements between the solution and the solid adsorbent easier. [127] However, the opposite has been observed during activated carbon adsorption. Zheng et al. [128] tested the adsorption capacity of copper and cadmium by areca waste and found that the adsorption capacity was decreased as the initial concentration was increased. The same trend was discovered for nickel by Malkoc and Nuhoglu [129] in their study on nickel adsorption by tea factory waste. This backs up the initial thought of activated carbon being used as a polishing step rather than a main treatment step. By having a step before the activated carbon which removes the majority of the element

concentrations, the adsorption capacity and life-time of the activated carbon can be enhanced.

As described in the previous sections, pH may influence the adsorption of trace elements. When the pH is somewhat acidic, elements that usually exist in the AMD is poorly retained. Those that exist as anions on the other hand will be retained easily due to the large amount of positively charged sites on the activated carbon surface. As the pH increase, less protons will occupy the functional groups, and exchange with the cations in the solution. Elements that easily form hydroxides will be adsorbed first, while those that stay as free dissolved ions in a wide pH range will be retained to a lesser extent. Again, a solution for increased removal of nickel, zinc, and cadmium could be to pre-treat the water. However, if some of the elements that easily hydrolyse are transformed into anionic complexes, they might be released from the activated carbon surface again. Different pH values could be tested to find the optimal range for maximum removal of all trace elements in the Killingdal AMD.

In conclusion, the granulated activated carbon that was tested in this thesis showed a high removal efficiency of iron, copper, arsenic, lead, and chromium. By combining activated carbon with a main treatment step that reduces the amount of elements in the water on beforehand, the adsorption capacity and operational time of the activated carbon could be suitable to use to treat the Killingdal water. As for nickel, zinc, and cadmium, the adsorption is not optimal. For the activated carbon to remove these trace elements, a main treatment step than can increase the pH might help. Another option could be to use a modified activated carbon that specifically target these elements. However, these modified versions can be more expensive, and may reduce the removal capacity of other elements.

4.6 Comparison of electrochemical treatment and activated carbon treatment as polishing steps

The two treatment methods tested in this thesis are very different, and the experiments were carried out in two types of setups. During planning of this thesis, it was planned for the electrochemical treatment to be performed in the same pipes as the activated carbon was tested in. However, this was not accomplished as it was decided that a setup at the laboratory at NTNU would be safer and more simple to use for the electrochemical experiments. It is therefore not possible to compare the removal from water running through a pipe, or to check if such a setup would even work in the Killingdal tunnel. It is however possible to compare solely removal efficiency percentages, and when doing this activated carbon outperforms electrochemical treatment, visible in table 4.13.

For aluminium, iron, chromium, copper, arsenic, and lead, the amounts removed even after 12 L of water has passed through the activated carbon are higher than that removed after 80 minutes of electrolysis. In addition, as mentioned earlier, if the main treatment step combined with the activated carbon could improve the removal efficiencies of nickel, zinc, and cadmium as well, this would potentially be the best combination. However, the maximal capacity of the electrochemical treatment may not have been reached during the experiments performed in the laboratory. Even though the water was stirred during the whole experiment, it may not have been enough to let all the water come in contact with the electrodes or the precipitating particles. By utilising a setup where these factors are in place, there is a possibility that the removal efficiency of the electrochemical treatment could have been improved.

One disadvantage with the activated carbon is that relatively large amounts are needed to remove relatively small amounts of contamination. According to the calculations in section 4.5.1, a total of 196 000 µg copper was removed per 220 g activated carbon from 12 L of water, which corresponds

Table 4.13: Summary of all the percentages removed (green cells) or increased (orange cells) of the trace elements in focus during the electrolysis experiments and the activated carbon experiments with water from Killingdal.

	Al	Fe	Cr	Ni	Cu	Zn	As	Cd	Pb
Experiment 1: Aluminium electrodes, 1.0 V									
Cleansed	206	36.2	2540	38.8	29.4	17.3	66.8	8.14	56.9
Experiment 2: Aluminium electrodes, 1.5 V									
Cleansed	246	40.2	6920	4.07	32.7	21.4	69.5	12.9	30.5
Not cleansed	51.1	24.1	1240	61.7	39.2	6.79	69.2	7.70	41.0
Experiment 6: Cylindrical graphite cathode and flat graphite anode, 1.5 V									
Cleansed	18.6	8.93	7.30	22.5	3.10	0.356	2.38	1.15	114
Not cleansed	0.409	8.53	6.61	80.5	12.2	7.34	17.0	0.752	137
Activated carbon treatment, Not cleansed									
3 L	99.8	99.3	81	5.30	93.2	40.7	72.9	28.6	98.5
6 L	99.5	91.6	31.2	9.34	69.6	15.2	84.8	4.61	97.6
12 L	98.4	70.2	46.7	44.4	42.1	16.4	76.1	11.3	94.1

to 0.89 mg copper per g activated carbon. This may be an underestimation, but it is still not a lot. Removal efficiencies up to 20 µg copper per g activated carbon have been reported [107]. Removing the majority of the contaminants before the polishing step would most likely enhance the time period the activated carbon can be used and the amount that is needed. Considering the large amount of water that the tunnel holds, estimates by Trondheim Municipality suggest 1578 m^3 or 1 578 000 L, and the fact that new water still keeps seeping into the tunnel, a great quantity of activated carbon will be consumed. There is however the possibility to remove the trace elements from the activated carbon after it is saturated with contaminants. This can be done by washing the activated carbon with e.g. acid, causing the contaminants attached to the surface to be exchanged for protons and be released into solution. Depending on the activated carbon, this can be rather successful [130].

A factor that needs to be considered when using electrochemical treatment in larger scales is the production of gases. As can be seen from the electrochemical series in table 2.4 in section 2.9.2 hydrogen gas production is favoured over several of the reduction reactions supposed to happen during the electrolysis. In the case of electroflotation the production of hydrogen gas and oxygen gas is useful, as it will assist the separation of contaminants from the water. However, hydrogen gas is flammable, and without sufficient ventilation it can accumulate in the Killingdal tunnel and potentially be very dangerous. The production of chlorine gas could also potentially be a problem. Chlorine gas is a toxic gas that when inhaled can cause respiratory distress, and in extreme cases it can be deadly. During the electrolysis of water which contains high amounts of chlorine, as the water at Killingdal does, it is possible that chlorine gas is produced [97]. It has a recognisable smell, and although it was not detected any gas production during the testing in the laboratory at NTNU, there could still have been produced small amounts. The experiments only lasted for 80 minutes, while treatment in the Killingdal tunnel would be continuous. It would therefore be important to have a good ventilating system and safety measures in place if electrochemical treatment were to be used to remove trace elements from the water at Killingdal. The electrochemical treatment setup would also need to have a power supply and electrical wires. The electricity system by itself is dangerous to come into contact with.

From both experiments there will most likely be some amounts of sludge produced. With the precipitates formed during electrolysis there will be the possibility of having a sedimentation tank afterwards, to give the contaminants time to settle out of solution. Trondheim Municipality already has this last sedimentation tank installed in their facility. The activated carbon on the other hand will most likely act as a filter, holding back the solids formed during the treatment. This could cause clogging of the system, and would have to be monitored and maintained regularly. In this case it would be wise to remove as much of the precipitates in the water before it is directed through the activated carbon. A main treatment step or a sedimentation tank before the polishing step could in this case be the solution.

4.7 Quality control and quality assurance

To make sure that the results are reproducible and represent the true concentrations in the different matrices, proper quality assurance and quality control is necessary. Quality control is needed to get accurate results, avoid contaminating the sample, and to identify possible errors that have occurred. Quality assurance on the other hand is considering the reliability of the of the results, and regulations are made to ensure reproducible and comparable results. It is important to incorporate these actions in all the stages of the process, from sampling to analysis.

In the monitoring of the Killingdal stream and the Trondheimsfjord, and the treatment experiments, all water samples were collected with a polypropylene syringe, a material that does not contaminate the samples with trace elements. This syringe was reused for approximately one month at the time, due to a limited budget, and regular replacement of the syringe was to avoid wear and tear of the syringe and non-optimal functionality. The syringe was thoroughly rinsed between each day it was used. In the laboratory before the electrochemical experiment, the syringe was rinsed with Milli-Q water, while it was generally rinsed with water from a tank at Killingdal before the monitoring samples and the activated carbon experiments. As the Milli-Q water from the laboratory is significantly cleaner than the water from the tanks at Killingdal, the electrochemistry experiment samples should not be contaminated by the water, while some effect may have appeared from the tank water in the other samples. However, it was decided that it was better to rinse the syringe with water to remove possible dust and other deposits, as the syringe was to be rinsed with water from the sample location afterwards anyways.

During the experiments carried out in the laboratory, all equipment that were to come into contact with the sample water, i.e. the container and the magnet used for stirring, were washed with soap and water, and then rinsed with Milli-Q water, to avoid any leftover contaminants from previous experiments to contaminate the samples. Then it was rinsed with parts of the sample water three times before the actual sample was collected for every sample collected. This was to avoid contamination by residues from the syringe from the production or from previous sample extractions.

The presumably least contaminated water was always sampled first, to avoid a large carry-over of elements from the previous sample that might impact the results. When the sample was collected in the syringe, it was filtered with a 0.45 µm filter. This filter was changed between each sample that was taken, to avoid a release of elements from this into a new sample. When transferring the sample to a polypropylene ICP-MS tube, the tube was first rinsed three times with the filtered sample before the actual sample was added, to remove all possible residues from the production and condition the tube. Gloves were worn during all sampling, to prevent contamination from hands. Containers and sample tubes made of inert plastic materials (teflon, polyethylene and polypropylene) were used to ensure that no contamination of the sample came from the storage equipment. The rinsing procedure and the use of gloves and container are in accordance with the standard NS-EN ISO 5667-6:2016 [84].

Normally it would be preferred to collect at least three parallels from each location at each sampling, as a mean of three parallels would even out the variances that might occur. However, due to the amount of samples that were going to be collected during this thesis and a limited budget, it was decided that one parallel would be sufficient enough to get the full picture of pollution in the waters

analysed. In the end the water samples were preserved with three droplets of Ultrapure HNO_3, to avoid analyte precipitation or adsorption to the container walls, in accordance with NS-EN ISO 17294-2:2016 [131]. All water samples were stored in racks in the refrigerator at 4.6 °C, as stated by the standard ISO 5667-3:2018 [85], to avoid any changes in the species distribution of trace elements in the solution.

The sediment cores were collected from the seafloor by a metallic box corer. To avoid contamination of elements from the equipment, the samples taken from this sediment core were taken of the parts that were furthest away from the edges that had been in contact with the box corer inner wall. Samples were collected in small plastic containers. These were new containers, so they were most likely clean from any trace elements. To get representative results, two parallels were sampled in each sampling location. It was decided that this was enough to show the full picture of pollution in the sediments, even though three parallels are often recommended. Sediment samples were stored in a freezer at −27 °C to avoid any microbial activity and to prepare the samples for further treatment.

To be able to analyse the sediment samples, a pre-treatment process had to be carried out. The freeze drying of the samples was conducted without lids. There is a possibility for the most volatile elements to escape (like mercury), but was most likely not a problem during this method as the sediments were frozen and transformed directly to solid powder, without letting the elements dissolve in water. The majority of the elements were therefore most likely preserved in the solid matrix. When transferring the sediment samples from the sampling containers and into tubes suitable for digestion, the bench was covered in a clean plastic film and gloves were used, so the chances of contamination is low. The digestion tubes are reusable, but had been rinsed with Milli-Q water and Ultrapure nitric acid before use, so there is most likely no contamination from them. Some of the sediment samples collected in the Trondheimsfjord were not homogeneous after freeze drying. Instead of extracting only one parallel from these sediment samples for decomposition and digestion, three parallels were extracted. This was done in an attempt to get a more representative result than only one sample would provide. In addition, three parallels of freshwater and seawater sediment reference materials with known concentrations of trace elements were analysed together with the sediment samples. This was to account for the possible loss of sample during the sample preparation procedures and analysis, and it could also be used to calibrate the instrument.

All the samples were analysed by ICP-MS at NTNU by Syverin Lierhagen. During the analysis, measured concentrations are verified against certified reference materials and standard solutions with high accuracy. This is important to ensure a high precision in the results. To ensure the reproducibility of the analyses, repeating tests of the certified reference material is carried out continuously. In addition, the RSD is calculated for each sample based on three scans. A high RSD value corresponds to a high uncertainty, and is an indication that these results might not need to be emphasized. In this thesis, some concentrations had high corresponding RSD values, e.g. arsenic, most likely due to low concentrations and interferences. When analyte concentrations in the sample are close to the detection limit, these problems are common. The detection limit for arsenic used in this thesis was 0.025 µg/L, as presented in appendix C. Many of the arsenic concentrations measured were from 0.4 µg/L and below, not very far from the detection limit. This was commented where it was necessary, and an evaluation was conducted for each sample to see if the concentration should be used or not. All these quality control and assurance factors increases the reliability of the results

obtained from the ICP-MS analysis.

Before the last analysis of samples, which included all the treatment experiment samples, the ICP-MS instrument ELEMENT 2 stopped working, and the analyses were performed with an Agilent 8800. From these results it was evident that some elements had interfering species that potentially could impact the results. Nickel was one of the affected trace elements. During the analysis, CaO was observed to interfere with ^{60}Ni by 0.000 35 %, which is a relatively small interference, but unnecessary. By analysing ^{62}Ni instead, this interference was avoided, and no other interfering analytes were observed for this isotope. Similarly for cadmium and the molecule MoO. MoO interfered by 0.05 %, which could have an impact on the results. By changing the tune mode of the ICP-MS machine, which is a mode used to remove interferences, from gaseous H_2 to gaseous O_2, the interference was reduced to 0.009 %.

Blanks account for the contamination that can occur from the air where the sample is taken, potential leakage from the containers during transport and storage, possible impurities in the chemicals used for preservation, decomposition, and analysis, loss of sample during sample preparation, or deviations in the sample analysis. Frequent analysis of blank samples could reveal defects in the sampling-to-analysis process. Three field blanks, i.e. sample that has been exposed to the sampling environment, were collected. Milli-Q water was brought in a clean container from the laboratory at NTNU to Killingdal, and sampled the same way as all the regular samples, as described above. This was to see if the samples are enriched in elements from the surroundings they are samples from, like particles in the air or gloves dirty because of contact with surfaces in the tunnel, which is nowhere near as clean as the laboratories. In addition, five method blanks were made in the laboratory at NTNU. This was to check the impact of the filter, syringe, ICP-MS tube, and acid. The impact of these potential sources would not be big, but it could still alter the concentrations of the elements found in small amounts.

The nitric acid used to preserve and decompose all the samples in this project was Ultrapure HNO_3, in accordance with NS-EN ISO 17294-2:2016 [131], produced in the laboratories at NTNU. Here, the acid is regularly checked to ensure that it is free from all possible contaminants that could be introduced during the production process. All equipment at the laboratory were rinsed with Milli-Q water purified at NTNU. This water is free for all ions and other possible contaminants to the analytes in the sample. By using this water in the equipment preparation and for the blanks, one can be sure that the amount of contamination or interruptive ions will be negligible.

Due to all these efforts to avoid contamination and increase the reliability of the results, the measured concentrations obtained during this project could be concluded to be reliable. Additional parallels could have been collected to even out the impact of errors done during sampling, pre-treatment, and analysis. However, it would either have been more expensive, or the amounts of samples would have been lower, causing the trends obtained in this thesis to be less descriptive. And since the standards for sample collection, handling, and analysis were followed, the contamination should be low. The concentrations give the general trends for contamination, and that is what was the focus of this thesis.

5 Conclusion

A monitoring program that lasts a whole year is a great method to observe the changes that might occur in a body of water. In this thesis, the Killingdal stream was monitored from 11.10.2018 to 12.11.2019. The results from this monitoring indicated that the stream had elevated concentrations of trace elements compared to background levels, but all were generally in class II, which will not cause any toxic effects to the organisms living there. Due to these low concentrations it was also concluded that this stream is by itself not the source of trace elements into the Killingdal tunnel. However, parts of the stream may find its way into the tunnel, and by flowing through residues from the ore processing facility that used to be at the Killingdal area, it can mobilise contaminants, transport them into the tunnel water and end up in the fjord. Fluctuations during the year were observed in the stream, with the highest concentrations during high water flow and lowest concentrations in the driest periods. Due to varying lengths between the samplings, the conclusions of trends were only based on the periods with frequent sampling. It is not possible to say if these trends are consistent during the whole year.

In addition to the stream, the location in the Trondheimsfjord where water from the Killingdal tunnel leaked out was monitored. This was to see the impact of this effluent in the fjord, and also record how the input changes during the year. The concentrations of trace elements in this effluent were found to be considerably high, especially copper and zinc which were found in class V. Arsenic and cadmium were also found in high concentrations, class III and IV respectively. These concentrations could pose a health risk to the aquatic organisms that come into contact with this water. When comparing the concentrations measured in the effluent to the concentrations inside the tunnel, it was discovered that the concentrations in the effluent were lowest. This could indicate that the elements precipitate either on the way from the tunnel and to the release point into the fjord, or when they reach the fjord water. The release into a fjord that moves due to natural waves and shipping traffic could also contribute to dilute the elements rather quickly. The concentrations of copper and zinc are still far above the lower limit of class V, which indicates a need for treatment of the water inside the Killingdal tunnel.

To get a fuller picture of the impact the water from the Killingdal tunnel has on the fjord, the sediments close to where the effluent is released into the fjord was sampled and analysed. The results indicate significant contamination of iron, copper, zinc, and arsenic, and elevated concentrations of cadmium and lead. By comparing with previous investigations of the sediments in this area, it was discovered that all the elements in focus were reduced in the sediments during the past 40 years, but in the case of copper, zinc, cadmium, and lead there has been an increase since 1994, and in the last decade there has been a decrease in concentration for all elements except zinc. This could be attributed to variation in sampling locations the different years, and some could be a result from increased activity in the area due to the clean-up of the Killingdal area on land.

The high concentrations measured in the top sediments indicate that the new sediment layer put out by Trondheim Municipality during the *Cleaner Harbour* project has become contaminated. It can also be concluded that a lot of this contamination originate from the Killingdal effluent. One reason for this is the trends found in the sediments right outside the Killingdal area. Considerable pollution was found both 20 m away from the effluent release location and 170 m away. While some of the pollution at 170 m from shore could be explained by other factors, such as release from the

Høvringen water treatment plant, the high amounts 20 m from the shore is most likely due to release from Killingdal. A correlations analysis showed that the trace elements found in high concentrations in the sediments were strongly correlated, indicating that they have the same source into the fjord. An explanation is that when there is more water from Killingdal released, more of these elements will end up in the sediments. In the end, the relationship between the trace element concentrations and the lithium concentration was investigated in each location, as it can give an indication of anthropogenic exposure. It was found that iron, copper, zinc, arsenic, cadmium, and lead relationships with lithium varied between locations, indicating their non-natural presence. This overlapped well with the measured concentrations saying that these elements are present in concentrations above background levels. All these factors indicate that iron, copper, zinc, arsenic, cadmium, and lead all have a common, anthropogenic source, and that there is a high probability that this source is the Killingdal tunnel.

In addition to the monitoring program, two different treatment methods were tested to investigate their ability to remove trace elements from the Killingdal water as a polishing step. The first method included was electrochemical treatment, where both aluminium electrodes, graphite electrodes and a combination were tested. It was found that the experiment including only aluminium electrodes worked best for removal of iron, copper, zinc, arsenic, and cadmium, and to some extent lead, with a maximal removal of 40.2 %, 39.2 %, 21.4 %, 69.5 %, 12.9 %, and 41.0 %, respectively. However, this method released high amounts of aluminium, chromium, and nickel into the water. When only graphite electrodes were used, both aluminium and chromium were removed, with 18.6 % and 7.30 % respectively, but the other elements had relatively bad removal efficiencies in this experiment compared to the experiment with only aluminium electrodes. In addition, nickel was released more or less in all experiments. More testing should be conducted before deciding which method is the best.

The total concentrations of particulate and dissolved elements were not measured, only the dissolved. By measuring both, a more in-depth knowledge could have been gained on the total removal capacities of the elements in the water. However, as the dissolved fractions of elements are often the most toxic and bioavailable, these are the most important to remove. For this, it can be concluded that despite the high release of aluminium and chromium, the experiment with only aluminium electrodes was the most successful, but it is not optimal. The best option would be to find a method that does not release iron or aluminium, but cause them to precipitate and adsorb the other elements.

The second remediation method tested was activated carbon. The removal efficiency was high for iron, copper, arsenic, lead, and chromium after a while, with a measured maximum removal of 99.8 %, 93.2 %, 84.8 %, 98.5 %, and 46.7 %. In addition, it removed aluminium efficiently, with a maximum removal of 99.8 %. It did not work as well for nickel, zinc, and cadmium, as these elements were released into the water after a while. After 12 L of water had passed, the concentrations of these elements were increased by 44.4 %, 16.4 %, and 11.3 %, respectively. For most elements the optimal pH for adsorption was not yet reached. An increase in pH in the water before treatment with activated carbon might improve both removal of those elements the method worked for, and also the elements it did not work that well for. This is due to more seats available and possibly some precipitation where the activated carbon work as a filter. A problem with increased removal of precipitates could be clogging of the system, as the precipitates might fill the pores in the activated carbon and obstruct the water from flowing through.

It is complicated to compare these two experiments as they are quite different. There was most likely a longer and better contact between the contaminants in the water and the functional groups on the activated carbon, compared to the electrodes in the electrochemical experiments, even with stirring of the water. In addition, the activated carbon was exposed to two rounds of water, while the electrochemical treatment used the same water throughout the experiment. However, removal percentages were compared to see the differences. From these percentages activated carbon appears to be the best method for trace element removal, and the potential for large-scale water treatment should be investigated further. In addition, there is no chance for production of gases as there is for electrochemical treatment, and there is no risk for electrocution when adjusting the activated carbon setup.Problems identified for the activated carbon, however, are the potential clogging of the system, causing it to need regular maintenance, and that relatively large amounts of the granulate is needed which can be costly. More testing and optimisation of the electrochemical treatment method should be conducted to get a definitive answer of which method is the most suitable.

The results presented in this thesis are of special interest for Trondheim Municipality and other participants that are involved in the cleanup of the Killingdal area and the Ilsvika sediments. From the monitoring program it is revealed that the fjord is continuously contaminated by the water released from the Killingdal tunnel. As for the *Cleaner Harbour* project, they have gotten additional data showing how the sediments again are polluted by the release from Killingdal, and the sediments will not be clean before the release of contaminants from the Killingdal area is stopped. This project has also assisted Trondheim Municipality in the investigation of potential treatment methods. Results show that activated carbon have a great potential when it comes to removing trace elements from the Killingdal water, and could be implemented on a larger scale, in combination with a main treatment step that increases the pH and removes particles in the water.

6 Further work

There are many aspects of this thesis that would be interesting to continue working on. In the monitoring project a more frequent sampling of the Killingdal stream and the Trondheimsfjord than what was acquired during this thesis could be beneficial. As mentioned in previous sections, it appears as if there are some trends of high element concentrations in the stream when the water flow is strong, and low concentrations when the water flow is small. By planning according to the weather forecast, samples could be taken the days before, during, and after a period with heavy rainfall. This could have revealed even better correlations between element concentrations and water flow in the Killingdal stream, or it could have shown a completely different picture. However, several of the samplings were planned but not executed, as the weather conditions made it hard to reach the sampling locations. In addition, it would have been interesting to collect samples from the middle of the Trondheimsfjord, to get updated samples of the current conditions.

If the treatment experiments were to be conducted one more time the total concentrations in the water, both particulate and dissolved, should be measured. It would have been very interesting to see in what form the elements existed in. Especially interesting would it be to see how much of the particulate-bound elements were released during electrolysis and how the distribution of species changed after the water had been in contact with the activated carbon. All filters were orange after use which may indicate that a large portion of the elements are on particulate form, and the treatment experiments may change that, even though there were no visible changes in the water after treatment. As investigations of interactions between elements was not the main focus in the planning phase, measurements of the total fraction was not thought of.

Specifically for the electrochemical treatment, the current through the system should have been measured, and a better measurement of the voltage applied should have been performed. However, this experiment was mainly intended to assess different methods for trace element removal. To get a more accurate description of the elements removed during the electrolysis, it might have been a good idea to test synthetic AMD water, to investigate the individual reactions happening during the experiments. Since this was a project to test the treatment efficiency of the water from Killingdal, the testing was done with *Cleansed* and *Not cleansed* water, and a stable removal efficiency during the testing period would show the robustness and reliability of the method. However, varying water content made it hard to compare treatment methods and to conclude which method was the best. Further work could include testing of other electrodes, e.g. an iron anode, to see if they would have been more effective, as several studies have found that sacrificial electrodes of iron have a better removal efficiency that aluminium. A higher applied voltage could be investigated, but this should be performed in safe surroundings with good ventilation, in the case of gas production. In addition, a setup suitable for the pipes used for the activated carbon experiments would be a necessary second step to see if the method could compete with the activated carbon in the field. A suggestion to such a setup could be to have several cathodes in parallel to increase the contact time between the contaminants and the deposition electrode.

In the experiments with activated carbon the pH of the water should have been measured. As mentioned, several studies have discovered how the optimal pH for the different trace elements in focus in this thesis varies from element to element. In addition, the pH can change significantly during the experiment, so it would be interesting to follow these variations. Testing *Cleansed* water

to see the performance of the activated carbon as a polishing step could increase the application potential of the results. The experiments performed with the *Not cleansed* water show the capacity of the activated carbon as a treatment method, but the actual abilities may have been affected by the high concentrations and low pH of the water. Perhaps the removal efficiencies would have been sufficient for nickel, zinc, and cadmium, or the capacity for iron, copper, arsenic, and lead would be lower. These are questions that could have been answered had the experiment been conducted on *Cleansed* water as well. More tests with different types of activated carbon, to see if different modifications could have improved the removal capacity, could be initiated. Since the activated carbon was only tested with *Not cleansed* water with a pH of approximately 3.5, one could see if and how the removal efficiencies change when the pH is increased. Due to the optimal removal pH for most of the elements started at 4, it could be assumed that the removal efficiency would increase. One could also find the saturation limit for activated carbon with the contaminated water. For both activated carbon and electrochemical treatment it would have been interesting to combine them with a main treatment step, to see how they perform in a more realistic setup.

References

[1] Norges Geologiske Undersøkelse. Forekomstområde 1644-011, 2019. Url is `http://aps.ngu.no/pls/oradb/minres_deposit_fakta.Main?p_objid=4403&p_spraak=N`.

[2] Google Maps. Directions for Driving from Killingdal Mines, Holtålen to Ilsvika, Trondheim, February 2019. Url is `maps.google.com`.

[3] A. Revdal and K. K. Ness. Slik blir nye Fagervika, 2010.

[4] Wikipedia. Det gamle anlegget til Killingdal gruver i Ilsvika rives., 2010.

[5] E. Lande, T. Holthe, A. Langeland, E. Sakshaug, and T. Strømgren. Resipientundersøkelsen av Trondheimsfjorden 1972-1975. Universitetet i Trondheim, 1977.

[6] J. Skei. Trondheimsfjorden 1981. Delrapport III. Sedimentundersøkelser. Overvåkningsrapport 103/83. Norsk Institutt forvannforskning (NIVA), 1983.

[7] B. Rygg. Trondheimsfjorden 1981. Delrapport I. Biologi. (Overvåkningsrapport 61/82). Norsk Institutt forvannforskning (NIVA), 1982.

[8] Ø. Stokland. Resipientundersøkelse av Ilsvikaområdet 1991. OCEANOR Oceanographic Company of Norway A/S, 1991.

[9] R. M. Konieczny and A. Juliussen. Sonderende undersøkelser i norske havner og utvalgte kystområder. Fase 1: Miljøgifter i sedimenter på strekningen Narvik-Kragerø. Norsk Institutt forvannforskning (NIVA), 1995.

[10] R. T. Ottesen, M. Langedal, J. Cramer, H. Elvebakk, T. E. Finne, T. Haugland, Ø. Jæger, O. Longva, T. M. Storstad, and T. Volden. Forurenset grunn og sedimenter i Trondheim kommune: Datarapport. Norges Geologiske Undersøkelse (NGU), 2001.

[11] Multiconsult. Killingdal. Opprydding av forurenset grunn til grøntanlegg., 2011.

[12] E. and Ytterås. Killingdalområdet, Trondheim. Opprydding i forurenset grunn. Sluttrapport. Multiconsult, 2011.

[13] S. Salomonsen. Erfaringer fra Renere Havn i Trondheim 2009-2016. Trondheim Municipality and Norwegian Enviromental Agency, 2019.

[14] P. L. A. Erftemeijer and R. R. R. Lewis. Environmental impacts of dredging on seagrasses: A review. *Marine Pollution Bulletin*, 52(12):1553 – 1572, 2006.

[15] A. W. Nybakk. Renere Havn - Overvåkning Årsrapport 2019. Norwegian Geotechnical Institute (NGI) on behalf of Trondheim Municipality, 2019.

[16] F. Fifield and P. Haines. *Environmental analytical chemistry*. Blackwell Science, Oxford, 2nd ed. edition, 2000.

[17] A. D. McNaught and A. Wilkinson, editor. *Compendium of Chemical Terminology*. Blackwell Scientific Publications, Oxford, 2nd ed. edition, 1997. Url is `http://goldbook.iupac.org/terms/view/T06421`.

[18] D. G. Barceloux and D. Dr. Barceloux. Copper. *Journal of Toxicology: Clinical Toxicology*, 37(2):217–230, 1999.

[19] M. Barwick and W. Maher. Biotransference and biomagnification of selenium copper, cadmium, zinc, arsenic and lead in a temperate seagrass ecosystem from Lake Macquarie Estuary, NSW, Australia. *Marine Environmental Research*, 56(4):471 – 502, 2003.

[20] S. J. Clearwater, A. M. Farag, and J. S. Meyer. Bioavailability and toxicity of dietborne copper and zinc to fish. *Comparative Biochemistry and Physiology Part C: Toxicology & Pharmacology*, 132(3):269–313, 2002.

[21] Y. M. Nor. Ecotoxicity of copper to aquatic biota: A review. *Environmental Research*, 43(1):274–282, 1987.

[22] J. L. Fitzpatrick, S. Nadella, C. Bucking, S. Balshine, and C. M. Wood. The relative sensitivity of sperm, eggs and embryos to copper in the blue mussel (Mytilus trossulus). *Comparative Biochemistry and Physiology Part C: Toxicology & Pharmacology*, 147(4):441–449, 2008.

[23] M. Hudspith, A. Reichelt-Brushett, and P. L. Harrison. Factors affecting the toxicity of trace metals to fertilization success in broadcast spawning marine invertebrates: A review. *Aquatic Toxicology*, 184:1–13, 2017.

[24] S. Schäfer, U. Bickmeyer, and A. Koehler. Measuring Ca2+-signalling at fertilization in the sea urchin Psammechinus miliaris: Alterations of this Ca2+-signal by copper and 2,4,6-tribromophenol. *Comparative Biochemistry and Physiology Part C: Toxicology & Pharmacology*, 150(2):261–269, 2009.

[25] H. Y. Sohn. Chapter 2.1 - Copper Production. In Seshadri Seetharaman, editor, *Treatise on Process Metallurgy*, chapter 2.1, pages 534–624. Elsevier, Boston, 2014.

[26] Y. Li, N. Kawashima, J. Li, A. P. Chandra, and A. R. Gerson. A review of the structure, and fundamental mechanisms and kinetics of the leaching of chalcopyrite. *Advances in Colloid and Interface Science*, 197-198:1–32, 2013.

[27] B. J. Alloway. *Heavy Metals in Soils: Trace Metals and Metalloids in Soils and their Bioavailability*. Environmental Pollution volume 22. Springer, 3rd ed. edition, 2013.

[28] M. F. C. Leal and C. M. G. Van Den Berg. Evidence for Strong Copper(I) Complexation by Organic Ligands in Seawater. *Aquatic Geochemistry*, 4:49–75, 1998.

[29] R. D. Cardwell, D. K. DeForest, K. V. Brix, and W. J. Adams. *Do Cd, Cu, Ni, Pb, and Zn Biomagnify in Aquatic Ecosystems?*, pages 101–122. Springer New York, New York, NY, 2013.

[30] L. M. Campbell, R. J. Norstrom, K. A. Hobson, D. C. G. Muir, S. Backus, and A. T. Fisk. Mercury and other trace elements in a pelagic Arctic marine food web (Northwater Polynya, Baffin Bay). *Science of The Total Environment*, 351-352:247–263, 2005.

[31] M. Kohlmeier. Chapter 11 - Minerals and Trace Elements. In Martin Kohlmeier, editor, *Nutrient Metabolism*, pages 673–807. Academic Press, San Diego, second edition, 2015.

[32] H. Y. Sohn and M. Olivas-Martinez. Chapter 2.3 - Lead and Zinc Production. In Seshadri Seetharaman, editor, *Treatise on Process Metallurgy*, chapter 2.3, pages 671–700. Elsevier, Boston, 2014.

[33] Z. Zhang, H. Cheng, Y. Wang, S. Wang, F. Xie, and S. Li. Acrosome Reaction of Sperm in the Mud Crab Scylla serrata as a Sensitive Toxicity Test for Metal Exposures. *Arch Environ Contam Toxicol*, 58:96–104, 2010.

[34] K. Vercauteren and R. Blust. Bioavailability of dissolved zinc to the common mussel Mytilus edulis in complexing environments . *Marine Ecology Progress Series*, 137:123–132, 1996.

[35] L. Shi, N. Wang, X. Hu, D. Yin, C. Wu, H. Liang, W. Cao, and H. Cao. Acute toxic effects of lead (Pb2+) exposure to rare minnow (Gobiocypris rarus) revealed by histopathological examination and transcriptome analysis. *Environmental Toxicology and Pharmacology*, 78:103385, 2020.

[36] E. S. Bakker, E. Van Donk, and A. K. Immers. Lake restoration by in-lake iron addition: a synopsis of iron impact on aquatic organisms and shallow lake ecosystems. *Aquat Ecol*, 50:121–135, 2016.

[37] P. K. Abraitis, R. A. D. Pattrick, and D. J. Vaughan. Variations in the compositional, textural and electrical properties of natural pyrite: a review. *International Journal of Mineral Processing*, 74(1):41–59, 2004.

[38] T. Sanyal, A. Kaviraj, and S. Saha. Toxicity and bioaccumulation of chromium in some freshwater fish. *Human and Ecological Risk Assessment: An International Journal*, 23(7):1655–1667, 2017.

[39] Greg Pyle and Patrice Couture. 5 - nickel. In C. M. Wood, A. P. Farrell, and C. J. Brauner, editors, *Homeostasis and Toxicology of Essential Metals*, volume 1 of *Fish Physiology*, pages 253–289. Academic Press, 2011.

[40] K. V. Brix, C. E. Schlekat, and E. R. Garman. The mechanisms of nickel toxicity in aquatic environments: An adverse outcome pathway analysis. *Environmental Toxicology and Chemistry*, 36(5):1128–1137, 2017.

[41] G. M. Mudd. Global trends and environmental issues in nickel mining: Sulfides versus laterites. *Ore Geology Reviews*, 38(1):9–26, 2010.

[42] B. Kumari, V. Kumar, A. K. Sinha, J. Ahsan, A. K. Ghosh, H. Wang, and G. DeBoek. Toxicology of arsenic in fish and aquatic systems. *Environ Chem Lett*, 15:43–64, 2017.

[43] M. Bissen and F. H. Frimmel. Arsenic — a Review. Part I: Occurrence, Toxicity, Speciation, Mobility. *Acta hydrochimica et hydrobiologica*, 31(1):9–18, 2003.

[44] A. Adra, G. Morin, G. Ona-Nguema, N. Menguy, F. Maillot, C. Casiot, O. Bruneel, S. Lebrun, F. Juillot, and J. Brest. Arsenic Scavenging by Aluminum-Substituted Ferrihydrites in a Circumneutral pH River Impacted by Acid Mine Drainage. *Environmental Science & Technology*, 47(22):12784–12792, 2013.

[45] J. S. Espana, E. L. Pamo, E. S. Pastor, J. R. Andrés, and J. A. M. Rubí. The Removal of Dissolved Metals by Hydroxysulphate Precipitates during Oxidation and Neutralization of Acid Mine Waters, Iberian Pyrite Belt. *Aquatic Geochemistry*, 12:269–298, 2006.

[46] D. Mohan and C. U. Pittman. Arsenic removal from water/wastewater using adsorbents — A critical review. *Journal of Hazardous Materials*, 142(1):1 – 53, 2007.

[47] R. C. Okocha and O. B. Adedeji. Overview of Cadmium Toxicity in Fish. *Journal of Applied Sciences Research*, 7(7):1195–1207, 2011.

[48] J. S. Becker. Chapter 13 - Inorganic Mass Spectrometry of Radionuclides. In Michael F. L'Annunziata, editor, *Handbook of Radioactivity Analysis (Third Edition)*, pages 833–870. Academic Press, Amsterdam, third edition edition, 2012.

[49] D. A. Skoog, D. M. West, F. J. Holler, and S. R. Crouch. *Fundamentals of Analytical Chemistry, 9th Edition*. Brooks/Cole Cengage Learning, 9th ed. edition, 2014.

[50] C. Dass. *Fundamentals of Contemporary Mass Spectrometry*. John Wiley & Sons, 1st ed. edition, 2007.

[51] P Atkins and J. de Paula. *Atkins' Physical Chemistry*. Oxford University Press, 10th ed. edition, 2014.

[52] Operating Manual Freeze-dryer ALPHA 1-4 LDplus ALPHA 2-4 LDplus. Martin Christ Gefriertrocknungsanlagen GmbH, 2006.

[53] W. Stumm and J. J. Morgan. *AQUATIC CHEMISTRY Chemical Equilibria and Rates in Natural Waters*. John Wiley & Sons, Inc., 3rd ed. edition, 1996.

[54] International Organization for Standardization. ISO 5667-9 Water quality - Sampling - Part 9: Guidance on sampling from marine waters. International Organization for Standardization, 1992.

[55] G. Nichols. *Sedimentology and stratigraphy*. Wiley-Blackwell, Chichester, 2nd ed. edition, 2009.

[56] International Organization for Standardization. ISO 5667-19 Water quality - Sampling - Part 19: Guidance on sampling of marine sediments. International Organization for Standardization, 2004.

[57] J. A. Berge. Resipientundersøkelse i Trondheimsfjorden 2001. Miljøgifter i sediment. Norsk Institutt forvannforskning (NIVA), 2003.

[58] W. P. Ridley, L. J. Dizikes, and J. M. Wood. Biomethylation of Toxic Elements in the Environment. *Science*, 197(4301):329–332, 1977.

[59] R. C. Aller. Bioturbation and Manganese Cycling in Hemipelagic Sediments. *Philosophical Transactions of the Royal Society of London. Series A, Mathematical and Physical Sciences*, 331(1616):51–68, 1990.

[60] Norwegian Enviromental Agency. Grenseverdier for klassifisering av vann, sediment og biota. Norwegian Enviromental Agency based on data from Aquateam, Norwegian Institute for Water Research (NIVA) and Norwegian Geotechnical Institute (NGI), 2016.

[61] Direktoratsgruppen for gjennomføringen av vannforskriften. Direktoratsgruppen vanndirektiv 2018. Veileder 02:2018 Klassifisering. Miljødirektoratet, Fiskeridirektoratet, Folkehelseinstituttet, Havforskningsinstituttet, Kystverket, Mattilsynet, NGU, NVE, Landbruksdirektoratet, and Statens vegvesen, 2018.

[62] A. Akcil and S. Koldas. Acid Mine Drainage (AMD): causes, treatment and case studies. *Journal of Cleaner Production*, 14(12):1139–1145, 2006.

[63] P. C. Singer and W. Stumm. Acidic Mine Drainage: The Rate-Determining Step. *Science*, 167(3921):1121–1123, 1970.

[64] G. S. Simate and S. Ndlovu. Acid mine drainage: Challenges and opportunities. *Journal of Environmental Chemical Engineering*, 2(3):1785–1803, 2014.

[65] J. S. Espana. Chapter 7 - The Behavior of Iron and Aluminum in Acid Mine Drainage: Speciation, Mineralogy, and Environmental Significance. In Trevor M. Letcher, editor, *Thermodynamics, Solubility and Environmental Issues*, chapter 7, pages 137–150. Elsevier, 2007.

[66] G. Lee, J. M. Bigham, and G. Faure. Removal of trace metals by coprecipitation with Fe, Al and Mn from natural waters contaminated with acid mine drainage in the Ducktown Mining District, Tennessee. *Applied Geochemistry*, 17(5):569–581, 2002.

[67] F. Fu and Q. Wang. Removal of heavy metal ions from wastewaters: A review. *Journal of Environmental Management*, 92(3):407–418, 2011.

[68] A. A. Peláez-Cid, V. Romero-Hernández, A. M. Herrera-González, A. Bautista-Hernández, and O. Coreño-Alonso. Synthesis of activated carbons from black sapote seeds, characterization and application in the elimination of heavy metals and textile dyes. *Chinese Journal of Chemical Engineering*, 2019.

[69] J. Taylor, S. Pape, and N. Murphy. A Summary of Passive and Active Treatment Technologies for Acid and Metalliferous Drainage (AMD). The Australian Centre for Minerals Extension and Research (ACMER), 2005.

[70] Moodley, I. and Sheridan, C. M. and Kappelmeyer, U. and Akcil, A. Environmentally sustainable acid mine drainage remediation: Research developments with a focus on waste/by-products. *Minerals Engineering*, 126:207–220, 2018.

[71] Jeffrey G. Skousen, Paul F. Ziemkiewicz, and Louis M. McDonald. Acid mine drainage formation, control and treatment: Approaches and strategies. *The Extractive Industries and Society*, 6(1):241–249, 2019.

[72] S. Steen. Treatment and monitoring of polluted leakage water from the former killingdal concentration plant area in trondheim - comparable studies of olivine and lime in a semi-scale water treatment system. Master's thesis, Norwegian University of Science and Technology (NTNU), May 2020.

[73] E. Nariyan, M. Sillanpää, and C. Wolkersdorfer. Electrocoagulation treatment of mine water from the deepest working European metal mine – Performance, isotherm and kinetic studies. *Separation and Purification Technology*, 177:363–373, 2017.

[74] X. Chen and G. Chen. *Electroflotation*, pages 263–277. Springer New York, 2010.

[75] M. Borówko. Adsorption on Heterogeneous Surfaces. In Jósef Tóth, editor, *ADSORPTION Theory, Modeling, and Analysis*, chapter 2, page 105. Taylor & Francis Group, 2002.

[76] Z. Adamczyk. Irreversible Adsorption of Particles. In Jósef Tóth, editor, *ADSORPTION Theory, Modeling, and Analysis*, chapter 5, page 251. Taylor & Francis Group, 2002.

[77] R. C. Bansal and M. Goyal. *ACTIVATED CARBON ADSORPTION*. Taylor & Francis Group, 2005.

[78] D. Prahas, Y. Kartika, N. Indrawati, and S. Ismadji. Activated carbon from jackfruit peel waste by H_3PO_4 chemical activation: Pore structure and surface chemistry characterization. *Chemical Engineering Journal*, 140(1-3):32–42, 2008.

[79] A. A. Peláez-Cid, A. M. Herrera-González, A. B. Hernández, and M. S. Villanueva. Preparation and characterization of activated carbon from Agave tequilana Weber for the removal of textile dyes and heavy metals. *Desalination and Water Treatment*, 57(44):21105–21117, 2016.

[80] Z. Hu and M. P. Srinivasan. Preparation of high-surface-area activated carbons from coconut shell. *Microporous and Mesoporous Materials*, 27(1):11–18, 1999.

[81] A. Bhatnagar, W. Hogland, M. Marques, and M. Sillanpää. An overview of the modification methods of activated carbon for its water treatment applications. *Chemical Engineering Journal*, 219:499–511, 2013.

[82] J. Valentín-Reyes, R. B. García-Reyes, A. García-González, E. Soto-Regalado, and F. Cerino-Córdova. Adsorption mechanisms of hexavalent chromium from aqueous solutions on modified activated carbons. *Journal of Environmental Management*, 236:815–822, 2019.

[83] NVE Atlas. NVE Atlas, April 2020. Url is `https://atlas.nve.no/Html5Viewer/index.html?viewer=nveatlas#`.

[84] International Organization for Standardization. ISO 5667-6 Water quality - Sampling - Part 6: Guidance on sampling of rivers and streams. International Organization for Standardization, 2014.

[85] International Organization for Standardization. ISO 5667-3 Water quality - Sampling - Part 3: Preservation and handling of water samples. International Organization for Standardization, 2018.

[86] Standard Norge. NS 4784 Vannundersøkelse. Prøvetaking av vann for bestemmelse av spormetaller. Standard Norge, 1988.

[87] ArcGlobe. Map of Ilsvika, Trondheim, 2020.

[88] J. Engebretsen. Tiltak for rensing av Killingdalområdet. Master's thesis, Norwegian University of Science and Technology (NTNU), 2017.

[89] T. Nøklegaard. Miljøovervåkning Nordgulen 2013/2014: Metaller i sedimenter, biota og vann samt bunnfaunaundersøkelse. DNV GL on behalf of Elkem AS Bremanger Smelteverk, 2014.

[90] M. Moseid. Trondheim havn. Helhetlig tiltaksplan for Trondheim havnebasseng. Norwegian Geotechnical Institute (NGI) on behalf of Trondheim Municipality, 2011.

[91] P. T. Gauthier, W. P. Norwood, E. E. Prepas, and G.G. Pyle. Metal-PAH mixtures in the aquatic environment: A review of co-toxic mechanisms leading to more-than-additive outcomes. *Aquatic Toxicology*, 154:253–269, 2014.

[92] A. S. Sheoran and V. Sheoran. Heavy metal removal mechanism of acid mine drainage in wetlands: A critical review. *Minerals Engineering*, 19(2):105–116, 2006.

[93] Late lessons from early warnings: science, precaution, innovation. European Environment Agency, 2013.

[94] Google Maps. Map of Korsfjorden in relation to Trondheim, May 2020.

[95] J. W. Morse, R. S. Arvidson, and A. Lüttge. Calcium Carbonate Formation and Dissolution. *Chemical Reviews*, 107(2):342–381, 2007.

[96] M. Aloupi and M. O. Angelidis. Normalization to lithium for the assessment of metal contamination in coastal sediment cores from the Aegean Sea, Greece. *Marine Environmental Research*, 52(1):1–12, 2001.

[97] R. Das and P. D. Blanc. Chlorine Gas Exposure and the Lung: A Review. *Toxicology and Industrial Health*, 9(3):439–455, 1993.

[98] C. A. Cravotta Iii and M. K. Trahan. Limestone drains to increase pH and remove dissolved metals from acidic mine drainage. *Applied Geochemistry*, 14(5):581–606, 1999.

[99] S. Liu, H. A. Abu Hajar, G. Riefler, and B. J. Stuart. Investigation of electrolytic flocculation for microalga Scenedesmus sp. using aluminum and graphite electrodes. *Royal Society of Chemistry*, 8:38808–38817, 2018.

[100] M. Bissen and F. H. Frimmel. Arsenic — a Review. Part I: Occurrence, Toxicity, Speciation, Mobility. *Acta hydrochimica et hydrobiologica*, 31(1):9–18, 2003.

[101] J. W. Wang, D. Bejan, and N. J. Bunce. Removal of Arsenic from Synthetic Acid Mine Drainage by Electrochemical pH Adjustment and Coprecipitation with Iron Hydroxide. *Environmental Science & Technology*, 37(19):4500–4506, 2003.

[102] P. Ratna Kumar, S. Chaudhari, K. C. Khilar, and S. P. Mahajan. Removal of arsenic from water by electrocoagulation. *Chemosphere*, 55(9):1245–1252, 2004.

[103] I. Giannopoulou and D. Panias. Differential precipitation of copper and nickel from acidic polymetallic aqueous solutions. *Hydrometallurgy*, 90(2):137–146, 2008.

[104] C. Escobar, C. Soto-Salazar, and M. Inés Toral. Optimization of the electrocoagulation process for the removal of copper, lead and cadmium in natural waters and simulated wastewater. *Journal of Environmental Management*, 81(4):384–391, 2006.

[105] A. Milchev and T. Zapryanova. Nucleation and growth of copper under combined charge transfer and diffusion limitations — Part II. *Electrochimica Acta*, 51(23):4916–4921, 2006.

[106] D. Eeshwarasinghe, P. Loganathan, and S. Vigneswaran. Simultaneous removal of polycyclic aromatic hydrocarbons and heavy metals from water using granular activated carbon. *Chemosphere*, 223:616–627, 2019.

[107] T. A. Kurniawan, G. Y. S. Chan, W. Lo, and S. Babel. Comparisons of low-cost adsorbents for treating wastewaters laden with heavy metals. *Science of The Total Environment*, 366(2-3):409–426, 2006.

[108] W. Stumm and G.F. Lee. The chemistry of aqueous iron. *Schweiz. Z. Hydrologie*, 22:295–319, 1960.

[109] M. A. Kahn and Y. I. Khattak. Adsorption of copper from copper sulfate solution on carbon black "Spheron 9"-—II. *Carbon*, 30(7):957–960, 1992.

[110] M. Kavand, P. Eslami, and L. Razeh. The adsorption of cadmium and lead ions from the synthesis wastewater with the activated carbon: Optimization of the single and binary systems. *Journal of Water Process Engineering*, 34, 2020.

[111] J. P. Chen and X. Wang. Removing copper, zinc, and lead ion by granular activated carbon in pretreated fixed-bed columns. *Separation and Purification Technology*, 19(3):157–167, 2000.

[112] Meenakshi Goyal, V.K Rattan, Diksha Aggarwal, and R.C Bansal. Removal of copper from aqueous solutions by adsorption on activated carbons. *Colloids and Surfaces A: Physicochemical and Engineering Aspects*, 190(3):229–238, 2001.

[113] M. A. Ferro-García, J. Rivera-Utrilla, J. Rodríguez-Gordillo, and I. Bautista-Toledo. Adsorption of zinc, cadmium, and copper on activated carbons obtained from agricultural by-products. *Carbon*, 26(3):363–373, 1988.

[114] D.P. Sounthararajah, P. Loganathan, J. Kandasamy, and S. Vigneswaran. Effects of Humic Acid and Suspended Solids on the Removal of Heavy Metals from Water by Adsorption onto Granular Activated Carbon. *International Journal of Environmental Research and Public Health*, 12(9):10475–10489, 2015.

[115] J. Zhu, P. Zhang, S. Yuan, and M. Tong. Arsenic oxidation and immobilization in acid mine drainage in karst areas. *Science of The Total Environment*, 727:138629, 2020.

[116] S. K. Gupta and K. Y. Chen. Arsenic Removal by Adsorption. *Journal (Water Pollution Control Federation)*, 50(3):493–506, 1978.

[117] M. A. Hashim, A. Kundu, S. Mukherjee, Y. S. Ng, S. Mukhopadhyay, G. Redzwan, and B. Sen Gupta. Arsenic removal by adsorption on activated carbon in a rotating packed bed. *Journal of Water Process Engineering*, 30:100591, 2019. SI: Sust Water Processing.

[118] S. Vega-Hernandez, J. Weijma, and C. J. N. Buisman. Immobilization of arsenic as scorodite by a thermoacidophilic mixed culture via As(III)-catalyzed oxidation with activated carbon. *Journal of Hazardous Materials*, 368:221–227, 2019.

[119] T. W. J. Albrecht, J. Addai-Mensah, and D. Fornasiero. Effect of pH, concentration and temperature on copper and zinc hydroxide formation/precipitation in solution. Ian Wark Research Institute, University of South Australia, 2011.

[120] R. Leyva-Ramos, J. R. Rangel-Mendez, J. Mendoza-Barron, L. Fuentes-Rubio, and R. M. Guerrero-Coronado. Adsorption of cadmium(II) from aqueous solution onto activated carbon. *Water Science & Technology*, 35(7):205–211, 1997.

[121] S. A. Maddodi, H. A. Alalwan, A. H. Alminshid, and M. N. Abbas. Isotherm and computational fluid dynamics analysis of nickel ion adsorption from aqueous solution using activated carbon. *South African Journal of Chemical Engineering*, 32:5–12, 2020.

[122] A.K. Bhattacharya, S.N. Mandal, and S.K. Das. Adsorption of Zn(II) from aqueous solution by using different adsorbents. *Chemical Engineering Journal*, 123(1):43–51, 2006.

[123] A. Seco, P. Marzal, C. Gabaldón, and J. Ferrer. Adsorption of Heavy Metals from Aqueous Solutions onto Activated Carbon in Single Cu and Ni Systems and in Binary Cu–Ni, Cu–Cd and Cu–Zn Systems. *Journal of Chemical Technology & Biotechnology*, 68(1):23–30, 1997.

[124] H. Yanagisawa, Y. Matsumoto, and M. Machida. Adsorption of Zn(II) and Cd(II) ions onto magnesium and activated carbon composite in aqueous solution. *Applied Surface Science*, 256(6):1619–1623, 2010.

[125] Amir [Fouladi Tajar], Tahereh Kaghazchi, and Mansooreh Soleimani. Adsorption of cadmium from aqueous solutions on sulfurized activated carbon prepared from nut shells. *Journal of Hazardous Materials*, 165(1):1159–1164, 2009.

[126] S. B. Lalvani, T. Wiltowski, A. Hübner, A. Weston, and N. Mandich. Removal of hexavalent chromium and metal cations by a selective and novel carbon adsorbent. *Carbon*, 36(7-8):1219–1226, 1998.

[127] M. Ahmaruzzaman. Industrial wastes as low-cost potential adsorbents for the treatment of wastewater laden with heavy metals. *Advances in Colloid and Interface Science*, 166(1-2):36–59, 2011.

[128] W. Zheng, X. M. Li, F. Wang, Q. Yang, P. Deng, and G. M. Zeng. Adsorption removal of cadmium and copper from aqueous solution by areca — A food waste. *Journal of Hazardous Materials*, 157(2):490–495, 2008.

[129] E. Malkoc and Y. Nuhoglu. Investigations of nickel(II) removal from aqueous solutions using tea factory waste. *Journal of Hazardous Materials*, 127(1):120–128, 2005.

[130] D. Kołodyńska, Krukowska. J., and P. Thomas. Comparison of sorption and desorption studies of heavy metal ions from biochar and commercial active carbon. *Chemical Engineering Journal*, 307:353–363, 2017.

[131] Standard Norge. NS 4784 Vannundersøkelse. Bruk av induktivt koblet plasmamassespektrometri (ICP-MS). Del 2: Bestemmelse av utvalgte elementer inkludert uraniumsisotoper. Standard Norge, 2016.

Appendix

A Classification of conditions in freshwater, seawater, and sediments

Table A.1: Classification for freshwater, in µg/L. For cadmium, the hardness of the Killingdal stream is calculated to be <40 mg $CaCO_3$/L. All the values are upper limit for the respective category. [60]

Element	Background (I)	Good (II)	Moderate (III)	Bad (IV)	Very bad (V)
Cadmium (Cd)	0.003	0.08	0.45	4.5	> 4.5
Chromium (Cr)	0.1	3.4	-	-	> 3.4
Copper (Cu)	0.3	7.8	-	15.6	> 15.6
Zinc (Zn)	1.5	11	-	60	> 60
Nickel (Ni)	0.5	4	34	67	> 67
Arsenic (As)	0.15	0.5	8.5	85	> 85
Lead (Pb)	0.02	1.2	14	57	> 57

Table A.2: Classification for seawater, in µg/L. For cadmium, the hardness of the Trondheimsfjord is calculated to be >200 mg $CaCO_3$/L. All the values are upper limit for the respective category. [60]

Element	Background (I)	Good (II)	Moderate (III)	Bad (IV)	Very bad (V)
Cadmium (Cd)	0.03	0.2	1.5	15	> 15
Chromium (Cr)	0.1	3.4	36	358	> 358
Copper (Cu)	0.3	2.6	-	5.2	> 5.2
Zinc (Zn)	1.5	3.4	6	60	> 60
Nickel (Ni)	0.5	8.6	34	67	> 67
Arsenic (As)	0.15	0.6	8.5	85	> 85
Lead (Pb)	0.02	1.3	14	57	> 57

Table A.3: Classification for sediments, in µg/g dry solids. All the values are upper limit for the respective category. [60]

Element	Background (I)	Good (II)	Moderate (III)	Bad (IV)	Very bad (V)
Cadmium (Cd)	0.2	2.5	16	157	> 157
Chromium (Cr)	60	660	6000	15500	15500-25000
Copper (Cu)	20	84	-	147	> 147
Zinc (Zn)	90	139	750	6690	> 6690
Nickel (Ni)	30	42	271	533	> 533
Arsenic (As)	15	18	71	580	> 580
Lead (Pb)	25	150	1480	2000	2000-2500

B Sediment sample collection and pre-treatment procedures

B.1 Sediment sampling location coordinates

Table B.1: The coordinates where the sediment samples in the Trondheimsfjord are taken.

Sample location	Coordinates	Approximate distance from shore
1	63°26'6.97"N 10°21'15.25"E	170 m
2	63°26'6.67"N 10°21'11.68"E	120 m
3	63°26'6.30"N 10°21'7.94"E	70 m
4	63°26'6.00"N 10°21'4.88"E	20 m
5	63°26'9.49"N 10°21'13.93"E	170 m
6	63°26'8.56"N 10°21'10.85"E	120 m
7	63°26'7.73"N 10°21'7.92"E	70 m
8	63°26'6.86"N 10°21'5.03"E	20 m
9	63°26'4.17"N 10°21'15.71"E	170 m
10	63°26'4.54"N 10°21'12.03"E	120 m
11	63°26'4.88"N 10°21'8.46"E	70 m
12	63°26'5.20"N 10°21'5.14"E	20 m

B.2 Weight of sediment samples

Table B.2: Weight of sample extracted from sediment samples and reference material, and weight of samples and reference material after digestion and dilution. Ref1 is reference material for seawater sediments, Ref2 is reference material for freshwater sediments.

Sample number	Start weight (mg)	Final weight sediment (g)
1	295.2	108.29
2	275.9	108.99
3	292.0	107.72
4	292.6	107.48
5	334.7	107.71
6	272.5	107.80
7.1	299.6	107.67
7.2	260.9	108.37
7.3	250.0	107.37
8	319.7	109.31
9	312.7	111.41
10	300.2	107.37
11	294.6	108.38
12	275.4	108.38
13	258.5	108.80
14	322.5	107.47
15	298.2	108.40
16	336.5	107.62
17	343.2	107.29
18	317.6	108.38
19	335.6	108.38
20	268.8	107.74
21.1	269.5	108.36
21.2	333.8	107.92
21.3	257.7	108.02
22	341.3	108.47
23	343.3	111.67
24	345.4	107.87
25	279.7	108.11
Ref1.1	101.3	108.66
Ref1.2	100.4	108.61
Ref1.3	108.7	108.00
Ref2.1	121.0	107.17
Ref2.2	111.9	111.21
Ref2.3	101.9	108.95

B.3 Microwave Program

Table B.3: The program used to operate the MLS Microwave.

Step	Time [hh:mm:ss]	Temp 1 [°C]	Temp 2 [°C]	Press [bar]	Energy [W]
1	00:05:00	50	60	160	1000
2	00:10:00	50	60	160	1000
3	00:10:00	100	60	160	1000
4	00:08:00	110	60	160	1000
5	00:15:00	190	60	160	1000
6	00:05:00	210	60	160	1000
7	00:15:00	245	60	160	1000
8	00:10:00	245	60	160	1000

C Detection limits for ICP-MS used in this thesis

Table C.1: ICP-MS detection limits for all the elements analysed in this thesis, according to results obtained from the ICP-MS laboratory at NTNU. Detection limits (D. limit) denoted QL-25% are listed in this table.

Element	Isotope	D. limit (µg/L)
Ag	109	0.02
Al	27	0.2
As	75	0.025
Au	197	0.0002
B	11	0.05
B	11	0.08
Ba	137	0.013
Be	9	0.002
Be	9	0.008
Bi	209	0.001
Br	81	3
Ca	44	2
Cd	111/114	0.002
Cd	111/114	0.01
Ce	140	0.0002
Cl	35	100
Co	59	0.004
Cr	53	0.02
Cs	133	0.0005
Cu	63/65	0.03
Dy	163	0.0008
Er	166	0.0003
Eu	153	0.0008
Fe	56	0.02
Ga	69	0.007
Gd	155	0.02
Ge	72	0.02
Hf	178	0.001
Hg	202	0.002
Ho	165	0.0002
I	127	1
In	115	0.0005
Ir	193	0.0005
K	39	1
La	139	0.0005
La	139	0.002
Li	7	0.005
Li	7	0.03
Lu	175	0.0002
Mg	24	0.1
Mg	25	0.5
Mn	55	0.006
Mo	98	0.02
Na	23	10
Nb	93	0.001
Nb	93	0.025
Nd	146	0.0002
Ni	60	0.015
P	31	0.4
Pb	208	0.002
Pd	104	0.05
Pr	141	0.0003
Pt	195	0.001
Rb	85	0.012
Re	185	0.04
Rh	103	0.0005
Rh	103	0.01
Ru	85	0.001
S	32	5
S	34	20
Sb	121	0.002
Sc	45	0.004
Se	82	0.05
Se	78	0.15
Si	29	10
Sm	147	0.0005
Sn	118	0.001
Sn	118	0.01
Sr	88	0.025
Ta	181	0.0002
Tb	159	0.0002
Te	125	0.1
Th	232	0.0005
Ti	47	0.02
Tl	205	0.0003
Tm	169	0.0005
U	238	0.0003
V	51	0.003
W	182	0.001
Yb	172	0.0004
Yb	89	0.0004
Zn	66	0.025
Zn	67	0.04
Zr	90	0.0005
Zr	90	0.025

D Summary of method

Table D.1: Sampling and analysis procedures for monitoring samples. *Pre-treatment: Freeze dried, Ultraclave.

Sample location	Matrix	Sampling equipment	Preservation	Analysis
Killingdal stream	Freshwater	Syringe	HNO_3	ICP-MS
Trondheimsfjord coast	Seawater	Syringe	HNO_3	ICP-MS
Trondheimsfjord sediment	Sediment	Box corer	HNO_3	ICP-MS*
Trondheimsfjord deep sea	Seawater	Rosette sampler	HNO_3	ICP-MS

Table D.2: Setup, sampling, and analysis procedures for laboratory experiments. MP stands for mechanical pencil, C stands for cylindrical electrode, and F stands for flat electrode.

Exp.	Cathode	Anode	Type of water	Voltage	Equipment	Preservation	Analysis
1	Aluminium	Aluminium	Cleansed	1	Syringe	HNO_3	ICP-MS
2	Aluminium	Aluminium	Cleansed, Not cleansed	1.5	Syringe	HNO_3	ICP-MS
Blank	Aluminium	Aluminium	0.0001M NaSO4	None, 1.5	Syringe	HNO_3	ICP-MS
3	Aluminium	Graphite MP	Not cleansed	1.5	Syringe	HNO_3	ICP-MS
4	Aluminium	Graphite C	Cleansed, Not cleansed	1.5	Syringe	HNO_3	ICP-MS
5	Aluminium	Graphite F	Cleansed, Not cleansed	1.5	Syringe	HNO_3	ICP-MS
6	Graphite C	Graphite F	Cleansed, Not cleansed	1.5	Syringe	HNO_3	ICP-MS

Table D.3: Equipment used in both the monitoring and the treatment experiments of water at Killingdal.

Equipment	Material	Reusable	Cleaning
Syringe	Polypropylene	Yes	Rinsed with clean water or Milli-Q, and rinsed three times with sample water
Gloves	Nitrile	No	-
Filter 0.45 µm membrane	Polyethersulfone	No	Flushed three times with sample water
ICP-MS tubes	Polypropylene	No	-
Nitric acid	Ultrapure HNO_3	No	-
Box corer	Steel	Yes	Seawater
Rosette sampler		Yes	Seawater
Experiment pipes	Plexiglass	Yes	Rinsed with *Not cleansed* water from Killingdal
Container for electrolysis	Glass	Yes	Washed with soap and water, and then rinsed Milli-Q water
Magnet	Ceramic	Yes	Washed with soap and water, and then rinsed Milli-Q water
Al electrodes	Al wire fence	No	-
Graphite electrodes	Carbon	Yes	Rinsed with Milli-Q water
10 L containers	Polyethylene	Yes	Rinsed with sample water

E Results from monitoring of the Killingdal stream, effluent into the Trondheimsfjord, and sediments i the Trondheimsfjord

E.1 Killingdal stream concentrations

Table E.1: Concentrations of elements in the Killingdal stream from 12.12.2018 until 12.11.2019. The RSD, i.e. uncertainty, is given for each value and a red number indicates relatively high uncertainty ($> 10\,\%$). The unit is µg/L for all the concentrations, and the RSD values have the unit %.

Date	Fe	(RSD)	Cr	(RSD)	Ni	(RSD)	Cu	(RSD)	Zn	(RSD)	As	(RSD)	Cd	(RSD)	Pb	(RSD)
11.10.2018	33.6	(4.7)	0.209	(10.0)	0.639	(4.1)	3.34	(7.3)	8.07	(6.3)	0.0783	(19.1)	0.0102	(6.1)	0.0231	(23.3)
12.12.2018	54.7	(4.7)	0.456	(3.2)	1.22	(10.3)	4.36	(4.9)	13.3	(6.7)	0.0876	(18.9)	0.0181	(10.7)	0.103	(6.1)
17.12.2018	18.0	(0.7)	0.261	(9.2)	0.558	(14.2)	2.32	(2.3)	4.34	(6.7)	0.0673	(33.5)	0.00704	(59.2)	0.0292	(9.3)
18.01.2019	21.6	(2.2)	0.336	(16.2)	0.580	(14.1)	2.54	(1.2)	4.39	(3.5)	0.0546	(40.4)	0.00965	(29.4)	0.0315	(10.1)
31.01.2019	2250	(0.3)	0.262	(5.6)	29.9	(1.9)	6710	(0.8)	9650	(0.9)	0.314	(8.0)	34.3	(1.9)	4.36	(2.0)
07.02.2019	24.0	(2.7)	0.221	(5.2)	4.59	(2.9)	2.46	(4.9)	5.24	(12.2)	0.0433	(87.2)	0.00785	(14.1)	0.0386	(3.1)
02.03.2019	57.3	(1.1)	0.317	(15.0)	0.591	(15.0)	3.32	(2.8)	9.43	(3.2)	0.0657	(66.8)	0.0139	(21.9)	0.0757	(10.6)
05.03.2019	18.9	(3.4)	0.232	(7.3)	0.553	(4.9)	2.35	(3.6)	5.48	(5.7)	0.0449	(66.1)	0.00973	(21.1)	0.0219	(12.2)
22.03.2019	38.1	(0.9)	0.328	(10.3)	0.503	(5.8)	2.40	(7.3)	7.87	(7.4)	0.0294	(56.8)	0.00897	(28.1)	0.0555	(8.1)
24.05.2019	7.22	(3.6)	0.138	(8.1)	0.480	(12.9)	2.17	(2.5)	2.51	(8.8)	0.129	(110.3)	0.00292	(53.3)	0.00632	(26.3)
28.05.2019	11.4	(0.7)	0.219	(20.5)	0.552	(14.7)	2.38	(8.4)	4.48	(7.9)	0.0687	(0.0)	0.00796	(32.7)	0.0175	(8.7)
03.06.2019	20.8	(2.6)	0.273	(9.5)	0.521	(30.1)	2.51	(5.5)	4.43	(19.0)	0.0902	(69.5)	0.0107	(75.4)	0.0280	(10.4)
09.06.2019	26.7	(2.8)	0.291	(13.8)	0.512	(25.1)	4.13	(6.8)	5.52	(12.4)	0.0371	(173.2)	0.0111	(10.2)	0.0435	(3.1)
12.09.2019	9.70	(0.2)	0.193	(4.8)	0.481	(10.9)	2.62	(2.9)	2.32	(9.2)	0.0471	(48.2)	0.00818	(13.4)	0.00675	(11.3)
19.09.2019	77.2	(2.8)	0.418	(6.5)	0.652	(4.8)	3.76	(3.3)	6.64	(8.6)	0.0795	(8.3)	0.0159	(15.4)	0.0861	(3.9)
02.10.2019	118.9	(2.3)	0.409	(14.1)	0.647	(13.7)	4.43	(2.2)	8.79	(8.6)	0.103	(48.3)	0.0148	(22.1)	0.139	(5.1)
18.10.2019	11.8	(1.5)	0.180	(1.0)	0.646	(4.7)	2.56	(1.4)	2.55	(5.4)	0.0489	(14.1)	0.00811	(19.3)	0.0177	(2.6)
12.11.2019	16.9	(0.8)	0.203	(2.2)	0.665	(6.0)	2.88	(2.3)	3.61	(3.5)	0.0528	(32.0)	0.00951	(16.0)	0.0228	(2.3)

E.2 Trondheimsfjord water concentrations

Table E.2: Concentrations of elements in the Trondheimsfjord from 12.12.2018 until 19.09.2019. The RSD, i.e. uncertainty, is given for each value and a red number indicates relatively high uncertainty ($> 10\,\%$). The unit is µg/L for all the concentrations, and the RSD values have the unit %.

Date	Fe	(RSD)	Cr	(RSD)	Ni	(RSD)	Cu	(RSD)	Zn	(RSD)	As	(RSD)	Cd	(RSD)	Pb	(RSD)
12.12.2018	37.5	(2.9)	0.0707	(15.6)	5.36	(7.2)	830	(2.8)	1614	(2.8)	0.679	(32.0)	6.17	(4.2)	0.172	(6.9)
02.03.2019	65.0	(2.0)	0.204	(6.2)	4.38	(4.3)	512	(1.8)	1505	(0.4)	0.418	(58.4)	5.93	(3.7)	0.132	(4.9)
05.03.2019	18.2	(1.5)	-0.0640	(2.9)	0.788	(13.2)	56.9	(1.4)	174	(5.4)	1.29	(21.5)	0.699	(14.2)	0.0524	(7.1)
11.03.2019	5.35	(3.4)	0.0210	(19.8)	0.425	(10.9)	27.5	(1.3)	82.8	(5.5)	1.22	(18.2)	0.346	(5.3)	0.0362	(4.7)
22.03.2019	15.4	(3.3)	0.0550	(28.8)	1.81	(14.6)	142	(2.7)	390	(2.7)	1.01	(31.3)	1.72	(7.4)	0.0983	(21.6)
28.05.2019	7.62	(2.5)	0.0496	(16.5)	0.489	(8.1)	4.92	(3.9)	7.23	(11.6)	0.519	(12.5)	0.0325	(12.9)	0.0210	(10.5)
03.06.2019	2.95	(5.0)	0.0365	(26.2)	0.297	(20.8)	14.2	(2.5)	61.4	(2.6)	1.08	(27.5)	0.294	(5.7)	0.00937	(32.4)
09.06.2019	10.4	(3.1)	0.0550	(11.6)	1.37	(0.6)	114	(2.2)	428	(1.8)	0.706	(24.0)	1.51	(0.5)	0.0346	(10.0)
19.09.2019	37.2	(1.6)	1.58	(18.0)	2.63	(16.8)	141	(1.8)	510	(5.5)	1.45	(28.7)	2.08	(5.0)	0.154	(1.8)

E.3 Trondheimsfjord sediment concentrations

Table E.3: Average concentrations of elements in the sediment samples collected at sample points 1-12. The unit is µg/g for all the values.

Element	1	2	3	4	5	6	7	8	9	10	11	12	25
Al	16300	14600	4630	11300	20600	17000	6600	9060	7690	4300	7260	7220	25200
S	143000	158000	3290	15600	83600	29600	10900	193000	11100	2440	22000	9550	200000
Fe	173000	175000	10400	38200	168000	83100	23900	167000	32900	7940	42200	18700	234000
Cr	61.6	57.6	12.4	35.3	84.5	57.9	19.4	38.9	25.4	11.5	25.2	31.0	121
Ni	30.1	17.3	5.00	15.0	31.2	21.0	7.47	20.9	8.93	4.99	9.43	8.13	32.1
Cu	1740	1310	51.1	286	1160	481	137	2070	162	32.9	280	110	2270
Zn	4180	4270	102	649	2610	895	251	8430	352	69.2	724	385	7460
As	455	495	22.3	82.8	414	218	63.0	457	89.3	16.5	113	29.5	754
Cd	9.51	9.69	0.150	1.45	4.73	1.03	0.358	22.9	0.394	0.118	1.33	1.01	17.8
Pb	791	1010	29.3	101	612	277	80.5	1090	113	18.3	166	41.0	1650
Ca	25500	47900	268000	211000	25500	134000	287000	139000	272000	332000	289000	264000	10700
Hg	0.595	0.491	0.0475	0.171	0.480	0.246	0.0857	1.05	0.120	0.0421	0.152	0.0772	0.980
K	5520	4920	1710	4330	6610	5370	2380	2380	2780	1640	2460	2020	8230
Li	11.3	10.0	3.41	8.08	14.68	12.68	3.70	4.04	5.33	2.28	4.81	4.85	15.8
Mg	10200	8540	3640	8080	12900	10500	4760	5670	5410	3590	5260	4680	13200
Mn	351	373	75.7	186	416	293	106	238	140	70.8	130	173	566
Na	12400	7220	4330	14200	11700	9070	5750	4350	6340	3980	5610	4070	6740
P	489	381	281	720	1050	929	282	187	471	174	399	273	757

F Average concentration of trace elements in sediments at each distance from shore

Table F.1: Average concentrations (Conc.) of sediment samples collected in four different distances from shore. Distance group 1 is 20 m from shore (include sample location 4, 8, and 12), distance group 2 is 700 m from shore (include sample locations 3, 7, and 11), distance group 3 is 120 m from shore (include sample locations 2, 6, and 10), and distance group 4 is 170 m from shore (include sample locations 1, 5, and 9). Included are also the standard deviation (SD) and standard error (SE) obtained when finding the average concentrations.

Distance group		1	2	3	4
Fe	Conc.	74600	25500	88600	125000
	SD	65800	13000	68200	65000
	SE	38000	7510	39400	37500
Cr	Conc.	35.0	19.0	42.4	57.1
	SD	3.20	5.22	21.8	24.3
	SE	1.85	3.01	12.6	14.1
Ni	Conc.	14.7	7.30	14.4	23.4
	SD	5.22	1.81	6.85	10.3
	SE	3.02	1.05	3.95	5.92
Cu	Conc.	822	156	608	1022
	SD	886	94.2	528	653
	SE	511	54.4	305	377
Zn	Conc.	3160	359	1750	2380
	SD	3730	265	1820	1570
	SE	2160	153	1050	907
As	Conc.	190	65.9	243	319
	SD	190	36.9	196	164
	SE	110	21.3	113	94.4
Cd	Conc.	8.46	0.612	3.61	4.88
	SD	10.2	0.513	4.31	3.72
	SE	5.91	0.296	2.49	2.15
Pb	Conc.	410	91.9	434	505
	SD	480	56.4	419	287
	SE	277	32.6	242	166

G Results from Shapiro-Wilk normality test and Kruskal-Wallis H Test analysis of the trends in the sediments in different distances from shore (groups 1-4).

Table G.1: Results from Shapiro-Wilk normality test of the trends in the sediments in different distances from shore (groups 1-4). A confidence interval of 95 % was used.

Element	Location	Statistic	n	p-value
Fe	1	0.734	8	0.005
	2	0.862	8	0.127
	3	0.872	6	0.235
	4	0.724	6	0.011
Cr	1	0.948	8	0.694
	2	0.935	8	0.565
	3	0.655	6	0.002
	4	0.883	6	0.285
Ni	1	0.883	8	0.203
	2	0.961	8	0.821
	3	0.806	6	0.066
	4	0.686	6	0.004
Cu	1	0.647	8	0.001
	2	0.816	8	0.042
	3	0.845	6	0.143
	4	0.882	6	0.278
Zn	1	0.535	8	0.000
	2	0.789	8	0.022
	3	0.766	6	0.029
	4	0.922	6	0.52
As	1	0.73	8	0.005
	2	0.858	8	0.115
	3	0.854	6	0.170
	4	0.848	6	0.150
Cd	1	0.515	8	0.000
	2	0.74	8	0.006
	3	0.702	6	0.006
	4	0.926	6	0.548
Pb	1	0.579	8	0.000
	2	0.826	8	0.054
	3	0.816	6	0.082
	4	0.858	6	0.181

Table G.2: Result from analysis with the Kruskal-Wallis H Test in SPSS for the trends between the sample locations 1-12. A confidence interval of 95 % was used and n=28.

Element	Test statistics	Degree of freedom	p-value
Fe	5.312	3	0.150
Cr	9.286	3	0.026
Ni	8.435	3	0.038
Cu	4.943	3	0.176
Zn	4.187	3	0.242
As	5.772	3	0.123
Cd	4.421	3	0.219
Pb	5.531	3	0.137

H Correlation between elements in sediment samples

Table H.1: Correlation between elements found in sediment samples from Ilsvika obtained from result excel sheet from NTNU.

	Cd	Hg	Li	Na	Mg	Al	P	S	K	Ca	Cr	Mn	Fe	Ni	Cu	Zn	Pb	As
Cd	1.00																	
Hg	0.98	1.00																
Li	0.24	0.41	1.00															
Na	-0.03	0.11	0.62	1.00														
Mg	0.28	0.46	0.98	0.71	1.00													
Al	0,35	0.51	0.98	0.60	0.99	1.00												
P	-0.09	0.09	0.84	0.73	0.86	0.80	1.00											
S	0.91	0.93	0.48	0.15	0.51	0.58	0.07	1.00										
K	0.29	0.46	0.97	0.67	0.98	0.99	0.82	0.53	1.00									
Ca	-0.60	-0.72	-0.86	-0.56	-0.88	-0.89	-0.58	-0.80	-0.87	1.00								
Cr	0.44	0.59	0.93	0.49	0.94	0.97	0.70	0.65	0.95	-0.88	1.00							
Mn	0.54	0.67	0.91	0.48	0.92	0.96	0.62	0.75	0.93	-0.95	0.98	1.00						
Fe	0.74	0.83	0.74	0.37	0.77	0.81	0.39	0.93	0.77	-0.93	0.86	0.92	1.00					
Ni	0.61	0.75	0.86	0.58	0.90	0.90	0.63	0.75	0.88	-0.94	0.90	0.92	0.90	1.00				
Cu	0.91	0.96	0.54	0.22	0.58	0.64	0.16	0.98	0.59	-0.83	0.71	0.78	0.94	0.84	1.00			
Zn	0.99	0.99	0.33	0.03	0.37	0.44	-0.02	0.94	0.38	-0.68	0.53	0.62	0.81	0.68	0.95	1.00		
Pb	0.90	0.94	0.56	0.14	0.57	0.65	0.16	0.98	0.61	-0.82	0.73	0.81	0.93	0.78	0.97	0.94	1.00	
As	0.73	0.81	0.72	0.33	0.75	0.81	0.36	0.93	0.76	-0.90	0.86	0.91	0.99	0.86	0.92	0.80	0.94	1.00

I Trace element/lithium relationship

Table I.1: Relationships between trace elements and Li in the sediment samples.

	1	2	3	4	5	6	7	8	9	10	11	12
Al/Li	1440	1460	1360	1400	1400	1340	1780	2240	1440	1890	1510	1490
Fe/Li	15300	17400	3060	4740	11400	6550	6440	41300	6170	3480	8770	3850
Cr/Li	5.45	5.75	3.64	4.37	5.75	4.56	5.25	9.62	4.75	5.07	5.23	6.40
Ni/Li	2.67	1.72	1.47	1.86	2.12	1.66	2.02	5.18	1.67	2.19	1.96	1.68
Cu/Li	154	130	15.0	35.5	79.1	38.0	37.1	513	30.3	14.5	58.1	22.6
Zn/Li	370	426	29.8	80.3	177	70.6	67.7	2090	66.1	30.40	150	79.4
As/Li	40.2	49.3	6.55	10.3	28.2	17.2	17.0	113	16.8	7.23	23.4	6.09
Cd/Li	0.842	0.966	0.0440	0.179	0.323	0.0812	0.0966	5.67	0.0738	0.0519	0.276	0.207
Pb/Li	70.0	100	8.59	12.5	41.7	21.9	21.8	269	21.2	8.03	34.5	8.46

J Results from the Shapiro-Wilk normality test and Kruskal-Wallis H Test for trace element/lithium relationships.

Table J.1: Results from the Shapiro-Wilk normality test for trace element/lithium relationships. All locations 1-12 were tested, but as only locations 4 and 11 had more parallels than 3 they are the only locations results were obtained for. A confidence interval of 95 % was used.

Element	Location	Statistic	n	p-value
Al	11	0.75	4	0.039
	4	0.97	4	0.839
Fe	11	0.688	4	0.008
	4	0.883	4	0.351
Cr	11	0.921	4	0.543
	4	0.905	4	0.459
Ni	11	0.915	4	0.507
	4	0.881	4	0.343
Cu	11	0.788	4	0.082
	4	0.962	4	0.791
Zn	11	0.788	4	0.082
	4	0.831	4	0.169
As	11	0.668	4	0.005
	4	0.868	4	0.292
Cd	11	0.767	4	0.055
	4	0.817	4	0.136
Pb	11	0.809	4	0.12
	4	0.835	4	0.181

Table J.2: Result from analysis with the Kruskal-Wallis H Test in SPSS for the element/Li relationships. A confidence interval of 95 % was used and $n = 28$.

Element	Test statistics	Degree of freedom	p-value
Fe	25.33	11	0.008
Cr	16.37	11	0.128
Ni	16.15	11	0.136
Cu	25.12	11	0.009
Zn	24.95	11	0.009
As	25.67	11	0.007
Cd	25.91	11	0.007
Pb	25.66	11	0.007
Al	13.62	11	0.255

K Results from experiments with electrolysis

K.1 Results from electrolysis with aluminium electrodes

Table K.1: Results for electrolysis of *Cleansed* water at 1 V with aluminium electrodes and the accompanying percentage indicating how much of a given element is left in the water after 80 minutes. The RSD, i.e. uncertainty, is given for each value and a red number indicates relatively high uncertainty. The concentrations have the unit µg/L, and the RSD values have the unit %.

Time [min]	Al	(RSD)	Fe	(RSD)	Cr	(RSD)	Ni	(RSD)	Cu	(RSD)	Zn	(RSD)	As	(RSD)	Cd	(RSD)	Pb	(RSD)
0	387	(0.2)	5940	(1.9)	0.0563	(2.3)	25.2	(2.8)	9803	(0.1)	7140	(0.1)	0.695	(11.1)	24.7	(2.4)	2.56	(0.8)
20	471	(1.2)	5600	(2.0)	0.295	(2.1)	27.9	(1.8)	9143	(1.6)	6920	(1.2)	0.644	(1.7)	24.6	(2.3)	2.65	(1.4)
40	673	(1.3)	5070	(2.0)	0.649	(3.8)	32.4	(2.0)	8716	(1.9)	6880	(1.8)	0.456	(18.1)	23.2	(0.8)	2.92	(2.2)
60	900	(2.0)	4620	(2.6)	1.04	(5.7)	34.0	(0.9)	8148	(2.4)	6530	(0.6)	0.279	(15.7)	22.6	(2.5)	3.34	(1.8)
80	1190	(4.1)	3790	(4.7)	1.49	(11.3)	35.0	(0.3)	6930	(1.5)	5900	(0.7)	0.231	(14.6)	22.7	(2.0)	4.01	(1.3)
% left	306		63.8		2640		139		70.6		82.7		33.2		91.9		157	

Table K.2: Results for electrolysis of *Cleansed* water at 1.5 V with aluminium electrodes and the accompanying percentage indicating how much of a given element is left in the water after 80 minutes. The RSD, i.e. uncertainty, is given for each value and a red number indicates relatively high uncertainty. The concentrations have the unit µg/L, and the RSD values have the unit %.

Time [min]	Al	(RSD)	Fe	(RSD)	Cr	(RSD)	Ni	(RSD)	Cu	(RSD)	Zn	(RSD)	As	(RSD)	Cd	(RSD)	Pb	(RSD)
0	356	(2.4)	6110	(2.9)	0.0296	(12.9)	26.2	(1.3)	10200	(2.0)	7500	(1.6)	0.728	(11.1)	26.4	(1.9)	2.84	(1.2)
20	531	(1.9)	5540	(1.1)	0.429	(2.8)	29.2	(2.5)	9460	(2.9)	7230	(1.4)	0.557	(15.1)	24.5	(2.2)	2.72	(2.6)
40	782	(1.9)	5020	(0.3)	0.928	(7.9)	29.6	(0.6)	8650	(1.6)	6800	(0.3)	0.427	(12.7)	23.9	(1.5)	3.12	(1.5)
60	1070	(0.3)	4450	(1.5)	1.63	(5.6)	29.0	(1.6)	7930	(2.3)	6440	(0.8)	0.295	(2.1)	23.0	(1.4)	3.55	(1.6)
80	1230	(1.3)	3650	(0.9)	2.08	(4.8)	27.3	(2.5)	6840	(1.5)	5890	(1.0)	0.222	(21.5)	23.0	(2.3)	3.71	(2.0)
% left	346		59.8		7020		104		67.3		78.6		30.5		87.1		130	

Table K.3: Results for electrolysis of *Not cleansed* water at 1.5 V with aluminium electrodes and the accompanying percentage indicating how much of a given element is left in the water after 80 minutes. The RSD, i.e. uncertainty, is given for each value and a red number indicates relatively high uncertainty. The concentrations have the unit µg/L, and the RSD values have the unit %.

Time [min]	Al	(RSD)	Fe	(RSD)	Cr	(RSD)	Ni	(RSD)	Cu	(RSD)	Zn	(RSD)	As	(RSD)	Cd	(RSD)	Pb	(RSD)
0	1490	(1.6)	2720	(1.1)	0.129	(12.4)	15.3	(5.0)	5110	(1.0)	5170	(0.1)	0.487	(8.5)	19.2	(1.0)	6.06	(1.4)
20	1880	(4.1)	2610	(2.7)	0.663	(3.4)	23.1	(1.2)	4470	(1.0)	5090	(1.8)	0.395	(14.9)	19.3	(0.8)	4.82	(1.1)
40	2010	(3.2)	2440	(1.8)	1.09	(5.6)	24.7	(2.1)	3960	(2.5)	5160	(1.3)	0.242	(6.6)	18.9	(1.6)	4.35	(1.1)
60	2310	(2.1)	2270	(0.2)	1.43	(6.8)	24.9	(2.3)	3420	(1.0)	4990	(0.4)	0.208	(10.1)	18.6	(1.2)	4.30	(2.2)
80	2250	(1.7)	2070	(0.8)	1.72	(10.9)	24.8	(0.6)	3110	(0.5)	4820	(0.8)	0.150	(24.1)	17.7	(0.6)	3.58	(3.1)
% left	151		75.9		1340		162		60.8		93.2		30.8		92.3		59.0	

K.2 Results from blank experiment with aluminium electrodes

Table K.4: Results from blank experiment without applied voltage. The RSD, i.e. uncertainty, is given for each value and a red number indicates relatively high uncertainty (>10 %). The concentrations have the unit µg/L, and the RSD values have the unit %.

Time [min]	Al (RSD)		Fe (RSD)		Cr (RSD)		Ni (RSD)		Cu (RSD)		Zn (RSD)		As (RSD)		Cd (RSD)		Pb (RSD)	
0	-0.0277	(6.6)	-0.147	(3.5)	-0.00656	(35.9)	0.570	(8.5)	4.05	(2.9)	2.38	(2.5)	-0.000757	(N/A)	0.00277	(N/A)	0.0384	(10.7)
20	0.517	(3.6)	0.118	(1.6)	0.0189	(8.5)	27.5	(2.6)	28.1	(3.1)	19.1	(1.4)	0.00317	(62.3)	-0.0106	(N/A)	0.106	(7.8)
40	0.805	(2.3)	0.190	(2.2)	0.0207	(30.7)	40.9	(0.6)	38.8	(0.8)	31.5	(1.8)	0.00204	(205.3)	-0.00132	(N/A)	0.108	(3.8)
60	0.557	(1.8)	0.339	(3.0)	0.0233	(17.1)	48.4	(1.0)	47.8	(0.6)	42.8	(0.6)	0.00206	(97.5)	-0.00261	(N/A)	0.113	(6.9)
80	0.683	(5.3)	0.588	(0.5)	0.0298	(3.7)	53.3	(1.3)	52.9	(1.9)	53.4	(2.4)	0.00177	(39.8)	-0.00460	(N/A)	0.116	(10.7)

Table K.5: Results from blank experiment with an applied voltage of 1.5 V. The RSD, i.e. uncertainty, is given for each value and a red number indicates relatively high uncertainty (>10 %). The concentrations have the unit µg/L, and the RSD values have the unit %.

Time [min]	Al (RSD)		Fe (RSD)		Cr (RSD)		Ni (RSD)		Cu (RSD)		Zn (RSD)		As (RSD)		Cd (RSD)		Pb (RSD)	
0	0.0268	(9.7)	-0.0643	(3.4)	-0.00802	(10.6)	0.713	(6.1)	5.92	(2.2)	4.48	(1.0)	0.000647	(487.4)	0.00361	(N/A)	0.0956	(0.7)
20	9.13	(3.9)	0.501	(1.8)	0.00142	(9.6)	7.32	(1.2)	15.5	(3.0)	15.8	(1.6)	0.000647	(723.3)	-0.00528	(N/A)	0.115	(4.2)
40	12.4	(1.5)	1.16	(0.5)	-0.00344	(24.2)	10.8	(3.5)	20.1	(2.3)	26.0	(1.4)	0.00533	(21.8)	-0.00697	(N/A)	0.116	(5.9)
60	11.5	(2.0)	1.80	(1.6)	0.00886	(15.0)	12.2	(2.0)	21.8	(0.7)	36.1	(0.7)	0.0000496	(N/A)	-0.0106	(N/A)	0.112	(10.4)
80	10.7	(1.3)	2.37	(0.5)	0.00226	(8.4)	13.4	(2.6)	24.1	(3.3)	47.2	(0.7)	-0.00112	(N/A)	-0.00828	(N/A)	0.112	(6.8)

K.3 Results from electrolysis with aluminium and graphite from a mechanical pencil as electrodes

Table K.6: Results for electrolysis of *Not cleansed* water at 1.5 V with aluminium electrode combined with graphite from a mechanical pencil, and the accompanying percentage indicating how much of a given element is left in the water after 80 minutes. The RSD, i.e. uncertainty, is given for each value and a red number indicates relatively high uncertainty (>10 %). The concentrations have the unit µg/L, and the RSD values have the unit %.

Time [min]	Al (RSD)		Fe (RSD)		Cr (RSD)		Ni (RSD)		Cu (RSD)		Zn (RSD)		As (RSD)		Cd (RSD)		Pb (RSD)	
0	1930	(0.7)	6350	(3.0)	2.29	(3.4)	14.1	(2.4)	6120	(1.3)	3980	(2.1)	0.327	(20.8)	16.0	(0.7)	17.6	(3.7)
20	2060	(0.4)	6250	(0.6)	2.46	(3.8)	33.4	(3.5)	6130	(1.4)	4060	(3.1)	0.227	(11.0)	16.0	(0.5)	18.1	(1.2)
40	2440	(3.3)	6050	(2.2)	2.71	(2.1)	62.4	(2.3)	5990	(2.0)	4100	(0.7)	0.292	(26.4)	16.2	(3.0)	17.5	(3.6)
60	3060	(4.0)	6030	(1.4)	3.17	(8.2)	80.6	(3.1)	5740	(0.8)	4130	(3.4)	0.176	(21.3)	16.2	(1.6)	17.2	(0.6)
80	3530	(2.0)	5700	(1.2)	3.52	(3.2)	100	(0.9)	5310	(0.3)	4250	(4.6)	0.189	(37.2)	16.3	(1.7)	16.0	(0.7)
% left	183		89.7		154		713		86.7		107		57.6		102		91.0	

K.4 Results from electrolysis with an aluminium and a cylindrical graphite electrode

Table K.7: Results for electrolysis of *Not cleansed* water at 1.5 V with aluminium electrode combined with a cylindrical graphite electrode, and the accompanying percentage indicating how much of a given element is left in the water after 80 minutes. The RSD, i.e. uncertainty, is given for each value and a red number indicates relatively high uncertainty (>10 %). The concentrations have the unit µg/L, and the RSD values have the unit %.

Time [min]	Al	(RSD)	Fe	(RSD)	Cr	(RSD)	Ni	(RSD)	Cu	(RSD)	Zn	(RSD)	As	(RSD)	Cd	(RSD)	Pb	(RSD)
0	2180	(0.2)	6980	(0.8)	1.34	(6.3)	22.2	(5.3)	5880	(1.0)	5370	(1.3)	0.386	(14.3)	20.9	(2.3)	18.3	(2.1)
20	2250	(1.4)	6440	(2.4)	1.47	(6.2)	22.5	(6.7)	5750	(1.6)	5220	(5.0)	0.526	(39.0)	20.7	(2.4)	23.1	(1.2)
40	2500	(4.1)	6360	(1.1)	1.59	(5.8)	23.8	(4.8)	5630	(1.6)	5340	(1.2)	0.553	(10.8)	20.5	(1.8)	23.8	(2.2)
60	2820	(1.9)	6430	(2.0)	1.75	(3.4)	23.7	(4.8)	5610	(0.3)	5700	(4.4)	0.451	(24.6)	21.2	(0.6)	25.0	(1.5)
80	3000	(1.6)	6050	(3.4)	1.95	(8.3)	22.7	(5.0)	5510	(2.7)	5460	(1.6)	0.340	(24.6)	21.1	(0.8)	24.8	(1.3)
% left	138		86.7		145		102		93.8		102		88.1		101		136	

Table K.8: Results for electrolysis of *Cleansed* water at 1.5 V with aluminium electrode combined with a cylindrical graphite electrode, and the accompanying percentage indicating how much of a given element is left in the water after 80 minutes. The RSD, i.e. uncertainty, is given for each value and a red number indicates relatively high uncertainty (>10 %). The concentrations have the unit µg/L, and the RSD values have the unit %.

Time [min]	Al	(RSD)	Fe	(RSD)	Cr	(RSD)	Ni	(RSD)	Cu	(RSD)	Zn	(RSD)	As	(RSD)	Cd	(RSD)	Pb	(RSD)
0	680	(0.3)	2820	(1.1)	0.343	(12.8)	15.3	(10.5)	4130	(2.2)	4410	(1.9)	0.255	(12.4)	17.3	(2.3)	2.78	(4.4)
20	658	(1.1)	2870	(1.3)	0.239	(25.8)	14.8	(6.0)	4030	(2.9)	4580	(3.7)	0.236	(38.6)	18.0	(1.9)	2.84	(0.6)
40	646	(1.1)	2790	(1.9)	0.410	(15.0)	16.7	(4.8)	4040	(1.3)	4560	(0.4)	0.304	(24.2)	18.0	(1.0)	2.83	(9.6)
60	663	(1.0)	2620	(1.3)	0.387	(15.5)	15.7	(8.0)	3900	(1.0)	4480	(1.2)	0.232	(14.1)	17.6	(0.9)	2.64	(3.3)
80	709	(0.4)	2530	(2.1)	0.481	(15.7)	15.9	(6.7)	3870	(3.3)	4500	(2.4)	0.123	(93.2)	17.6	(0.6)	2.76	(5.9)
% left	104		89.9		140		104		93.8		102		48.4		102		99.3	

K.5 Results from electrolysis with an aluminium and a flat graphite electrode

Table K.9: Results for electrolysis of *Not cleansed* water at 1.5 V with aluminium electrode combined with a flat graphite electrode, and the accompanying percentage indicating how much of a given element is left in the water after 80 minutes. The RSD, i.e. uncertainty, is given for each value and a red number indicates relatively high uncertainty (>10 %). The concentrations have the unit µg/L, and the RSD values have the unit %.

Time [min]	Al	(RSD)	Fe	(RSD)	Cr	(RSD)	Ni	(RSD)	Cu	(RSD)	Zn	(RSD)	As	(RSD)	Cd	(RSD)	Pb	(RSD)
0	2280	(0.7)	6090	(1.8)	1.32	(8.9)	20.7	(3.2)	5950	(1.1)	5340	(2.3)	0.460	(4.9)	20.6	(1.2)	36.4	(0.8)
20	2360	(0.7)	6050	(0.7)	1.40	(2.1)	37.8	(10.1)	6010	(2.1)	5850	(1.9)	0.286	(35.7)	21.1	(0.7)	113	(1.9)
40	2450	(2.1)	5560	(0.5)	1.52	(4.0)	50.8	(0.9)	6110	(0.4)	5750	(5.2)	0.382	(6.4)	20.8	(0.5)	130	(0.4)
60	2770	(0.7)	5280	(1.1)	1.60	(2.6)	66.4	(4.4)	6120	(1.5)	6000	(1.2)	0.350	(7.6)	21.2	(2.5)	140	(2.6)
80	3080	(0.4)	4900	(3.9)	1.76	(3.4)	76.2	(4.8)	6000	(1.4)	6040	(1.7)	0.189	(13.4)	21.3	(0.2)	148	(0.9)
% left	135		80.5		133		368		101		113		40.9		103		406	

Table K.10: Results for electrolysis of *Cleansed* water at 1.5 V with aluminium electrode combined with a flat graphite electrode, and the accompanying percentage indicating how much of a given element is left in the water after 80 minutes. The RSD, i.e. uncertainty, is given for each value and a red number indicates relatively high uncertainty (>10 %). The concentrations have the unit µg/L, and the RSD values have the unit %.

Time [min]	Al	(RSD)	Fe	(RSD)	Cr	(RSD)	Ni	(RSD)	Cu	(RSD)	Zn	(RSD)	As	(RSD)	Cd	(RSD)	Pb	(RSD)
0	646	(0.5)	2700	(1.7)	0.300	(16.4)	15.3	(1.4)	4140	(2.9)	4480	(2.3)	0.214	(38.8)	17.3	(1.1)	2.95	(6.5)
20	598	(1.4)	2620	(4.2)	0.259	(40.6)	19.9	(7.5)	4130	(1.6)	4460	(1.7)	0.272	(44.8)	17.2	(2.1)	8.57	(3.5)
40	565	(0.8)	2470	(0.5)	0.306	(20.1)	22.7	(0.7)	4080	(0.6)	4510	(2.8)	0.191	(19.0)	17.3	(1.5)	10.6	(1.8)
60	587	(1.6)	2510	(2.2)	0.383	(25.4)	25.9	(1.3)	4070	(1.5)	4790	(2.1)	0.103	(65.0)	18.3	(1.1)	12.6	(3.2)
80	581	(2.2)	2210	(0.6)	0.315	(9.3)	29.4	(1.1)	4160	(4.3)	4720	(2.6)	0.126	(27.1)	17.5	(1.0)	14.5	(3.4)
% left	90.0		79.8		105		192		100		105		58.8		101		490	

K.6 Results from electrolysis with a cylindrical graphite and a flat graphite electrode

Table K.11: Results for electrolysis of *Not cleansed* water at 1.5 V with a cylindrical graphite electrode combined with a flat graphite electrode, and the accompanying percentage indicating how much of a given element is left in the water after 80 minutes. The RSD, i.e. uncertainty, is given for each value and a red number indicates relatively high uncertainty (>10 %). The concentrations have the unit µg/L, and the RSD values have the unit %.

Time [min]	Al	(RSD)	Fe	(RSD)	Cr	(RSD)	Ni	(RSD)	Cu	(RSD)	Zn	(RSD)	As	(RSD)	Cd	(RSD)	Pb	(RSD)
0	2330	(0.9)	5790	(1.5)	1.33	(8.7)	23.1	(3.3)	5910	(2.2)	5400	(5.4)	0.527	(13.1)	20.6	(1.9)	20.4	(2.6)
20	2350	(1.4)	5760	(2.4)	1.29	(12.3)	29.6	(2.6)	6060	(1.9)	5570	(2.0)	0.397	(12.3)	20.8	(1.4)	30.7	(2.3)
40	2360	(0.9)	5720	(1.3)	1.27	(4.0)	32.5	(10.5)	6170	(3.6)	5740	(1.9)	0.423	(14.6)	20.9	(1.4)	35.8	(2.2)
60	2300	(0.7)	5430	(2.9)	1.24	(6.8)	37.0	(6.2)	6240	(1.4)	5600	(1.2)	0.518	(16.0)	20.2	(1.6)	41.2	(2.3)
80	2340	(1.5)	5300	(2.0)	1.24	(11.4)	41.7	(1.6)	6630	(4.0)	5800	(6.6)	0.437	(18.7)	20.8	(1.3)	48.3	(1.3)
% left	100		91.5		93.4		180		112		107		83.0		101		237	

Table K.12: Results for electrolysis of *Cleansed* water at 1.5 V with a cylindrical graphite electrode combined with a flat graphite electrode, and the accompanying percentage indicating how much of a given element is left in the water after 80 minutes. The RSD, i.e. uncertainty, is given for each value and a red number indicates relatively high uncertainty (>10 %). The concentrations have the unit µg/L, and the RSD values have the unit %.

Time [min]	Al	(RSD)	Fe	(RSD)	Cr	(RSD)	Ni	(RSD)	Cu	(RSD)	Zn	(RSD)	As	(RSD)	Cd	(RSD)	Pb	(RSD)
0	629	(1.0)	2820	(3.0)	0.277	(2.5)	15.9	(4.7)	4090	(2.7)	4540	(0.7)	0.274	(35.1)	18.0	(1.7)	3.39	(7.8)
20	570	(3.1)	2730	(0.9)	0.214	(41.5)	18.3	(4.4)	4130	(2.8)	4560	(2.7)	0.249	(50.6)	17.5	(1.1)	5.64	(1.8)
40	541	(1.0)	2730	(3.3)	0.230	(22.1)	19.1	(7.8)	4350	(0.8)	4610	(4.1)	0.293	(23.7)	17.6	(0.9)	6.77	(1.0)
60	510	(1.3)	2560	(1.8)	0.276	(11.6)	20.1	(4.6)	4240	(1.4)	4540	(1.2)	0.174	(4.7)	17.7	(0.2)	6.88	(1.6)
80	512	(1.2)	2570	(1.0)	0.257	(34.2)	19.5	(1.7)	4220	(2.5)	4560	(4.0)	0.268	(32.3)	17.8	(0.3)	7.23	(3.3)
% left	81.4		91.1		92.7		123		103		100		97.6		98.9		214	

L Results from Shapiro-Wilk normality test and Mann-Whitney U test performed in SPSS on the concentrations in Not cleansed water before and after rinsing gravel.

Table L.1: Results from the Shapiro-Wilk normality test to check the normality of concentrations in *Not cleansed* water before and after rinsing gravel. A confidence interval of 95 % was used.

Element	Type of water	Statistic	n	p-value
Fe	Rinsed	0.772	5	0.048
	Not cleansed	0.905	3	0.400
Cr	Rinsed	0.829	5	0.137
	Not cleansed	0.995	3	0.864
Ni	Rinsed	0.838	5	0.159
	Not cleansed	0.935	3	0.507
Cu	Rinsed	0.630	5	0.002
	Not cleansed	0.973	3	0.683
Zn	Rinsed	0.892	5	0.366
	Not cleansed	0.896	3	0.373
As	Rinsed	0.734	5	0.021
	Not cleansed	0.777	3	0.061
Cd	Rinsed	0.843	5	0.174
	Not cleansed	0.893	3	0.363
Pb	Rinsed	0.816	5	0.109
	Not cleansed	0.953	3	0.582

Table L.2: Results from Mann-Whitney U test performed in SPSS on the concentrations in *Not cleansed* water before and after rinsing gravel.

	Fe	Cr	Ni	Cu	Zn	As	Cd	Pb
Mann-Whitney U	7.000	7.000	7.000	7.000	7.000	7.000	6.000	5.000
p-value	0.881	0.881	0.881	0.881	0.881	0.881	0.655	0.456

M Results from treatment with activated carbon

Table M.1: Results for treatment of *Not cleansed* water from Killingdal with activated carbon. The RSD, i.e. uncertainty, is given for each value and a red number indicates relatively high uncertainty (>10 %). The concentrations have the unit µg/L, and the RSD values have the unit %.

Volume (L)	Fe	(RSD)	Cr	(RSD)	Ni	(RSD)	Cu	(RSD)	Zn	(RSD)	As	(RSD)	Cd	(RSD)	Pb	(RSD)
0	5670	(1.9)	0.492	(3.5)	51.6	(2.1)	20500	(0.9)	13200	(1.6)	0.258	(23.6)	50.0	(1.0)	3.35	(1.8)
3.85	39.1	(2.6)	0.891	(3.5)	48.8	(7.1)	1390	(3.3)	7820	(2.8)	0.0699	(78.1)	35.7	(2.4)	0.0490	(58.0)
7.7	476	(4.1)	0.338	(18.5)	56.4	(4.4)	623	(0.3)	11200	(2.7)	0.0393	(76.3)	47.7	(1.1)	0.0790	(34.3)
15.4	1700	(5.1)	0.262	(22.0)	74.4	(1.6)	11900	(2.0)	15300	(1.7)	0.0615	(53.3)	55.6	(1.9)	0.198	(19.7)

N Weather data from 01.10.2018 to 04.02.2020

This section contains 10 pages of weather data obtained at the weather station at Sverresborg. The data is collected from YR.no at `https://www.yr.no/nb/historikk/tabell/1-211143/Norge/Tr%C3%B8ndelag/Trondheim/Ila?q=2020`. Information included is minimum temperature (°C), maximum temperature (°C), average temperature (°C), precipitation (mm), and snow depth (cm). Precipitation was measured at 07.00 am every day. The cells with precipitation are colour coded based on the amount of rain or snow that came that day. The classifications are

- Blue: $<$2.4 mm/24 hours, which indicates *no precipitation*.
- Green: 2.4 mm to 12 mm/24 hours, which indicates *light precipitation*.
- Yellow: 12 mm to 24 mm/24 hours, which indicates *precipitation*.
- Orange: $>$24 mm/24 hours, which indicates *heavy precipitation*.

and are based on the classification obtained from YR.no at `https://hjelp.yr.no/hc/no/articles/115003696813-Hva-er-grensene-for-lett-og-kraftig-nedb%C3%B8r-`.

Date	Min. temp.	Max temp.	Avg. temp.	Precip. mm	Snow depth cm
01.10.2018	2.7	8	4.4	30.9	0
02.10.2018	-0.7	5.8	2.3	0.1	0
03.10.2018	0.5	7.4	4.2	2.4	0
04.10.2018	2.5	6.2	4.7	0.6	0
05.10.2018	3.2	9.8	6.5	8.6	0
06.10.2018	3	6.7	3.9	8	0
07.10.2018	-0.1	7.2	3	8.2	0
08.10.2018	0.9	9	6.2	2.6	0
09.10.2018	4.3	8.1	6.2	3.2	0
10.10.2018	3.9	10.5	7.5	4.7	0
11.10.2018	3.4	14.2	8.5	0.1	0
12.10.2018	7.9	17	12.9	0	0
13.10.2018	10.8	18.5	13.9	4.8	0
14.10.2018	8.1	20.8	13.6	3.1	0
15.10.2018	3.7	9.1	4.8	18.9	0
16.10.2018	1.9	9.2	6.4	0	0
17.10.2018	6.3	11	7.8	0.8	0
18.10.2018	3.4	7.7	5.7	5	0
19.10.2018	4.8	8.7	6.4	5.7	0
20.10.2018	4.9	9.4	7	0.6	0
21.10.2018	5.5	9.4	7.1	8.2	0
22.10.2018	1.1	5.5	2.9	16	0
23.10.2018	1.5	4.2	2.4	13.9	0
24.10.2018	1.1	4.1	2.8	23.3	0
25.10.2018	0.8	3.7	2.2	8.6	0
26.10.2018	-0.4	3.2	1.3	18.5	0
27.10.2018	-3.6	1.3	-2.1	1.6	0
28.10.2018	-5.9	-1.7	-4.3	0	0
29.10.2018	-7.8	-0.2	-3.3	0	0
30.10.2018	-2.4	2	0.8	0	0
31.10.2018	0.6	6.9	4.9	0.1	0
01.11.2018	-0.9	7.7	3.7	6.5	0
02.11.2018	3.9	8.6	5	0	0
03.11.2018	0.5	4.5	2.5	13.6	0
04.11.2018	3.2	10.7	8.3	3.9	0
05.11.2018	4.8	9.9	6.8	0	0
06.11.2018	-0.9	5.1	0.8	0	0
07.11.2018	-1	3.6	1.4	0	0
08.11.2018	-0.2	6.2	2.1	0	0
09.11.2018	-0.5	4.4	1.2	0	0
10.11.2018	-1.6	8.6	5.3	0	0
11.11.2018	5.5	10.5	8.9	1	0
12.11.2018	4.8	10.1	7	0.9	0
13.11.2018	0.3	6.1	2.3	4.4	0
14.11.2018	-0.5	3.4	1.6	0	0
15.11.2018	0.9	7.3	4.9	0	0
16.11.2018	3.6	10.6	7.9	0.4	0
17.11.2018	3.4	7.9	5.8	7.3	0
18.11.2018	-0.6	6.1	1.3	0.1	0

19.11.2018	-3.2	-0.2	-1.8	0	0
20.11.2018	-1.1	0.8	0	0	0
21.11.2018	-3.6	1.8	-1.8	0	0
22.11.2018	-5.6	-0.6	-2.1	0	0
23.11.2018	-1.2	0.8	0.1	0	0
24.11.2018	0.5	3	1.6	0	0
25.11.2018	0.5	2.4	1.3	0	0
26.11.2018	-0.1	2	0.8	1.8	0
27.11.2018	-5.2	0.3	-3.2	2.2	0
28.11.2018	-8.4	-4.3	-5.1	0	0
29.11.2018	-4.4	4.8	4.2	0	0
30.11.2018	4.1	8.5	7.2	0.5	0
01.12.2018	5.4	8.7	6.3	0	0
02.12.2018	-1.8	6.5	3.2	0	0
03.12.2018	-1.3	6.3	0.8	0	0
04.12.2018	-0.2	2.6	0.7	10.2	0
05.12.2018	-1.7	0.3	-0.6	10.4	10
06.12.2018	-7.2	-0.5	-4.1	6.3	18
07.12.2018	-6.9	-0.8	-3	0.3	16
08.12.2018	-2.2	0.8	0	0	14
09.12.2018	-0.9	1.1	0.4	5.2	17
10.12.2018	0.8	2.6	2.1	3	16
11.12.2018	-2.6	3.1	-0.2	2.8	13
12.12.2018	-8.8	-1.1	-7.4	0	13
13.12.2018	-11.1	-8	-10.2	0	13
14.12.2018	-12.8	-10.5	-12.2	0	13
15.12.2018	-14.2	-9.2	-11.5	0	14
16.12.2018	-11.7	0.9	-1.2	0	14
17.12.2018	-6.8	0	-4.4	0	13
18.12.2018	-9.1	-3	-5.9	0	13
19.12.2018	-11.2	3.2	-1.9	0	14
20.12.2018	1.8	3.5	2.2	0	13
21.12.2018	-1.9	1.9	-1.2	0	13
22.12.2018	-8.1	-1.9	-4.6	0	13
23.12.2018	-7.5	-2.2	-4.7	0	13
24.12.2018	-5.7	1.3	0.9	0.1	14
25.12.2018	0.8	6	4.4	32.8	11
26.12.2018	2.6	6.5	4.2	14.4	2
27.12.2018	1.5	5.2	3.5	8.5	0
28.12.2018	0.9	5.2	3.3	6	0
29.12.2018	0.9	4.7	2.2	5.6	0
30.12.2018	0.1	2.2	0.4	17.7	0
31.12.2018	-1	6.5	3.4	7.5	0
01.01.2019	-0.3	5.5	1.8	15.5	0
02.01.2019	-1.2	1.9	0.8	4.6	0
03.01.2019	1.7	5.3	4.5	16.4	0
04.01.2019	4.8	7.2	6.2	36.4	0
05.01.2019	3.5	6.3	4.7	13.5	0
06.01.2019	3.6	6	4.4	6.2	0
07.01.2019	-0.4	3.9	0.7	4.4	0

08.01.2019	-0.2	2.1	0.9	0.1	0
09.01.2019	-2.5	0.8	-0.6	3.2	3
10.01.2019	-1.1	7.3	3.7	6.1	7
11.01.2019	0.3	6.7	1	5.3	0
12.01.2019	-1	1.5	-0.1	5.3	4
13.01.2019	-3.3	1.5	-1.4	2.4	8
14.01.2019	-3.1	2.1	-0.8	9.7	18
15.01.2019	-9.7	-1.1	-6.1	4.7	23
16.01.2019	-13	-5.1	-8.1	0	20
17.01.2019	-9.3	-0.8	-4.2	5.6	25
18.01.2019	-3.3	-1.5	-2.3	8.2	37
19.01.2019	-4.1	-0.9	-2.8	12.2	52
20.01.2019	-8.2	-2.9	-6	9.8	60
21.01.2019	-14.8	-5.3	-9.5	0.4	53
22.01.2019	-13.4	-4.5	-12.1	0.3	48
23.01.2019	-14.6	-10.7	-13.1	0	44
24.01.2019	-15	-6.2	-9.6	0	42
25.01.2019	-12.5	-5.1	-9.4	0	40
26.01.2019	-12.5	-4.5	-5.8	0	38
27.01.2019	-11.1	-4.9	-7.1	0	36
28.01.2019	-12.4	-5.1	-7.8	0	36
29.01.2019	-12.6	-6.5	-9.3	0	35
30.01.2019	-13.2	-4	-8.8	0	35
31.01.2019	-10	-0.6	-3.2	0	35
01.02.2019	-4.8	-1.7	-3	0	34
02.02.2019	-6.5	-3.2	-6.3	0	34
03.02.2019	-14.2	-5.8	-9.7	0	34
04.02.2019	-11.9	-5	-7.3	1.2	37
05.02.2019	-14.9	-5.9	-9.2	0	36
06.02.2019	-13.9	-4	-7.6	0	35
07.02.2019	-4.4	1.2	-2.1	0.6	36
08.02.2019	-4.5	0	-1.8	0	36
09.02.2019	-4.3	1.7	-0.3	0.4	37
10.02.2019	-0.9	1.8	-0.3	3.2	42
11.02.2019	-3.8	0.6	-1.2	4.2	47
12.02.2019	-2.5	0.8	-0.5	5	52
13.02.2019	-0.1	5.3	3.7	16	52
14.02.2019	-0.6	9.5	6.5	2.3	42
15.02.2019	0.9	8	3.6	3.8	26
16.02.2019	-0.3	7.2	2.7	0.9	24
17.02.2019	-1.9	2.4	0.4	2.6	24
18.02.2019	0.2	8.3	4.9	0	23
19.02.2019	-0.2	6.3	3	0	23
20.02.2019	-2.8	3.2	-0.4	1.7	23
21.02.2019	-2.4	1.4	-0.2	1	24
22.02.2019	-1.9	2.8	1	5.9	26
23.02.2019	1	5.5	2.8	2.4	24
24.02.2019	0.1	6.4	4.7	3.7	21
25.02.2019	0.8	7.7	5.5	0.1	15
26.02.2019	-0.3	6.7	3.9	0.6	11

27.02.2019	2.5	7.5	5.2	0.1	9
28.02.2019	0.2	3.7	1.1	12.5	4
01.03.2019	-0.6	1.1	0	26.2	19
02.03.2019	-1.1	1.4	0.1	5.3	19
03.03.2019	-1.5	2	-0.5	11.4	23
04.03.2019	-3.8	-0.7	-3	1.3	23
05.03.2019	-13.6	-3.8	-9.1	0	22
06.03.2019	-14.7	-4	-9.7	0	22
07.03.2019	-11.3	-1.9	-3.3	0	21
08.03.2019	-3.5	1.5	-1.5	1.9	24
09.03.2019	-6.9	-0.6	-3.1	0.7	25
10.03.2019	-8.7	-1.6	-4.3	0.3	25
11.03.2019	-9.6	0.3	-2.9	1.7	26
12.03.2019	-10.2	0.3	-3	1.9	29
13.03.2019	-2.7	0.2	-1.6	0	27
14.03.2019	-3	3.3	-0.7	0.8	28
15.03.2019	-3.4	3.1	-1.6	0	28
16.03.2019	-9.7	0.7	-3.8	0	27
17.03.2019	-7.2	1.4	-1	0	27
18.03.2019	-1.4	3.1	0.4	0	27
19.03.2019	-2.5	5.6	2.5	1	27
20.03.2019	1.2	4.3	2.7	4.1	25
21.03.2019	0.7	6.5	3.3	11.7	22
22.03.2019	-0.5	7.9	4.8	1	18
23.03.2019	0.5	7.5	1.8	4.5	15
24.03.2019	-0.5	2	0.4	11.1	29
25.03.2019	-1.8	2.2	0.4	26	35
26.03.2019	-0.7	2.6	1.1	3.7	38
27.03.2019	0.7	6.3	4.2	4.8	31
28.03.2019	1.4	12.8	8.1	2.1	24
29.03.2019	0.5	10.8	3.4	2.7	12
30.03.2019	0.3	4.1	1	26.6	13
31.03.2019	-1.9	2.5	-0.7	14.3	22
01.04.2019	-3.4	6.5	1.2	4.6	27
02.04.2019	-3.4	7	1.5	0	22
03.04.2019	-2.7	8.7	3.3	0	21
04.04.2019	-0.3	6.8	3.6	0	20
05.04.2019	0.2	8.1	5	0	18
06.04.2019	-3.2	5.4	2.3	0	16
07.04.2019	2.1	3.8	2.8	0	14
08.04.2019	-2.3	3.5	1.1	0	14
09.04.2019	-1.8	2	-0.6	0.3	15
10.04.2019	-8.2	1.4	-2.7	0	15
11.04.2019	-8.3	2.7	-1.9	0	14
12.04.2019	-6.9	5.2	-0.2	0	14
13.04.2019	-5	5.8	0.6	0	14
14.04.2019	-5.3	7.7	1.3	0	13
15.04.2019	-4	8.5	2.3	0	12
16.04.2019	-2.4	13.5	6	0	12
17.04.2019	0.6	14	8.2	0	9

18.04.2019	0.7	12.3	7.2	0	6
19.04.2019	2.8	16	8.8	0	0
20.04.2019	0.2	16.6	8.6	0	0
21.04.2019	4.8	10.9	6.2	0.4	0
22.04.2019	2.8	19.3	9.8	1.5	0
23.04.2019	1.3	20.9	11	0	0
24.04.2019	4	18.6	12.8	0	0
25.04.2019	3.1	19.3	12.8	0	0
26.04.2019	5.4	19.5	13.3	0	0
27.04.2019	4.4	19.7	12.9	0	0
28.04.2019	4.9	18.8	13.4	0	0
29.04.2019	5.2	18	12.2	0	0
30.04.2019	6.6	13	8.5	2.5	0
01.05.2019	2.8	7.3	4.5	3.9	0
02.05.2019	0.2	4.3	2.1	11.1	0
03.05.2019	-0.6	4	1.6	1.2	0
04.05.2019	0.6	3.9	1.9	1	0
05.05.2019	0.6	4.2	1.7	13.2	0
06.05.2019	-1.7	4.9	1.4	6.2	0
07.05.2019	-1.4	6	2.4	1.2	0
08.05.2019	-0.2	8.3	3.3	1	0
09.05.2019	-1.8	9.3	5.8	0	0
10.05.2019	6.9	12.8	8.7	0	0
11.05.2019	3.2	9.3	4.3	6.9	0
12.05.2019	2.2	7	3.9	6.3	0
13.05.2019	0.4	6.9	3.6	2.5	0
14.05.2019	1.1	10.5	6.2	4.3	0
15.05.2019	6.3	11.9	8.8	2.4	0
16.05.2019	3.8	15.6	9.3	0.1	0
17.05.2019	4.6	19.2	12.7	0	0
18.05.2019	8	21.2	15.9	0	0
19.05.2019	11.4	20.2	13.8	0	0
20.05.2019	11	18.4	14.5	0.9	0
21.05.2019	10.3	21.2	15.8	0	0
22.05.2019	11.7	22.7	17.8	0	0
23.05.2019	11.7	21.3	12.9	1.3	0
24.05.2019	6.3	16.6	10.9	0.7	0
25.05.2019	6.2	10.1	7.8	0.3	0
26.05.2019	4.9	9.1	6.3	0.1	0
27.05.2019	2	7.9	5.1	0	0
28.05.2019	0.4	8.9	4.5	1.5	0
29.05.2019	2.4	10.2	5.8	2.7	0
30.05.2019	1.2	10.1	4.6	0.5	0
31.05.2019	1.5	7.3	4.4	16.7	0
01.06.2019	1.8	12.8	7.5	33.5	0
02.06.2019	5.1	11.4	8.6	0	0
03.06.2019	8.6	20.9	14.1	1	0
04.06.2019	7.3	19	12.4	1.7	0
05.06.2019	6.3	18	12.8	4.7	0
06.06.2019	10.7	25.2	18.2	0.4	0

07.06.2019	10.1	23.3	13.1	2.4	0
08.06.2019	9	19.8	14.1	21.4	0
09.06.2019	11.1	19.9	14.4	1.7	0
10.06.2019	8.4	12.9	10.1	4.6	0
11.06.2019	6.3	15.7	12.2	1.1	0
12.06.2019	7.3	18.8	12.7	0	0
13.06.2019	8.3	17.6	12.9	4	0
14.06.2019	8.3	18.1	13.9	4.5	0
15.06.2019	10.1	20.4	15.7	0	0
16.06.2019	10.5	23.1	16.7	0	0
17.06.2019	10	18.2	12.7	4.6	0
18.06.2019	10.5	17	12.9	1.5	0
19.06.2019	7.9	18.1	13.7	14.3	0
20.06.2019	12	19.5	14.7	2.5	0
21.06.2019	10.4	15.4	11	8.6	0
22.06.2019	7.3	13.4	10.4	4.1	0
23.06.2019	7.8	13.4	10.7	1.4	0
24.06.2019	8.1	14.7	11.7	0.8	0
25.06.2019	7.7	15.9	12.5	0	0
26.06.2019	9.1	13.7	10.5	1.3	0
27.06.2019	8.7	10.2	9.5	0.3	0
28.06.2019	7.7	13.5	10.9	4.4	0
29.06.2019	10.7	13.2	11.3	6.4	0
30.06.2019	10.5	14.8	12	11.5	0
01.07.2019	8.2	12.7	9.2	16.4	0
02.07.2019	4.3	11.3	6.5	6.4	0
03.07.2019	4.1	7.8	6.2	6.9	0
04.07.2019	4.2	9.7	7	18	0
05.07.2019	7.3	9.8	8.2	5.1	0
06.07.2019	5.8	13.2	9.6	1.3	0
07.07.2019	8.4	14.9	10.7	0.2	0
08.07.2019	7	14.1	9.7	1.1	0
09.07.2019	10.1	15.7	11.9	0.5	0
10.07.2019	6.5	18.5	11.9	0.1	0
11.07.2019	6.3	18.2	12	0	0
12.07.2019	6.3	17.6	11.5	0	0
13.07.2019	8.3	14	11.4	0	0
14.07.2019	8.2	12.6	10	0	0
15.07.2019	8.1	10.7	9.5	2.6	0
16.07.2019	8.5	13.7	10.7	9.1	0
17.07.2019	6.7	17	12.7	0	0
18.07.2019	10.9	21.8	16.5	0.4	0
19.07.2019	12.5	24.6	16.9	0	0
20.07.2019	10	23.7	17.3	0	0
21.07.2019	15.4	22	16.6	0.4	0
22.07.2019	10.9	19	15.1	5.3	0
23.07.2019	14.2	20.1	17.1	0	0
24.07.2019	15.5	23.9	19.8	0.2	0
25.07.2019	17.2	27.5	21.2	0	0
26.07.2019	14.3	27.3	21.4	0	0

27.07.2019	17.9	29.9	24.7	0	0
28.07.2019	17.1	29	23.8	0	0
29.07.2019	17.6	27.4	22.6	0	0
30.07.2019	15	25.2	16.5	0	0
31.07.2019	12.5	21.4	16.7	0	0
01.08.2019	9.9	21.7	15.7	0	0
02.08.2019	10.9	17.9	14	0	0
03.08.2019	10.9	15.5	12.5	0	0
04.08.2019	9.3	15.6	12.5	0	0
05.08.2019	9.1	14.8	12	0	0
06.08.2019	6.5	17.5	12.7	0	0
07.08.2019	8.5	20.1	14.3	0	0
08.08.2019	12.5	16.8	13.8	0	0
09.08.2019	11.6	16.1	13.9	0.1	0
10.08.2019	12	21.6	17.4	0	0
11.08.2019	13.5	26	18.4	0.2	0
12.08.2019	11.6	18.9	13.2	3.5	0
13.08.2019	10	12.8	10.5	34.5	0
14.08.2019	7.7	15.1	10.9	6.2	0
15.08.2019	7.8	15.3	11.9	0	0
16.08.2019	8.3	15.9	12.8	0.7	0
17.08.2019	10.4	18.3	14.8	0.1	0
18.08.2019	11.6	17.8	13.2	1.9	0
19.08.2019	7.5	17.9	12.6	0.9	0
20.08.2019	8.7	17	12.6	2.3	0
21.08.2019	8.1	16.2	11.2	2	0
22.08.2019	5	17.7	12	0	0
23.08.2019	9.9	17.2	12.9	4	0
24.08.2019	9.8	16.6	13.7	0.3	0
25.08.2019	13.9	18	14.9	0	0
26.08.2019	11.8	21	16	0.4	0
27.08.2019	10.5	23.4	17.3	0	0
28.08.2019	12.2	27	19.1	0	0
29.08.2019	11.7	21.8	14.5	0	0
30.08.2019	8.6	18.4	14.1	22.8	0
31.08.2019	13.6	20.1	16.5	0.1	0
01.09.2019	12.4	19	14.8	0	0
02.09.2019	7.9	13.3	9.4	1.9	0
03.09.2019	3.4	13.4	8.2	0	0
04.09.2019	4.8	13.1	9.5	2	0
05.09.2019	8	11.6	8.3	5.7	0
06.09.2019	5.2	11	8.2	14.1	0
07.09.2019	6.9	11.5	8.5	9.2	0
08.09.2019	3	11.9	7.6	0.4	0
09.09.2019	4.5	15.8	10.5	0	0
10.09.2019	7.8	15.9	12.3	0	0
11.09.2019	10.4	20	14.5	0	0
12.09.2019	7.9	13.2	9.7	6.5	0
13.09.2019	6.1	9.2	7.2	13.4	0
14.09.2019	5	9.7	7.5	31.4	0

15.09.2019	5.2	11.7	8.4	15.3	0
16.09.2019	6.7	9.7	7.6	35.7	0
17.09.2019	3.9	9.7	6.8	9.6	17
18.09.2019	5.6	8.9	6.9	3.6	0
19.09.2019	4.8	8.4	6.1	17.7	0
20.09.2019	4.6	11.7	9.3	27.2	0
21.09.2019	10.5	13.1	11.7	21.5	0
22.09.2019	7.6	11.4	8.7	2.9	0
23.09.2019	3.7	11.4	7.7	0.6	0
24.09.2019	2.8	10.7	6.4	0	0
25.09.2019	1.4	11.7	6.2	0	0
26.09.2019	1.8	14.1	7.3	0	0
27.09.2019	3.6	13.8	10.7	0	0
28.09.2019	8.5	15.2	11.6	0.2	0
29.09.2019	6.5	12.1	8.1	0	0
30.09.2019	1	6.7	2.5	14.4	0
01.10.2019	-1.6	5.4	2.5	1.4	0
02.10.2019	3.7	7.3	5.8	19.8	0
03.10.2019	3.6	6.7	4.5	3.8	0
04.10.2019	-1.6	4.8	1.1	0.7	0
05.10.2019	-3.9	2.6	-1.4	0	0
06.10.2019	-4.1	3.6	-0.1	0	0
07.10.2019	-0.1	6.4	2.6	0	0
08.10.2019	-1.9	6.7	1.5	0	0
09.10.2019	-0.9	8.7	2.7	0	0
10.10.2019	-1.1	5.9	1.5	0	0
11.10.2019	0.2	8.7	4.7	0.8	0
12.10.2019	1	6.3	3.8	0	0
13.10.2019	0.6	7.4	2.8	0	0
14.10.2019	-2.3	3.3	-0.2	0	0
15.10.2019	-2.7	4.1	0.7	0	0
16.10.2019	-0.3	8.9	5.2	0	0
17.10.2019	2	8.8	4.6	4.1	0
18.10.2019	2	9.1	6	0	0
19.10.2019	2.8	6.1	4.8	1.1	0
20.10.2019	0.6	6.3	3.1	0.5	0
21.10.2019	0.8	5.4	4.1	0	0
22.10.2019	3.4	11.8	7.2	0.6	0
23.10.2019	3.6	6.5	5.1	1.1	0
24.10.2019	4.7	10.1	6.9	1.7	0
25.10.2019	2.9	7.8	4.1	2.9	0
26.10.2019	0.5	3.9	1.1	14.8	0
27.10.2019	-1.6	3.6	1.3	0.5	0
28.10.2019	0.2	3.7	2.1	11.1	0
29.10.2019	0.7	4.2	2.6	7.9	0
30.10.2019	1.6	4.3	3.1	7.5	0
31.10.2019	2.4	4.5	3.2	31.1	0
01.11.2019	-0.2	4.5	2.1	4.7	0
02.11.2019	0	3.5	0.9	0.5	0
03.11.2019	-5.4	1.3	-4.5	0.3	0

04.11.2019	-8.6	-0.9	-6.1	0	0
05.11.2019	-8.6	-5.2	-7.4	0	0
06.11.2019	-8.2	-3	-5.9	0	0
07.11.2019	-8.3	-2.2	-5.8	0	0
08.11.2019	-7.5	-2.7	-5.4	0	0
09.11.2019	-11.1	-3.2	-7.8	0	0
10.11.2019	-8.9	-4.2	-6.4	0	2
11.11.2019	-9.2	-4.2	-7.4	1.1	3
12.11.2019	-10.7	3.2	-3.3	0	3
13.11.2019	-3.1	2.1	-1.3	0	3
14.11.2019	-6	-1.2	-3.9	0.2	3
15.11.2019	-5.8	-0.5	-2.6	0	3
16.11.2019	-5.6	-0.3	-2.8	0	3
17.11.2019	-3.2	2.7	1.4	0	3
18.11.2019	-4.1	2.9	-0.4	0	2
19.11.2019	0.1	2.7	0.6	5.3	2
20.11.2019	-4.1	0.8	-1.9	12.9	2
21.11.2019	-4.9	3.9	-0.1	0	3
22.11.2019	-0.8	6.1	2.3	0	2
23.11.2019	0	5.6	2.1	0	2
24.11.2019	-2.5	1.8	-1.3	0	2
25.11.2019	-1.8	0.5	-0.1	0	2
26.11.2019	-0.2	1	0.4	0	2
27.11.2019	-1.6	0.9	-0.4	1	2
28.11.2019	-4.3	0.6	-1.4	0	2
29.11.2019	-2.6	1.7	0.1	6.5	9
30.11.2019	-2.8	0.7	-1.4	9.7	20
01.12.2019	-1.5	1.1	-0.4	5.2	25
02.12.2019	-2.1	-0.1	-0.8	15.9	40
03.12.2019	-1.1	6.9	3.7	11.8	38
04.12.2019	0.1	7.1	3.2	23.6	18
05.12.2019	0.2	4.6	1.7	1.2	16
06.12.2019	0.4	1.9	1.4	13.5	19
07.12.2019	-0.1	2	0.6	2.1	18
08.12.2019	-3.8	0	-1.9	6.8	25
09.12.2019	-4.1	0	-1.5	11.3	34
10.12.2019	-5.2	-0.7	-2	8.1	40
11.12.2019	-2.3	5.7	3.6	3.3	39
12.12.2019	3.4	5.1	4.2	0	35
13.12.2019	-2.6	3.7	0.8	0	35
14.12.2019	1.3	4	2.7	0	34
15.12.2019	-1.9	3.2	0.2	0	33
16.12.2019	-2.8	0.4	-1.1	0	32
17.12.2019	-4.8	0.7	-1.5	0.6	34
18.12.2019	-5.8	0.5	-1.6	0	33
19.12.2019	-4.6	0.9	-1.8	2.8	33
20.12.2019	-4.6	1.8	-0.7	0	33
21.12.2019	0	6.1	2.5	0	33
22.12.2019	0.7	2.8	1	4.2	32
23.12.2019	-3.7	1	-2.6	0	31

24.12.2019	-8	-3.2	-6.1	0	31
25.12.2019	-7.9	-2.7	-4.7	0	31
26.12.2019	-4.1	-0.4	-1.3	0.5	33
27.12.2019	-9.2	-0.3	-5.8	2.5	35
28.12.2019	-9.7	1.8	-1.4	1.7	36
29.12.2019	0.3	7.5	4.9	5.6	33
30.12.2019	3.5	7.5	4.3	12.3	23
31.12.2019	0.7	3.8	1.9	26.8	19
01.01.2020	1.1	9.2	7	19.3	15
02.01.2020	3	9.5	5.5	0.6	9
03.01.2020	-2.8	7.2	-0.2	4.2	6
04.01.2020	-2	2.6	0.4	18.9	28
05.01.2020	-1.2	3.8	1.1	6.9	31
06.01.2020	0.8	5.7	3.5	14.8	25
07.01.2020	0.6	6.7	5.1	0.1	20
08.01.2020	0.9	7.5	3	4	15
09.01.2020	-0.6	3.2	1	6	18
10.01.2020	-1.1	2.3	0.2	0	18
11.01.2020	-2.3	5.6	3.5	0.4	17
12.01.2020	-0.4	5.3	1.2	9	15
13.01.2020	-1.5	3.2	1	1.8	17
14.01.2020	-1.8	5.5	3.3	0	17
15.01.2020	-2	3.9	1.5	0	15
16.01.2020	-1.8	5.4	3.6	0	15
17.01.2020	-0.1	4.9	1.9	5.6	15
18.01.2020	-2.2	2.6	0	0.2	15
19.01.2020	1.4	3.8	2.8	10.7	13
20.01.2020	2.1	11.3	7.3	1.9	10
21.01.2020	0.6	8.4	2	22.2	3
22.01.2020	0.3	1.9	1.1	16.9	7
23.01.2020	-0.3	6.6	3.3	5.3	10
24.01.2020	-0.6	3.8	0.4	14.9	6
25.01.2020	-0.9	1.5	0.6	16	15
26.01.2020	1.1	4.9	3.2	8.2	12
27.01.2020	-1.9	1.8	-0.4	0.1	10
28.01.2020	-5.3	1.4	-2.3	0.5	10
29.01.2020	-6.6	1.6	-0.3	0	10
30.01.2020	-5.8	0.1	-4.2	0	10
31.01.2020	-6.3	4	1.8	0	10
01.02.2020	0	4.3	2	0	10
02.02.2020	0.5	2.8	1.4	13.7	11
03.02.2020	-4.8	1.9	-2.8	14.5	12
04.02.2020	-8.4	1.1	-2.7	0	12

O All results from the ICP-MS analyses

This section contains all the concentrations measured in the samples collected in this thesis.

- Samples 1-61 are corrected by blank samples 55 and 56. Started the counting from start, therefore the next samples start on 1 again.
- Samples 3-35 are corrected by blank samples that belong to samples 1-61 (55 and 56).
- Samples 36-77 are corrected for blank samples that belong to samples 82-162 (152-156).
- Samples 82-156 are corrected for blank samples 152-156.

When repeating tests were performed, the values in the repeating test furthest up were used consistently. Empty cells indicate that no concentration was obtained. For samples 82-156, when two or more modes existed for an element, the one with the lowest RSD values were used.

Some abbreviations were made of the sample names.

- GNR: gravel not rinsed
- GR: gravel rinsed LStream: lower part of the Killingdal stream where the stream flows into the fjord
- C: cleansed
- N: not cleansed
- EC: electrochemical treatment
- Alu: aluminium electrode
- Graph: graphite electrode
- Cyl: cylindrical
- m: minutes
- AC: activated carbon treatment
- Loc: location
- Sed: sediment

			Li7(LR)		Be9(LR)		B11(LR)		Y89(LR)		Zr90(HR)		Nb93(HR)		Cd114(LR)	
Date	Sample name	Number	Conc. µg/L	RSD, %	Conc. µg/L	RSD, %	Conc. µg/L	RSD, %	Conc. µg/L	RSD, %	Conc. µg/L	RSD, %	Conc. µg/L	RSD, %	Conc. µg/L	RSD, %
12.12.2018	Stream	1	0.145793591	2.5	0.008617801	73	2.385782007	2.9	0.437941635	2.9	0.08871783	5.9	0.00243894	4.9	0.018081538	10.7
12.12.2018	Tunnel	2	12.40076113	1.9	0.272146533	3.5	30.37614716	2.4	13.27018243	3.2	0.16339182	36.3	0.004531006	72.5	35.56209876	2.2
12.12.2018	Fjord	6	113.6626442	5.3	0.025426111	90.5	3042.796711	0.5	0.789311478	2.4	-0.046555448	34.6	0.062648106	29	6.174759461	4.2
12.12.2018	Fjord	6	117.9404182	2.9	0.016664941	118.4	3157.781226	1.8	0.841508334	9.1	-0.095810465	97.2	-0.00197702	57.7	6.498759404	3.8
17.12.2018	Stream	7	0.025193171	3.2	0.007541552	36.7	2.095222099	1.3	0.17030564	4.2	0.03272291	20.7	-0.003491478	173.2	0.007040973	59.2
18.01.2019	Stream	13	0.098421671	5.3	0.004135638	58.2	2.335298056	3.6	0.184228895	1.1	0.043984668	6.8	0.001369111	173.2	0.009645199	29.4
31.01.2019	Stream	19	0.084479881	6.5	0.005857162	49.5	3.06348065	1.4	0.105106422	3.8	0.035184946	37.9	0	0	0.003378239	7
07.02.2019	Stream	34	0.116499858	4.5	0.003732171	106.4	2.794455725	2.5	0.131122528	2.7	0.026900415	47.2	-0.004091222	173.2	0.007850614	14.1
02.03.2019	Stream	39	0.13504195	9	0.009312938	33.6	2.927290253	3.1	0.357518544	3.1	0.06233436	30.1	-0.006015611	0	0.013949459	21.9
02.03.2019	Fjord	43	115.8947143	5.5	0.021950144	74.2	3039.970113	2	0.486098303	8	-0.066682556	117.8	-0.05512497	173.2	5.929324951	3.7
05.03.2019	Stream	45	0.114033139	1.9	0.003674184	120.2	2.986217484	3	0.191994252	0.8	0.037320793	14.3	0.002297263	86.8	0.009728791	21.1
05.03.2019	Fjord	50	134.8675004	1.6	0.015588182	7.5	3540.359066	3.1	0.143927173	2.4	0.006679553	27.1	-0.03869016	173.2	0.698980483	14.2
11.03.2019	Fjord	54	126.7058188	0.2	0.003697724	173.2	2943.425308	1.9	0.095197653	5.5	0.124632534	62.4	0.022731263	52.2	0.345841882	5.3
11.03.2019	Blank	55	0.00000000	1.1	0.00000000	173.2	0.00000000	2.0	0.00000000	78.1	0.00000000	0.0	0.00000000	100.0	0.00000000	139.5
11.03.2019	Blank	56	0.00000000	3.5	0.00000000	0.0	0.00000000	2.2	0.00000000	82.8	0.00000000	0.0	0.00000000	41.7	0.00000000	87.2
22.03.2019	Fjord	60	153.6874637	2.5	0.000480593	173.2	4010.244365	2.8	0.23756172	1.9	-0.12705585	87.7	-0.03465071	112.8	1.799129471	2.4
22.03.2019	Stream	61	0.103153236	5.4	0.003903047	114.6	3.545493657	0.6	0.257527336	1	0.075685005	47.8	0.00229547	173.2	0.008970188	28.1

			Tl205(LR)		Pb208(LR)		Bi209(LR)		Th232(LR)		U238(LR)		Na23(MR)		Mg25(MR)	
Date	Sample name	Number	Conc. µg/L	RSD, %	Conc. µg/L	RSD, %	Conc. µg/L	RSD, %	Conc. µg/L	RSD, %	Conc. µg/L	RSD, %	Conc. µg/L	RSD, %	Conc. µg/L	RSD, %
12.12.2018	Stream	1	0.004075812	29.2	0.102545095	6.1	0.001040202	34.7	0.033634809	25.3	0.124929387	5.2	4398.06269	2.1	691.0646983	3.2
12.12.2018	Tunnel	2	1.002167281	0.9	47.64350699	1.4	0.047250816	12.8	1.64800432	3.3	1.612212817	2.5	50102.96501	2.3	12601.24004	2.5
12.12.2018	Fjord	6	0.129375905	8.2	0.171924018	6.9			0.184842551	16	1.992516203	4.3			851879.7475	4
12.12.2018	Fjord	6	0.139121845	1.9	0.164290788	6.3			0.052707319	7.9	2.134635558	1.9			1004386.909	2.4
17.12.2018	Stream	7	0.003055918	15.8	0.029168516	9.3	0.00220148	13.8	0.0065292	3.5	0.034932608	7.5	4884.020928	1	963.8323477	2
18.01.2019	Stream	13	0.003826386	17.8	0.031503072	10.1	6.1089E-05	50	0.011441145	10.6	0.040384802	6	8392.56219	3.2	830.0671809	2.3
31.01.2019	Stream	19	0.003413742	9.3	0.025514595	3.7	0.000518949	45.2	0.092941236	12.3	0.020573671	4.9	48397.59396	2.2	1120.156445	0.5
07.02.2019	Stream	34	0.002432866	15.5	0.038596071	3.1	5.07576E-05	20.8	0.011117912	10	0.029036514	7.2	6816.418028	0.8	968.6945076	1.9
02.03.2019	Stream	39	0.003574209	20.3	0.075721734	10.6	0.000162395	30.5	0.012589179	13.7	0.083127694	6.1	4581.452446	2.9	737.4875956	1
02.03.2019	Fjord	43	0.086649746	24.5	0.131721207	4.9			0.028700518	22.2	1.976173631	1.3			991229.638	1.1
05.03.2019	Stream	45	0.002866174	7.1	0.021876917	12.2	0.000913279	17.5	0.002547035	8.6	0.039700571	5.6	4927.14833	2.4	863.1415844	1.1
05.03.2019	Fjord	50	0.009640774	44.8	0.05242266	7.1			0.0095757	33	2.265792089	0.5			1120532.887	0.5
11.03.2019	Fjord	54	0.016863723	25.5	0.036185082	4.7			0.013792877	9.8	1.856070269	2.6			964538.0643	2.4
11.03.2019	Blank	55	0.00000000	17.3	0.00000000	23.6	0.00000000	43.9	0.00000000	28.6	0.00000000	173.2	4.57968032	11.1	0.00000000	20.6
11.03.2019	Blank	56	0.00000000	173.2	0.00000000	19.5	0.00000000	26.5	0.00000000	17.2	0.00000000	87.0	4.50933891	5.6	0.00000000	24.3
22.03.2019	Fjord	60	0.044530568	4.2	0.087790167	13.4			0.001816042	44.2	2.600417304	1.2			1215257.578	4.1
22.03.2019	Stream	61	0.002880286	23.6	0.05552577	8.1	0.000436174	22.1	0.015843989	6.5	0.054077316	4.3	4195.738437	1.5	656.652871	3

			Mo98(MR)		Sn118(LR)		Cs133(LR)		La139(MR)		Ce140(LR)		Pr141(LR)		Nd146(LR)	
Date	Sample name	Number	Conc. µg/L	RSD, %	Conc. µg/L	RSD, %	Conc. µg/L	RSD, %	Conc. µg/L	RSD, %	Conc. µg/L	RSD, %	Conc. µg/L	RSD, %	Conc. µg/L	RSD, %
12.12.2018	Stream	1	0.042568385	12.2	0.015654603	12.7	0.002068506	21.7	0.393105437	6.7	0.857541957	3.2	0.115723605	2.4	0.481036377	3.6
12.12.2018	Tunnel	2	0.043051859	59.1	0.011456215	5.1	0.20045729	4.9	25.58894128	8.1	52.26991603	0.5	5.200137001	1.4	21.32177541	1.5
12.12.2018	Fjord	6	5.49840453	9.7	0.137764359	3.3	0.185251354	4.2	1.738421425	8.2	2.796402687	4.6	0.28357854	7.2	0.986479898	3.2
12.12.2018	Fjord	6	6.792562425	1.6	0.117391706	17.9	0.217818369	5.9	2.142730032	7.7	2.938508366	0.2	0.30459714	9.4	1.08661111	5.4
17.12.2018	Stream	7	0.084593883	13.1	0.00764485	46.5	0.002771932	21.8	0.116348621	5.3	0.211091013	3.5	0.036837846	5.6	0.151957009	7.7
18.01.2019	Stream	13	0.078250806	17.6	0.01111557	12.9	0.002583153	3.1	0.160302968	7	0.255982283	2.9	0.039956023	4.3	0.18427077	4.3
31.01.2019	Stream	19	0.120718233	35.6	0.01286802	39.4	0.003860872	13.8	0.065893958	11.7	0.086741389	3.7	0.019605289	15.5	0.094943097	9
07.02.2019	Stream	34	0.070178677	30.8	0.007626316	13.3	0.003144634	28	0.100213257	6.1	0.151196198	2.2	0.026265991	8.8	0.107919079	7.8
02.03.2019	Stream	39	0.048490665	36.1	0.001940737	28	0.001659835	7.8	0.368846666	10.6	0.720246701	1.1	0.0952082	3.8	0.403520532	6.1
02.03.2019	Fjord	43	6.036822512	7.7	0.10386611	16.5	0.184325189	6.2	1.191032861	1.1	1.348700188	4.4	0.130922546	6.7	0.427326258	5.5
05.03.2019	Stream	45	0.065714648	38.9	0.004038296	7.8	0.002011365	34.2	0.147119499	16	0.277165562	1.1	0.037803793	3.7	0.182607933	3.8
05.03.2019	Fjord	50	7.426829726	2.8	0.091239199	19.6	0.199281648	6.6	0.199067891	30.9	0.229309662	1.9	0.028110514	17.1	0.066526043	34.8
11.03.2019	Fjord	54	6.104644	3.3	0.322903115	9.1	0.1731143	2	0.101367521	12.3	0.118546341	5	0.016220561	7.6	0.061700952	12.7
11.03.2019	Blank	55	0.00000000	16.2	0.00000000	49.2	0.00000000	43.4	0.00000000	86.6	-0.00021647	50.0	0.00000000	43.7	0.00000000	173.2
11.03.2019	Blank	56	0.00000000	22.9	0.00000000	40.2	0.00000000	18.6	0.00000000	86.9	-0.00008244	132.4	0.00000000	107.2	0.00000000	86.6
22.03.2019	Fjord	60	7.79419961	4.3	0.110146387	12.8	0.216739541	14.3	0.343663967	9.1	0.486094046	4.8	0.056792524	10.3	0.213271786	17.9
22.03.2019	Stream	61	0.024678647	29.3	0.002419155	33	0.001379636	16.9	0.247611143	3.9	0.490437023	2.4	0.06719205	5.1	0.276385783	5.6

			Al27(MR)		Si29(MR)		P31(MR)		S34(MR)		Cl35(MR)		K39(MR)		Ca44(MR)	
Date	Sample name	Number	Conc. µg/L	RSD, %	Conc. µg/L	RSD, %	Conc. µg/L	RSD, %	Conc. µg/L	RSD, %	Conc. µg/L	RSD, %	Conc. µg/L	RSD, %	Conc. µg/L	RSD, %
12.12.2018	Stream	1	175.8526592	2.2	1791.008	0.8	4.669487251	10.5	1102.426445	3.1	8043.439676	1.5	142.9870183	2.9	3614.917349	6.7
12.12.2018	Tunnel	2	5148.096774	1.3	11417.15698	2.1	6.799595494	1.3	197889.9161	2.8	54783.14537	2.8	6232.10578	2.7	145765.0981	1.2
12.12.2018	Fjord	6	72.20205859	3.5	1061.787821	3.9	8.280710949	12.9	546900.123	5.9	11311263.13	3.8	217521.4456	4.6	288025.3521	3.9
12.12.2018	Fjord	6	83.43737855	1.4	2235.910365	3.8	9.79652716	4.8	663915.2635	1	13648504.64	3	269243.9755	3.7	340550.5261	0.2
17.12.2018	Stream	7	59.64465986	2.8	1766.499892	1.2	4.126394093	2.3	1429.35974	4.6	8733.176107	3.1	201.9606859	3.5	5084.689062	2.2
18.01.2019	Stream	13	77.9388929	1.8	1699.249506	0.2	2.00566305	2.3	1261.45393	1.3	15584.07955	3.7	214.3163323	3.1	4319.846629	1.6
31.01.2019	Stream	19	42.55972016	2.1	1891.89057	3.5	1.967492077	7	1712.074954	1.1	88464.6898	2	309.5680437	2	5549.062468	0.2
07.02.2019	Stream	34	50.4455651	3.6	1776.592502	1.1	1.724097545	12.8	1456.030637	3.2	12340.14458	3.6	233.4340489	2.1	5127.391567	0.7
02.03.2019	Stream	39	168.1759368	1.5	1437.648871	0.3	1.618070375	8.6	788.9614919	3.5	10128.61584	2.2	182.1276076	2.2	3160.249997	1.2
02.03.2019	Fjord	43	65.01003362	2.2	1986.070533	0.8	4.790986343	14.7	641834.3562	0.9	12914690.89	2.9	250429.8731	3	324285.6903	2.4
05.03.2019	Stream	45	77.17009831	0.5	1633.732872	3.2	2.754968313	13	1054.741582	2.2	11828.05598	2.3	223.5683834	3.1	4210.978891	1.3
05.03.2019	Fjord	50	27.02767019	2.2	<200	2.9	18.05357831	9.3	712117.5274	2.6	15195918.92	1.7	297197.0346	2.1	346174.72	1.6
11.03.2019	Fjord	54	16.29975399	2.2	<200	3.2	15.46514039	3.4	606675.9394	2.2	14094146.56	4.9	283297.974	3	306820.0255	0.9
11.03.2019	Blank	55	0.00000000	9.5	0.00000000	11.6	1.59014607	11.3	0.00000000	13.7	0.00000000	7.9	1.54498245	12.6	9.39474897	3.4
11.03.2019	Blank	56	0.00000000	11.4	0.00000000	7.8	2.14641554	1.5	0.00000000	16.7	0.00000000	9.6	3.71086944	7.3	7.67116337	9.1
22.03.2019	Fjord	60	53.50588184	3.8	<200	0.7	11.60563663	9.2	785313.7583	5.6	16376137.01	0.9	317881.5793	2.4	374430.7756	3.2
22.03.2019	Stream	61	116.2305191	2.1	1324.918187	3.5	1.514448493	9	781.5983723	3.4	16554.69182	3.3	170.1219487	3.1	2988.566162	2.9

			Sm147(LR)		Eu151(LR)		Gd157(HR)		Tb159(LR)		Dy163(LR)		Dy161(LR)		Ho165(LR)	
Date	Sample name	Number	Conc. µg/L	RSD, %	Conc. µg/L	RSD, %	Conc. µg/L	RSD, %	Conc. µg/L	RSD, %	Conc. µg/L	RSD, %	Conc. µg/L	RSD, %	Conc. µg/L	RSD, %
12.12.2018	Stream	1	0.090623713	14.1	0.014719406	16.2	0.08047334	85	0.011712656	5.7	0.070052958	9.2	0.068467633	11.2	0.014642864	7.9
12.12.2018	Tunnel	2	3.656029798	2.1	0.485713902	2.4	2.954310265	9.2	0.453754895	5.2	2.368915055	4.3	2.594608912	2.6	0.477121329	2.1
12.12.2018	Fjord	6	0.158211122	2.4	0.01626587	29.8	0.086382665	173.2	0.020104144	22.2	0.105227816	19.2	0.105944414	9.2	0.02211708	17.6
12.12.2018	Fjord	6	0.171095528	7.6	0.021112476	10.6	0.350641166	114.6	0.018783067	18.7	0.100121622	17.3	0.122311585	12.9	0.024428988	20.8
17.12.2018	Stream	7	0.028687897	23	0.004237997	48.9	0.00909877	173.2	0.003919419	13.8	0.024471209	10	0.025515709	9.1	0.006571933	8.9
18.01.2019	Stream	13	0.028292252	13.8	0.005345896	47.5	0.007397309	173.2	0.005247344	24	0.029188682	2.7	0.026287705	3.3	0.005780315	15.4
31.01.2019	Stream	19	0.016369103	31.5	0.002437558	50	0	0	0.002261459	11.2	0.015461963	8.4	0.01820111	11	0.00406574	7.5
07.02.2019	Stream	34	0.019845314	6.2	0.00444886	20.7	0.029892891	86.6	0.003900874	16.7	0.018950138	5.3	0.022843248	14.5	0.003989582	9.2
02.03.2019	Stream	39	0.062266198	8.7	0.009732443	4.4	0.053137316	89.2	0.009664395	4.4	0.053354212	17.6	0.059760329	11.9	0.012068269	6.6
02.03.2019	Fjord	43	0.051511799	74.3	0.007434411	31.3	0.088937918	86.6	0.0072212	42.7	0.054808741	11.8	0.052351446	4.4	0.011481034	13.1
05.03.2019	Stream	45	0.031489355	10.9	0.00570735	25.8	0.030929728	86.6	0.00430039	27.7	0.030646975	11.4	0.031586859	9.8	0.0056243	19.9
05.03.2019	Fjord	50	0.016151317	32.8	0.000730524	173.2	0.045746586	173.2	0.003913351	19.9	0.017909805	51.8	0.015914366	66.1	0.003541101	43.9
11.03.2019	Fjord	54	0.006657575	49.5	0.001153616	45.8	0.030460496	173.2	0.001551398	23	0.006495992	10.2	0.011571958	9.1	0.00205041	33.5
11.03.2019	Blank	55	0.00000000	0.0	0.00000000	0.0	0.00000000	0.0	0.00000000	173.2	0.00000000	173.2	0.00000000	100.0	0.00000000	100.0
11.03.2019	Blank	56	0.00000000	173.2	0.00000000	173.2	0.00000000	0.0	0.00000000	93.3	0.00000000	173.2	0.00000000	173.2	0.00000000	121.2
22.03.2019	Fjord	60	0.018998395	60.4	0.001707227	87.7	0.094048424	86.6	0.003091974	45.3	0.028624569	22.3	0.033590205	13.9	0.005059025	15.6
22.03.2019	Stream	61	0.047426949	12	0.008871974	1.7	0.101893429	103.1	0.005620032	17.9	0.04055188	8.4	0.049595661	0.9	0.010700451	6.9

			Sc45(MR)		Ti49(MR)		V51(MR)		Cr53(MR)		Mn55(MR)		Fe56(MR)		Co59(MR)	
Date	Sample name	Number	Conc. µg/L	RSD, %	Conc. µg/L	RSD, %	Conc. µg/L	RSD, %	Conc. µg/L	RSD, %	Conc. µg/L	RSD, %	Conc. µg/L	RSD, %	Conc. µg/L	RSD, %
12.12.2018	Stream	1	0.043409465	30.3	1.146188374	13.4	0.128318491	13.7	0.45616471	3.2	0.686833465	5.6	54.70415935	4.7	0.091792563	13.7
12.12.2018	Tunnel	2	0.636751236	2	2.540611426	6.2	0.026051233	40.8	6.740654423	3	481.9894467	0.9	15235.3555	0.3	81.25714529	0.9
12.12.2018	Fjord	6	0.015385209	37.7	0.18364534	10.8	0.416864734	25.1	0.070662627	15.6	58.91999254	4.9	37.48991578	2.9	8.531917635	3.2
12.12.2018	Fjord	6	0.015546791	19.9	0.222068848	43.2	0.471188918	12	0.060841868	18.7	68.15052829	2.5	43.61037951	1.3	9.33195478	9.4
17.12.2018	Stream	7	0.014062139	37	0.365235884	29.6	0.079331647	6.2	0.261222843	9.2	0.459963495	3.8	17.99289927	0.7	0.048262896	4.9
18.01.2019	Stream	13	0.020850943	21.4	0.440302578	29.1	0.069159777	13.1	0.336128591	16.2	0.532964338	6.1	21.62155015	2.2	0.063064466	17
31.01.2019	Stream	19	0.0208549	41	0.238281708	30.2	0.056810735	10.6	0.260677673	3.8	1.1487266	2.2	12.1773607	2.8	0.159800014	4.9
07.02.2019	Stream	34	0.019114239	15.5	0.312939817	22.7	0.064343385	19.5	0.22056906	5.2	0.553300334	4.5	24.03187455	2.7	0.105184288	16.2
02.03.2019	Stream	39	0.035613537	8	0.98112539	12.7	0.113359132	7	0.31660978	15	0.666278637	5.5	57.34032515	1.1	0.050981061	15.3
02.03.2019	Fjord	43	0.015708372	27.2	0.157643248	66	0.210812858	14.4	0.203925938	6.2	42.82361012	2.2	64.99066578	2	6.764976385	3.2
05.03.2019	Stream	45	0.021746741	24.1	0.447872774	35.4	0.070821138	6.6	0.232362967	7.3	0.457844623	7.3	18.90263757	3.4	0.048779439	11.6
05.03.2019	Fjord	50	0.007292323	34.6	0.161082237	57.3	0.906243287	6.1	-0.064007567	2.9	8.028637429	6.2	18.23401588	1.5	0.911256208	10.9
11.03.2019	Fjord	54	0.006950785	58.8	0.168958644	12.2	0.823792837	4.3	0.020978861	19.8	4.150169183	5.1	5.352557813	3.4	0.414990191	11.4
11.03.2019	Blank	55	0.00000000	17.3	0.03111338	18.3	0.00000000	34.6	0.00000000	11.6	0.00000000	7.9	0.89106629	7.2	0.00000000	88.2
11.03.2019	Blank	56	0.00000000	48.4	0.03563945	37.8	0.00000000	37.8	0.00000000	23.0	0.00000000	31.3	0.02515034	10.4	0.00000000	142.0
22.03.2019	Fjord	60	0.010804728	28.9	0.122888113	13.3	0.714558324	1.8	-0.056229284	17.3	20.21781408	5.4	14.87430328	0.9	2.764691802	8.3
22.03.2019	Stream	61	0.033931262	20.3	0.765365348	9.1	0.073016004	23.8	0.328333564	10.3	0.645812627	1.1	38.10820421	0.9	0.041025289	2.9

			Er166(LR)		Tm169(LR)		Yb172(LR)		Lu175(LR)		Hf178(LR)		Ta181(LR)		W182(LR)	
Date	Sample name	Number	Conc. µg/L	RSD, %	Conc. µg/L	RSD, %	Conc. µg/L	RSD, %	Conc. µg/L	RSD, %	Conc. µg/L	RSD, %	Conc. µg/L	RSD, %	Conc. µg/L	RSD, %
12.12.2018	Stream	1	0.050782031	5.4	0.007293667	16.4	0.061534409	4.2	0.007862104	11.8	0.004278924	27.1	0.000382458	87.4	-0.001316238	44.1
12.12.2018	Tunnel	2	1.391810459	3.4	0.180392873	3	1.333471436	2.5	0.183318859	3.9	0.008289685	49.9	0.001296853	23.1	0.006495217	27.8
12.12.2018	Fjord	6	0.059826924	5.9	0.011263575	27.8	0.062040078	28.2	0.00669621	16.5	0.013671539	17.2	0.002632882	30.7	0.006571331	12.4
12.12.2018	Fjord	6	0.059016879	5.7	0.008794488	22.2	0.075471761	21.1	0.0106747	14.5	0.004465765	13.3	0.0009464	120.2	0.000366123	21.8
17.12.2018	Stream	7	0.019700459	9	0.003312661	17.2	0.020820863	28.2	0.003572195	19.8	0.001498404	28.6	0	107.9	0.002664796	27.2
18.01.2019	Stream	13	0.020928094	14.9	0.003081708	32	0.020811129	14.2	0.002984267	31.6	0.000926998	32.7	0.000198751	97.9	0.007881173	24.6
31.01.2019	Stream	19	0.012025718	35.9	0.002931531	14.8	0.016144963	2.5	0.00176043	44.9	0.001040672	124.9	0.000178044	94.4	0.219381396	6.5
07.02.2019	Stream	34	0.017754395	16.7	0.002123245	13.3	0.017874533	25.3	0.003138733	19.5	0.002932484	74	5.87891E-05	173.2	0.01235104	12
02.03.2019	Stream	39	0.034560736	8.8	0.005882096	21.9	0.043130227	6.8	0.006376726	5	0.003622101	49.4	0.000639671	76.2	0.004413417	2.3
02.03.2019	Fjord	43	0.020522851	17.3	0.003069664	10.8	0.024751336	14.3	0.004313932	20.9	0.005792601	25	0.000428618	118.4	0.012052917	15.6
05.03.2019	Stream	45	0.024260548	12.1	0.003510788	20.7	0.025127924	18.4	0.0032391	29.9	0.001509132	11.2	0.000227529	124.9	0.003348098	24.3
05.03.2019	Fjord	50	0.006046316	93.9	0.000518128	93.3	0.007327799	84	0.001623118	20	0.00787076	50	9.64654E-05	91.7	-0.006262211	11.1
11.03.2019	Fjord	54	0.004037073	25.9	0.000756779	37.9	0.007584025	58.3	0.000856664	75.1	0.000911417	13.3	0.000273705	53.9	0.001727793	40.2
11.03.2019	Blank	55	0.00000000	173.2	0.00000000	173.2	0.00000000	0.0	0.00000000	173.2	0.00000000	10.2	0.00000000	68.9	0.00000000	24.9
11.03.2019	Blank	56	0.00000000	0.0	0.00000000	0.0	0.00000000	0.0	0.00000000	87.7	0.00000000	173.2	0.00000000	14.2	0.00000000	4.1
22.03.2019	Fjord	60	0.018031169	25.9	0.003829917	9.3	0.011312814	81.1	0.002102598	104.9	0.009268151	55.1	0.000781458	51.9	0.018790968	29
22.03.2019	Stream	61	0.029072139	27.9	0.003417247	5.7	0.032745903	20.2	0.00464399	28.9	0.003181473	25	0.000359531	57.1	0.001807184	19.3

			Ni60(MR)		Cu63(MR)		Zn66(MR)		Ga69(MR)		As75(HR)		Rb85(MR)		Sr88(MR)	
Date	Sample name	Number	Conc. µg/L	RSD, %	Conc. µg/L	RSD, %	Conc. µg/L	RSD, %	Conc. µg/L	RSD, %	Conc. µg/L	RSD, %	Conc. µg/L	RSD, %	Conc. µg/L	RSD, %
12.12.2018	Stream	1	1.221830112	10.3	4.355856014	4.9	13.32421565	6.7	0.008439944	77.1	0.087579423	18.9	0.261958357	11.8	6.840658104	4.8
12.12.2018	Tunnel	2	36.08545988	5.1	16299.58585	1.2	11156.94871	0.8	0.474840636	4.4	3.277976672	9.1	6.966142132	2	458.7593536	2.9
12.12.2018	Fjord	6	5.35755704	7.2	830.1387763	2.8	1613.9107	2.8	0.019796983	60.3	0.679331753	32	66.66910809	1.8	4606.853357	2.8
12.12.2018	Fjord	6	5.808884963	10	964.0862653	3.5	1900.487685	3.8	0.027505678	107.9	0.783754037	4.9	81.0928685	3.7	5453.011063	2.3
17.12.2018	Stream	7	0.558073036	14.2	2.31504954	2.3	4.340401055	6.7	0.001360558	100	0.067304416	33.5	0.394272794	2.6	8.911561394	2.8
18.01.2019	Stream	13	0.580331111	14.1	2.539479633	1.2	4.386894118	3.5	0.001846451	95.2	0.054647215	40.4	0.477023767	8.3	8.250220058	0.9
31.01.2019	Stream	19	0.547036336	12.5	2.044038912	3.2	4.392414432	7.6	0.006300264	64	0.018094812	39.7	0.534434112	14.2	16.36220802	2.8
07.02.2019	Stream	34	4.586156022	2.9	2.464411429	4.9	5.239238133	12.2	-4.09626E-05	100	0.043269901	87.2	0.468315635	8.3	9.167363486	2.1
02.03.2019	Stream	39	0.590974432	15	3.320032765	2.8	9.430611953	3.2	0.003951064	57.7	0.065727819	66.8	0.317098126	3.9	6.2204608	2.9
02.03.2019	Fjord	43	4.384167153	4.3	511.5643645	1.8	1504.714132	0.4	0.009184404	100	0.418043676	58.4	77.97339279	2.7	5377.881212	0.7
05.03.2019	Stream	45	0.552970839	4.9	2.34619551	3.6	5.481306694	5.7	0.005734049	14.2	0.044896248	66.1	0.450652879	7.2	7.67736191	3.3
05.03.2019	Fjord	50	0.788473548	13.2	56.93417592	1.4	174.2962277	5.4	0.003276833	173.2	1.285450714	21.5	88.24856186	2.1	6013.171634	1.5
11.03.2019	Fjord	54	0.424537434	10.9	27.53188182	1.3	82.80029765	5.5	0.008392116	21.7	1.222618958	18.2	76.0503006	2.5	5327.901784	1.1
11.03.2019	Blank	55	0.00000000	33.3	0.00000000	10.8	0.14040150	16.7	0.00000000	0.0	0.00000000	173.2	0.00000000	101.7	0.00000000	18.7
11.03.2019	Blank	56	0.00000000	87.2	0.00000000	13.9	0.20536541	31.5	0.00000000	173.2	0.00000000	173.2	0.00000000	23.6	0.00000000	24.1
22.03.2019	Fjord	60	1.646986539	25.8	135.2117448	4.3	377.838519	2.2	0.011645354	93.9	0.791664758	18.3	93.48957937	3.4	6520.834769	3
22.03.2019	Stream	61	0.503273761	5.8	2.398675603	7.3	7.870423505	7.4	0.004155027	48.8	0.029396773	56.8	0.286929763	5.1	5.782861437	1.2

			Ir193(LR)		Pt195(LR)		Au197(LR)		Hg202(LR)	
Date	Sample name	Number	Conc. µg/L	RSD, %	Conc. µg/L	RSD, %	Conc. µg/L	RSD, %	Conc. µg/L	RSD, %
12.12.2018	Stream	1	0	0	0.000380466	69.3	0.002277742	34.4	0.011479454	6.9
12.12.2018	Tunnel	2	0.000261775	86.6	0.000380398	34.6	0.007539691	37.5	0.063695948	3.3
12.12.2018	Fjord	6								
12.12.2018	Fjord	6								
17.12.2018	Stream	7	0	0	0.001290659	56.8	1.97375E-05	101.7	0.010865482	14.1
18.01.2019	Stream	13	0	0	0.000359734	43.4	0.002304975	12.6	0.046599964	2.3
31.01.2019	Stream	19	0	0	0	173.2	6.143437601	173	0.078184178	5.3
07.02.2019	Stream	34	4.99659E-05	173.2	0.000398202	25.8	0.000135513	55.1	0.031677447	3.6
02.03.2019	Stream	39	0.000129968	173.2	0.000149275	88.2	0.000174526	33.3	0.016717217	2.1
02.03.2019	Fjord	43								
05.03.2019	Stream	45	0	0	0.000437696	91.7	0.000738381	37.8	0.051190381	3.7
05.03.2019	Fjord	50								
11.03.2019	Fjord	54								
11.03.2019	Blank	55	0.00000000	173.2	0.00000000	89.2	0.00000000	36.7	0.00000000	1.0
11.03.2019	Blank	56	0.00000000	173.2	0.00000000	91.7	0.00000000	33.3	0.00000000	2.3
22.03.2019	Fjord	60								
22.03.2019	Stream	61	0.000150185	106.4	0.000556652	91.7	0.001365226	83.3	0.038467023	8.9

			Ag109(MR)		Sb121(MR)		Ba137(MR)		Br81(HR)	
Date	Sample name	Number	Conc. µg/L	RSD, %	Conc. µg/L	RSD, %	Conc. µg/L	RSD, %	Conc. µg/L	RSD, %
12.12.2018	Stream	1	0.009779496	83.3	0.057283952	27.6	2.580034426	0.8	38.09588029	12.8
12.12.2018	Tunnel	2	0.128628516	9.1	0.081892607	18.3	13.82584386	10.9	62.39390727	0.6
12.12.2018	Fjord	6	0.029858899	40.1	0.156598372	27	7.837172481	7.9	1779.296201	6.6
12.12.2018	Fjord	6	-0.006484248	0	0.161703763	72.6	8.72898075	9.8	2120.039575	3.3
17.12.2018	Stream	7	0.001997413	100	0.031945432	48.3	3.116750129	5.6	39.38615804	3.5
18.01.2019	Stream	13	0.007572919	118.4	0.014857191	57.7	2.917274082	7.5	40.26128678	4.9
31.01.2019	Stream	19	0.002212008	10.8	0.02485179	0	3.72902005	5.2	68.52999161	16.4
07.02.2019	Stream	34	0.000544456	173.2	0.165224203	20.4	3.226746825	5.9	45.80860857	6.8
02.03.2019	Stream	39	0.002097114	88.6	0.032163238	36.5	2.3615985	6.6	31.1450217	6
02.03.2019	Fjord	43	0.049627979	103.6	0.15557015	28.2	8.360100217	5.9	2183.945752	2.4
05.03.2019	Stream	45	0.003054282	173.2	0.01360272	94.4	2.767395311	2.1	31.06071903	4.3
05.03.2019	Fjord	50	0.028894891	121.8	0.13718821	20	5.410353404	11.8	2407.299481	3.6
11.03.2019	Fjord	54	0.005609041	100	0.173085063	19.5	4.899097565	4.2	2530.537386	2.7
11.03.2019	Blank	55	0.00000000	87.1	0.00000000	173.2	0.00000000	86.8	0.00000000	28.6
11.03.2019	Blank	56	0.00000000	86.6	0.00000000	86.6	0.00000000	75.5	0.00000000	69.3
22.03.2019	Fjord	60	0.001767777	173.2	0.110399608	25	7.234966048	7.4	2507.37689	3.7
22.03.2019	Stream	61	0.006103513	24.7	0.01200588	65.5	2.235757085	5.5	32	18.2

Date	Sample name	Number	Li7(LR) Conc. µg/L	Li7(LR) RSD, %	Y89(LR) Conc. µg/L	Y89(LR) RSD, %	Zr90(LR) Conc. µg/L	Zr90(LR) RSD, %	Cd114(LR) Conc. µg/L	Cd114(LR) RSD, %	Mo98(MR) Conc. µg/L	Mo98(MR) RSD, %	Sn118(LR) Conc. µg/L	Sn118(LR) RSD, %
24.05.2019	Stream	3	0.226888376	0.8	0.096222199	4.8	0.025069589	9.9	0.002918909	53.3	0.087127599	39.2	0.005287428	6.3
24.05.2019	Stream	3	0.218867831	3.8	0.085425505	4	0.022046903	10.8	0.004016141	23.4	0.0808591	44.2	0.001243787	24.7
28.05.2019	Fjord	6	54.20228384	0.9	0.079299326	6.7	0.015464984	12.7	0.032468709	12.9	2.909789504	7.4	0.158993004	7.9
28.05.2019	Fjord	6	51.15548295	1.3	0.068536272	6.5	0.014728612	17	0.035269307	11.5	2.95961221	9.8	0.145205491	6.2
28.05.2019	Stream	7	0.078123173	4.3	0.128889335	1	0.035362864	8.9	0.007960908	32.7	0.087461347	46.6	0.001554341	48.8
03.06.2019	Fjord	11	134.0669102	0.8	0.091418496	2.5	0.027954286	4.3	0.294147851	5.7	7.354267071	2.2	0.386497075	6.6
03.06.2019	Stream	12	0.041372719	2.8	0.192134932	4.2	0.039804285	5.1	0.010691494	75.4	0.058528556	28.6	0.000583908	45.8
06.06.2019	GNR	21	10.74319505	2.3	14.30602447	1.7	0.079975502	1.8	28.36315647	1.6	0.031523857	121.4	0.006728687	37.8
06.06.2019	GR	22	10.81175749	1.6	14.64840874	3.7	0.084187913	12.8	28.38664336	1.6	0.048711252	55.1	0.011741801	21.6
09.06.2019	Fjord	34	78.2525761	0.6	0.171748473	2.9	0.012982439	27	1.514540643	0.5	3.883542337	3.6	0.193386791	9
09.06.2019	Stream	35	0.103744433	4	0.238119813	4.9	0.042364982	10	0.01113539	10.2	0.043166373	12.8	0.0028558	55.3

Date	Sample name	Number	Hg202(LR) Conc. µg/L	Hg202(LR) RSD, %	Tl205(LR) Conc. µg/L	Tl205(LR) RSD, %	Pb208(LR) Conc. µg/L	Pb208(LR) RSD, %	U238(LR) Conc. µg/L	U238(LR) RSD, %	Dy161(LR) Conc. µg/L	Dy161(LR) RSD, %	Na23(MR) Conc. µg/L	Na23(MR) RSD, %
24.05.2019	Stream	3	0.057856243	2.5	0.004431856	38.4	0.006322173	26.3	0.01729316	6.8	0.016587231	16.5	5450.511183	2.4
24.05.2019	Stream	3	0.055670728	11.2	0.002862306	17.4	0.010452899	7.4	0.013791615	9.3	0.015515233	6.7	5268.31955	1.4
28.05.2019	Fjord	6	kan ikke		0.005386336	11.6	0.021047706	10.5	0.948674557	1.4	0.007777948	25		
28.05.2019	Fjord	6	bestemmes i		0.004159296	14.5	0.020402577	19.3	0.886528582	0.6	0.011612833	25		
28.05.2019	Stream	7	0.055135227	9.9	0.003040815	32.5	0.017538333	8.7	0.023462861	13.1	0.022976459	29.8	5507.26541	2.4
03.06.2019	Fjord	11	sjøvann		0.01101079	23	0.009369865	32.4	2.348364693	0.8	0.007751998	71.5		
03.06.2019	Stream	12	0.018071787	5.6	0.002624458	28	0.028041049	10.4	0.040490466	8.4	0.03826458	23.7	4670.269414	2.6
06.06.2019	GNR	21	0.047591852	4.2	0.802043385	2.3	22.86196397	1.5	1.31595026	0.3	2.728511265	1.7	57070.31802	2.9
06.06.2019	GR	22	0.042047142	15.5	0.780420443	4.2	22.80552469	2.6	1.317971865	3.2	2.715786501	3.4	56009.35907	2.4
09.06.2019	Fjord	34			0.030143424	13.2	0.034647255	10	1.322714891	1.2	0.019577481	33.8		
09.06.2019	Stream	35	0.060704446	6.7	0.003208876	31.2	0.043459848	3.1	0.049880007	5.5	0.04225238	13.9	4426.27873	1.8

Date	Sample name	Number	V51(MR) Conc. µg/L	V51(MR) RSD, %	Cr53(MR) Conc. µg/L	Cr53(MR) RSD, %	Mn55(MR) Conc. µg/L	Mn55(MR) RSD, %	Fe56(MR) Conc. µg/L	Fe56(MR) RSD, %	Fe57(MR) Conc. µg/L	Fe57(MR) RSD, %	Co59(MR) Conc. µg/L	Co59(MR) RSD, %
24.05.2019	Stream	3	0.071280036	9.8	0.138054411	8.1	0.31194818	18.7	7.223330931	3.6	9.659396628	9.4	0.031556248	34.6
24.05.2019	Stream	3	0.045949083	30	0.089876759	27.4	0.288106717	15.5	7.347720209	1.4	8.268996069	8.1	0.040694713	35.1
28.05.2019	Fjord	6	0.353181062	15.7	0.049588896	16.5	2.224875411	2.2	7.615816764	2.5	9.651212902	8.3	0.08421585	16.1
28.05.2019	Fjord	6	0.31038557	12.3	0.054131227	18.2	2.104258306	3.7	7.08209998	0.4	9.916984023	19.8	0.063874836	47.4
28.05.2019	Stream	7	0.065135302	6.2	0.218634557	20.5	0.441421748	12.7	11.43168153	0.7	13.0470093	5.9	0.053033784	32
03.06.2019	Fjord	11	0.863482374	2.3	0.03645507	26.2	2.657850156	4.4	2.947146929	5	3.902927322	27.7	0.256413257	10.6
03.06.2019	Stream	12	0.094429725	19.4	0.273342899	9.5	0.522435888	10	20.79274615	2.6	23.05376444	19.1	0.044784675	42.5
06.06.2019	GNR	21	0.008709508	53.9	3.081323484	4.6	521.4401035	2.4	10360.28939	2.1	10610.15014	2.5	79.33496083	2.6
06.06.2019	GR	22	0.003077736	82.9	3.286929854	3.7	524.3134022	3	9723.451707	1.7	9918.727893	4.3	80.6816199	4.7
09.06.2019	Fjord	34	0.359985223	7.2	0.054986977	11.6	17.28244461	1	10.36350347	3.1	10.54609169	21.7	2.43912592	3.3
09.06.2019	Stream	35	0.099726109	14.8	0.290909376	13.8	0.615204305	9.3	26.67144188	2.8	29.98546038	5.6	0.048271532	40.6

Date	Sample name	Number	La139(LR) Conc. µg/L	RSD, %	Ce140(LR) Conc. µg/L	RSD, %	Pr141(LR) Conc. µg/L	RSD, %	Nd146(LR) Conc. µg/L	RSD, %	Eu153(LR) Conc. µg/L	RSD, %	Gd160(LR) Conc. µg/L	RSD, %
24.05.2019	Stream	3	0.073361593	5	0.073812477	15.7	0.018048221	14.8	0.077492275	10.5	0.003382863	28.6	0.012760739	32.8
24.05.2019	Stream	3	0.071370077	8.8	0.072453508	5	0.016659696	9.7	0.074366786	14.9	0.004987407	21	-0.026370202	31.4
28.05.2019	Fjord	6	0.056740287	6.5	0.07421488	4.3	0.012697437	8.9	0.056399855	20.2	-0.003769593	18.3	0.08218416	28.6
28.05.2019	Fjord	6	0.056833744	9.8	0.068354148	9.7	0.011019239	3	0.056508412	14.7	-0.003502138	33.6	-0.040020435	9.2
28.05.2019	Stream	7	0.101184	2.3	0.128594917	4	0.02589195	10.8	0.1126469	5.5	0.004871892	8	-0.0222923	26.1
03.06.2019	Fjord	11	0.077873062	11.8	0.086525138	3.8	0.010791029	6.4	0.051303601	30.1	-0.006676157	23.3	-0.031732529	51.7
03.06.2019	Stream	12	0.184644842	3.5	0.286322983	4.1	0.046649659	5.6	0.18485637	3.5	0.006485154	16.5	-0.007653917	5.1
06.06.2019	GNR	21	27.93903257	0.7	54.22829599	0.8	5.824422447	0.9	24.35322579	1	0.502575805	1.2	3.516552899	2.4
06.06.2019	GR	22	28.51250022	0.2	54.61915873	1	5.745498584	5.1	23.95204669	4	0.501925499	3.7	3.409604016	5.7
09.06.2019	Fjord	34	0.268467166	4.1	0.322823955	4.2	0.037313799	6	0.125358158	16	-0.004527974	38	-0.021363772	11.3
09.06.2019	Stream	35	0.233334953	5.6	0.396831451	1.4	0.057187053	5.4	0.237468531	12.8	0.012766193	16.7	-0.034522682	22.2

Date	Sample name	Number	Mg25(MR) Conc. µg/L	RSD, %	Al27(MR) Conc. µg/L	RSD, %	Si29(MR) Conc. µg/L	RSD, %	P31(MR) Conc. µg/L	RSD, %	S34(MR) Conc. µg/L	RSD, %	Cl35(MR) Conc. µg/L	RSD, %
24.05.2019	Stream	3	1085.825702	4.9	41.43866307	1.2	1924.677554	2.1	3.005658545	16.7	1456.387453	5.5	13842.63667	1
24.05.2019	Stream	3	1062.815582	1.5	39.67244979	3.6	1846.672089	1.5	2.977353042	15.9	1429.752552	3.6	13379.63228	2.6
28.05.2019	Fjord	6	342307.0144	3.5	20.01494875	3.8	460.2676001	8.1	4.0270606	15	264802.376	15.4	4752108.643	21
28.05.2019	Fjord	6	313564.5683	1	18.05174412	1.7	471.8035013	1.6	4.689379845	5.8	266404.0868	4.1	5204031.37	1.3
28.05.2019	Stream	7	1178.106703	5.9	47.21669292	2.9	1849.716616	0.7	2.720212305	4.2	1446.857505	6.6	13986.86643	1
03.06.2019	Fjord	11	795490.0424	2.9	9.702285597	2.1	212.4802835	2.8	5.734294346	10.4	695917.8231	2.9	12096667.17	3.3
03.06.2019	Stream	12	845.5725193	3.2	85.82245144	4.2	1517.636375	2.6	2.975769354	9.5	1082.630492	6	11859.80487	0.6
06.06.2019	GNR	21	12456.13469	4.4	4337.96841	1.6	11131.65128	3.2	4.003506681	14.4	199396.366	3.8	72836.64446	2.8
06.06.2019	GR	22	12419.27468	3.5	4311.365343	3.4	11012.07909	3.6	3.515831909	3.6	197742.4008	3.3	72130.66289	3.5
09.06.2019	Fjord	34	459438.0843	3.2	31.5578708	4.1	1030.376186	2.1	4.363931713	7.6	406632.4698	2.8	7380859.322	1.9
09.06.2019	Stream	35	791.9452191	1.8	102.32776	3.6	1501.018443	2	3.029435247	22.4	951.2935178	4.1	6724.95163	1.9

Date	Sample name	Number	Ni60(MR) Conc. µg/L	RSD, %	Cu63(MR) Conc. µg/L	RSD, %	Zn66(MR) Conc. µg/L	RSD, %	Rb85(MR) Conc. µg/L	RSD, %	Sr88(MR) Conc. µg/L	RSD, %	Ba137(MR) Conc. µg/L	RSD, %
24.05.2019	Stream	3	0.479932334	12.9	2.167363975	2.5	2.507081587	8.8	0.646726412	8	9.941606104	2.8	4.470414984	15.3
24.05.2019	Stream	3	0.443890684	18.7	2.322650493	14.9	2.408987073	3.8	0.636373395	7.5	9.862930334	2.6	3.898912632	9
28.05.2019	Fjord	6	0.489000779	8.1	4.9204463	3.9	7.234575655	11.6	30.80905718	1.7	2180.820814	2.4	2.857610652	7.5
28.05.2019	Fjord	6	0.476088006	9.4	4.549859179	4.8	7.261289485	20.5	28.65667519	2	2018.901077	1.3	3.007921901	3.4
28.05.2019	Stream	7	0.552234407	14.7	2.383664764	8.4	4.477169459	7.9	0.49836628	4.4	11.09593196	4.7	4.554318305	8.7
03.06.2019	Fjord	11	0.297251471	20.8	14.18377894	2.5	61.38443668	2.6	73.55377902	1.7	5111.976272	2.1	3.639379384	5.4
03.06.2019	Stream	12	0.520653341	30.1	2.5096061	5.5	4.428907182	19	0.455668527	5.2	7.804492454	2.3	3.30835127	8.7
06.06.2019	GNR	21	36.88521538	6.6	11699.2802	2	8119.447717	2.9	6.740006127	3.6	432.2021462	3.7	12.89830181	7
06.06.2019	GR	22	37.52251776	4.6	11659.41539	4.3	8072.545833	3.2	6.727754432	3.1	424.1783202	3.6	13.33366791	1.4
09.06.2019	Fjord	34	1.37258039	0.6	113.771228	2.2	427.7661486	1.8	40.7209309	2.5	2960.106503	2.6	3.31629821	4.6
09.06.2019	Stream	35	0.512047047	25.1	4.127839066	6.8	5.521469519	12.4	0.382442247	1.2	7.617734897	2	3.189524742	17

			Ho165(LR)		Er166(LR)		W182(LR)	
			Conc.		Conc.		Conc.	
Date	Sample name	Number	µg/L	RSD, %	µg/L	RSD, %	µg/L	RSD, %
24.05.2019	Stream	3	0.002945723	31.5	0.014271771	28.2	0.002192151	86.6
24.05.2019	Stream	3	0.003484459	19.6	0.012193145	14.8	0.000607238	12.4
28.05.2019	Fjord	6	0.002254763	22.5	0.007649365	23.2	0.004558726	44.7
28.05.2019	Fjord	6	0.001450267	27.9	0.007141973	59	0.003419178	77.1
28.05.2019	Stream	7	0.004985549	16.5	0.013974567	20.3	0.002675156	23
03.06.2019	Fjord	11	0.002929551	94.6	0.00630306	35.7	0.010209787	43.5
03.06.2019	Stream	12	0.005687573	9.1	0.023677034	6.6	0.004372417	25
06.06.2019	GNR	21	0.502713939	2.2	1.571867321	3.5	0.007732473	17
06.06.2019	GR	22	0.491097094	5.9	1.5406736	6.2	0.006824851	0.9
09.06.2019	Fjord	34	0.003919211	26.3	0.012193771	22.4	0.007687508	18.1
09.06.2019	Stream	35	0.008373767	28.4	0.025724222	19.2	0.002565645	41.8

			K39(MR)		Ca44(MR)		Ti49(MR)	
			Conc.		Conc.		Conc.	
Date	Sample name	Number	µg/L	RSD, %	µg/L	RSD, %	µg/L	RSD, %
24.05.2019	Stream	3	220.6572931	3.4	5179.512076	3.1	0.213580245	11.3
24.05.2019	Stream	3	208.24123	3.5	5102.790499	2.8	0.200330398	42.8
28.05.2019	Fjord	6	95206.01673	29.5	104521.2915	22.7	0.212175465	32.9
28.05.2019	Fjord	6	103152.8537	3.5	109403.9982	1.9	0.139855973	32.8
28.05.2019	Stream	7	199.5229571	3.3	5647.531254	4	0.265491306	64.5
03.06.2019	Fjord	11	266921.8598	4.6	276670.3846	3.7	0.069822045	8.7
03.06.2019	Stream	12	160.3590777	2.9	3910.981737	3.2	0.427610249	10.2
06.06.2019	GNR	21	5535.331093	0.9	173165.7003	3.9	0.569337348	27.4
06.06.2019	GR	22	5584.828543	1.9	169014.6892	3.2	0.472489625	22.4
09.06.2019	Fjord	34	156272.6664	2.3	168880.8284	3	0.128983177	21.6
09.06.2019	Stream	35	134.8940278	1.9	3745.626688	1.5	0.571079443	12.4

			As75(HR)		Se78(HR)		Br81(HR)	
			Conc.		Conc.		Conc.	
Date	Sample name	Number	µg/L	RSD, %	µg/L	RSD, %	µg/L	RSD, %
24.05.2019	Stream	3	0.129393064	110.3	<1.0	52.3	35.77997391	1.6
24.05.2019	Stream	3	0.070598565	53.9	<1.0	103.2	30.06133152	20
28.05.2019	Fjord	6	0.518654281	12.5	<1.0	111.1	20716.63584	1
28.05.2019	Fjord	6	0.523706626	37.8	<1.0	26.3	19476.27749	0.5
28.05.2019	Stream	7	0.068731723	0	<1.0	79.1	35.81999929	14
03.06.2019	Fjord	11	1.075063243	27.5	<1.0	15.9	51889.30208	2.2
03.06.2019	Stream	12	0.090247528	69.5	<1.0	58.7	21.69464723	17.5
06.06.2019	GNR	21	0.623590452	11.8	<1.0	20.1	50.63468826	1.3
06.06.2019	GR	22	0.760621706	23.9	<1.0	30.6	50.20744123	8.1
09.06.2019	Fjord	34	0.706421636	24	<1.0	106.7	28112.42428	0.4
09.06.2019	Stream	35	0.0371446	173.2	<1.0	107.5	33.40220605	5.2

Date	Sample name	Number	Li7(LR) Conc. µg/L	RSD, %	Y89(LR) Conc. µg/L	RSD, %	Cd114(LR) Conc. µg/L	RSD, %	Mo98(MR) Conc. µg/L	RSD, %	Sn118(LR) Conc. µg/L	RSD, %	La139(LR) Conc. µg/L	RSD, %
12.09.2019	GNR	36	9.428959016	2.8	11.2524304	4.4	32.68564688	1.2	0.070913075	28.2	0.017362899	9.8	22.15479463	2.1
	GR	36	10.06350295	1.5	11.72147386	2	34.99205609	2.6	0.039419556	20.3	0.013950482	26.9	23.47385574	1.6
	GR	37	10.09263136	2.9	12.10246427	2.2	33.85005592	0.6	0.032533946	22.4	0.01412158	10.6	23.12954127	0.9
12.09.2019	Stream	43	0.115317721	2.2	0.076285746	5.5	0.00818331	13.4	0.111210235	38.4	0.002115971	28.9	0.063977447	5.6
12.09.2019	LStream	44	0.177011113	2.7	0.092577027	1.8	0.01767257	31	0.135589916	3.6	0.009081584	14.6	0.099217258	5.5
19.09.2019	Stream	48	0.130462217	4.2	0.376771983	3	0.015893635	15.4	0.044238096	13.2	0.00461306	24.9	0.466438676	2.8
19.09.2019	LStream	49	0.13361179	4.4	0.417486876	2.4	0.018910087	23.2	0.039398182	22.3	0.006960722	19.5	0.502651656	1.3
19.09.2019	Fjord	50	134.3064881	4.7	0.186939284	9.3	2.077192926	5	8.348228599	8	0.766651247	8.2	0.289728118	11.1
02.10.2019	Stream	55	0.137932138	2.9	0.521845304	0.8	0.014820699	22.1	0.03939494	27	0.002894239	15.4	0.727931141	1.5
02.10.2019	LStream	56	0.131335605	4.5	0.436639278	5.7	0.016776012	7.1	0.049082594	13.7	0.00481473	37.9	0.563931691	2
02.10.2019	EC.Alu.C.1V0m	57	9.402627914	4.7	9.816283104	4.5	24.69354386	2.4	0.026713157	40.9	0.003234933	35.3	20.27311594	0.2
02.10.2019	EC.Alu.C.1V20m	58	9.177039618	0.5	9.155660249	1	24.551353	2.3	0.018378734	48.7	1.540836853	4.4	19.6110121	3.8
02.10.2019	EC.Alu.C.1V40m	59	8.99410158	1.8	8.591769112	1.4	23.2230874	0.8	0.017579945	61.6	1.709391302	1.6	18.04016631	2.6
02.10.2019	EC.Alu.C.1V60m	60	9.251096691	1	8.233866679	0.6	22.64358168	2.5	0.018236196	62.6	1.838791182	0.6	17.33826211	1.8
02.10.2019	EC.Alu.C.1V80m	61	9.678390217	2.4	7.980081555	2.4	22.68280233	2	0.041302081	22.2	2.037513484	2.6	16.6645015	2.7
02.10.2019	EC.Alu.C.1.5V0m	62	9.928612772	1.9	10.16205992	2.7	26.39984936	1.9	0.023155159	42.8	0.004852172	30.3	21.72248902	3.9
02.10.2019	EC.Alu.C.1.5V20m	63	9.467808229	1.6	9.06225272	0.8	24.53278492	2.2	0.026221755	64.6	0.899232731	2.8	19.68888109	1.6
02.10.2019	EC.Alu.C.1.5V40m	64	9.37321183	0.6	8.885480379	1.4	23.87128117	1.5	0.01898729	34.5	0.991207502	2.1	18.7305307	1.5
02.10.2019	EC.Alu.C.1.5V60m	65	9.814932734	2.5	8.167036064	1	23.01024035	1.4	0.0328216	9.3	1.050419387	3.5	17.78692342	1.3
02.10.2019	EC.Alu.C.1.5V80m	66	10.2233656	3.3	7.809873227	2.5	22.99602247	2.3	0.030289002	32.9	1.144862651	5.1	16.56798193	1.6
02.10.2019	EC.Alu.NC.1.V0m	67	6.42628157	1.7	5.539164839	4.2	19.15543437	1	0.000348579	54.6	0.004328345	17	10.60495241	0.6
02.10.2019	EC.Alu.NC.1.5V20m	68	6.428148442	1	5.28656226	0.7	19.3388224	0.8	0.024259077	35	2.36717991	2.3	10.54651673	1.2
02.10.2019	EC.Alu.NC.1.5V40m	69	6.354213736	2.6	5.224726472	1.3	18.89244191	1.6	0.044262197	35.1	2.517258533	1.2	10.31638168	1.9
02.10.2019	EC.Alu.NC1.5V60m	70	6.670465881	2.4	5.010122167	3.1	18.60492465	1.2	0.022572358	9.2	2.641659821	1.4	10.20315262	1.2
02.10.2019	EC.Alu.NC.1.5V80m	71	6.064099654	1.9	4.646144102	1.4	17.67980077	0.6	0.028305216	31.2	2.433225016	3.9	9.298865177	3.1
11.10.2018	Fjord	72	3.205867064	1.3	0.679046574	3.1	2.572201979	1	0.263835774	3.1	0.007034825	17.1	1.480290047	1.8
11.10.2018	Stream	77	0.120348837	2.5	0.200021153	3.7	0.010242409	6.1	0.06789009	34	0.003189522	56.2	0.175141689	1.6

			Ce140(LR)		Pr141(LR)		Nd146(LR)		Eu151(LR)		Eu153(LR)		Gd157(LR)	
			Conc.		Conc.		Conc.		Conc.		Conc.		Conc.	
Date	Sample name	Number	µg/L	RSD, %	µg/L	RSD, %	µg/L	RSD, %	µg/L	RSD, %	µg/L	RSD, %	µg/L	RSD, %
12.09.2019	GNR	36	43.70405834	1.6	4.648033423	0.4	19.07996823	0.5	0.460640678	2.3	0.431398003	3.6	2.791025094	4
	GR	36	46.82293312	3.1	4.864473632	1.5	20.23470078	1.8	0.490865364	5.2	0.457180696	3.8	2.932306917	0.6
	GR	37	47.35738069	1.9	4.838169858	0.7	20.13457493	2	0.476185957	0.6	0.458440799	2.6	2.929090332	2.2
12.09.2019	Stream	43	0.066430359	5.4	0.015640453	6.4	0.066287083	9.6	0.001701118	41	0.003375677	10.2	0.009739293	26.8
12.09.2019	LStream	44	0.107230181	2.6	0.022753752	7.8	0.101796526	4.5	0.003045807	22.4	0.003734601	30.5	0.018813435	5.6
19.09.2019	Stream	48	0.804866388	0.7	0.109743471	1.2	0.453597621	5.6	0.01440707	7.3	0.011863681	10.6	0.065954126	4.4
19.09.2019	LStream	49	0.868780585	1.2	0.117133845	3.2	0.48277661	0.4	0.015302953	16.7	0.01402724	2.2	0.079177994	8.8
19.09.2019	Fjord	50	0.405593457	6	0.070071356	16.6	0.150646348	19.9	0.032559823	29.4	0.078289184	33.6	0.080699952	13.5
02.10.2019	Stream	55	1.317060455	2.4	0.156118842	2.6	0.662982085	4.1	0.018924748	5.3	0.019795292	19.7	0.10306189	20.4
02.10.2019	LStream	56	1.001688655	1	0.130102932	4.6	0.558209728	5.8	0.014640891	11.6	0.014834993	4.7	0.089419748	24.4
02.10.2019	EC.Alu.C.1V0m	57	37.09093635	2.6	3.776263147	0.5	15.12823051	2	0.29333674	4	0.293966116	5.6	2.100476318	1.6
02.10.2019	EC.Alu.C.1V20m	58	36.40977036	4	3.623189318	0.9	14.30106133	0.9	0.293499724	2.8	0.287402239	2.3	2.030102695	2.6
02.10.2019	EC.Alu.C.1V40m	59	34.54579207	0.6	3.355503668	1.1	13.52489023	1.6	0.286682422	6.6	0.26090036	4	1.958881025	2.9
02.10.2019	EC.Alu.C.1V60m	60	31.49630955	2.9	3.227154748	2.5	12.90322026	1.9	0.261389932	2.9	0.252511399	4.3	1.771326896	0.9
02.10.2019	EC.Alu.C.1V80m	61	31.00405143	1.4	3.325899644	2	12.96896162	1	0.261735441	3.2	0.240441437	0.7	1.757608349	1.9
02.10.2019	EC.Alu.C.1.5V0m	62	41.94441596	1.5	4.008141256	1.4	15.89634176	1.5	0.324566957	4	0.30660984	1.7	2.249314869	0.7
02.10.2019	EC.Alu.C.1.5V20m	63	36.95617989	1.7	3.621396315	1	14.36278818	1.6	0.29211654	2.2	0.28231116	3.2	2.06979934	3
02.10.2019	EC.Alu.C.1.5V40m	64	36.04407336	1.8	3.483496475	1.3	13.70117405	2.3	0.286995926	6.1	0.273367211	0.7	1.926234293	1.8
02.10.2019	EC.Alu.C.1.5V60m	65	33.39003303	3.3	3.254932314	0.9	12.96578289	1.6	0.25765353	2.6	0.254825818	4.4	1.802114581	3.9
02.10.2019	EC.Alu.C.1.5V80m	66	30.88363953	2.1	3.305232818	3	13.00643803	3.3	0.259857055	3.1	0.248284616	4.5	1.774479111	1.1
02.10.2019	EC.Alu.NC.1.V0m	67	19.68870746	1.6	2.264119875	1.1	8.899741204	1.4	0.192271975	0.4	0.185461998	5.2	1.253886128	3.3
02.10.2019	EC.Alu.NC.1.5V20m	68	19.29123622	1.5	2.235244938	0.8	8.713605462	3.2	0.178086226	1.4	0.183663602	4.6	1.205044379	4.3
02.10.2019	EC.Alu.NC.1.5V40m	69	19.06884088	1	2.199492936	1.8	8.570376931	1.1	0.177842181	7.3	0.168081456	2.2	1.202170975	3.1
02.10.2019	EC.Alu.NC1.5V60m	70	18.62164079	1.8	2.11296831	1.4	8.471245384	0.9	0.16418674	2.8	0.162777554	3.8	1.142404338	2.8
02.10.2019	EC.Alu.NC.1.5V80m	71	16.96844828	0.6	1.916705812	0.3	7.61404309	3.7	0.153127222	6.8	0.152316965	4.3	1.046293353	5.1
11.10.2018	Fjord	72	2.331925523	3	0.310372419	3.2	1.255368996	3	0.030223036	14.5	0.026406335	6.5	0.159332571	10.1
11.10.2018	Stream	77	0.280941792	2.6	0.044196626	9.5	0.180657733	2.2	0.006696908	14	0.007142624	14.4	0.032428524	11.9

			Dy163(LR)		Ho165(LR)		Er166(LR)		W182(LR)		Hg202(LR)		Tl205(LR)	
			Conc.		Conc.		Conc.		Conc.		Conc.		Conc.	
Date	Sample name	Number	µg/L	RSD, %	µg/L	RSD, %	µg/L	RSD, %	µg/L	RSD, %	µg/L	RSD, %	µg/L	RSD, %
12.09.2019	GNR	36	2.107907674	1.1	0.406056886	2.1	1.246338788	2.4	0.004378326	21.2	0.014232482	19.1	0.772128455	0.7
	GR	36	2.209852341	2.2	0.426946612	3.1	1.296678678	2.4	0.004106868	19.2	0.014793544	9.7	0.82333587	0.1
	GR	37	2.224854393	3.1	0.428784368	1.5	1.317094845	3.9	0.002479992	60	0.01190758	10.1	0.80030699	1.5
12.09.2019	Stream	43	0.012252025	11.4	0.003044415	29.5	0.008477687	4.5	0.00276768	63.3	0.009737561	12.6	0.002910683	3.2
12.09.2019	LStream	44	0.013467084	13.2	0.003215822	29.4	0.013915572	31.1	0.019502589	17.3	0.008855868	14.1	0.004179087	22.3
19.09.2019	Stream	48	0.066084154	5.1	0.012335648	1.1	0.040170512	3.6	0.002486118	58	0.007709078	18.1	0.003310392	28.9
19.09.2019	LStream	49	0.068347032	7.9	0.014697755	15	0.046291066	17.3	0.005673517	21.7	0.006502737	14.4	0.004154016	19.4
19.09.2019	Fjord	50	0.013521291	31.4	0.014126448	39.2	0.03109225	37.9	-0.024873561	46.5	sjøvann umulig		0.09994683	19.9
02.10.2019	Stream	55	0.085467064	0.2	0.019841592	10.6	0.056613364	16.2	0.003237459	50	0.010940698	10.3	0.003927088	13
02.10.2019	LStream	56	0.065344377	6.5	0.014176237	10.8	0.049849179	10.5	0.004389769	36.4	0.006989519	10	0.003511558	11.4
02.10.2019	EC.Alu.C.1V0m	57	1.58126909	3.1	0.312827205	4.6	0.963705629	0.5	0.002925821	4.6	0.012033372	5.9	0.700943705	4.7
02.10.2019	EC.Alu.C.1V20m	58	1.520581247	2.7	0.303458533	2.9	0.898066868	1.3	0.001813466	36.5	0.013601195	4.6	0.95540545	4
02.10.2019	EC.Alu.C.1V40m	59	1.396336966	1.4	0.282546628	0.9	0.826570086	3.5	0.001412588	27	0.018642833	10.5	0.939052992	2.2
02.10.2019	EC.Alu.C.1V60m	60	1.333971673	1.8	0.27578623	1.7	0.814189345	3.1	0.002724779	43	0.016360064	3.9	0.935737585	2.6
02.10.2019	EC.Alu.C.1V80m	61	1.333226503	2.1	0.271476793	4.9	0.799976212	3.8	0.002454111	78.6	0.019851531	8.2	1.002609617	2.8
02.10.2019	EC.Alu.C.1.5V0m	62	1.640030974	1.7	0.322663135	2.3	0.961363703	1.3	0.001462335	11.1	0.012653487	9	0.74672845	2.9
02.10.2019	EC.Alu.C.1.5V20m	63	1.493883427	1.6	0.306955302	2	0.906310169	1.7	0.002914423	17.4	0.021784726	26.4	0.691594828	1.5
02.10.2019	EC.Alu.C.1.5V40m	64	1.456381265	1	0.286591084	3.9	0.882996264	4.7	0.002082998	56.9	0.013931438	7.9	0.696004981	2.4
02.10.2019	EC.Alu.C.1.5V60m	65	1.343435648	1.5	0.26805674	3.1	0.827139045	3.2	0.001682289	61.5	0.015781314	9.7	0.69139274	2.3
02.10.2019	EC.Alu.C.1.5V80m	66	1.329961158	1.8	0.264351512	2	0.800632755	4.4	0.001231579	55.5	0.017592108	5.9	0.724777879	2.1
02.10.2019	EC.Alu.NC.1.V0m	67	0.950184508	2	0.188986753	3.4	0.562277359	6	0.003223878	10.9	0.014350056	17.5	0.425384451	1.8
02.10.2019	EC.Alu.NC.1.5V20m	68	0.932522102	1.3	0.179458479	3.3	0.552704533	6.2	0.001741958	17.2	0.012430576	10.2	0.427046264	4.2
02.10.2019	EC.Alu.NC.1.5V40m	69	0.879022362	2.8	0.175071296	5.7	0.528637097	3.1	0.000400419	47.6	0.013762409	21.4	0.428071421	5.7
02.10.2019	EC.Alu.NC1.5V60m	70	0.85878015	4.2	0.173962668	2.4	0.515412009	3.4	0.001411364	37.6	0.021123475	29.6	0.417608658	2.3
02.10.2019	EC.Alu.NC.1.5V80m	71	0.768594495	3.1	0.15445876	3.8	0.479143596	1.7	0.002532249	46.4	0.010679932	12.3	0.401209826	3.8
11.10.2018	Fjord	72	0.109311422	5.3	0.02138985	13.1	0.069472696	9.2	0.061555553	3.8	0.015666318	12.3	0.180598158	4.1
11.10.2018	Stream	77	0.031737988	9.2	0.00718488	22.7	0.021882089	25.1	0.003000536	38.5	0.014275822	3.7	0.003796815	10.5

			Pb208(LR)		U238(LR)		Na23(MR)		Mg25(MR)		Al27(MR)		Si29(MR)	
			Conc.		Conc.		Conc.		Conc.		Conc.		Conc.	
Date	Sample name	Number	µg/L	RSD, %	µg/L	RSD, %	µg/L	RSD, %	µg/L	RSD, %	µg/L	RSD, %	µg/L	RSD, %
12.09.2019	GNR	36	31.52399178	0.8	1.518410386	0.7	44976.32072	5.2	11352.23715	5.1	5013.835701	7.8	10339.56025	1.6
	GR	36	33.18717333	1	1.587050447	2.2	46283.17159	1.1	11944.55622	2.2	5124.316403	1.9	10393.02869	0.4
	GR	37	31.06263245	1.8	1.604577435	1.2	46982.1491	1.1	12080.10945	1.6	5311.860251	1.4	10462.51684	1.1
12.09.2019	Stream	43	0.006754807	11.3	0.013617653	10.2	4687.773221	7	1049.196087	1	30.41202391	0.8	1531.048029	2.1
12.09.2019	LStream	44	0.066531443	8.8	0.023513477	7	5634.307006	1.1	1096.777628	1.7	41.61855728	2.7	1587.064251	0.6
19.09.2019	Stream	48	0.086047941	3.9	0.083160322	4.7	3884.293262	2.5	685.0117805	1.9	187.0674508	1.9	1396.235352	1.8
19.09.2019	LStream	49	0.964654907	3.7	0.094887794	3.5	3934.36858	1.8	652.2821044	2.1	207.0649236	4.6	1319.928195	2.6
19.09.2019	Fjord	50	0.153732748	1.8	2.428271687	2.1	7512536.451	3.8	893111.8371	2.5	36.38899541	3.5	512.6477789	2.9
02.10.2019	Stream	55	0.13941663	5.1	0.113569111	2.1	3643.938274	1.8	615.1643546	0.7	270.9242964	0.6	1307.742222	1.5
02.10.2019	LStream	56	0.465419734	4.4	0.094313631	7.2	3875.25104	1.7	646.9925207	0.7	231.0715173	3.1	1390.767725	2.1
02.10.2019	EC.Alu.C.1V0m	57	2.558160105	0.8	0.472959083	1.2	37396.88078	1.4	10137.518	3.1	387.2597691	0.2	10412.11549	1.8
02.10.2019	EC.Alu.C.1V20m	58	2.647236145	1.4	0.451322868	1.9	37309.439	0.9	9899.068333	1.3	470.9865384	1.2	10101.36548	2.2
02.10.2019	EC.Alu.C.1V40m	59	2.917137408	2.2	0.433113303	2.3	38949.06014	1.8	10325.99331	2.2	673.2512163	1.3	10311.59927	1
02.10.2019	EC.Alu.C.1V60m	60	3.34050696	1.8	0.446805927	3.6	38769.55112	2.2	10354.79843	1.5	899.6800061	2	9586.779391	2.4
02.10.2019	EC.Alu.C.1V80m	61	4.014047467	1.3	0.47893943	3.7	36967.59535	2.3	9901.16324	3.8	1186.323713	4.1	9089.073376	1.2
02.10.2019	EC.Alu.C.1.5V0m	62	2.841097403	1.2	0.490020724	3.8	39686.67559	1.7	10837.2747	2.8	356.1014816	2.4	11041.8225	1
02.10.2019	EC.Alu.C.1.5V20m	63	2.721459981	2.6	0.444748758	1.9	40580.06454	1.6	10397.44122	2	531.1090381	1.9	10748.51444	2.3
02.10.2019	EC.Alu.C.1.5V40m	64	3.121631857	1.5	0.450028461	1.1	40670.39602	0.7	10535.48475	1.9	781.5272794	1.9	10129.4819	5
02.10.2019	EC.Alu.C.1.5V60m	65	3.546561952	1.6	0.44739182	2.1	40296.8886	2.8	10759.57907	2.7	1067.231953	0.3	9746.20901	1.3
02.10.2019	EC.Alu.C.1.5V80m	66	3.706263849	2	0.449353262	2.9	38199.16321	2	10299.81784	0.6	1233.289485	1.3	9171.512761	1.4
02.10.2019	EC.Alu.NC.1.V0m	67	6.064181988	1.4	0.526110401	0.8	28141.57906	1.2	7670.020351	1.8	1485.653351	1.6	7192.518489	1.3
02.10.2019	EC.Alu.NC.1.5V20m	68	4.818082838	1.1	0.48180583	1.7	28758.08669	2.7	7546.498337	2.1	1875.311891	4.1	7177.431131	2.3
02.10.2019	EC.Alu.NC.1.5V40m	69	4.34591901	1.1	0.471893058	2.2	28201.25422	2.1	7803.812609	1	2011.096456	3.2	7034.014346	1.8
02.10.2019	EC.Alu.NC1.5V60m	70	4.300761693	2.2	0.445606647	1.2	27743.13312	0.8	7898.154808	1.9	2305.714009	2.1	7085.879951	1.2
02.10.2019	EC.Alu.NC.1.5V80m	71	3.580693983	3.1	0.402659276	4.7	28008.09581	1.2	7508.368855	0.9	2245.376871	1.7	6860.382591	2.2
11.10.2018	Fjord	72	2.041146041	1.5	0.182786765	1.1	20610.53062	1.4	2528.196861	3	103.6877048	1.4	4472.019883	1.4
11.10.2018	Stream	77	0.023087197	23.3	0.040060146	6.2	4964.116757	2.8	945.2864428	2.1	93.99036527	0.5	1850.442978	3

			P31(MR)		S34(MR)		Cl35(MR)		K39(MR)		Ca44(MR)		Ti49(MR)	
			Conc.		Conc.		Conc.		Conc.		Conc.		Conc.	
Date	Sample name	Number	µg/L	RSD, %	µg/L	RSD, %	µg/L	RSD, %	µg/L	RSD, %	µg/L	RSD, %	µg/L	RSD, %
12.09.2019	GNR	36	11.11855506	1.6	207077.7298	3.8	39477.29293	1.4	6319.446257	6.8	129004.8896	7.2	5.755944857	7.5
	GR	36	11.49319065	2.1	216377.3559	2.2	41466.44486	2.9	6664.519145	3.3	133221.7424	1.5	5.848844264	3.7
	GR	37	12.82573825	3.7	218611.4659	0.9	40892.99852	3.2	6569.124262	2.4	135494.9362	1.2	5.610393299	2.4
12.09.2019	Stream	43	1.505173348	1.8	1300.061588	1.6	6548.059598	3.1	132.1334284	5.4	5458.599232	1.7	0.163571481	8.6
12.09.2019	LStream	44	1.875534321	7.7	2551.776997	1.4	7406.991866	2.5	274.9003373	1.7	7570.239237	3.1	0.239278347	12.2
19.09.2019	Stream	48	2.487248253	8.2	897.5980136	3.1	5401.805371	3.6	108.1325718	3.4	3048.226528	2	1.3736167	8.4
19.09.2019	LStream	49	2.431832872	5	966.6181135	1.5	5572.599177	0.8	113.6718083	3.6	2927.413646	2.6	1.511522434	2.8
19.09.2019	Fjord	50	30.77395709	4.5	681963.2145	1.9	14487148.1	4.4	278958.6967	4	288708.7398	1.3	-0.020269213	17.3
02.10.2019	Stream	55	2.516108965	3.5	767.1502263	3.8	5495.274718	1.3	97.45861615	0.9	2576.590367	1.9	2.171980609	8.4
02.10.2019	LStream	56	2.440460918	6.8	923.9246278	1.8	5601.402235	2.6	120.5686127	1.7	2951.5092	2.8	1.783360231	7.3
02.10.2019	EC.Alu.C.1V0m	57	1.95278421	13.6	185675.3639	4	28314.20227	2.1	6501.089548	2.4	156161.9081	2.9	0.008630137	43.4
02.10.2019	EC.Alu.C.1V20m	58	2.554277784	6.8	187017.5739	1.5	27826.86869	1.3	6344.335447	2.4	152517.4719	0.9	0.294103538	113.7
02.10.2019	EC.Alu.C.1V40m	59	2.274923495	5.9	188410.6484	1.9	29966.57404	3.8	6727.336775	7.2	153205.9817	2.3	0.014178682	29.3
02.10.2019	EC.Alu.C.1V60m	60	1.991873925	3.1	183919.5364	3.1	29187.2307	1.6	6621.938455	3.1	158843.4811	2	0.761556975	87.7
02.10.2019	EC.Alu.C.1V80m	61	1.538494838	1.9	179587.6188	1.7	28497.21075	1.6	6109.22431	6	150886.0094	2.9	-0.005292095	9.4
02.10.2019	EC.Alu.C.1.5V0m	62	2.103833211	6.1	196497.4935	3	31163.3007	0.7	6780.709134	0.8	164644.881	3.5	0.056126269	27.8
02.10.2019	EC.Alu.C.1.5V20m	63	2.502569542	1.7	195588.532	1.4	30360.3391	0.7	6840.668085	1	162222.6787	2.5	0.000184199	71.4
02.10.2019	EC.Alu.C.1.5V40m	64	2.095605823	1.2	192217.761	3	30649.1399	2	6699.487521	4.5	162550.3526	2.2	0.017081013	10.9
02.10.2019	EC.Alu.C.1.5V60m	65	2.588105459	4.4	193488.2918	1.7	29952.74686	2.5	6724.585606	5.2	162925.1804	1	0.240223327	122.5
02.10.2019	EC.Alu.C.1.5V80m	66	2.211145494	6.6	183653.4083	3.5	29127.4632	2	6369.643984	3.3	155417.7918	1.9	0.021101215	46.4
02.10.2019	EC.Alu.NC.1.V0m	67	1.208181919	6.3	114112.8916	1	22795.00282	1.7	4286.757305	4	90424.99352	1.3	0.014244849	35.2
02.10.2019	EC.Alu.NC.1.5V20m	68	1.804527491	3.4	114786.953	1.4	22957.70221	1.8	4401.593181	2.6	91280.29457	3.2	0.039479679	55.4
02.10.2019	EC.Alu.NC.1.5V40m	69	1.584294081	9.1	114922.4287	1.9	22604.80774	3.7	4550.877147	1.8	89465.58875	1.7	0.292168193	115.9
02.10.2019	EC.Alu.NC1.5V60m	70	2.361922047	5.7	115620.0121	1.4	23390.82938	3.6	4311.973576	0.6	87588.23096	1	0.047841922	75.2
02.10.2019	EC.Alu.NC.1.5V80m	71	1.659535039	3.1	110944.081	2.6	22576.72203	1	4365.386183	2.7	88486.98222	2.6	0.011586796	18.3
11.10.2018	Fjord	72	3.790547065	7	40988.89542	0.4	22324.24412	1.7	2851.887084	1.3	45007.21192	0.7	0.462078963	12.5
11.10.2018	Stream	77	3.357956338	2.7	1346.931873	1.8	9392.028191	0.8	171.7905799	4.6	4337.297489	1.2	0.51019695	18.1

			V51(MR)		Cr53(MR)		Mn55(MR)		Fe56(MR)		Co59(MR)		Ni60(MR)	
			Conc.		Conc.		Conc.		Conc.		Conc.		Conc.	
Date	Sample name	Number	µg/L	RSD, %	µg/L	RSD, %	µg/L	RSD, %	µg/L	RSD, %	µg/L	RSD, %	µg/L	RSD, %
12.09.2019	GNR	36	0.075701229	7.9	6.40297133	2.7	520.7152377	1.6	27011.30463	6.4	68.98885622	1	31.41558437	1.7
	GR	36	0.0638283	22.1	6.216153183	1.2	525.8286874	2.2	29131.21191	3.5	69.81417452	4.6	33.21630141	5.3
	GR	37	0.063448159	2.2	6.330143228	2.4	623.4354934	1.3	27866.83979	1.3	74.91493142	4.1	33.8794323	4.2
12.09.2019	Stream	43	0.067917905	9	0.193082157	4.8	0.507213805	7.1	9.695339659	0.2	0.031086793	31	0.480700872	10.9
12.09.2019	LStream	44	0.11404086	10.8	0.2071029	3.6	0.439487386	9.3	13.36576091	1.9	0.05228656	14.3	0.777532937	5.3
19.09.2019	Stream	48	0.130160775	22	0.418017196	6.5	1.21716178	4.8	77.15700014	2.8	0.073255319	18.9	0.651534535	4.8
19.09.2019	LStream	49	0.156013994	12.6	0.389242582	3	1.304714042	4	85.73532038	1.5	0.087885126	8.3	0.6925968	8.9
19.09.2019	Fjord	50	0.87294688	3.2	1.58392127	18	17.0699831	1.3	37.24819844	1.6	2.061996926	11.6	2.631468828	16.8
02.10.2019	Stream	55	0.143195053	6.3	0.408793834	14.1	1.360174532	3.1	118.8705988	2.3	0.077025692	13	0.646551003	13.7
02.10.2019	LStream	56	0.168693422	7.5	0.470102856	9.5	1.371170986	6.8	104.9904006	0.6	0.080046415	15.4	0.752454361	11.1
02.10.2019	EC.Alu.C.1V0m	57	0.016712285	28.2	0.056291684	2.3	348.3306193	2.2	5935.974245	1.9	59.8856474	2.6	25.18415824	2.8
02.10.2019	EC.Alu.C.1V20m	58	0.022130481	10.5	0.295113195	2.1	346.8798047	0.5	5595.21003	2	58.94174787	1.4	27.88868857	1.8
02.10.2019	EC.Alu.C.1V40m	59	0.020469858	34.1	0.648614307	3.8	348.6735206	1.2	5073.819894	2	59.44089053	2.4	32.426591	2
02.10.2019	EC.Alu.C.1V60m	60	0.022982165	12.8	1.040772596	5.7	350.0507045	1.6	4623.429307	2.6	58.49781384	1	33.95362391	0.9
02.10.2019	EC.Alu.C.1V80m	61	0.013389697	16.7	1.486155122	11.3	328.316258	1.2	3788.695554	4.7	55.10374684	2	34.961246	0.3
02.10.2019	EC.Alu.C.1.5V0m	62	0.015073192	11.5	0.029637495	12.9	371.0291514	1.7	6111.84127	2.9	63.19034154	1.2	26.24355438	1.3
02.10.2019	EC.Alu.C.1.5V20m	63	0.019263563	25	0.428705766	2.8	367.4504725	2	5538.281279	1.1	61.67425737	1.3	29.20172242	2.5
02.10.2019	EC.Alu.C.1.5V40m	64	0.016757653	21.9	0.928438946	7.9	350.9942881	0.9	5020.523782	0.3	59.22557914	0.7	29.55520649	0.6
02.10.2019	EC.Alu.C.1.5V60m	65	0.018020985	28.8	1.624502886	5.6	350.8200677	1.6	4453.248621	1.5	58.28190081	1.4	29.04676605	1.6
02.10.2019	EC.Alu.C.1.5V80m	66	0.024739649	34.3	2.081752147	4.8	335.4458269	0.9	3652.117768	0.9	55.0309512	0.6	27.31250573	2.5
02.10.2019	EC.Alu.NC.1.V0m	67	0.02140259	33.3	0.128633249	12.4	193.4389809	0.7	2721.590534	1.1	29.51449889	1.7	15.34286994	5
02.10.2019	EC.Alu.NC.1.5V20m	68	0.026864283	5.1	0.662856341	3.4	188.8565204	1.5	2606.509795	2.7	28.73071314	1.8	23.138035	1.2
02.10.2019	EC.Alu.NC.1.5V40m	69	0.034014651	16.7	1.093270866	5.6	195.8672389	1	2435.561038	1.8	29.27314712	1.7	24.66466247	2.1
02.10.2019	EC.Alu.NC1.5V60m	70	0.040757346	23.1	1.430334293	6.8	191.4884748	1.2	2269.402763	0.2	28.60964368	3.2	24.8515475	2.3
02.10.2019	EC.Alu.NC.1.5V80m	71	0.026067303	36.1	1.720045261	10.9	190.0039579	1	2066.553357	0.8	28.41325753	2.7	24.81496019	0.6
11.10.2018	Fjord	72	0.103785206	11.7	0.331110238	13	26.96597134	1.1	482.7049549	0.8	3.351978182	1.6	5.194920539	3.2
11.10.2018	Stream	77	0.107334547	11.6	0.208584966	10	0.522499	12.2	33.56010281	4.7	0.07343645	10.2	0.638645012	4.1

			Cu63(MR)		Zn66(MR)		Rb85(MR)		Sr88(MR)		Ba137(MR)		As75(HR)	
			Conc.		Conc.		Conc.		Conc.		Conc.		Conc.	
Date	Sample name	Number	µg/L	RSD, %	µg/L	RSD, %	µg/L	RSD, %	µg/L	RSD, %	µg/L	RSD, %	µg/L	RSD, %
12.09.2019	GNR	36	17370.5041	5.3	9157.377969	4.5	7.550387437	0.5	455.3431661	1.3	14.04609248	2	10.32414576	3.9
	GR	36	18074.2438	2.2	9496.824462	0.5	7.853662825	1	469.8215287	0.4	13.65661686	2.9	10.27162186	7.2
	GR	37	18602.25582	0.6	9681.467173	2.8	7.727661669	0.8	462.2161991	1.5	24.21609471	1.5	9.757882121	8.2
12.09.2019	Stream	43	2.620390867	2.9	2.317916034	9.2	0.414123746	1.7	11.20325448	1.6	3.803586531	3.3	0.047096779	48.2
12.09.2019	LStream	44	4.342358358	4.3	5.501334892	3.1	0.591299473	2.6	17.05225989	0.7	4.569045478	9.4	0.190048748	13.7
19.09.2019	Stream	48	3.762635428	3.3	6.639358407	8.6	0.294354049	2.1	6.606995957	2	2.415497137	5.8	0.079486553	8.3
19.09.2019	LStream	49	5.115144306	4.9	7.169751798	2.9	0.282445526	4.1	6.381713622	2.1	2.502175428	9.3	0.076871735	10.1
19.09.2019	Fjord	50	140.9940374	1.8	510.2613561	5.5	74.02891919	3.3	5351.055412	2.2	7.812871929	13.3	1.445677729	28.7
02.10.2019	Stream	55	4.430276189	2.2	8.787613595	8.6	0.236244869	17.6	5.656921035	4	2.322374348	5.1	0.102637647	48.3
02.10.2019	LStream	56	5.002690881	4.6	8.635322275	2	0.308532996	7.5	6.488866595	1	2.352496665	6.9	0.074016574	30.8
02.10.2019	EC.Alu.C.1V0m	57	9803.193998	0.1	7137.472172	0.1	6.395297092	1	428.0447654	1.6	14.14820768	2.4	0.694928524	11.1
02.10.2019	EC.Alu.C.1V20m	58	9143.456567	1.6	6917.24726	1.2	5.975898417	3.5	410.1709809	2.3	13.91495457	1.7	0.644373078	1.7
02.10.2019	EC.Alu.C.1V40m	59	8715.765177	1.9	6875.062538	1.8	6.35929727	3.6	424.0162128	0.8	14.37791323	2.8	0.455708065	18.1
02.10.2019	EC.Alu.C.1V60m	60	8147.512912	2.4	6529.810765	0.6	6.479664429	0.9	436.4945593	0.9	14.0115691	4.4	0.279397651	15.7
02.10.2019	EC.Alu.C.1V80m	61	6925.565718	1.5	5899.514553	0.7	6.205971851	4.2	416.0590952	1.9	13.21246844	6.6	0.230651454	14.6
02.10.2019	EC.Alu.C.1.5V0m	62	10168.07957	2	7499.14941	1.6	6.728884961	1.8	440.6715062	2.6	14.57758654	3.4	0.728125057	11.1
02.10.2019	EC.Alu.C.1.5V20m	63	9457.039962	2.9	7229.241438	1.4	6.529120774	0.9	434.7002034	2.1	14.74422122	3.9	0.557392045	15.1
02.10.2019	EC.Alu.C.1.5V40m	64	8649.816616	1.6	6799.07259	0.3	6.546224073	1.5	433.7148924	0.4	14.64099532	2.5	0.42741062	12.7
02.10.2019	EC.Alu.C.1.5V60m	65	7925.865351	2.3	6441.595912	0.8	6.61875798	1.9	441.7074287	1.1	14.37448674	0.6	0.294897608	2.1
02.10.2019	EC.Alu.C.1.5V80m	66	6842.052815	1.5	5891.857107	1	6.245218411	3.1	409.4855513	1.1	13.83171234	3	0.221954775	21.5
02.10.2019	EC.Alu.NC.1.V0m	67	5113.381753	1	5171.24125	0.1	4.716613215	0.6	278.5101197	1.1	14.86098486	4.6	0.487372434	8.5
02.10.2019	EC.Alu.NC.1.5V20m	68	4466.266433	1	5094.6068	1.8	4.599471569	3.8	275.3314286	1.4	14.15809067	3.1	0.395403519	14.9
02.10.2019	EC.Alu.NC.1.5V40m	69	3956.957208	2.5	5161.228289	1.3	4.672655302	1.5	283.5888632	2	14.53434157	6.5	0.241668166	6.6
02.10.2019	EC.Alu.NC1.5V60m	70	3419.489467	1	4985.9266	0.4	4.580515182	1.9	285.9864472	1.5	14.63102491	2	0.207922758	10.1
02.10.2019	EC.Alu.NC.1.5V80m	71	3106.801667	0.5	4820.139044	0.8	4.443970542	2.9	279.9186179	2.3	13.76529408	1.4	0.149931431	24.1
11.10.2018	Fjord	72	183.7466837	0.8	871.8457446	1.4	3.51436757	3.9	168.291143	1.1	6.589730581	5.5	0.481872928	7
11.10.2018	Stream	77	3.335084935	7.3	8.0672781	6.3	0.427731229	6.6	8.751654736	3.1	3.36093045	6.6	0.078331408	19.1

Date	Sample name	Number	Br81(HR) Conc. µg/L	RSD, %
12.09.2019	GNR	36	65.08636785	5.3
	GR	36	60.0738985	12
	GR	37	57.88603526	9
12.09.2019	Stream	43	43.31002625	8.6
12.09.2019	LStream	44	48.64619756	3.6
19.09.2019	Stream	48	35.60208572	15.2
19.09.2019	LStream	49	35.87611788	15.7
19.09.2019	Fjord	50	52169.15571	2.6
02.10.2019	Stream	55	34.90669216	10.3
02.10.2019	LStream	56	34.56234512	4.4
02.10.2019	EC.Alu.C.1V0m	57	43.95187436	3.5
02.10.2019	EC.Alu.C.1V20m	58	43.36669488	5.2
02.10.2019	EC.Alu.C.1V40m	59	40.81481213	7.8
02.10.2019	EC.Alu.C.1V60m	60	39.90481515	13.4
02.10.2019	EC.Alu.C.1V80m	61	37.92986335	8.3
02.10.2019	EC.Alu.C.1.5V0m	62	46.02727753	8
02.10.2019	EC.Alu.C.1.5V20m	63	38.73380452	4.4
02.10.2019	EC.Alu.C.1.5V40m	64	43.14118619	15.4
02.10.2019	EC.Alu.C.1.5V60m	65	40.0268612	5.9
02.10.2019	EC.Alu.C.1.5V80m	66	41.81186411	5.3
02.10.2019	EC.Alu.NC.1.V0m	67	39.02010992	12.4
02.10.2019	EC.Alu.NC.1.5V20m	68	37.68895495	9
02.10.2019	EC.Alu.NC.1.5V40m	69	32.70206437	13.8
02.10.2019	EC.Alu.NC1.5V60m	70	34.31042925	11
02.10.2019	EC.Alu.NC.1.5V80m	71	28.18806162	8.3
11.10.2018	Fjord	72	39.60706447	5.6
11.10.2018	Stream	77	33.62933021	16.7

			7 -> 7 Li [H2]		23 -> 23 Na [O2]	
Date	Sample name	Numbers	Conc. [ug/l]	Conc. RSD	Conc. [ug/l]	Conc. RSD
18.10.2019	Stream	82	0.002242855	N/A	5524.933408	1.784310648
18.10.2019	Lstream	83	0.081349731	80.69878884	5690.4185	1.943490957
12.11.2019	Stream	90	0.057036531	255.2262916	5751.304925	1.532165735
18.12.2019	GNR/AC0L	95	14.24194824	10.98165055	100793.8441	0.94204452
18.12.2019	GR	96	11.75411743	12.88891554	97621.39811	1.554227024
18.12.2019	GR	97	11.02434577	21.55855893	98060.40346	1.301624566
18.12.2019	AC3L	98	20.08412623	23.21568681	99540.9993	3.269033002
18.12.2019	AC6L	100	16.66200601	17.6750289	99623.89894	1.980363238
18.12.2019	AC12L	103	19.57436642	35.27959409	106709.9185	1.010681721
15.01.2020	ECAluBlank0V0min	104	0.086082765	316.0837806	4975.708904	2.635817825
15.01.2020	ECAluBlank0V20min	105	0.082908741	213.3510722	4996.109912	2.651261256
15.01.2020	ECAluBlank0V40min	106	0.112320704	144.8242371	4938.340727	1.012333062
15.01.2020	ECAluBlank0V60min	107	-0.025244661	N/A	5127.475362	0.484830448
15.01.2020	ECAluBlank0V80min	108	0.002121284	N/A	5082.759905	1.596275413
15.01.2020	ECAluBlank1.5V0min	109	0.028472084	2952.119173	4973.24806	2.236573985
15.01.2020	ECAluBlank1.5V20min	110	0.084729728	321.109177	4955.119124	3.445088487
15.01.2020	ECAluBlank1.5V40min	111	0.058350581	440.0093377	5054.380213	2.1505948
15.01.2020	ECAluBlank1.5V60min	112	-0.025423622	N/A	5067.630089	1.211287415
15.01.2020	ECAluBlank1.5V80min	113	-0.025459414	N/A	5175.161885	2.808839569
22.01.2020	ECAluPencilNotCleansed1.5V0min	114	7.723554905	11.82884798	65887.93495	2.585406317
22.01.2020	ECAluPencilNotCleansed1.5V20min	115	7.417660153	12.39557183	66615.56475	1.758283353
22.01.2020	ECAluPencilNotCleansed1.5V40min	116	4.734377776	10.6583869	67229.68122	1.400639457
22.01.2020	ECAluPencilNotCleansed1.5V60min	117	7.121633268	5.879875073	67162.31954	1.406557589
22.01.2020	ECAluPencilNotCleansed1.5V80min	118	6.541693347	10.13177534	66848.54815	0.726209091
31.01.2020	ECAluCylGraphNotcleansed1.5V0min	119	8.08149861	16.97146481	62559.148	1.318221805
31.01.2020	ECAluCylGraphNotcleansed1.5V20min	120	7.734771848	17.54455836	61992.631	0.933923497
31.01.2020	ECAluCylGraphNotcleansed1.5V40min	121	5.308289574	36.42265559	61928.42715	1.767020991
31.01.2020	ECAluCylGraphNotcleansed1.5V60min	122	6.436251951	16.9193177	62562.41562	0.598214328
31.01.2020	ECAluCylGraphNotcleansed1.5V80min	123	6.953440417	20.75270644	63430.9394	1.207459129
31.01.2020	ECAluCFlatGraphNotcleansed1.5V0min	124	5.347756198	38.52754066	61985.48255	1.105880156
31.01.2020	ECAluCFlatGraphNotcleansed1.5V20min	125	7.985586892	58.65023464	61527.06834	2.075788436
31.01.2020	ECAluCFlatGraphNotcleansed1.5V40min	126	7.447093962	18.7067374	62431.04104	0.701613352
31.01.2020	ECAluCFlatGraphNotcleansed1.5V60min	127	6.585582462	40.13081729	62484.09272	2.625785565
31.01.2020	ECAluCFlatGraphNotcleansed1.5V80min	128	6.556695076	38.82397236	62656.33019	0.795569977
31.01.2020	ECGraphNotcleansed1.5V0min	129	6.393339971	49.5785448	62371.62267	1.167178011
31.01.2020	ECGraphNotcleansed1.5V20min	130	8.25732574	22.04026049	62863.07706	3.058910474
31.01.2020	ECGraphNotcleansed1.5V40min	131	9.584457273	11.48485143	61598.34065	2.550655989
31.01.2020	ECGraphNotcleansed1.5V60min	132	8.219330819	47.68061918	61664.70992	1.660509285
31.01.2020	ECGraphNotcleansed1.5V80min	133	7.778779603	19.77612493	63528.32337	2.264120644
04.02.2020	ECAluCylGraphNCleansed1.5V0min	134	8.411458904	14.77414483	60140.38374	3.578623285
04.02.2020	ECAluCylGraphCleansed1.5V20min	135	8.181487874	6.880673361	60056.83366	2.383464235
04.02.2020	ECAluCylGraphCleansed1.5V40min	136	7.133645643	16.61765858	61284.45548	1.810476297
04.02.2020	ECAluCylGraphCleansed1.5V60min	137	6.680613129	35.8632923	59382.32832	1.207622303
04.02.2020	ECAluCylGraphCleansed1.5V80min	138	7.341186901	13.46802414	59944.42082	2.891358743
04.02.2020	ECAluCFlatGraphCleansed1.5V0min	139	6.615488053	31.11225847	59989.04686	1.045877396
04.02.2020	ECAluCFlatGraphCleansed1.5V20min	140	6.52077377	15.30764249	60186.30885	0.836705098
04.02.2020	ECAluCFlatGraphCleansed1.5V40min	141	5.495957427	19.51725881	59928.57595	0.467473623
04.02.2020	ECAluCFlatGraphCleansed1.5V60min	142	6.975689057	27.48098333	60536.53045	0.686271212
04.02.2020	ECAluCFlatGraphCleansed1.5V80min	143	6.583799785	58.1602688	60390.84872	3.173272865
04.02.2020	ECGraphCleansed1.5V0min	144	6.555246062	8.055779021	61466.83016	1.401340398
04.02.2020	ECGraphCleansed1.5V20min	145	6.329324398	19.85893012	60021.17253	1.867208128
04.02.2020	ECGraphCleansed1.5V40min	146	7.831796136	13.47567622	61155.6596	0.396422123
04.02.2020	ECGraphCleansed1.5V60min	147	6.480324026	10.11899283	60179.27605	0.206198534
04.02.2020	ECGraphCleansed1.5V80min	148	6.411096588	43.41418964	60694.02604	1.744640836
04.02.2020	Blank	152	-0.025745751	N/A	1.878912711	12.30318073
04.02.2020	Blank	153	0	N/A	1.42474188	7.436575561
04.02.2020	Blank	154	0	1201.790588	8.238872879	2.138376738
04.02.2020	Blank	155	0	N/A	30.9625575	0.855558631
04.02.2020	Blank	156	0	145.9366614	2.236102144	5.586185184

	24 -> 24 Mg [H2]		24 -> 24 Mg [O2]		27 -> 27 Al [H2]		29 -> 45 Si [O2]	
Numbers	Conc. [ug/l]	Conc. RSD	Conc. [ug/l]	Conc. RSD	Conc. [ug/l]	Conc. RSD	Conc. [ug/l]	Conc. RSD
82	1261.273993	2.480542014	1299.997355	0.870703271	48.05556832	0.913426893	1787.588687	7.980137951
83	1182.501925	1.194728142	1201.199442	2.522846864	68.49167467	1.145473346	1741.011785	6.713678258
90	1231.029743	2.204258946	1272.750576	1.94267106	61.52979885	1.368726279	1747.356529	7.600782208
95	14804.13061	1.895147571	14843.79576	0.967271325	2508.497638	2.299059691	10707.85522	8.278961213
96	14111.28656	1.265138867	14259.11929	1.605241941	2177.429057	2.340944158	10346.70268	8.875762501
97	13709.26712	1.980828842	14374.38889	1.655261177	2195.10481	0.496318247	10179.10999	9.34455005
98	15359.20971	1.317656816	14787.74329	3.232260587	6.023111795	7.159279437	8477.226432	9.291706466
100	14771.70213	3.731927614	14966.58752	1.612111428	11.91197635	8.557766939	9358.634371	7.208234862
103	15980.99001	1.539786741	15649.60363	1.12651227	38.96942821	2.296580441	10996.24129	6.991248754
104	5.420134447	1.206850867	6.003664006	0.459988268	-0.027660397	6.624416491	0.410561621	N/A
105	8.672571713	2.504880151	9.21943883	2.643571194	0.516865892	3.562423278	0.974031816	285.6683275
106	9.746515361	0.853781263	10.28638873	4.041208071	0.805369669	2.28015329	3.592127863	23.5896588
107	10.5057593	0.485200619	11.37451454	2.280624321	0.557260532	1.806080804	2.45605368	42.80586322
108	10.81857618	1.898906232	11.83085821	1.08312234	0.683228342	5.292812432	1.164098364	69.93632119
109	11.20383825	0.68075247	12.32225262	1.945802999	0.026788743	9.725235894	-0.631775377	N/A
110	14.92563178	2.286812736	16.42840119	4.511076918	9.134116846	3.935275887	0.344293416	N/A
111	16.15360201	1.722437562	18.07634965	1.808797481	12.42116103	1.520711582	1.174345587	140.9916107
112	17.10759171	2.551278744	18.77578461	1.598264007	11.49824668	1.967195234	1.304282441	179.8011247
113	17.95841734	2.015095784	20.1504597	2.447839159	10.74442011	1.281664057	1.833466743	56.04319626
114	8343.949835	0.952477205	8253.489671	2.252562418	1927.19756	0.724838214	7828.058808	8.253222116
115	8372.23906	1.352109652	8507.253715	2.060774337	2061.547268	0.427552224	7874.854724	8.223439696
116	8384.86971	0.692332144	8522.742499	4.425573348	2438.691383	3.26243357	7916.426413	7.945599157
117	8543.836267	2.76232286	8400.365197	1.406541299	3060.254679	4.03831633	7834.465763	8.628166779
118	8650.43303	2.158244866	8416.748375	1.574559937	3531.675906	1.962232479	7864.988018	7.643099503
119	10412.07058	1.238512913	10362.82299	3.642397525	2181.558003	0.208426342	8598.190242	7.484431684
120	10079.69231	1.917094746	10446.96208	1.689781633	2252.1567	1.383028406	8435.080837	6.000084222
121	10352.26128	2.521077095	10250.65519	3.286767302	2495.407595	4.07677853	8581.720219	7.785655582
122	10636.68842	2.843910942	10409.43756	2.938107382	2820.787222	1.853869643	8874.453101	8.3142032
123	10522.70826	1.851035459	10681.65493	2.33653327	3000.978325	1.561928717	8736.861196	10.41488379
124	10169.06753	1.390515645	10513.54946	1.329985197	2283.786388	0.697351871	8574.480355	8.598626373
125	10415.24333	2.517821005	10354.51368	0.501080903	2356.513825	0.732024575	8700.05464	8.997236065
126	10079.22437	0.794709717	10332.97011	1.564445581	2453.907405	2.118437664	8778.020103	8.558741291
127	10501.12732	0.647242323	10414.17438	1.889065073	2774.129455	0.650010606	8798.631909	7.590281595
128	10261.99994	1.360602039	10590.74789	2.135096534	3082.933283	0.410987633	8577.177003	8.954137402
129	10454.64606	3.049340172	10353.66098	2.332519376	2334.7087	0.914635636	8777.782866	9.21576351
130	10256.38433	0.745371394	10348.55501	3.815995609	2354.647383	1.378457828	8757.722784	8.101347108
131	10568.26118	1.045485722	10337.17375	2.626435483	2362.953627	0.915666001	8650.72186	9.546253751
132	9967.078716	4.552326389	10333.51374	2.404084693	2298.771504	0.699419716	8753.305523	8.827564002
133	10400.72515	0.680041497	10397.44885	1.983655049	2344.249641	1.453144883	8821.540543	9.031355868
134	8369.198817	2.569694629	8743.088858	4.137708034	680.0895434	0.335830976	7572.868173	9.029786922
135	8849.528282	2.050343968	8534.180781	1.519039525	658.3533056	1.131079286	7568.384869	9.564467693
136	8527.53724	2.256359181	8839.711837	2.570599267	645.5183834	1.088561481	7629.936273	8.655832141
137	8644.36141	1.058224932	8576.196561	1.690491272	663.2549186	0.979983653	7476.62172	7.941043446
138	8554.123542	5.255839483	8680.43352	2.493376446	708.6859253	0.420304236	7702.460637	9.81283821
139	8600.177269	1.756549413	8529.519868	2.525596409	645.8851283	0.496596465	7602.18537	8.07948139
140	8423.307107	3.332987991	8556.261819	0.34050245	597.7031733	1.423272306	7639.011752	8.715099152
141	8373.923572	1.806465615	8716.184323	1.74729567	565.2948636	0.837069355	7671.718895	9.249785486
142	8816.37533	1.792615486	8674.284485	1.528638643	587.4666279	1.638588238	7637.678395	8.915111071
143	8615.95883	1.890252199	8796.627251	3.506831666	581.4710911	2.170823246	7554.308709	6.429943376
144	8765.38139	3.580012036	8544.277074	0.559938807	628.8831062	1.006449868	7680.939087	6.45468177
145	8543.771228	5.85761332	8733.034873	2.285224957	569.9140902	3.060751107	7653.79142	8.872526478
146	8716.285061	1.241741131	8862.065646	0.730812833	541.0027542	1.03233535	7709.00115	7.428957717
147	8568.099327	1.663227553	8769.504999	0.746144242	510.4296945	1.258634024	7766.322681	10.24436087
148	8718.759266	2.473127694	8861.660055	1.367956577	512.0447663	1.197218057	7669.631707	8.562670815
152	0.266793593	22.28185164	0.270042523	2.851245351	0.131228192	23.25565154	-0.333928564	N/A
153	0.667368002	1.793902666	0.672488562	2.830624409	1.004838164	3.329265041	0	26.89787856
154	0.739020884	21.9193059	0.718056628	11.56633389	0.304303561	15.66929125	0	N/A
155	1.566757346	2.047012003	1.630416179	2.011527854	0.462943486	12.71234695	0	N/A
156	0.204071689	8.215289179	0.230683311	5.234910009	0.414551378	2.372605207	0	N/A

	31 -> 47 P [O2]		32 -> 48 S [O2]		35 -> 51 Cl [O2]		39 -> 39 K [H2]	
Numbers	Conc. [ug/l]	Conc. RSD	Conc. [ug/l]	Conc. RSD	Conc. [ug/l]	Conc. RSD	Conc. [ug/l]	Conc. RSD
82	1.165644595	5.15278819	1572.226545	0.251775106	7243.163116	4.496688467	201.4269667	4.356715859
83	1.302056809	4.505203096	1680.147415	2.819447571	7328.575044	1.640313601	226.7207537	1.714760884
90	1.119534743	5.298880967	1541.685005	2.733718354	7403.51292	3.564400385	198.17472	3.561261265
95	2.538845985	16.6141313	192935.5695	1.06725083	52235.34798	3.08273144	5866.577215	1.697754521
96	2.291728637	22.08449169	187874.5692	0.300139112	51570.131	1.088495604	5825.298059	2.601327615
97	2.596714147	36.64828492	189424.314	0.763042947	50710.48805	3.291877302	5747.260824	0.311322413
98	2.080309471	13.54125656	170733.9399	1.90596246	45476.95329	3.210429583	6108.259899	2.228422525
100	2.406660308	46.71494493	176837.6438	1.160595815	48082.05167	4.570868272	5999.597906	0.197796023
103	2.955618546	14.85867159	194384.0018	1.796738795	45684.01271	3.900961148	6108.744409	1.504732878
104	1.051823158	14.03780759	3200.673032	1.651931165	16.59056381	N/A	12.7775361	1.669781084
105	3.511815097	2.587230959	3325.512787	2.105510779	-45.21673872	N/A	19.76627241	2.008772561
106	3.225974938	7.355703629	3264.079931	3.091668803	-17.83763156	N/A	20.64794097	0.776977693
107	3.441062477	11.38372113	3363.936032	0.474602521	-99.59443477	N/A	21.68120116	1.558112762
108	2.955417604	5.770234075	3360.72692	0.340751824	-67.3183181	N/A	23.7562121	1.124439712
109	0.545037846	11.35689754	3206.988476	1.227009293	-137.9277323	N/A	13.43370496	1.107321533
110	0.409831594	14.11355016	3208.948919	1.686003727	33.61330892	1468.393332	16.9600249	1.117632815
111	0.529904763	10.14420687	3304.805387	0.542660987	-95.41296882	N/A	17.57994311	1.482701219
112	0.215194831	8.088286365	3321.934379	1.523141756	-130.7633954	N/A	18.46285102	0.935152173
113	0.312511081	10.31176185	3443.977163	2.783259167	-32.98001286	N/A	18.56895729	0.322075367
114	2.584901926	40.2242877	105611.128	1.953951985	93254.17928	4.640944278	5216.73025	2.20759564
115	3.23606686	20.19497757	107131.5706	1.347134209	95092.82669	3.374600194	5186.389293	2.226239821
116	2.384178146	27.23809515	105661.2766	1.108081538	92235.68189	3.838695419	5301.132977	1.529879091
117	1.962195814	28.4865908	106640.5128	0.741430699	92236.51463	1.744852703	5280.275765	0.28227224
118	1.615116555	11.10798762	106003.2398	1.321925447	95328.21311	3.088161474	5310.309012	2.728542644
119	2.887325683	37.25202899	138494.2695	0.875355852	78631.55789	2.341111995	6156.673086	1.678017221
120	2.404194641	14.23363047	136234.7994	0.543554569	75864.02461	0.627936116	6115.952805	1.143602945
121	1.271858398	35.41942427	136779.3733	2.613585747	79598.89054	0.972284202	6113.997658	1.02199252
122	2.303825092	7.91480064	137764.4626	0.412116406	81709.06908	0.626327253	6470.158963	1.461383799
123	2.218511312	30.85142429	134525.9966	3.903566649	77265.46099	5.145611327	6258.358372	1.621712184
124	2.543629472	35.94060862	135433.5477	0.985277389	81052.71858	1.370959117	8625.077723	0.899888862
125	1.984633886	20.38724618	136887.2755	1.718425761	79861.46863	3.109957772	9567.698814	1.044756798
126	2.424820781	8.191669571	137186.2838	1.341586084	78875.38457	1.376812254	9265.067993	3.295162822
127	1.630450321	19.85843117	136969.4277	1.570635236	80959.82233	2.109481947	9400.663511	2.585762417
128	1.246500843	32.98319916	135946.7386	0.76711908	80179.51086	0.08553504	9707.009448	0.981649777
129	1.345335014	37.86683964	138957.2732	1.175471759	78460.01913	4.467511321	6148.506674	1.148450968
130	0.832857914	4.71164074	135045.5197	1.695615413	74275.46133	1.626124379	6396.100176	1.885664605
131	0.885040704	37.6980886	134810.3135	1.666234717	75623.78701	6.50087414	6441.847607	3.156299592
132	1.056270194	24.0342968	135911.3345	0.458633483	77792.02861	1.872086484	6084.778454	3.218385812
133	1.048109293	39.1845765	134964.6198	2.493950702	76789.13084	1.718393129	6353.415262	1.163863055
134	0.382291741	17.56173374	105285.6459	1.266889357	71638.66444	4.205793326	5128.107188	3.203770945
135	1.674570374	31.85632774	106838.0161	1.709168935	72868.15713	2.455023804	5503.462945	1.007346079
136	1.072641393	53.45994203	107752.529	0.308106537	72248.71307	1.883821085	5491.302685	1.153223453
137	0.266726119	51.62708568	105784.9018	2.063467187	71869.05314	3.32505663	5387.145457	1.922700439
138	1.31237354	18.11894675	107695.8853	1.724640053	76276.48227	1.352740739	5450.240745	1.584084493
139	0.904739249	62.66058481	105845.9749	0.789904347	72619.69158	1.538960621	5357.080838	1.452615839
140	0.184109636	50.61209821	107243.723	0.879977788	73693.53634	4.560188254	5395.86643	1.878064436
141	2.102850602	33.29924452	108396.7222	1.98465155	76752.02232	2.174577984	5294.28022	3.094262404
142	0.983428383	29.71745566	109596.0513	1.89046121	72772.12549	2.109729935	5535.15632	1.916274278
143	1.117248277	44.28413877	106794.514	1.176022679	73960.07545	1.759230681	5402.931112	1.57150578
144	1.3874521	67.50191362	106074.8948	0.920096657	74596.80102	4.632660745	5612.301858	1.569280049
145	1.29853967	36.61939707	107363.1507	0.875037974	73023.98918	3.833620418	5458.69179	1.842182938
146	0.183121029	5.340454731	107189.5994	1.407901131	75711.36975	6.371538777	5397.855944	1.33855833
147	0.830954193	31.37014698	105952.6973	0.711272518	73874.28158	3.789877053	5370.321221	0.743438212
148	0.487866771	66.00747243	107072.3004	0.801069013	73494.8859	1.005376396	5693.859443	2.58616998
152	0.634128406	22.86432943	4.402032403	20.80907114	0	484.0008962	2.311142936	4.270654606
153	0.940398868	19.74252455	3.217113137	23.07303024	0	N/A	2.738987925	2.852681017
154	1.72797457	8.931212386	4.421998342	6.552826393	0	N/A	11.69594792	1.719840762
155	1.275145425	16.60771365	2.815534136	8.166087416	0	N/A	6.747420781	2.769103645
156	1.074476809	6.905302204	1.583884852	12.56994414	0	N/A	5.733203983	2.78687611

	39 -> 39 K [O2]		40 -> 40 Ca [H2]		44 -> 60 Ca [O2]		47 -> 63 Ti [O2]	
Numbers	Conc. [ug/l]	Conc. RSD	Conc. [ug/l]	Conc. RSD	Conc. [ug/l]	Conc. RSD	Conc. [ug/l]	Conc. RSD
82	204.9793933	2.009827665	6014.27005	0.988214817	5408.353686	6.418814873	0.227264038	6.744767885
83	240.3975115	1.136433469	6171.155868	1.298246942	5655.367813	4.950278636	0.33679176	2.214035715
90	209.1889555	0.941676518	5638.466961	3.425013571	4999.174753	5.501546634	0.296035002	4.254712287
95	6566.398779	0.844863559	143215.6153	0.812565942	154534.0366	5.987530058	0.074072268	23.42720156
96	6385.305851	1.328979894	139930.5816	1.634916527	144776.2005	7.287012149	0.083078645	42.43652218
97	6580.512922	1.292394478	136425.8184	1.023704989	147579.9466	6.822905107	0.083835713	39.72062508
98	6545.284601	1.929899603	145222.7149	0.528612531	151917.9609	5.758389517	0.029207074	39.08665523
100	6624.474369	0.228995673	147290.4772	1.228975838	153614.8284	6.380168022	0.025919882	51.40951804
103	6707.86859	0.779447024	150857.6295	2.990047833	157866.7855	8.689965887	0.024131656	12.87966275
104	14.29556388	2.721188897	30.84163845	0.965387298	27.57626017	6.001586584	0.00894688	27.78274367
105	21.47557549	2.172884707	48.37394919	2.328254901	44.75560789	2.542202472	0.006933052	24.56230739
106	22.30482219	0.78766131	55.50826416	3.91708008	49.1158856	6.260967441	-0.003719825	34.67908015
107	24.09882532	0.981079752	60.70126231	2.558950856	50.97755554	6.844840344	-0.000729309	23.48002634
108	25.91927695	0.995311718	64.82523585	5.538363988	55.27705524	8.027139753	0.011954614	3.487827937
109	14.98936686	1.367267288	34.81485726	0.476018371	31.42817896	7.67593591	-0.001576942	27.9697133
110	18.98787368	1.815961561	44.85874784	1.696413119	40.69996502	7.524198018	-0.011464737	11.83219015
111	20.19085315	1.509216616	47.06886978	1.188532001	43.38078322	11.57277231	0.012967313	20.1701373
112	20.42688782	0.922494877	49.08596756	0.910061499	44.25274328	5.504302851	-0.005057441	13.12616407
113	21.07719071	1.593285587	48.74425304	0.629941198	43.47435187	8.414572462	0.013373154	14.94956533
114	5725.224591	2.260068507	103723.5403	2.595823293	100407.9602	7.612643669	0.900116468	9.310386016
115	5703.35284	1.27573867	104630.9385	0.665174266	101052.387	6.907679053	1.129255141	13.84737178
116	5849.196968	2.677477486	107213.2743	0.991743937	100631.0897	7.034340589	0.663717258	20.79869253
117	5801.449424	0.806685764	106081.6404	1.533947374	101268.9322	6.325207418	0.517632063	37.56280419
118	5762.580121	1.20846982	107371.2116	1.32601153	102103.2537	6.153873518	0.308852493	4.549154381
119	6877.308201	0.096801575	138184.2984	1.127197372	146699.4746	5.893757909	1.04822885	21.86597997
120	6902.062509	2.094549013	135036.6785	1.000297003	146094.8661	5.981355432	0.673278455	19.09933513
121	6824.899401	0.986703089	136539.418	1.633951009	148574.4114	6.020355479	0.726449435	17.0910478
122	6992.195211	2.105095277	141233.9897	1.558973736	149771.5399	8.09148733	0.4066823	6.058921132
123	7114.869324	1.487033162	139472.2749	2.828216006	144891.0595	10.50809595	0.400418658	17.36046865
124	9345.407633	0.729635936	140297.1487	0.228044806	142452.6145	7.892505574	0.43711379	11.01298247
125	10426.36819	1.19131367	140498.1619	1.208343558	147254.9726	4.192095187	0.327021766	28.48194061
126	10467.28927	0.990463065	136353.5914	2.342715952	146263.0263	5.541156644	0.261934315	35.02405546
127	10495.19132	1.492975491	137873.6715	0.671460502	146374.539	8.455404909	0.229691167	32.35491194
128	10702.62856	0.824716872	138494.0378	0.216415353	143580.1805	6.956164061	0.12323223	55.22268462
129	6958.345995	1.462095263	136075.1678	0.640109086	147697.1702	7.288018527	0.208687455	11.00604476
130	6908.329469	2.523584273	137698.8725	2.142709025	149254.231	5.90072989	0.214137537	49.83468787
131	6896.27429	4.133093192	142617.3844	1.108601126	144583.8309	8.370635434	0.266433489	43.14559562
132	6859.882483	2.120568395	136168.9073	2.396139446	148070.4719	8.325243496	0.176983589	27.13819236
133	7122.774534	1.025926313	138614.6635	1.40439996	148562.6405	8.361290984	0.129780079	23.9303138
134	5995.382043	2.213741831	112063.4163	1.623050352	112546.281	10.58136295	0.049286708	43.38344911
135	5926.086591	1.349297741	116665.7931	0.495783749	113308.9038	10.76234709	0.01619763	72.3718454
136	6067.015083	0.553281634	116524.2285	1.192195847	115944.4785	12.47297324	0.049540926	22.23092173
137	5894.758336	0.450344497	115072.656	0.85327167	111065.9219	7.595524888	0.028561727	68.75924652
138	5915.315316	2.16971305	113801.4601	0.693928417	118426.9589	15.49823001	0.026058401	33.79571201
139	5950.883087	3.119621186	113221.3081	1.808613849	115489.4872	11.81679872	0.596379361	163.2962014
140	5919.475233	0.534516641	113098.4529	3.039149137	113747.4732	10.4442375	0.068489242	36.53223088
141	5960.095287	0.666145098	111039.148	3.218209079	115397.4596	10.81723835	0.022392616	46.87111065
142	5950.897884	1.307341131	116739.4683	0.879324714	116482.6842	11.78568413	0.048146396	0.986557053
143	5943.603093	2.22627426	114503.5068	0.263534431	114163.0618	11.47194083	0.033758619	49.13560408
144	6181.237571	1.783701063	115429.1846	1.336065976	111881.9616	5.884964205	-0.020680413	117.4633269
145	5961.149191	2.349400697	113112.1403	1.281588111	115186.8201	11.18459355	0.022003945	82.76569982
146	6074.323121	1.108862592	112736.7384	1.618392486	116035.6367	10.22595794	0.061334623	82.50641492
147	6002.594839	2.262855025	115829.8016	2.023815135	116278.8426	12.87330332	0.065070304	58.79898247
148	6002.772383	2.295125301	116629.305	1.846635789	111958.4262	6.858227261	0.07039374	48.19064117
152	2.70325271	1.350991575	3.008354242	2.183172231	3.152814568	2.196180676	0.026920112	27.57325459
153	2.807846183	3.425040787	5.073957808	0.737597846	4.749716049	13.02413413	0.041210607	24.18067261
154	12.36627454	1.872116791	8.075201232	5.118437939	7.303663279	7.549772305	0.042910673	29.78543077
155	7.261008517	0.517643076	7.120811368	0.565053734	6.816612872	6.726869419	0.025922129	22.28254037
156	5.860571216	2.349330952	4.482828025	0.655016875	3.822325314	15.91553015	0.031810352	15.10364807

	51 -> 67 V [O2]		52 -> 52 Cr [H2]		52 -> 52 Cr [O2]		55 -> 55 Mn [O2]	
Numbers	Conc. [ug/l]	Conc. RSD	Conc. [ug/l]	Conc. RSD	Conc. [ug/l]	Conc. RSD	Conc. [ug/l]	Conc. RSD
82	0.067898248	10.27706728	0.179567716	1.025859376	0.257105575	2.272410699	0.477632428	5.843203563
83	0.097049989	4.18997347	0.232207908	3.694840921	0.312990024	1.508937695	0.387102241	1.467838785
90	0.075850345	9.540386059	0.203031471	2.189930717	0.196698014	4.918629476	0.580735985	3.155371916
95	0.030270399	38.29656375	0.491715225	3.47426236	0.300757714	20.77988138	747.0147001	0.940389347
96	0.038311436	37.32526049	0.518680988	15.56979935	0.264253283	27.60368481	724.5439162	2.183839999
97	0.040349501	50.70505682	0.559951959	3.498773907	0.314438581	9.523183335	732.4197453	1.449054373
98	0.086246818	17.95790138	0.890532134	3.470710204	0.680496706	8.80584474	721.1108963	6.444848354
100	0.031175093	25.99725132	0.338450756	18.46631344	0.190589931	15.3722463	779.1471642	2.736254289
103	0.029631109	46.22592444	0.261926033	21.99046029	0.079630778	67.44122227	889.9350373	1.538434349
104	0.002108608	29.27907771	-0.006559922	35.94008136	-0.005451212	33.61477137	0.024744264	16.47827483
105	0.006522555	45.4795322	0.018885386	8.48682352	0.012026709	5.528485027	0.06262549	17.14667633
106	0.007278025	12.34108906	0.02065598	30.73398254	0.022407422	13.4481631	0.063005176	5.667305938
107	0.00903919	17.73372104	0.023301507	17.11405897	0.019334322	24.12160834	0.069044753	4.437105009
108	0.011866904	7.523046704	0.029771009	3.741410283	0.021350813	1.871318788	0.070534639	12.33273485
109	0.002693552	50.23760163	-0.008021338	10.63633899	-0.013983509	95.56469636	0.048317899	6.183940179
110	0.006024608	23.6916869	0.001416095	9.602781092	0.004742393	23.00826799	0.065174566	7.057973642
111	0.009810005	9.66538694	-0.003440962	24.19448434	0.000387577	29.1798213	0.073552689	5.035806302
112	0.00903842	13.84554161	0.008862624	15.01458579	-0.003148663	20.02618177	0.076803028	10.58289201
113	0.013426825	27.89280549	0.002261592	8.43437515	-0.000493933	42.86939059	0.094882419	4.339129531
114	0.029080952	9.827624777	2.285566563	3.363762498	2.063514313	4.070380127	162.3441093	1.70596876
115	0.035033895	33.08176358	2.463661157	3.834620694	2.390812226	4.172302152	165.6065078	1.799437138
116	0.018586644	60.97421611	2.709675584	2.103339974	2.764481245	1.045367734	167.7476714	0.806445643
117	0.028141358	37.92266341	3.174599461	8.224137632	3.107293999	0.757369084	169.7321567	0.811052671
118	0.02381785	20.7343778	3.516064322	3.158843349	3.321173555	6.834259783	171.869114	1.286537619
119	0.020396725	24.90176197	1.338191081	6.344519783	1.150081001	2.077745099	278.5244127	0.37616959
120	0.039030479	37.74792474	1.470302042	6.165309784	1.292243729	3.858648056	277.1244366	0.816272586
121	0.042752603	33.67933849	1.590743732	5.809429006	1.409242524	4.22395815	276.8352885	1.808567932
122	0.037263886	49.17679172	1.749800754	3.356025395	1.707651659	10.62865113	284.993643	0.086105718
123	0.024016319	23.17983209	1.945078766	8.311357826	1.902037195	1.190016028	285.1869693	1.951506389
124	0.022404622	28.80166557	1.32064068	8.948932531	1.208302476	9.340876459	281.5071318	1.31400794
125	0.040281402	17.9666838	1.395277099	2.120881311	1.302578972	5.162771228	277.4133323	1.589092518
126	0.043061088	32.04875294	1.519399169	4.020317412	1.368589228	0.178384179	282.0705663	0.512817739
127	0.028084499	39.02347196	1.595201643	2.618356071	1.531742671	5.026780234	281.0392929	1.925212428
128	0.042976969	80.81509191	1.758997735	3.415077544	1.641835772	2.708654593	283.9853732	1.105138205
129	0.043258143	58.55628149	1.330997557	8.699402345	1.0331664	1.515181425	282.7008653	1.151311422
130	0.033266437	24.85816641	1.292433959	12.29370165	1.096719042	8.97012235	280.1646373	2.647339902
131	0.033433834	61.90218332	1.274096141	4.033910627	1.129005495	9.759075522	279.2894743	3.274138395
132	0.022052486	48.11186001	1.24317935	6.797857295	1.068440826	5.986606742	277.2702922	1.739276416
133	0.023709914	69.23656761	1.243033371	11.39765482	1.040092706	0.671341748	285.4254568	1.955142385
134	0.03158742	41.91411297	0.342987431	12.8272648	0.109344948	31.37590653	185.2551816	3.559089212
135	0.035281556	32.69422379	0.239292711	25.84744292	0.090247751	73.20786438	182.8526142	1.839474265
136	0.044214416	9.935458092	0.409577132	14.99121415	0.18014052	28.39840431	186.585426	0.150987438
137	0.028364792	81.39057183	0.387024601	15.49032805	0.171825755	20.70588153	181.4109531	1.225787464
138	0.031455402	44.22515213	0.481053711	15.72766405	0.200581311	48.47488688	185.8006077	2.763676574
139	0.035052047	53.08446458	0.299837438	16.42435943	0.159567528	32.84469474	184.5098867	1.8607877
140	0.042336524	49.20576739	0.258775809	40.64571256	0.088331571	50.93120018	183.3850698	0.631929871
141	0.026301111	52.58929396	0.306238181	20.12779836	0.084239022	109.4981789	182.8295594	0.979760413
142	0.039204966	33.03953558	0.382612744	25.35101291	0.032807963	41.95237076	184.1180712	0.611232678
143	0.044786729	9.698989088	0.315481888	9.3290594	0.158045309	19.36674732	183.7065624	2.439173551
144	0.024124415	54.83216415	0.277015714	2.503463728	0.020185413	101.1427717	186.4686634	1.156584549
145	0.039013073	44.66283573	0.213875387	41.51543921	0.018794292	72.46490542	182.6255415	1.682458196
146	0.030969933	40.30410993	0.229935913	22.09901047	0.086006781	75.37996943	188.4016355	1.15840285
147	0.077499583	12.3576179	0.275995492	11.62597062	-0.029483278	N/A	182.9213873	0.558487994
148	0.031977335	26.74960585	0.256781255	34.23070894	0.019405344	254.220457	184.4330612	1.505224097
152	0	53.80421172	0.015781519	26.41121895	0.020203602	1.28801435	0	N/A
153	0	49.26587928	0.020660127	9.44584265	0.015350498	21.86903971	0	807.8488684
154	0	33.94686186	0.021919413	11.73085445	0.011535474	13.36816117	0	N/A
155	0	85.02333325	0.017935225	17.94619502	0.018607821	12.98948817	0	N/A
156	0	23.36601159	0.021990307	22.83693135	0.015859623	48.77062457	0	N/A

	56 -> 56 Fe [H2]		59 -> 59 Co [O2]		60 -> 60 Ni [H2]		60 -> 60 Ni [O2]	
Numbers	Conc. [ug/l]	Conc. RSD	Conc. [ug/l]	Conc. RSD	Conc. [ug/l]	Conc. RSD	Conc. [ug/l]	Conc. RSD
82	11.83716969	1.465991671	0.054292324	18.30385212	0.669461225	9.081520283	0.645832143	4.733028688
83	21.38736532	1.844134336	0.08163659	3.243726919	0.852669475	4.647412801	0.770281743	5.474078891
90	16.94272677	0.788724668	0.047198743	7.700172878	0.680019812	13.47243276	0.66466859	5.975589497
95	5698.665859	1.866787286	117.411404	0.531854363	52.82970131	2.215392452	53.21730507	2.107316257
96	5332.40577	1.270250768	106.3109854	0.260294208	45.01454713	5.369610819	49.85850247	1.207615082
97	5378.776163	2.880807981	108.5999306	1.512880659	47.87727925	4.768365675	50.70310761	0.294735427
98	39.1375619	2.643056457	100.2294528	2.441344846	52.41738476	3.943378204	51.15805088	2.268412987
100	476.488347	4.116398954	117.5828274	2.207776428	62.3389492	2.454856393	59.07170773	1.793453927
103	1700.064449	5.096591178	143.5842367	2.081526126	77.34800055	2.650569287	78.65335997	1.328331877
104	-0.147351832	3.545373281	0.001323118	182.6933546	0.555706153	5.606010961	0.570166448	8.521482908
105	0.118300117	1.58991081	0.010066937	46.85056644	27.13659824	2.859285656	28.67943298	2.745926815
106	0.190196782	2.163041735	0.017520769	16.43141799	41.24691031	2.050718378	42.49675709	1.071941231
107	0.33928114	3.021579435	0.015358299	13.32188584	48.35607461	0.749843599	51.0528463	1.0021545
108	0.588437994	0.518368961	0.020762074	13.14245147	53.45287292	2.220369191	55.66115884	0.938400511
109	-0.06432352	3.384145394	0.002073786	50.70307365	0.65343286	3.777057871	0.712620159	6.149855987
110	0.501299127	1.823457296	0.003206572	129.9552444	6.772538315	2.271774552	7.324440007	1.178261353
111	1.156466729	0.543551554	0.005498657	50.91611588	10.49541327	2.908158645	11.01540768	0.467880103
112	1.799508679	1.648862544	0.004628091	29.28986258	11.84501754	2.726834733	12.51983603	2.415839445
113	2.371298747	0.535602682	0.00774018	72.13308557	12.83538398	1.173549221	13.95425953	1.264104109
114	6348.832068	3.020448987	33.31822776	3.718679077	15.54769471	12.52816299	14.67551992	2.726916811
115	6248.483834	0.589034345	33.72544011	1.568842422	33.70129259	0.699123871	34.58283014	3.154671953
116	6048.772017	2.171305392	34.75026421	1.647229446	61.74586995	5.968253408	64.29761843	0.832469331
117	6030.693862	1.424161105	34.6328365	2.307335562	83.71215559	2.06003964	87.20298955	0.915728573
118	5697.031787	1.190937688	34.48593821	2.789231779	104.2354616	2.817936703	106.3296501	1.175743807
119	6978.601439	0.797840581	48.42190257	1.770989196	21.35228187	6.580824563	22.89681927	3.784041626
120	6444.071326	2.364416027	47.79576408	0.523730989	25.10509621	4.093917162	23.38902697	1.920674589
121	6361.864353	1.083192424	48.35303327	0.349448444	23.08390539	3.780431234	23.47207582	0.418537046
122	6431.86736	1.965074434	49.08138731	1.20241678	26.32129712	3.204532591	24.98258689	2.368092107
123	6051.815589	3.444400628	49.32224577	1.735167359	25.4611739	11.3868742	25.71535735	0.796272378
124	6091.842252	1.818980601	49.24732054	1.862468078	21.67588416	4.597005534	22.25778214	1.58886374
125	6049.482539	0.710905655	48.02248783	0.858661067	38.43502032	4.110839455	36.39340706	1.32499946
126	5556.158296	0.459030332	49.02274053	1.325595318	53.12007071	3.197177175	54.0476324	2.239734877
127	5277.656357	1.149424703	48.77986474	1.101729224	66.71384748	0.874470469	67.43951196	1.607842235
128	4902.347286	3.933734489	48.72504287	1.267452766	75.31643323	4.364104236	78.18211953	2.85239789
129	5790.446954	1.464038232	48.59399733	1.509583349	23.84999999	6.965381771	24.62661413	2.164132471
130	5759.306752	2.352397504	48.80359419	3.06541393	29.84012174	4.702712802	30.34556189	0.915889195
131	5719.083613	1.334735347	48.31609614	3.338110043	34.14541682	4.678595029	34.00912791	4.056680574
132	5432.208284	2.85724181	48.16897261	2.139988691	37.7591618	3.347008974	38.13785409	1.295121541
133	5296.698535	2.029686565	49.70913885	2.238395713	42.93580368	7.38233342	43.83286979	0.754287873
134	2818.582415	1.104401849	32.15688038	3.581123961	14.97411297	8.960630112	17.2601875	6.25443446
135	2871.760414	1.271072584	32.17829902	3.880507008	15.54826067	8.603579144	16.62056802	5.918389545
136	2791.432895	1.887608733	32.58389561	1.358907842	16.28195898	12.93295166	16.94483689	9.163458869
137	2624.046622	1.342267301	31.5910764	1.344931753	15.56885015	14.64734883	16.15896124	2.456047026
138	2533.257116	2.07454872	32.44006802	3.352164246	17.20908085	3.053428328	16.88983427	9.064268622
139	2764.710186	1.702809964	32.28427278	1.20385872	16.09005633	10.60992631	16.17377086	1.822671133
140	2616.983071	4.207481007	31.9729852	0.781462572	18.27617884	8.24680841	19.05629265	3.005852598
141	2469.583454	0.493208622	31.97332921	2.765392475	21.05163928	7.446219066	23.76140533	0.22843194
142	2510.088566	2.158781289	32.02531392	0.140807316	26.47817009	3.169581901	26.64105729	2.65536344
143	2205.125396	0.561288944	32.65589936	1.206561181	30.54316702	7.122228138	30.2425837	2.298124252
144	2821.61053	2.988899679	32.32214146	1.029274512	18.43481367	2.926607237	16.357946	4.29072085
145	2730.063133	0.907602722	31.98679898	1.833456645	17.92821137	5.816479667	18.27757055	2.368469164
146	2728.943759	3.260742592	32.3824659	2.769194857	20.7042836	5.826041243	21.30688939	2.928641302
147	2555.506835	1.844367597	31.76283262	0.749537467	21.31258397	11.39418276	21.01352444	2.822799377
148	2569.526585	0.958324475	32.30093455	0.487242931	21.07350013	5.352614497	20.68471012	8.774748229
152	0.098799934	7.648744962	0	56.51249815	-1.04043E-05	4293.406034	-1.10349E-05	60.33662866
153	0.683393437	7.795349146	0	55.74687977	-1.56741E-05	35.52740691	-1.6624E-05	32.32252925
154	0.278294643	2.03641867	0	N/A	-2.41021E-05	67.02005699	-2.55628E-05	13.85273467
155	0.178524219	5.359722222	0	154.8208372	-2.24948E-05	73.28908989	-2.38581E-05	26.0286365
156	0.126488225	4.609180537	0	269.1437091	-1.26137E-05	134.9382284	-1.33781E-05	46.85503159

	62 -> 62 Ni [H2]		62 -> 62 Ni [O2]		63 -> 63 Cu [O2]		66 -> 66 Zn [H2]	
Numbers	Conc. [ug/l]	Conc. RSD	Conc. [ug/l]	Conc. RSD	Conc. [ug/l]	Conc. RSD	Conc. [ug/l]	Conc. RSD
82	0.733923594	21.99291167	0.650986944	3.638986639	2.557781534	1.353578328	2.553862571	5.425687314
83	0.746166039	10.19580262	0.77495862	7.642612952	4.993972033	2.049552703	5.101650091	3.735762556
90	0.560497295	26.34368562	0.631949172	2.710775646	2.88494365	2.329980786	3.607966644	3.528136713
95	52.05914256	6.400093676	51.55759953	2.085783845	20491.63417	0.922907624	13188.17032	1.582157119
96	46.35768657	2.396182924	47.9675375	1.496446934	18293.69959	1.581301988	12783.35468	2.018817902
97	47.76332479	2.789220348	49.65545287	5.252773411	18658.45202	0.673699744	12428.4771	4.332393086
98	49.18108122	2.899421795	48.82467178	7.087242458	1393.144764	3.270142872	7820.243418	2.770252059
100	55.09727626	6.415212573	56.37069018	4.399912972	6226.689414	0.320345158	11184.25355	2.74211082
103	72.7571921	7.999205484	74.43252358	1.566894608	11872.21776	1.955911416	15347.75201	1.687239202
104	0.627883428	23.67954549	0.532853459	13.11576419	4.046809474	2.869591137	2.377732156	2.54022849
105	26.97770233	1.516595455	27.47986147	2.557663126	28.1165606	3.114089906	19.13689043	1.362369284
106	41.12918794	0.661093671	40.86559873	0.618816239	38.80535936	0.774786765	31.48610221	1.813485145
107	47.78448771	1.846135091	48.43873751	0.974571479	47.75221691	0.633392779	42.83837487	0.637795579
108	52.9641094	1.986591834	53.305152	1.301045205	52.91977798	1.927472581	53.39515113	2.395390124
109	0.60535085	28.40843627	0.720889683	10.88771793	5.91681627	2.15021333	4.48352507	0.981461282
110	6.635217765	5.235824272	7.050451722	4.973264742	15.51857542	2.979184291	15.77388826	1.636910889
111	10.72063317	6.222179874	10.8096898	3.504702766	20.07564856	2.331641067	26.02044339	1.37076164
112	11.97469572	6.581525586	12.24523103	2.013780226	21.80848174	0.734133852	36.0537982	0.72697771
113	12.7920209	1.350088997	13.40421596	2.620490266	24.11878391	3.252942723	47.24527472	0.718961368
114	14.42390331	6.653868599	14.08606556	2.424113698	6123.508593	1.278782031	3979.878885	2.135571257
115	31.53148043	15.28167785	33.37571713	3.5077571	6130.893816	1.4492751	4063.217981	3.096157959
116	61.63327388	7.829700186	62.39413356	2.261770563	5993.200137	2.030687827	4095.571888	0.720278499
117	77.10233761	5.579434535	80.55077902	3.060590546	5735.168805	0.840807609	4134.15858	3.418233395
118	99.3570944	2.743156078	100.4739764	0.930962792	5311.403469	0.275605421	4253.24378	4.590191345
119	19.56006424	0.849923881	22.23437263	5.284943261	5877.513895	0.955687078	5369.144908	1.25632665
120	20.02956671	17.94399165	22.48242619	6.669198414	5753.172908	1.615834695	5221.632011	4.988902146
121	23.99677028	14.61567629	23.78428443	4.800369208	5626.923391	1.561183414	5340.040528	1.226082793
122	22.1117895	10.24607934	23.73703371	4.77956871	5605.799769	0.273530674	5701.194281	4.367444829
123	23.92742206	17.53634795	22.66657605	4.997218146	5512.431816	2.7360691	5455.078293	1.61686976
124	22.23727387	7.778182833	20.68879147	3.233550954	5951.26886	1.05293405	5335.817341	2.252521495
125	31.80739904	10.2096252	37.78945373	10.10940293	6006.089176	2.137204251	5849.178826	1.871504116
126	49.10748289	9.766956122	50.84431476	0.906392047	6113.117628	0.430039148	5752.36872	5.155160165
127	62.15733736	7.007687654	66.42494005	4.409341045	6123.234469	1.468388366	5999.956399	1.236652232
128	75.97667467	9.411319162	76.15350283	4.836750917	5995.25243	1.405787011	6035.369338	1.731944678
129	26.00865434	7.081137462	23.12362706	3.279023347	5908.453786	2.194299992	5403.030154	5.421070578
130	30.67764717	5.807687714	29.6225314	2.639932102	6058.291761	1.94768848	5572.482832	2.012353387
131	32.41674111	11.70093759	32.47960346	10.51995722	6172.166962	3.632708291	5736.547352	1.900984024
132	33.21216356	2.953763547	36.95306364	6.200454106	6238.048687	1.407793707	5597.662836	1.179214615
133	41.4954368	12.72824593	41.73121484	1.563428121	6627.177325	4.046241393	5799.746308	6.646598346
134	14.60861047	9.175152945	15.30279744	10.53322121	4128.994723	2.229158909	4412.159098	1.872971367
135	15.13703106	4.488281647	14.82238698	5.981247529	4027.251304	2.901023072	4578.686546	3.707103949
136	15.80473482	10.07392118	16.67642624	4.798282062	4044.438249	1.257892742	4563.960622	0.398283048
137	14.98591432	14.34066694	15.71729517	8.001068658	3899.696386	0.998365578	4482.162819	1.160180097
138	15.75344381	2.798358132	15.9319881	6.667221332	3872.500918	3.266569708	4496.970035	2.370147184
139	16.10631218	16.67572085	15.32081357	1.430114241	4144.087259	2.898026136	4481.000339	2.32676424
140	17.22139339	12.91513892	19.85543101	7.478168414	4129.058118	1.630852906	4463.583876	1.657304067
141	20.44791109	11.45495758	22.70340688	0.668919136	4083.684538	0.60073174	4512.680625	2.786783369
142	26.08636731	4.754782494	25.87486798	1.290735841	4067.583403	1.458764867	4791.327088	2.142106426
143	28.15677625	5.090168762	29.41568391	1.121615997	4157.546688	4.31640996	4716.689516	2.599822966
144	17.1956053	13.77932354	15.91844757	4.746816248	4091.975901	2.742355724	4540.635933	0.689446549
145	18.69736991	1.922200533	18.26118591	4.436878626	4133.053266	2.796150361	4557.333035	2.735200781
146	17.8744372	3.396906794	19.12890955	7.825975823	4351.6602	0.849289197	4611.053273	4.052475616
147	19.77619122	20.50891895	20.07017518	4.626776892	4243.441809	1.419665944	4544.748538	1.154075166
148	19.26226341	9.978588613	19.50342489	1.72824298	4218.865711	2.528352712	4556.804144	4.040327572
152	0	48.92552298	0	413.9852506	0.032665086	9.903424097	0.116177941	10.0318079
153	0	12.09512926	0	60.04669155	0.032847989	27.57859357	0.015383098	108.496731
154	0	52.27559378	0	38.05328626	0.340463628	6.337881606	0.069935033	35.83342403
155	0	122.7266585	0	87.65212078	0.108171371	18.37631834	0.035654733	26.6396159
156	0	109.132278	0	115.3636412	0.103039698	16.12062398	0.014818147	141.1143554

	75 -> 91 As [O2]		79 -> 79 Br [O2]		79 -> 95 Br [O2]		85 -> 85 Rb [H2]	
Numbers	Conc. [ug/l]	Conc. RSD	Conc. [ug/l]	Conc. RSD	Conc. [ug/l]	Conc. RSD	Conc. [ug/l]	Conc. RSD
82	0.048853217	14.10551112	36.65505385	4.972108611	37.25095267	6.811109366	0.566127359	1.195445268
83	0.113376234	11.60606028	36.62006057	5.096204999	36.0057293	1.557348648	0.589329596	5.057103212
90	0.052807836	31.99475875	36.41144829	9.526143865	36.35357293	3.090157873	0.496317843	4.589416624
95	0.257917049	23.61707467	46.34679713	11.06914952	53.42144048	13.72483273	7.683010147	2.244447807
96	0.263801316	25.41354	58.03335042	20.94897429	51.66632416	14.68469748	7.618412072	4.233730273
97	0.178319513	40.16602285	52.59087656	29.4588747	48.25258337	15.55302618	7.341310414	0.456268145
98	0.069948323	78.09273071	32.11794872	4.548710058	36.9997563	14.6108536	7.754354978	1.511306188
100	0.039279224	76.33180506	29.31182532	35.53003776	29.55112064	14.36471632	7.619789059	3.500513152
103	0.061521419	53.26616941	25.85201256	39.32631264	30.42148975	28.85979948	7.948413111	1.036145672
104	-0.000756762	N/A	0.193716048	234.879898	0.792731912	88.2407915	0.015665064	15.53314499
105	0.003165651	62.28253726	0.583903254	96.86993995	0.725082554	84.08834224	0.023770409	4.184888418
106	0.002044734	205.2580121	0.076582225	N/A	0.541247022	266.6022662	0.02467709	9.56258289
107	0.002058295	97.52050285	0.227573869	N/A	0.288697187	N/A	0.026713172	13.97609783
108	0.001768984	39.8346462	-0.01628897	N/A	0.537499756	561.508371	0.027690026	26.13588828
109	0.000646822	487.3598592	0.160249846	N/A	0.509314923	886.2779003	0.016784572	23.02032477
110	0.000647067	723.2836616	-0.05063629	N/A	0.501733381	1347.797213	0.025792098	6.61417974
111	0.005331075	21.75643049	0.291118092	N/A	0.744365416	114.5390959	0.027567781	12.29091108
112	-4.96141E-05	N/A	-0.043983247	N/A	0.422757691	N/A	0.031241714	3.34333036
113	-0.001124353	N/A	-0.068477878	N/A	0.486484062	N/A	0.029738069	8.294786763
114	0.327332079	20.83886962	53.79087302	5.364100077	53.81279187	3.615382039	5.67398452	2.499182104
115	0.227160078	10.98090746	49.17050258	7.668384958	57.84046563	28.31260587	5.481776514	1.583464505
116	0.29188783	26.38276165	51.01581414	12.51359097	56.09856345	15.08182828	5.617253529	2.179429122
117	0.175874486	21.25391336	71.15146211	3.391899655	50.2662193	10.82145791	5.679657269	1.601967513
118	0.18869709	37.20201228	55.20671224	13.8407151	58.80655025	4.816265209	5.816610889	3.764111243
119	0.385528709	14.30559428	40.89178175	23.96343049	46.75399446	25.39149952	7.038949113	1.61520368
120	0.52550671	39.03577889	57.87903786	28.15831963	59.33655922	13.69214061	6.65554903	2.33823396
121	0.552561595	10.83688454	45.33619605	7.115874169	49.53807195	24.36656109	6.60100221	3.388801827
122	0.450862507	24.55983634	62.32288374	7.63135612	71.46478179	9.020250742	6.910621571	0.822018447
123	0.339818955	24.57229311	59.09593814	16.16998262	59.64471577	4.514413799	6.944118512	1.032683096
124	0.460401799	4.930709312	65.32970469	12.31001656	67.31037403	13.19582291	6.784980011	0.853029898
125	0.285743638	35.66360067	57.40659138	10.93608998	65.21063326	9.71096563	6.899711324	1.182826881
126	0.38150137	6.373355879	59.30597374	11.0593009	59.52696355	7.676177901	6.767996862	4.192905057
127	0.350237398	7.613932144	66.65437363	13.27615694	56.10743491	16.98777981	6.79823578	3.163281479
128	0.188510891	13.37707543	54.65635336	22.10187683	62.10943261	2.643187182	6.824352825	0.75549584
129	0.526615744	13.11315128	62.88668971	8.434240624	58.54735739	8.860073461	6.723358964	3.144156641
130	0.39677394	12.25629169	56.33931216	9.92097515	63.90016009	7.270852235	6.855887354	1.351647453
131	0.423491102	14.6254702	58.72449627	12.10783537	56.81168567	2.310290048	6.804158369	1.980522286
132	0.518487536	15.99232261	51.23237521	6.974393323	52.62021551	6.533015634	6.48397034	1.194665883
133	0.437082788	18.74096627	45.21375849	8.762517793	56.01161559	10.52506384	6.69358738	1.960453425
134	0.254821107	12.4006528	53.83025244	2.372282309	52.73336889	4.833206251	5.398085572	2.001789342
135	0.235658193	38.6154242	51.56324908	4.201248653	57.88265993	16.72308457	5.778155365	2.469242054
136	0.304379938	24.18377413	52.87514483	23.70512958	49.415332	13.38624625	5.62667241	3.574099847
137	0.232035537	14.10662045	52.35550531	8.799062441	50.68566613	16.24588346	5.66781896	2.123739879
138	0.12325331	93.16755568	58.55619582	24.59294834	46.66680325	19.99846683	5.949024974	0.215125877
139	0.214147835	38.84720652	54.08424227	10.56252444	51.33779848	11.18732749	5.42559059	2.86082025
140	0.272092078	44.7692663	56.66439757	3.242674988	46.34933958	23.42824422	5.507283703	4.14262003
141	0.190709609	18.986901	52.68678564	17.59270874	56.27768973	16.36610541	5.542229843	2.948164509
142	0.102703652	64.97631412	50.55518993	6.751165846	53.22437116	6.052282899	5.940689266	0.665348348
143	0.125995822	27.14816916	50.49566055	19.68350406	48.37583339	17.84582121	5.54068533	2.186345838
144	0.274038236	35.10090342	48.14151314	3.00881362	54.25375482	9.512604685	5.725698608	1.727641486
145	0.248752558	50.5705846	48.5524956	11.66959035	38.85550202	11.42615864	5.711370903	4.062772594
146	0.292813924	23.71085484	48.50207535	9.220198402	57.12720489	28.8426954	5.792564563	0.773429301
147	0.173748647	4.747632439	53.73423406	12.43880781	42.30060384	12.54632273	5.594285733	1.177454313
148	0.267511326	32.3068248	56.10178009	31.48378351	59.796986	24.10224998	5.788323171	1.429812611
152	0	286.9235455	0	245.4103168	0	N/A	0	72.00001316
153	0	N/A	0	N/A	0	N/A	0	1112.430818
154	0	N/A	0	N/A	0	N/A	0	57.37338995
155	0	N/A	0	N/A	0	997.2326987	0	96.8283372
156	0	N/A	0	N/A	0	N/A	0	248.6025194

	85 -> 85 Rb [O2]		88 -> 88 Sr [H2]		88 -> 88 Sr [O2]		98 -> 98 Mo [H2]	
Numbers	Conc. [ug/l]	Conc. RSD	Conc. [ug/l]	Conc. RSD	Conc. [ug/l]	Conc. RSD	Conc. [ug/l]	Conc. RSD
82	0.554727155	3.698223261	12.31019866	1.305672102	12.47667318	0.309072467	0.085127266	17.24554229
83	0.577254492	0.873504416	13.71799552	0.83744329	13.60126421	1.916678266	0.087001232	7.721623184
90	0.488235476	1.539967445	11.20626124	1.317520861	11.28374989	1.643166086	0.079915202	11.57708356
95	7.293553356	3.514225028	460.6749904	2.633119681	466.7902292	2.445053673	0.02287319	76.59302029
96	7.240770333	0.791854391	454.0737722	2.26646856	463.2764878	1.863115668	0.023022522	36.3335796
97	7.271568665	3.583745347	443.1393458	1.433550839	470.4790426	1.75714011	0.001472994	1061.056392
98	7.274966558	2.272216238	493.9830315	3.507133079	498.6444702	2.883378413	1.57051793	2.31523508
100	7.310841476	3.610118399	494.7719954	1.018741821	501.6445674	3.723792501	0.779993513	2.583561448
103	7.750060306	4.938251931	487.8559697	2.294565142	508.4672375	1.240876917	0.314891821	9.090962807
104	0.016691709	11.2239667	0.150071576	3.545383265	0.159004204	5.856765745	0.00405757	57.96304911
105	0.023728051	7.527562215	0.230674001	1.027680202	0.24056023	5.957527198	0.004476902	62.91792349
106	0.023526676	10.18102136	0.258877316	2.061683846	0.258112127	0.892577902	0.001684515	134.9580625
107	0.025208933	2.349442287	0.27061833	1.603474384	0.287046117	3.671648584	0.006283247	20.18362933
108	0.027649	8.653027393	0.279431642	3.647043038	0.291974478	1.427976119	0.003301372	85.95950421
109	0.018587225	19.66060584	0.256881071	3.436822667	0.268708984	6.172539258	0.001982623	95.13629965
110	0.02557544	6.98591752	0.299713944	1.499334731	0.303075293	1.114598822	0.004023847	25.28952575
111	0.025481992	6.196819871	0.301262935	3.336812231	0.316167385	2.184984727	0.001809423	75.94628067
112	0.025622482	8.68848446	0.308921229	3.55764757	0.320700227	3.069630889	0.002251663	23.20344796
113	0.031290703	7.205530614	0.311030843	3.91233985	0.328788857	3.92030387	0.003369781	45.44590266
114	5.445303359	3.584540901	341.3571162	3.287768066	352.6999744	1.937409913	0.010292964	236.1686219
115	5.536562968	2.753721131	346.5721996	2.163762946	349.9233907	3.680339539	0.008511048	333.673201
116	5.523554719	2.737265812	364.9971434	1.874968543	361.6029199	2.58603168	0.003558329	353.2115499
117	5.64884025	3.427347388	353.0717274	4.674740936	353.0694122	2.90128264	0.003622634	461.6581005
118	5.623977305	1.943367009	361.2471296	3.814419192	347.4306712	1.594720828	0.010251198	73.51825893
119	6.579661127	3.344625226	420.4554191	0.930865056	431.0197707	0.951678465	-0.005005462	N/A
120	6.457341785	1.269061477	414.1957659	2.970552056	418.5273098	1.318173782	0.008702874	144.6492567
121	6.663299329	0.989634464	417.7872402	1.384280008	445.273666	3.717645319	0.015140934	52.32523551
122	6.714617756	1.259567828	429.8472454	2.358224445	450.3207941	5.989557315	0.016577539	91.97795938
123	6.966171695	2.099537111	421.1176825	3.704557642	441.4604606	2.054198366	0.00684376	203.1873231
124	6.790258008	1.439561872	418.7064787	1.930420241	447.7147197	1.082861299	0.013869381	94.72416822
125	6.792668009	2.40052667	431.8447543	0.602739103	436.6388212	1.87200547	0.008546105	92.70489663
126	6.812553391	1.768825609	428.2869872	1.287108706	433.7100722	0.961897715	0.003733111	228.3651455
127	6.914269814	0.832335696	424.4948994	1.946445353	454.4905408	3.067716258	0.009018748	92.34149261
128	7.001953549	0.530287441	435.1240381	2.993947121	442.2411751	0.906472245	0.007237683	73.8591474
129	6.837110277	2.8478006	425.0486411	1.142946416	435.7625636	0.630333333	-0.008190642	N/A
130	6.828644275	5.432001084	417.7277789	2.568751391	447.1651782	3.012780277	-0.006345738	N/A
131	6.576199142	2.442242272	436.6022901	5.27078469	449.8506374	2.924378045	-0.001135324	N/A
132	6.783295413	4.070198172	419.2035853	2.83821954	435.4711262	2.690100851	0.002121164	272.7020373
133	6.843767411	2.312131506	417.5886804	1.812591008	443.4625141	1.77875245	0.016076329	131.3492715
134	5.68341882	4.665670214	343.5497115	2.134230506	376.1882444	2.975579854	-0.006543083	N/A
135	5.673574157	1.533550629	367.1839936	3.931618269	365.5644091	3.751178064	0.019377929	41.86784525
136	5.874256528	1.078248492	352.0601108	0.718716331	372.4207823	3.58342553	0.017917061	179.3892276
137	5.764164022	2.065335298	348.9778975	5.711260201	358.8194536	1.378968105	0.012469032	126.7479221
138	5.566271446	5.823783896	352.3877721	2.043613584	365.4418119	2.836184822	0.028485967	33.0367139
139	5.753430641	2.698703883	339.8908578	3.297653118	372.287546	1.230605639	-0.004422308	N/A
140	5.761400607	2.131127791	349.3736328	1.783374411	363.6180315	1.829739735	-0.001313547	N/A
141	5.788895279	2.824031252	328.6806125	1.880642376	364.4551221	3.054121108	0.005719387	194.1244535
142	5.737652726	2.811973203	359.9700321	1.09362627	362.3033203	1.656374316	0.006381429	360.7651317
143	5.772144871	2.35651837	353.0993739	2.175073798	358.2748858	2.691126392	0.004381852	578.6158787
144	5.966475387	2.66425015	355.0570356	4.5317812	376.7871232	2.777957496	0.017152127	161.4734214
145	5.685033378	1.439158772	363.825053	1.674602156	360.9048648	4.587829752	0.018493419	56.48452158
146	5.918162212	1.574369474	349.5148726	1.695798652	372.5145344	3.7314339	-0.006057906	N/A
147	5.782800285	0.425866452	352.818631	1.070724889	363.2588209	2.808475634	-0.005931731	N/A
148	5.869920877	2.158358064	341.2588089	0.908147217	367.1646511	1.076508121	0.008526466	195.5964543
152	0	251.2045231	0.008069413	20.37148012	0	25.84796306	0	61.81317233
153	0	N/A	0.010394493	7.621502397	0	6.83095139	0	167.9947878
154	0	41.14953548	0.026583501	110.6811809	0	12.35797864	0	97.20178321
155	0	95.64167199	0.011375657	9.933839616	0	16.15712883	0	70.14715018
156	0	N/A	0.002206766	13.56359782	0	12.69634171	0	30.3646088

	98 -> 130 Mo [O2]		114 -> 114 Cd [H2]		114 -> 114 Cd [O2]		118 -> 118 Sn [H2]	
Numbers	Conc. [ug/l]	Conc. RSD	Conc. [ug/l]	Conc. RSD	Conc. [ug/l]	Conc. RSD	Conc. [ug/l]	Conc. RSD
82	0.079380778	3.574004129	0.008110267	19.28966579	0.006894754	8.911457389	0.002775606	54.97562269
83	0.076084497	3.249666237	0.01606189	14.42130273	0.012634689	19.15591481	0.004621666	14.32835376
90	0.077996834	1.41891151	0.009513155	15.96573716	0.008846736	7.505288278	0.002694376	66.05152364
95	0.022044808	67.15354779	49.99135209	0.975558633	50.74551399	1.562317708	0.126382776	3.387566699
96	0.014390037	129.400664	48.24047296	1.88578149	47.72584588	1.374924718	0.050591977	50.00170357
97	0.01061459	44.28178677	47.59514473	1.348331791	47.78651347	0.988886947	0.03587487	20.07398098
98	1.512467288	5.319335456	35.68846349	2.364209557	34.99651851	2.227431537	0.027940579	82.50603692
100	0.751066715	1.841831728	47.68686102	1.094456958	47.26039786	1.544123761	0.043708519	40.90632466
103	0.299548523	16.04077017	55.62509342	1.895667146	55.79099003	1.08002251	0.040559226	33.45721066
104	0.002126843	50.75977526	-0.002766285	N/A	-0.004263435	N/A	1.038158692	2.666865521
105	0.00454663	36.54932778	-0.010584886	N/A	0.000675991	953.0411271	2.05254609	0.602221509
106	0.003776616	32.73196499	-0.001323179	N/A	-0.00350437	N/A	2.13164243	1.446168464
107	0.001515504	51.53976649	-0.00260957	N/A	-0.001477609	N/A	2.22384773	0.596060916
108	0.004810784	69.59998454	-0.004595695	N/A	-0.002529683	N/A	2.250612212	3.390972797
109	0.002104835	79.61890445	-0.003606706	N/A	-0.003096302	N/A	0.954864754	1.462731324
110	0.003509538	41.72370459	-0.005275065	N/A	-0.002493971	N/A	1.731538874	1.952672735
111	0.002596282	43.30485232	-0.006971186	N/A	-0.003965585	N/A	1.796722522	1.566349892
112	0.003310406	43.46318512	-0.010591853	N/A	-0.004709791	N/A	1.823461764	0.951543532
113	0.00336242	7.560254521	-0.008276632	N/A	-0.001531426	N/A	1.804768128	1.23550422
114	0.006620514	32.20016037	15.95546143	0.65875721	15.74071455	2.34363311	0.077670104	5.687724417
115	0.002563665	475.4035935	16.02063268	0.523589313	15.79541344	1.752828973	0.5503694	5.622700867
116	0.01192447	88.13354305	16.1718291	2.984101243	16.19309189	2.392195597	0.626978959	6.017985176
117	0.015966875	91.83311509	16.17489754	1.546994672	16.16775033	0.549146061	0.755253587	6.595195714
118	0.005275546	267.2737441	16.34627611	1.720345146	16.22696941	1.077731565	0.802861611	6.369585728
119	0.010564724	130.1344579	20.87816032	2.33095335	20.88187184	1.175550032	0.063678159	32.96763777
120	0.018734643	24.74485243	20.69461594	2.38515206	20.48759223	0.677428376	0.162335864	8.770693746
121	0.015001203	136.5871657	20.50039058	1.782555979	20.72801	1.889828807	0.207248543	13.07507993
122	0.017464547	87.59684989	21.17203142	0.569655562	20.83556557	1.290456555	0.23119415	18.77502898
123	0.010667665	22.68571899	21.11822024	0.831613934	21.22687958	2.935238441	0.254703839	8.139846859
124	0.010794265	112.9634942	20.64473779	1.234290517	20.80620672	1.697786166	0.120804923	9.806886171
125	0.021673204	75.05281523	21.0527656	0.697510396	20.86095343	0.807354777	0.207442632	4.695525276
126	0.001448501	1073.997888	20.78944218	0.455385689	21.3542538	1.418894945	0.233469843	18.77256018
127	0.008394321	128.5016651	21.20131786	2.44594491	21.57295728	1.671254232	0.233753958	22.90170568
128	0.01225136	206.963435	21.33860744	0.150441755	21.74887193	1.923110804	0.297949491	8.64390321
129	0.005666152	165.4945447	20.6180458	1.846103707	20.9509467	2.192073429	0.055903779	31.05413059
130	0.009641911	129.0790069	20.84687005	1.362420214	21.04036371	3.331881757	0.066801262	9.406383666
131	0.009776252	170.3567087	20.88673485	1.416850085	20.87981445	1.690427776	0.058621729	53.38827852
132	0.007220998	32.37016373	20.18941339	1.592143352	20.838787	2.723285038	0.090779583	32.83111097
133	0.01248131	95.77460914	20.77315153	1.326063037	21.14767454	2.866959262	0.0907562	17.79738832
134	0.00155198	857.7881654	17.29089621	2.264215824	17.97895673	3.044979047	0.047549323	20.06829723
135	0.008395137	128.2423854	17.99987056	1.870418831	17.69402538	1.725946936	0.149282956	19.50841123
136	0.016529328	1.214574006	18.03834518	1.028272337	18.28608508	0.79320677	0.20108293	19.71742909
137	0.015523757	137.3309408	17.59904177	0.865146269	17.51986275	1.243876227	0.174144347	11.1655905
138	0.01570054	75.7823151	17.57243735	0.556814519	17.86483291	2.40596556	0.199245419	11.95766559
139	0.018459552	104.2109144	17.27916043	1.12214335	18.00765672	2.382781104	0.084847082	7.556211796
140	0.00051491	2243.18638	17.22569052	2.138655851	18.03673807	0.512893609	0.271673347	12.80619848
141	0.008949048	187.6637595	17.3084283	1.532116908	17.80420894	1.926573022	0.351803834	11.68470556
142	0.006276324	157.9530198	18.30018314	1.100281781	17.63781828	0.824320058	0.339017659	3.327807028
143	0.005912464	83.18334587	17.52827689	1.011631387	17.5926762	0.997425654	0.380333341	10.77513498
144	0.001929232	336.815081	17.95565932	1.733834564	18.40550352	2.554585353	0.055002285	55.68752586
145	0.004677162	321.1912109	17.5197081	1.089318224	17.76805273	1.81754456	0.045887878	27.42149745
146	0.009131477	82.3678813	17.64802	0.888464547	18.30953691	1.781200424	0.045914451	15.75535097
147	0.008939503	1.637664091	17.68355662	0.201825215	18.04293249	1.596063001	0.04816109	39.74790127
148	0.010551159	84.31765396	17.74997405	0.277123275	18.10363569	0.744479492	0.058493888	5.885253461
152	0.00164194	77.31345655	0	N/A	0.000114641	N/A	0.00181436	32.13759895
153	0.001990863	48.1302091	0	N/A	0.000483698	202.104618	0.007314029	48.59283037
154	0.00252912	42.11628098	0	150.0267802	0.000559531	96.16122638	0.004485159	44.69103528
155	0.001108355	132.496225	0	N/A	0.000139057	N/A	0.004707867	10.79481208
156	0.00194129	32.64544963	0	1317.565216	0.000214808	N/A	0.005709605	8.852536062

	118 -> 118 Sn [O2]		137 -> 137 Ba [O2]		139 -> 155 La [O2]		140 -> 156 Ce [O2]	
Numbers	Conc. [ug/l]	Conc. RSD	Conc. [ug/l]	Conc. RSD	Conc. [ug/l]	Conc. RSD	Conc. [ug/l]	Conc. RSD
82	0.003319338	35.6161671	4.704988632	0.472356092	0.08570283	3.786311982	0.104826209	1.856483592
83	0.004563361	27.45746564	4.563446663	0.62933154	0.176560639	5.450169311	0.252921088	4.295680872
90	0.001833727	85.15052196	4.15337996	2.559499293	0.123935273	4.888190479	0.176454003	3.052545716
95	0.16542829	26.45727921	15.72931204	3.322474316	42.64497619	2.019098585	79.39609192	0.088471177
96	0.059213929	39.85767681	15.9050909	3.451755283	38.52578148	0.934314289	70.56144643	1.336755573
97	0.051339858	15.93182635	16.69721166	1.722066164	38.35211208	1.568168886	70.45625994	0.597051037
98	0.040382462	32.91096954	23.30995208	0.214532579	7.486384981	0.229602706	7.424205129	2.333569816
100	0.042330276	25.95932029	21.67941694	5.048598461	20.42193784	1.93755325	29.28191673	1.484182668
103	0.052467344	25.36182025	21.24660974	1.54007677	38.86264669	0.543772653	57.42725566	0.501153045
104	1.052117467	1.844552032	0.026538362	33.12450878	0.001953808	45.37408691	0.003217141	38.20306436
105	2.013842345	2.845605846	0.07082598	2.639366749	0.001527942	37.04882727	0.00264393	26.54482313
106	2.085718175	2.297968605	0.082638635	5.274485435	0.001223498	35.09468348	0.001484231	23.14488948
107	2.213257039	1.080733525	0.094504568	8.965229974	0.00099001	37.15368047	0.001654873	8.841006723
108	2.220471573	2.292061069	0.105540222	10.49646621	0.000798758	24.57025748	0.000671842	67.76020124
109	0.942792476	1.540713716	0.035568135	40.14402556	0.000658033	37.20827444	0.001407984	32.13389751
110	1.695974999	4.454208692	0.067661953	9.067860959	0.00013158	173.2050808	0.000195233	118.2097846
111	1.791765327	2.166917189	0.068050504	6.072280466	9.79233E-05	173.2050808	0.000268932	64.6218919
112	1.79706433	0.931829868	0.067069733	5.741081238	0.00016468	34.73967092	9.0985E-05	142.4720696
113	1.842406158	1.475116259	0.077096946	7.712884298	0	N/A	0.00016418	152.3251292
114	0.086927851	14.26180671	14.07765607	4.295574829	10.68952923	1.233018672	20.6561734	1.859785298
115	0.564561894	10.90416561	14.29653097	2.849185301	10.65955784	2.016312262	21.18467918	2.563988965
116	0.636688067	5.576442249	15.18694063	0.553222223	10.69375286	2.172805482	20.93139666	0.834120509
117	0.736359899	5.081780998	14.86596225	6.148863195	10.75412628	1.217051568	21.09783072	0.559793224
118	0.764094197	6.51155171	15.09770071	0.703266561	10.72901857	0.381622743	21.09763539	0.970651961
119	0.073381508	34.33521239	14.5631575	0.705854311	12.90633418	1.286277185	25.25111152	1.750476563
120	0.149823108	27.99819854	14.39249435	2.100747254	12.96405404	1.972149115	24.96747508	2.861329672
121	0.180902213	9.965602551	13.68129405	1.630344532	12.84944805	0.912180325	25.02839681	0.91419146
122	0.254692198	8.346386533	13.93867734	3.882590887	13.03737815	0.502191364	25.30499874	1.88599633
123	0.287213772	21.14520556	14.5827198	1.873389803	13.15097455	1.570715327	25.13549224	1.402285689
124	0.137611116	22.04632498	14.72079856	7.092476274	12.76832937	1.596247077	25.10299286	0.806259462
125	0.216313205	9.180965662	14.43197294	1.929134689	12.77797773	1.11047454	25.1696168	2.130132255
126	0.242668726	9.179477297	14.94403659	3.810996794	13.25636292	1.946353181	25.01333071	0.622661371
127	0.228304343	11.34037185	14.34227389	2.296358232	12.8748585	1.031665214	24.991	1.302863602
128	0.322332747	10.10078229	14.44963012	3.945768146	12.98114623	0.393073559	24.90113264	0.332384919
129	0.07324892	18.46058763	14.77270598	3.752792648	13.07155202	1.898558798	25.4269166	1.791583174
130	0.079718345	22.96262835	14.35954478	2.569004064	13.02151807	1.656798629	25.18027944	0.14592564
131	0.075792778	6.143119794	14.43671423	3.428084888	12.84621388	0.694444272	25.0781202	0.784460201
132	0.069453757	30.62000415	14.62031354	1.314267207	12.80665633	1.40024001	25.03028249	0.465347479
133	0.053315737	26.78171004	14.69639802	2.645612716	12.68329401	2.877590218	24.9564828	0.554395021
134	0.035756193	51.58741431	15.15551866	1.107751652	8.661976679	2.190765554	16.10780005	1.100444125
135	0.173879258	9.134819605	15.04435996	5.176550487	8.508867717	0.421639511	16.02124909	1.558529364
136	0.212722472	31.4864674	15.46123493	2.106899639	8.569975718	1.141829925	16.25579806	1.039259669
137	0.200548832	5.489479398	14.92461822	0.38657196	8.292879667	4.008684113	15.45129327	1.097480904
138	0.185697818	22.65161919	15.02438929	5.407278736	8.487043583	0.391457493	15.55941537	2.334176348
139	0.112210042	24.2283167	14.70001962	3.252997048	8.584721336	2.510985861	16.28437436	0.866065435
140	0.263651129	17.04839015	14.93518409	1.269597009	8.552480379	1.403494657	16.08673927	1.783514859
141	0.330712462	12.19491795	15.25558091	2.326897974	8.47470263	1.059788333	15.74263877	0.768963944
142	0.369783335	11.88298463	14.91187252	2.921928489	8.318809895	0.086549111	15.60132493	0.769601988
143	0.358278978	9.29548935	15.01283046	7.56486621	7.935232388	0.992583193	14.85289147	0.903760416
144	0.075852411	18.31848391	15.33054423	6.615070416	8.426059545	0.944597618	16.3904961	0.235092602
145	0.051543996	5.093841684	15.14161111	3.463561262	8.489130348	1.80062065	16.29198004	0.936509569
146	0.077430896	34.5520892	15.49623819	4.018018157	8.725779584	0.919169079	16.43939536	2.173652902
147	0.062207321	26.9779309	15.12102125	3.740286012	8.646374894	2.425142117	16.03161211	2.87140833
148	0.043317751	4.341671072	14.76410255	4.659111397	8.538953901	2.358284837	15.93307913	0.55344827
152	0.003823856	40.87972225	0	41.72389817	0.00020651	86.60984368	0.000314567	1.897751163
153	0.004697254	20.68998269	0	52.20785429	0.000322701	147.377283	0.001036011	34.92446974
154	0.004716046	14.76169537	0	32.08559618	6.46063E-05	86.60449997	0.00074741	59.03402907
155	0.003648404	40.07714191	0	125.6632216	3.19536E-05	173.2050808	0.000398929	98.30869755
156	0.004110133	41.35417436	0	81.94216849	6.454E-05	173.2050808	0.000192143	101.9681839

	146 -> 162 Nd [O2]		151 -> 151 Eu [O2]		151 -> 167 Eu [O2]		153 -> 153 Eu [O2]	
Numbers	Conc. [ug/l]	Conc. RSD	Conc. [ug/l]	Conc. RSD	Conc. [ug/l]	Conc. RSD	Conc. [ug/l]	Conc. RSD
82	0.088846486	8.879790306	0.003747195	36.34496206	0.003219727	50.64841376	0.004319271	29.44398175
83	0.181060791	7.884168316	0.006109547	12.21272459	0.006917779	31.07050677	0.004930822	21.57602886
90	0.120824188	11.41329685	0.00493545	11.5180754	0.004834281	13.34631219	0.005612617	34.04160671
95	31.24982426	0.869207982	0.71699159	2.008455423	0.771076072	8.468874998	0.691980916	7.09654124
96	27.91126694	1.342561342	0.623611721	20.20832867	0.602446993	2.665528608	0.656653819	5.53894465
97	27.24270985	2.790260341	0.644893061	6.732317826	0.630253764	7.438500127	0.652085591	9.881013529
98	1.877620512	6.798110861	0.027349589	18.74054814	0.016659764	87.83387302	0.022842852	13.4609024
100	9.435369669	2.589911806	0.182026825	14.50883449	0.159069144	33.22054603	0.192553142	12.93074513
103	18.30469481	2.883170616	0.345393582	17.42065544	0.290362577	27.98199601	0.293674089	16.13808551
104	0.000859355	69.7806032	0	N/A	0	N/A	0.000180012	173.2050808
105	0.001202071	24.82273687	0.000101677	173.2050808	0	N/A	0	N/A
106	0.001529255	56.85249113	0	N/A	0	N/A	0.000177304	173.2050808
107	0.000682623	114.1831637	0.000200833	173.2050808	0	N/A	0	N/A
108	0.000344422	173.2050808	0.000301397	173.2050808	0	N/A	0	N/A
109	0.000171935	173.2050808	9.82133E-05	173.2050808	0	N/A	8.9044E-05	173.2050808
110	0.000169989	173.2050808	0	N/A	0	N/A	0	N/A
111	0	N/A	9.81745E-05	173.2050808	0	N/A	0	N/A
112	0	N/A	0	N/A	0.000171005	173.2050808	0	N/A
113	0	N/A	0	N/A	0	N/A	9.15212E-05	173.2050808
114	9.461807194	2.760772894	0.165984332	16.63370671	0.179904218	7.365712245	0.176172923	13.89830788
115	9.501203214	3.12905949	0.174394241	8.612337633	0.194482774	30.37780732	0.224073246	11.0139182
116	9.247518835	3.110328662	0.219894358	5.278944555	0.232816281	8.753069855	0.182770725	8.502717365
117	9.085224369	4.369511354	0.193712279	5.678218433	0.215826266	24.16529534	0.179870957	14.97277533
118	9.307952864	3.005141258	0.222168526	12.25385427	0.206005963	17.7355274	0.222068011	1.792774765
119	11.46530823	2.014702152	0.259905077	6.23477191	0.206563287	21.41715481	0.265142473	8.375305658
120	10.89874718	4.01379101	0.289644307	3.657287243	0.232186898	15.66003993	0.232644528	5.916092962
121	10.79988048	1.845114173	0.263426265	18.05548979	0.204638728	25.4401749	0.26035087	13.7401405
122	11.05247128	1.474552085	0.253240272	9.258954491	0.233707523	25.90058383	0.24917384	13.75004088
123	10.80857675	2.999253857	0.243593886	11.70704195	0.240665407	3.91500173	0.289383477	4.514929808
124	10.84795058	2.205847106	0.270593545	12.75819456	0.285795161	21.47896941	0.241049862	16.90462027
125	11.06269594	4.496290926	0.277085936	14.5509619	0.300046909	3.833409977	0.252992921	18.47665446
126	11.05585313	1.03292143	0.247431635	15.86476963	0.251155805	17.9999868	0.29269325	8.730963468
127	10.86496186	4.881599252	0.291043652	16.69594041	0.21959868	14.82105514	0.270660447	6.408919087
128	10.74913683	1.686114851	0.245037885	13.07757197	0.263802148	16.86150237	0.230723654	12.2637614
129	11.28499496	2.92483366	0.248377116	11.85315621	0.292505901	16.25320189	0.241686981	7.263939518
130	10.79861786	0.457688409	0.259005497	8.187233524	0.317773092	8.513402847	0.272889056	6.077828026
131	10.63847232	3.323849491	0.257553623	28.46198732	0.230594418	14.66291209	0.252351336	3.173881309
132	10.72530165	5.102900282	0.268767017	6.439549057	0.244138435	26.95654983	0.272949733	24.80194659
133	11.04109977	0.495538372	0.25496703	9.009892804	0.264437991	24.98759659	0.243997027	8.901574333
134	6.713163804	3.028814258	0.151781556	9.85534805	0.168614327	8.31936315	0.147732908	29.27546972
135	6.857975186	1.168771528	0.158645956	16.92114529	0.155747248	15.83061881	0.13580231	17.6541425
136	6.841177811	4.586924026	0.165737682	10.48593609	0.147684981	37.80826279	0.143629425	8.804726718
137	6.809551307	5.876479469	0.154808149	1.943814368	0.17518733	13.00387998	0.168526059	15.2122508
138	6.516879377	4.428238335	0.143134086	16.6674796	0.175784926	18.25694815	0.134460327	3.561640239
139	7.01160229	2.611783992	0.164993668	7.241335185	0.171482662	20.45860032	0.181417981	22.63655242
140	6.700873167	0.281315834	0.151168105	10.19834265	0.128829889	14.07119864	0.158370243	20.89399872
141	6.996182763	4.222739725	0.171386091	6.449348682	0.176914657	17.1038524	0.156296302	11.01597178
142	6.737871433	5.938356046	0.129939751	23.37688202	0.181280165	17.40105006	0.143418121	6.881996444
143	6.092122473	2.110905943	0.177420351	3.528041762	0.161053889	18.87493198	0.156828865	10.8303314
144	6.893421898	3.827399759	0.165913066	17.09955016	0.158457442	23.52469365	0.139808523	31.50921773
145	6.859483678	3.496929992	0.153590382	24.66693004	0.156717477	9.519134841	0.171151413	14.69551102
146	6.785604495	6.745653442	0.143747252	25.90028964	0.169493289	25.92859912	0.176700284	8.797583518
147	6.817149821	6.554717938	0.174328452	20.27606412	0.176666516	33.36904015	0.138491345	17.7118466
148	6.863442777	7.05169376	0.156922302	20.59353062	0.177589587	11.36345376	0.14265239	23.65272638
152	0.000532111	99.50265247	0.000103972	173.2050808	0.000180424	173.2050808	0.000188291	173.2050808
153	0.000166251	173.2050808	0	N/A	0	N/A	0.000180507	173.2050808
154	0.000332972	173.2050808	9.71078E-05	173.2050808	0	N/A	0.000258433	173.2050808
155	0	N/A	0	N/A	0	N/A	0	N/A
156	0.00016495	173.2050808	0.00019451	173.2050808	0.000335805	173.2050808	0	N/A

	153 -> 169 Eu [O2]		157 -> 173 Gd [O2]		163 -> 179 Dy [O2]		165 -> 181 Ho [O2]	
Numbers	Conc. [ug/l]	Conc. RSD	Conc. [ug/l]	Conc. RSD	Conc. [ug/l]	Conc. RSD	Conc. [ug/l]	Conc. RSD
82	0.004522823	22.22980688	0.01582269	35.09808633	0.017900358	13.3307647	0.004286802	12.01284719
83	0.008427974	51.5836599	0.031592564	19.42542738	0.026762904	3.803282811	0.00619948	29.04553169
90	0.004421005	42.11049821	0.022229083	31.94594455	0.019636915	27.2931708	0.005037808	13.35155644
95	0.750957631	20.43318168	4.828052731	1.414016983	3.939305544	0.846739131	0.761377935	6.380757833
96	0.583642162	7.378676267	4.389526687	2.165588733	3.586467392	3.368179208	0.65067498	1.157141294
97	0.661120134	12.85590527	4.502141306	2.733144286	3.414103255	5.775782873	0.670569038	4.594027844
98	0.018736423	41.55275055	0.250809283	10.6322873	0.154124554	9.103291202	0.037939578	12.11167739
100	0.154345046	7.707595464	1.549770985	4.170104309	1.026656064	5.654375037	0.216901081	2.660626229
103	0.375976987	1.921312179	2.715672336	2.204447763	2.065455569	4.797124222	0.43438354	6.306432351
104	0	N/A	0	N/A	0.000334509	119.029869	0	N/A
105	0.000159183	173.2050808	0	N/A	0.000466433	98.35531993	3.37523E-05	173.2050808
106	0	N/A	0.000424848	86.62095795	0.000203401	227.0923281	0	N/A
107	0	N/A	0.000213874	173.2050808	6.64431E-05	338.1230688	3.34132E-05	173.2050808
108	0	N/A	0	N/A	7.14598E-05	326.5026833	0	N/A
109	0.000311491	173.2050808	0	N/A	0.000197128	228.7606006	0.000100581	100.6911652
110	0	N/A	0	N/A	-6.32114E-05	N/A	0	N/A
111	0	N/A	0.000211883	173.2050808	-6.31938E-05	N/A	0	N/A
112	0	N/A	0	N/A	-6.31762E-05	N/A	0	N/A
113	0	N/A	0	N/A	7.04652E-05	328.4505539	0	N/A
114	0.194428148	21.59253773	1.470777395	5.17032066	1.090829756	5.955997202	0.208942219	13.43145225
115	0.190165574	16.76600003	1.329129866	2.735064962	1.115488298	8.292604515	0.187175087	6.097579353
116	0.16295803	24.51540986	1.306630035	5.115864445	1.060150975	2.366691894	0.19903926	7.935694637
117	0.181774313	15.46079643	1.321557797	5.424396111	1.057271494	3.874274184	0.195056854	4.784016925
118	0.209394105	15.88044264	1.485780045	10.01605872	1.088273254	9.304319924	0.197103413	9.398687763
119	0.305912203	13.51022979	1.852853841	6.672243388	1.271497464	2.471842123	0.261757775	2.836115669
120	0.27511202	34.25240149	1.647062551	9.641921777	1.263443988	6.270915565	0.244667344	2.396802806
121	0.278125041	3.819689817	1.64310573	11.53708845	1.333483461	16.68664536	0.262443932	11.16234625
122	0.249948202	3.094784264	1.666760227	13.50868716	1.279720972	8.653577508	0.241452133	10.60368175
123	0.230023774	9.737076087	1.695454997	7.607638465	1.333498727	2.498629903	0.250576652	6.295755326
124	0.234990909	11.62549563	1.691926639	10.54720443	1.347613819	5.341865406	0.260380268	2.184985557
125	0.237235433	5.894542398	1.714335368	7.823012292	1.376815056	4.036855962	0.257839575	8.369485932
126	0.257502977	21.7041592	1.652342045	8.274666793	1.328515047	9.521870784	0.25117391	7.267680257
127	0.272454191	8.714918357	1.776692322	4.758962573	1.240959535	7.295487095	0.258678628	11.57513279
128	0.268581002	13.75715294	1.718317555	4.560949856	1.309420021	5.589911532	0.231357198	5.062633673
129	0.272364088	22.1296544	1.644965943	8.196103712	1.366093769	3.064010645	0.253298565	1.516017489
130	0.2690278	12.8294581	1.689496078	15.20458725	1.349353189	5.676776231	0.248134316	3.94765849
131	0.214115417	16.84333471	1.7014738	7.268753632	1.353640778	7.203232722	0.236948872	2.976475714
132	0.23887496	18.55938017	1.609619814	6.381085103	1.324071274	9.618425866	0.256837446	9.368163255
133	0.229148528	10.4643232	1.666773296	6.020567257	1.408506498	5.996190582	0.242573045	5.956330704
134	0.159214926	13.93781328	0.923050449	18.98678079	0.765649552	1.11577632	0.1590446	2.588463463
135	0.142048938	29.85846901	1.05865797	10.28105702	0.770275465	15.1660545	0.16292979	2.62775461
136	0.142069375	13.79949632	1.054914196	6.337312525	0.947683131	8.512613764	0.163498852	10.94090558
137	0.153540614	22.39874429	1.121893591	7.133929604	0.737385361	6.725294103	0.161985642	19.74095523
138	0.171141786	7.692268233	0.956318063	9.53665067	0.751316839	5.291089106	0.144456293	6.188397349
139	0.110326463	14.27720601	1.008811734	8.164294982	0.833727003	6.091096394	0.146065078	12.8149288
140	0.154966437	19.40663747	1.043964318	2.369839526	0.759517301	8.268278861	0.152454589	16.36385182
141	0.127475494	38.70500609	0.935232966	13.28263343	0.809451505	3.96622369	0.152765179	17.84124376
142	0.154483999	7.340832967	0.942049487	7.075094368	0.772801412	5.274094371	0.174502989	6.874396107
143	0.134669886	29.13563149	1.018788541	16.06205864	0.736305168	11.82345044	0.137561549	14.02033742
144	0.139241378	15.74752594	1.107612761	4.97863813	0.838775958	13.0024384	0.173653675	10.38234962
145	0.162680691	4.914456043	1.020624022	19.02863824	0.727326383	4.377421588	0.154776218	1.475512391
146	0.181958073	14.94775308	0.981702979	1.659655418	0.818207112	14.78076248	0.165300792	3.409998309
147	0.169838658	27.09249149	0.96102261	3.8640746	0.850907388	2.162829897	0.145663636	10.06169766
148	0.15674577	5.99197728	0.964851633	9.757312659	0.808521303	7.923235327	0.135777326	9.516384736
152	0	N/A	0	N/A	0.000212491	224.5722656	0	N/A
153	0	N/A	0	N/A	6.67512E-05	336.7234073	0	N/A
154	0	N/A	0	N/A	0.000196693	114.3489808	0	N/A
155	0	N/A	0	N/A	-6.3018E-05	N/A	0	N/A
156	0	N/A	0	N/A	-6.3018E-05	N/A	0	N/A

	166 -> 182 Er [O2]		182 -> 182 W [H2]		202 -> 202 Hg [O2]			208 -> 208 Pb [O2]	
Numbers	Conc. [ug/l]	Conc. RSD	Conc. [ug/l]	Conc. RSD	Conc. [ng/l		Conc. RSD	Conc. [ug/l]	Conc. RSD
82	0.012794157	16.90656855	0.001123604	28.16950095	0.15015015	<5.0	45.81603658	0.01765532	2.627818272
83	0.021338781	12.78186617	0.003552731	35.23308993	0.03003003	<5.0	43.75299855	0.179803453	2.808944908
90	0.016379091	19.1204772	0.001584689	50.59791896	0.600600601	<5.0	182.722548	0.022747354	2.301914417
95	2.153369948	2.191168752	0.016106328	79.11772277	2.72055E-15	<5.0	N/A	3.351133996	1.79329742
96	1.906431013	8.739757141	0.012608959	87.001736	0.720720721	<5.0	N/A	3.070908221	2.889866574
97	1.922992019	10.20669186	0.015875594	79.22892536	0.660660661	<5.0	N/A	3.217719172	5.795093965
98	0.100254108	30.62805862	0.105119587	10.00559025	0.24024024	<5.0	N/A	0.04896682	57.9963615
100	0.650044005	15.64163432	0.027695317	17.12570179	2.72055E-15	<5.0	N/A	0.079047635	34.27326504
103	1.225046863	5.603216012	0.016269554	59.94218771	0.06006006	<5.0	N/A	0.197598724	19.74548889
104	0.000205107	173.2050808	0.000495108	155.539457	-0.27027027	<5.0	N/A	0.03840379	10.74652292
105	0.000102005	173.2050808	0.000938729	146.6522526	0.15015015	<5.0	N/A	0.106004484	7.841634583
106	0	N/A	0.000946701	66.4547711	0.990990991	<5.0	787.2714231	0.108117379	3.772015665
107	0.000101588	173.2050808	0.000787811	71.94855605	0.630630631	<5.0	N/A	0.112589897	6.896252189
108	0	N/A	0.001117693	102.8662528	0.750750751	<5.0	N/A	0.115639638	10.65795418
109	0	N/A	1.1214E-05	N/A	-0.03003003	<5.0	N/A	0.095598898	0.676199948
110	0.00020184	86.61250647	0.000632783	194.5872683	0.15015015	<5.0	N/A	0.114693026	4.203623477
111	0	N/A	0.001560763	68.30858004	0.690690691	<5.0	N/A	0.116206337	5.903688272
112	0	N/A	0.000940079	132.8144846	1.171171171	<5.0	N/A	0.112203287	10.39302558
113	0	N/A	0.001236967	83.68702898	1.051051051	<5.0	N/A	0.111524804	6.809111209
114	0.617784677	5.842123911	0.010177235	67.34717109	1.201201201	<5.0	N/A	17.57647185	3.716230028
115	0.581710841	15.883182	-0.001010938	N/A	0.36036036	<5.0	N/A	18.11387756	1.195321276
116	0.594766777	7.354335209	0.004141076	95.57654831	-0.06006006	<5.0	N/A	17.48739578	3.642074591
117	0.567146882	4.374585304	0.002404741	186.1914444	0.06006006	<5.0	N/A	17.15758501	0.587588837
118	0.553228049	10.05075538	0.000682809	445.4859214	0.600600601	<5.0	N/A	15.99480969	0.716031533
119	0.73675868	4.257308031	0.004915871	52.39774401	0.540540541	<5.0	N/A	18.288707	2.140008623
120	0.643502166	10.33734533	0.004138415	37.24514879	0.12012012	<5.0	N/A	23.14475145	1.22312919
121	0.679639935	7.602859757	0.002423327	283.8617786	0.540540541	<5.0	N/A	23.82988906	2.242529108
122	0.773297183	11.73243088	0.004871667	89.89564793	1.771771772	<5.0	84.95158066	24.96093803	1.47372699
123	0.736453596	10.83198227	0.011809926	98.33152478	0.03003003	<5.0	N/A	24.82186546	1.310357328
124	0.713358977	10.34717506	0.000713462	568.0657949	0.03003003	<5.0	N/A	36.41157439	0.827562717
125	0.713397903	2.382675697	0.01005491	134.4973576	-0.03003003	<5.0	N/A	112.999561	1.944742631
126	0.74003673	5.95722029	0.000718583	210.1975667	0.15015015	<5.0	N/A	129.9304943	0.352559557
127	0.729450821	5.677973206	0.003328476	43.70790016	0.33033033	<5.0	N/A	140.1066062	2.564761664
128	0.739446198	5.872316459	0.000737273	209.7362654	-0.27027027	<5.0	N/A	147.7830429	0.869793483
129	0.715473176	17.21836244	0.003337355	197.4202166	-0.21021021	<5.0	N/A	20.35438433	2.554233209
130	0.704537682	8.244020919	0.003370419	162.6382544	0.21021021	<5.0	N/A	30.74675028	2.316065309
131	0.7687172	15.91636822	0.005984976	67.62241369	0.570570571	<5.0	N/A	35.84719739	2.197031215
132	0.713689984	7.143038863	0.007723004	69.18239994	0.27027027	<5.0	N/A	41.24922856	2.331519705
133	0.715870688	4.06894734	0.000760695	202.0785164	-0.09009009	<5.0	N/A	48.33892078	1.261007871
134	0.454187666	8.48960517	0.001589303	253.300946	0.27027027	<5.0	N/A	2.779140966	4.416979589
135	0.489981299	10.41422359	0.0024976	106.3759166	0.510510511	<5.0	N/A	2.840343741	0.61938243
136	0.421152546	16.33235962	0.004240359	72.13485136	-0.39039039	<5.0	N/A	2.830291414	9.613205139
137	0.460565396	6.990327644	0.002477417	183.6408547	-0.21021021	<5.0	N/A	2.637426159	3.290996295
138	0.496981395	20.4361738	0.004306487	71.98756723	-0.03003003	<5.0	N/A	2.759132354	5.909648442
139	0.435877679	5.910031946	0.006090101	153.628416	0.510510511	<5.0	N/A	2.952545196	6.478425542
140	0.480241015	8.56349035	-0.000114323	N/A	-0.03003003	<5.0	N/A	8.569177983	3.461456771
141	0.421090651	13.40927128	0.000761376	542.2805245	-0.21021021	<5.0	N/A	10.58738557	1.822891773
142	0.451224408	3.576254951	0.003503618	310.2813774	0.03003003	<5.0	N/A	12.63893993	3.192172983
143	0.396270609	5.536656325	0.001690965	91.35790782	0.09009009	<5.0	N/A	14.47617962	3.388796833
144	0.442764207	16.42250398	-0.0027356	0	-0.33033033	<5.0	N/A	3.387226039	7.78779201
145	0.488547684	9.099662571	0.002641752	205.9843666	-0.15015015	<5.0	N/A	5.635362645	1.815233169
146	0.455892169	13.45790083	0.001735694	239.4074076	-0.09009009	<5.0	N/A	6.76694332	0.957533143
147	0.423040535	12.1509644	0.00441343	126.8265533	0.21021021	<5.0	N/A	6.875335499	1.648099648
148	0.433355854	10.83135944	0.001789182	88.56774206	-0.21021021	<5.0	N/A	7.233632174	3.273859216
152	0	N/A	0.000391525	135.5617286	0		95.30372034	0	27.67156295
153	0	N/A	0.000400059	100.030334	0		65.0298981	0	95.93381995
154	0.00030264	99.95047522	0.000395531	220.3355963	0		N/A	0	243.2798323
155	0.000200256	173.2050808	0.000776447	105.8769134	0		N/A	0	115.623692
156	0	N/A	1.8134E-05	N/A	0		N/A	0	206.4775051

Date	Sample name	Number	Cd111(LR) Conc. µg/g	RSD, %	Mo98(MR) Conc. µg/g	RSD, %	Sn118(LR) Conc. µg/g	RSD, %	W182(LR) Conc. µg/g	RSD, %	Hg202(LR) Conc. µg/g	RSD, %	Tl205(LR) Conc. µg/g	RSD, %
18.11.2019	Loc1Sed	1	7.884992718	0.8	8.61945187	2.6	2.375107258	2.3	0.594622411	1.3	0.533618281	1.2	7.464181777	2.2
18.11.2019	Loc1Sed	1	7.340910974	0.8	7.556317191	4.4	2.170946481	1.1	0.53729712	3	0.476800644	4.2	6.954337965	2.1
18.11.2019	Loc1Sed	2	11.13658599	1.6	8.794597733	3.1	2.174669843	0.5	0.4446049	2.3	0.656628006	3.1	8.285049943	4.9
18.11.2019	Loc2Sed	3	9.710524071	1.3	7.724853236	1.6	2.37121738	0.9	0.379672772	1.3	0.49142421	0.8	11.63300015	3.3
18.11.2019	Loc2Sed	4	9.661050292	0.8	8.198119758	2	2.45149354	0.8	0.388175671	2.4	0.489991965	2.1	10.9666896	2.5
18.11.2019	Loc3Sed	5	0.160945758	6.7	0.675683098	13.3	0.329242114	4	0.010009289	3.9	0.046469702	10.1	0.423393402	1.8
18.11.2019	Loc3Sed	5	0.170457272	5.1	0.620942687	6.9	0.361156539	1.9	0.012505497	6.3	0.051361411	7.4	0.478994445	4.7
18.11.2019	Loc3Sed	6	0.138815847	7.4	0.6117057	3.5	0.383422079	0.6	0.040607006	9	0.048556602	4.4	0.524190465	1.8
18.11.2019	Loc4Sed	7	1.447704296	1.9	1.512942698	9.6	1.045718824	2	0.05541183	6	0.170868418	7.7	1.318045639	5.6
18.11.2019	Loc4Sed	8	1.251304123	3.5	1.581070649	10.3	0.998965628	0.6	0.043852521	7.8	0.16993207	3.7	1.171947651	4.4
18.11.2019	Loc5Sed	9	4.54025076	1	6.942276844	3.8	2.238213606	0.5	0.355182945	0.6	0.45646835	7	5.144492126	2.3
18.11.2019	Loc5Sed	10	4.928519968	0.6	7.58310771	2.3	2.195205789	1.4	0.397845613	0.9	0.503096119	5.9	5.636301081	5.8
18.11.2019	Loc5Sed	10	4.923436904	2.7	7.664154355	4.1	2.171797618	0.9	0.37340908	1.1	0.501125663	6.3	5.300326372	3.7
18.11.2019	Loc6Sed	11	1.041984836	2.7	4.317748688	1.8	1.377199889	1.7	0.166739139	5.7	0.242323503	8.3	3.235222612	6.5
18.11.2019	Loc6Sed	12	1.016295026	3.5	5.092181772	7.3	1.652016608	1	0.19856425	4	0.250460274	4.6	3.179376317	6.5
18.11.2019	Loc7Sed	13	0.348772626	4.5	1.764351948	8.8	0.743199741	5	0.099780743	26.6	0.09141087	2.6	1.104505407	1.1
18.11.2019	Loc7Sed	14	0.366981466	5.2	2.073419174	2.7	0.637806978	2.1	0.079232831	4.3	0.080054681	13.1	1.139887141	6.5
18.11.2019	Loc8Sed	15	7.071705931	1.7	5.841248475	2.2	1.388137759	0.8	0.275567257	5.1	0.381671856	0.8	6.886876427	1.7
18.11.2019	Loc8Sed	16	38.78530462	2.2	7.499920363	30.1	1.924659734	0.8	0.374266109	3	1.717855961	3.6	12.87267294	2.2
18.11.2019	Loc9Sed	17	0.420595231	1.1	2.449650884	1.2	0.944129663	1.6	0.10324973	3	0.130063384	1	1.442060125	1.2
18.11.2019	Loc9Sed	18	0.366912717	2.4	2.043374703	5.9	0.910028659	3.1	0.07991797	3.9	0.108995224	16.7	1.474596808	3.2
18.11.2019	Loc10Sed	19	0.115971645	0.7	0.344769857	0.8	0.370915726	6.3	0.03054936	39.1	0.043546454	11.7	0.311729257	6.1
18.11.2019	Loc10Sed	20	0.120201738	3.5	0.388017825	15.1	0.383468815	1.7	0.037808076	5.9	0.040737757	3.2	0.366331077	2.9
18.11.2019	Loc11Sed	21	1.706094355	4.4	4.345448297	5.3	1.374706305	3.5	0.164855484	4.9	0.183415038	4.6	2.069663088	3.4
18.11.2019	Loc11Sed	22	0.153677505	2.2	0.554416406	6.1	0.261738649	3.2	0.033193669	8.8	0.037253842	7.3	0.299542321	5.4
18.11.2019	Loc12Sed	23	1.223471911	1.5	0.972627693	9.6	0.720663266	2.1	0.053436709	6.8	0.092860651	6.1	0.966076437	2.2
18.11.2019	Loc12Sed	24	0.789389445	2.8	0.634619756	15.8	0.445038972	2.4	0.087676092	4.8	0.061473628	5.2	0.566418575	3
18.11.2019	Loc9Sed	25	17.7981139	0.3	8.377602604	0.4	4.754529359	1.3	0.639821529	2.6	0.979575822	4.7	17.44704692	2
18.11.2019	Loc4Sed	7.2	1.4878388	1	2.226616492	9.4	1.157706397	1	0.083340035	6.1	0.160963764	0.3	1.410571448	3.9
18.11.2019	Loc4Sed	7.3	1.610988524	2.4	2.028590025	8.6	1.217441463	2.9	0.092134048	7.7	0.183600154	6	1.580606544	5
18.11.2019	Loc11Sed	21.2	1.640468579	1.9	4.036762584	2.3	1.223230779	1.1	0.146216841	5.2	0.180676634	2.2	1.955625255	3.6
18.11.2019	Loc11Sed	21.3	1.811395582	2.1	3.876408997	9.7	1.107462467	2	0.174103122	2.5	0.20771028	9.5	2.065924191	7.7
17.01.2020	Blank	Blank UC	0	123.9	0	82.3	0	0.8	0.014532364	31.4	-0.003171957	46.6	0	173.2
17.01.2020	Blank	Blank UC	0	173.2	0	114.6	0	9.1	0.011837228	9.3	-0.007407572	37.1	0	173.2
17.01.2020	Blank	Blank UC	0	173.2	0	173.2	0	17.7	0.004994807	23.6	-0.008376228	23.4	0	173.2

Date	Sample name	Number	Li7(MR) Conc. µg/g	RSD, %	Na23(MR) Conc. µg/g	RSD, %	Mg25(MR) Conc. µg/g	RSD, %	Al27(MR) Conc. µg/g	RSD, %	Si29(MR) Conc. µg/g	RSD, %	P31(MR) Conc. µg/g	RSD, %
18.11.2019	Loc1Sed	1	11.59747501	3.8	17085.78122	2.8	10911.83762	1.7	16737.01035	1.6	2223.367248	1.8	611.4075886	0.1
18.11.2019	Loc1Sed	1	10.47918478	2.6	15654.77331	3.3	9523.702543	1.2	14952.21045	1.2	2148.244806	4	579.0898798	1.9
18.11.2019	Loc1Sed	2	11.00243684	1.3	7793.17286	1.7	9432.444611	2.3	15785.38753	2.5	2643.518585	2.2	367.4043922	2.2
18.11.2019	Loc2Sed	3	8.732972917	3.4	6755.194978	1.2	8719.445943	1.2	14699.22694	2.5	2153.503063	1.8	391.2075041	4.5
18.11.2019	Loc2Sed	4	11.33054649	3	7691.172936	0.7	8354.003123	3.2	14582.75674	1.1	2210.866129	6.4	371.1308883	3.6
18.11.2019	Loc3Sed	5	4.441751181	2	5117.20478	1.9	3880.748008	1.6	5203.419666	1.9	1125.858483	2.5	389.7759247	1.2
18.11.2019	Loc3Sed	5	4.45057859	1.4	5283.396951	3.4	4027.685858	1	5423.52222	1.3	1168.089178	0.6	397.2786188	1.6
18.11.2019	Loc3Sed	6	2.37753686	3.4	3551.057642	1.1	3395.405925	1.4	4056.826836	0.5	1926.712632	4	171.8671344	4.2
18.11.2019	Loc4Sed	7	6.984747065	0.4	14497.44283	1.9	8130.640712	2.2	10794.5319	1	1683.642517	3.9	726.5868668	1.5
18.11.2019	Loc4Sed	8	6.050765713	1.5	13230.36634	1.9	7337.137716	1.7	10010.2728	3.2	1419.659723	1.3	622.223642	1.7
18.11.2019	Loc5Sed	9	14.06135595	1.5	11123.74765	5.5	12578.67559	4.8	19856.83211	3	2045.76653	2.5	1003.458942	1.1
18.11.2019	Loc5Sed	10	15.29757582	2.1	12246.59294	1.5	13130.49034	1.1	21292.34402	1.2	2210.470104	5.6	1097.995144	2.6
18.11.2019	Loc5Sed	10	15.88229767	1.6	11809.23908	1.2	12915.51028	0.8	20876.92653	1.7	2127.83387	2.4	1081.815627	0.9
18.11.2019	Loc6Sed	11	13.08351741	1	8661.232355	3.1	10633.85523	4.4	17030.72006	2.7	2003.686529	4.4	942.1836673	0.6
18.11.2019	Loc6Sed	12	12.2708352	2.9	9476.760122	2.3	10429.56385	2.6	16977.39661	2.1	2208.898382	6.6	915.0953108	1
18.11.2019	Loc7Sed	13	4.483893049	2.5	6201.198543	1.9	5137.148826	0.8	7622.23122	2.3	2129.117835	2	296.0284849	2.6
18.11.2019	Loc7Sed	14	2.92339242	3.5	5299.812527	4.2	4373.50654	1.2	5574.463468	5.5	1774.83812	1.1	267.9334203	2.9
18.11.2019	Loc8Sed	15	3.630063502	2.3	4795.357097	3.6	5588.897544	2.6	8826.882013	0.2	2153.523651	4.1	265.872024	6.1
18.11.2019	Loc8Sed	16	4.451110537	1.1	3898.757228	2.8	5753.08437	3.1	9297.581044	1.3	2541.16541	1.3	108.4216941	1.7
18.11.2019	Loc9Sed	17	5.776089953	1	6732.785152	2.5	5634.875001	1.3	7918.71139	0.9	1740.089267	2.3	497.6859808	3.1
18.11.2019	Loc9Sed	18	4.889353649	1.2	5944.741489	2.8	5190.203484	1	7452.814846	1.4	1960.207512	1.1	444.0740393	1.4
18.11.2019	Loc10Sed	19	2.240353174	4.5	3692.787149	2.9	3472.684364	2.1	4170.602079	3.2	1736.319301	0.5	179.2500399	6.5
18.11.2019	Loc10Sed	20	2.31418849	2.5	4273.886586	2.9	3699.627834	1.3	4434.815775	0.7	2528.102626	2	168.1136702	1
18.11.2019	Loc11Sed	21	5.752787463	4.4	6729.770667	2.1	6011.242259	1.2	9048.502687	4.1	2462.887792	5.8	491.4539682	3.5
18.11.2019	Loc11Sed	22	0.957384722	3.7	2205.280378	1.4	2753.13369	2.8	2399.638934	0.9	2220.052594	0.7	95.27180361	4.7
18.11.2019	Loc12Sed	23	6.567329194	1.7	4185.933682	2.9	5365.522641	1.9	8958.416191	2.9	1867.444649	1.7	336.4061302	1.7
18.11.2019	Loc12Sed	24	3.134510536	1	3952.346503	1.9	3999.833381	0.9	5488.31322	3.6	1680.267474	3.6	209.617238	2.5
18.11.2019	Loc9Sed	25	15.80265084	3.8	6739.037298	1.4	13188.21276	1.3	25216.24363	1.9	3170.36884	0.8	757.0240271	2.7
18.11.2019	Loc4Sed	7.2	9.568302364	1.1	13943.0443	1.7	8017.233561	1	11327.93436	2.2	2121.442994	1.4	729.4501165	0.5
18.11.2019	Loc4Sed	7.3	9.705571849	2.3	14957.40194	3.1	8839.12322	1.5	13102.10152	2.2	2163.932596	0.8	799.8873457	1.2
18.11.2019	Loc11Sed	21.2	5.945103512	3.3	6364.974328	2.8	5806.597235	1.1	8249.575017	1.5	1862.667474	2.7	473.1485208	2.6
18.11.2019	Loc11Sed	21.3	6.592424563	2.2	7128.743553	2.3	6455.16498	0.6	9356.245364	0.7	2175.613793	2.8	536.1135239	2.6
17.01.2020	Blank	Blank UC	0	1.4	0	3.7	0	57.7	0	3.4	0	3.6	0	9.2
17.01.2020	Blank	Blank UC	0	3	0	3.7	0	15.1	0	4	0	3.3	0	38.3
17.01.2020	Blank	Blank UC	0	1.9	0	4	0	75.8	0	21.9	0	3.7	0	47

Date	Sample name	Number	S34(MR) Conc. µg/g	RSD, %	K39(MR) Conc. µg/g	RSD, %	Ca44(MR) Conc. µg/g	RSD, %	Ti47(MR) Conc. µg/g	RSD, %	V51(MR) Conc. µg/g	RSD, %	Cr52(MR) Conc. µg/g	RSD, %
18.11.2019	Loc1Sed	1	146306.8041	2.9	5637.330173	1.7	24504.29032	1.4	636.3095509	0.6	72.7347436	1.4	63.73759279	1.2
18.11.2019	Loc1Sed	1	128310.2778	2.9	5106.365112	3.1	21860.77529	3.5	572.4866905	1.5	66.06230801	1.2	56.62943623	0.4
18.11.2019	Loc1Sed	2	139087.6977	0.7	5406.672945	0.9	26573.91176	3.7	463.1213996	1.4	66.43714863	1.3	59.37635329	1.8
18.11.2019	Loc2Sed	3	152206.9805	3.7	4845.288084	0.3	52421.97014	0.9	462.1412806	1.4	56.65862404	2.4	57.3266393	1.9
18.11.2019	Loc2Sed	4	163403.5809	2.7	4990.411186	4.4	43294.15012	2.6	429.9925392	3	54.41107198	1.4	57.96164724	2.2
18.11.2019	Loc3Sed	5	3700.079835	1.3	1866.67177	1.8	238808.6482	2.5	167.4168905	2.2	18.20968855	2.7	12.98242758	2.7
18.11.2019	Loc3Sed	5	3790.185164	0.4	1953.72849	4.9	248414.5443	4	175.8832957	1.4	19.09525305	2.1	13.4650313	2.3
18.11.2019	Loc3Sed	6	2869.407884	0.6	1547.544577	1.4	297191.2057	1.5	229.8141559	2.4	15.84290088	0.7	11.82527015	2.5
18.11.2019	Loc4Sed	7	15572.61104	3.2	4331.652966	2.5	209153.5687	2.2	390.6821014	2.5	54.077439	1.4	34.71892949	1.6
18.11.2019	Loc4Sed	8	13373.23431	1	3845.953639	1.4	190845.9014	3.1	317.5638703	2.3	47.60358708	1.7	31.34224568	2.1
18.11.2019	Loc5Sed	9	83814.56878	3.9	6232.024088	3.5	29298.80226	5.4	566.1715768	2.2	103.1533749	1.9	81.91260022	1.1
18.11.2019	Loc5Sed	10	83470.77284	2.7	6983.264832	1.3	21749.00036	4.5	622.2459961	1.4	112.4497348	4.6	87.02430547	2.5
18.11.2019	Loc5Sed	10	78514.82148	0.3	6626.420533	2.5	20869.10657	1.2	587.1833767	1.7	107.7072592	1.8	84.07287953	3.8
18.11.2019	Loc6Sed	11	29767.29328	1.8	5434.322806	4.6	138773.3129	3.3	537.3865025	1.9	78.99887899	3.1	58.28365588	0.1
18.11.2019	Loc6Sed	12	29344.39995	3.1	5308.073074	1.3	129146.238	2.3	555.9421052	1.4	77.49264323	1.6	57.44269415	3
18.11.2019	Loc7Sed	13	10287.9295	2.1	2703.951053	4.8	292136.8776	2.5	390.4602756	2.4	30.27886706	1.9	22.18078694	1
18.11.2019	Loc7Sed	14	11450.43051	1	2050.217436	5	280951.0443	4.3	280.2876313	1.9	24.36487454	4.5	16.70050362	3.3
18.11.2019	Loc8Sed	15	118241.0632	2.7	2227.441547	2.6	219621.4005	2.3	335.9702933	3.4	36.20474085	1.4	34.87739471	1.3
18.11.2019	Loc8Sed	16	268299.0286	3.6	2537.959614	2.1	58640.60372	2.9	200.0710935	3.9	35.43517519	4.1	42.84326693	1.9
18.11.2019	Loc9Sed	17	11545.67594	1.5	2850.323983	0.7	269259.1028	1.5	344.4944569	0.5	38.82421908	1.6	26.17087154	1.6
18.11.2019	Loc9Sed	18	10577.62672	2	2700.196192	3.1	275730.2659	1.8	339.4651182	3.4	34.4333946	3	24.52923954	2.4
18.11.2019	Loc10Sed	19	2435.438545	1.2	1551.590629	3.9	321184.5	2.6	205.3366359	3.2	15.96427194	1.9	11.33238049	1.7
18.11.2019	Loc10Sed	20	2444.453157	4.7	1731.026061	3.3	342494.486	2.5	253.8638871	0.7	17.17357914	2.3	11.76552444	3.4
18.11.2019	Loc11Sed	21	27366.77666	0.3	3084.488267	1.9	258896.9359	3.5	427.9815513	1.4	44.14586692	1.7	31.62043614	0.4
18.11.2019	Loc11Sed	22	2328.107694	1.2	841.6436183	2.4	373946.1315	2.8	127.1665954	1.9	9.024075585	3.2	5.376509411	2.1
18.11.2019	Loc12Sed	23	11199.07506	2.9	2536.785171	4.2	247344.0248	2.6	364.3661197	4	31.39738595	1.3	27.24222865	2.1
18.11.2019	Loc12Sed	24	7904.115378	2.8	1511.615804	3.1	280540.588	5	281.7205836	2.6	21.13745352	3.1	34.81404138	3.8
18.11.2019	Loc9Sed	25	200154.3877	3.2	8228.594486	0.9	10692.36156	1	729.1560441	1.3	98.97858333	2.2	121.1378397	1.2
18.11.2019	Loc4Sed	7.2	15697.4237	2	4266.89458	2	227582.96	0.7	487.6996456	0.8	54.4711567	3.5	35.40139908	1.9
18.11.2019	Loc4Sed	7.3	17914.37197	1.6	4862.461285	2.6	215261.2825	1.8	466.401091	1.2	59.76297716	3.3	39.58308024	3
18.11.2019	Loc11Sed	21.2	27989.64522	2.2	2841.937355	3.3	263633.3056	0.5	385.6327325	1	41.45224219	3.8	29.72322279	1.5
18.11.2019	Loc11Sed	21.3	30362.86578	3.1	3077.730184	1.3	261094.4735	0.6	343.4029664	1.2	49.35397632	4.3	33.9031896	0.9
17.01.2020	Blank	Blank UC	0	6.7	2.702856441	8	0	8.1	7.149590775	18.8	0	41.7	0	26.6
17.01.2020	Blank	Blank UC	0	9	0.904792464	9.2	0	10.7	2.697016013	10.8	0	44.1	0	19.2
17.01.2020	Blank	Blank UC	0	31.5	2.142617451	16.6	0	23.4	0.1505668	64.3	0	173.2	0	14.3

Date	Sample name	Number	Mn55(MR) Conc. µg/g	RSD, %	Fe57(MR) Conc. µg/g	RSD, %	Co59(MR) Conc. µg/g	RSD, %	Ni62(MR) Conc. µg/g	RSD, %	Cu65(MR) Conc. µg/g	RSD, %	Zn67(MR) Conc. µg/g	RSD, %
18.11.2019	Loc1Sed	1	347.5873782	1.5	182564.1267	1.8	113.0005004	1.1	30.39612806	4	1642.150009	1.5	3597.245393	1
18.11.2019	Loc1Sed	1	309.3021895	1.2	167457.9587	2.2	98.90248723	2.9	27.334839	6.9	1476.152165	2.6	3229.787024	1.8
18.11.2019	Loc1Sed	2	355.0628599	0.8	164261.2857	1.4	134.3742501	0.8	29.90184533	2	1844.43774	0.8	4761.402878	2.4
18.11.2019	Loc2Sed	3	373.4477996	0.4	169452.2397	0.7	106.7719117	1.4	16.65421172	4.1	1278.100406	2.7	4230.451243	1.9
18.11.2019	Loc2Sed	4	372.83759	0.7	180033.688	1.2	116.1670912	1.8	17.94153216	2.3	1339.02395	1	4315.461422	1.8
18.11.2019	Loc3Sed	5	82.25319499	1.8	11984.59099	1.4	4.974609247	1.4	5.165190286	3.7	60.03063815	5.2	115.3336486	3.9
18.11.2019	Loc3Sed	5	87.00383713	3.3	12384.10761	1.1	5.231993193	1.4	6.216280957	12.2	63.18748029	5	122.6440718	9.1
18.11.2019	Loc3Sed	6	69.0808936	0.9	8911.080208	1.3	3.757046398	2.9	4.838161258	12.3	42.17526957	4.8	88.12511765	12.8
18.11.2019	Loc4Sed	7	178.9506837	1.6	37782.59207	5	15.45716823	0.2	14.62022291	7.5	272.4558052	2.2	650.931823	2.2
18.11.2019	Loc4Sed	8	180.2496151	2.4	33409.49438	0.6	13.66459156	2.2	12.92414584	1.9	249.1656849	0.8	582.4062756	5
18.11.2019	Loc5Sed	9	414.9049945	2.6	170134.0378	4.1	76.6017045	1.5	30.67889619	3.4	1100.113725	4.1	2441.612035	2
18.11.2019	Loc5Sed	10	417.153204	1.2	165568.6821	2	76.80923036	3.9	31.66941193	4.4	1222.040154	1	2769.262948	2.9
18.11.2019	Loc5Sed	10	396.4053373	1.8	164791.1779	1.3	74.22130282	0.6	29.09610657	5.1	1181.485551	2.7	2635.500479	2.1
18.11.2019	Loc6Sed	11	285.6963682	1.9	82115.44221	2.6	32.28652129	1.3	21.37697601	5.6	485.4296982	1.7	886.9912308	1.3
18.11.2019	Loc6Sed	12	300.5118476	2.8	84013.18987	0.5	32.84390772	0.5	20.6438855	6.2	477.2319087	2.9	903.8761048	3.7
18.11.2019	Loc7Sed	13	116.9627844	2.4	23472.80317	1.3	11.08976243	3.1	8.080569392	11.9	134.5287535	5.1	248.9204209	3.3
18.11.2019	Loc7Sed	14	95.21680454	1.7	24249.19969	0.6	11.1201527	0.9	6.858005753	9	140.3752339	2.1	252.3855355	4.8
18.11.2019	Loc8Sed	15	187.2257126	1.4	130520.4715	0.7	77.57322911	1	13.33751002	10.1	1179.204658	1.6	2962.961746	1.6
18.11.2019	Loc8Sed	16	289.0413828	2.1	203319.479	2.8	219.7990566	2	28.50162065	2.2	2962.625736	3.1	13901.5549	2.3
18.11.2019	Loc9Sed	17	146.510125	3.1	35727.04428	1.7	13.72499324	1.3	8.812691867	2.9	168.1773545	1.9	379.316754	3.1
18.11.2019	Loc9Sed	18	133.862382	1.1	30129.45916	1.6	12.0879234	3.1	9.039346853	5.8	155.1110931	1.1	325.6753314	8.2
18.11.2019	Loc10Sed	19	70.35295403	2.3	8022.163008	1	3.379302578	6.9	4.863024351	15.9	32.48646013	0.8	69.97738995	1.3
18.11.2019	Loc10Sed	20	71.1563005	0.7	7849.696565	0.4	3.413233774	0.8	5.11249325	29.3	33.31972938	4.5	68.32716847	7.9
18.11.2019	Loc11Sed	21	154.0077134	0.7	52123.22988	3.4	23.03085822	1.6	10.15080741	2.3	358.1123944	2.6	933.9698564	3.5
18.11.2019	Loc11Sed	22	45.14625532	1.8	5500.344509	1	2.346494671	5.2	2.511375659	21.9	33.5365273	2.6	75.14476298	9
18.11.2019	Loc12Sed	23	182.4245884	2.2	22703.25336	1.1	10.98830226	1.2	9.527379543	5	135.7687422	0.5	494.7529153	2.5
18.11.2019	Loc12Sed	24	164.167171	2.9	14669.859	3.3	7.472615921	4.2	6.73764208	14.1	83.81069773	2	275.969581	5.1
18.11.2019	Loc9Sed	25	566.487374	1.6	233856.5872	1	143.4849872	2.3	32.09984233	3.6	2265.282981	2.7	7457.230423	1.8
18.11.2019	Loc4Sed	7.2	180.4610305	3.1	38477.01847	2.5	15.64930238	1.7	15.3734543	16.5	287.6529636	1.1	661.6439353	2.4
18.11.2019	Loc4Sed	7.3	204.5852612	1.2	43327.15832	2.1	18.24345955	1.8	17.01853153	3.1	336.5642094	2.3	699.6142857	0.9
18.11.2019	Loc11Sed	21.2	149.9391435	2.1	52450.68738	3.7	22.72533462	2	9.694894196	8	350.9780529	0.9	865.4079816	4.1
18.11.2019	Loc11Sed	21.3	168.9773349	1.4	58725.14769	2.6	24.83014329	1.3	15.35681344	3.8	375.6918433	1.3	1019.498893	3.4
17.01.2020	Blank	Blank UC	0	100	0	38.5	0	173.2	0	0	0	86.8	0	0
17.01.2020	Blank	Blank UC	0	31.5	0	54.3	0	86.8	0	173.2	0	173.2	0	173.2
17.01.2020	Blank	Blank UC	0	173.2	0	52.9	0	114.6	0	0	0	65.5	0	0

Date	Sample name	Number	Rb85(MR) Conc. µg/g	RSD, %	Sr88(MR) Conc. µg/g	RSD, %	Y89(MR) Conc. µg/g	RSD, %	Ba137(MR) Conc. µg/g	RSD, %	La139(MR) Conc. µg/g	RSD, %	Ce140(MR) Conc. µg/g	RSD, %
18.11.2019	Loc1Sed	1	24.69757018	1.7	56.4672974	1.4	10.12407104	0.3	220.0345049	1.5	10.84614238	3.3	22.56799989	1.8
18.11.2019	Loc1Sed	1	22.37866124	2.6	50.41058742	1.2	9.058103527	2.7	203.0641306	3.3	10.05532172	1.6	21.09010532	2
18.11.2019	Loc1Sed	2	24.34807124	2.5	50.28557115	1.8	9.590731351	2.7	188.103113	1.1	10.63905357	0.8	21.54412788	1.6
18.11.2019	Loc2Sed	3	19.70752804	2.2	54.69896003	1.9	10.27897002	0.8	274.7536511	2.2	9.87168768	3.2	20.21862039	2.1
18.11.2019	Loc2Sed	4	20.13981031	3.3	49.78181036	3.6	10.24748663	1.2	249.3795068	1.3	10.23258301	4	20.64801832	2.3
18.11.2019	Loc3Sed	5	7.63331198	2.8	157.5253227	3.5	3.512017235	5.9	36.1494341	4.6	6.330890889	0.5	12.15774935	2.3
18.11.2019	Loc3Sed	5	8.140032839	4.8	163.7043998	0.8	3.669697335	3.6	38.68781095	0.4	6.611828514	2	12.64326758	1.1
18.11.2019	Loc3Sed	6	6.26073995	1.6	184.5328163	1.5	2.868964889	2.1	34.71085844	1	3.05809757	2.6	5.947047023	3.4
18.11.2019	Loc4Sed	7	18.40988739	3.5	186.9127101	0.8	7.009711104	1	89.3600907	1	8.98393245	3.3	17.62163579	0.8
18.11.2019	Loc4Sed	8	16.34314298	1.1	165.1591097	1.7	6.185264074	2.3	79.32995633	3.8	7.789467763	3.1	15.9417186	3.7
18.11.2019	Loc5Sed	9	30.91506016	1.3	69.41505413	1.9	13.04701767	2.3	190.3407873	1.9	15.28778042	6.7	31.30134229	2.9
18.11.2019	Loc5Sed	10	34.65248829	4.3	68.49244814	5.4	13.16006014	2.2	211.2911661	4.1	16.31948439	1.9	33.61307504	3
18.11.2019	Loc5Sed	10	32.54017082	3	66.48343023	0.4	12.8163474	3.4	204.4737665	2.2	16.43141482	2.7	33.26185575	2.5
18.11.2019	Loc6Sed	11	25.63898168	2.3	128.0569155	1.3	10.18274913	3.8	150.3796865	1.8	12.49371025	5	25.36385812	1.1
18.11.2019	Loc6Sed	12	24.9897928	3.9	128.0095282	0.2	10.96890007	2.4	147.5999746	1.7	11.80318999	1.4	24.31449172	4.8
18.11.2019	Loc7Sed	13	11.79861542	1.7	199.885975	1	4.549563743	1.1	62.91950459	3.7	5.268299368	0.4	10.35272113	2.5
18.11.2019	Loc7Sed	14	9.193609022	3.8	194.7505873	0.6	3.783785824	2.7	53.16041517	3.4	4.590674835	2.7	8.740586343	1.1
18.11.2019	Loc8Sed	15	9.181186288	2.9	154.278803	2.1	5.997462576	1	109.7397103	1.7	5.698577583	1.9	11.83700279	0.6
18.11.2019	Loc8Sed	16	10.93134357	1.3	47.86710751	3.4	6.699288671	3.6	59.63726263	2.4	5.304836812	4.9	11.24498289	2.2
18.11.2019	Loc9Sed	17	12.47398924	3	173.1423467	1.8	4.984466438	1.1	82.75866811	1.4	6.372504989	0.9	12.28174551	0.8
18.11.2019	Loc9Sed	18	11.57959972	2.8	175.8739769	3.5	4.945163235	2.1	80.83725523	2.2	5.604703488	1.7	11.31528799	3
18.11.2019	Loc10Sed	19	6.514846483	3.1	183.1943731	3.8	2.893327977	1.1	31.46486983	3.7	3.548630306	2.5	6.817525148	1.5
18.11.2019	Loc10Sed	20	7.115474502	3.2	196.4713993	2.6	2.792903222	4.7	34.62795724	4.7	3.214538993	4.1	6.374628111	5.1
18.11.2019	Loc11Sed	21	13.85319388	3.6	172.9517067	2.8	6.621437126	3.6	104.6912027	2.5	7.00365091	0.7	14.55204081	1.3
18.11.2019	Loc11Sed	22	3.303092578	2.2	207.2802515	1.3	2.082145693	4.9	20.27921665	0.8	1.880219497	5.2	3.526909103	2.5
18.11.2019	Loc12Sed	23	11.27747421	1.2	163.9389185	5.4	6.835835921	2.2	56.35228684	3.7	7.457209789	3.7	15.01530702	3.4
18.11.2019	Loc12Sed	24	6.395888085	8.3	171.185988	3	5.136978772	5.4	31.19377211	4.8	4.068679432	0.5	8.617240673	4
18.11.2019	Loc9Sed	25	36.48756211	1.1	43.82689219	1.7	18.68464744	1.5	588.3682209	1.8	18.96085034	3.3	37.76450408	3.5
18.11.2019	Loc4Sed	7.2	18.63171731	3.4	187.0293055	2	6.918357994	4.1	91.11591432	1	8.937425711	1.5	17.53704223	1
18.11.2019	Loc4Sed	7.3	20.32609574	2.5	195.9468979	1.6	7.964381847	3.8	105.1456087	2.6	10.24253782	3.6	20.17807974	2.4
18.11.2019	Loc11Sed	21.2	12.72674903	1.9	168.0968546	0.7	6.175954343	4.8	90.30457818	1.5	7.093986137	2.6	13.47373098	3.8
18.11.2019	Loc11Sed	21.3	13.9854603	1.8	167.1865392	2.4	6.764413041	1.2	97.85789693	1.2	7.754794361	2	15.72913964	2.1
17.01.2020	Blank	Blank UC	0	54.5	0	32.8	0	173.2	0	173.2	0	173.2	0	173.2
17.01.2020	Blank	Blank UC	0	54.5	0	52.1	0	0	0	173.2	0	0	0	0
17.01.2020	Blank	Blank UC	0	86.6	0	86.6	0	173.2	0	173.2	0	0	0	173.2

Date	Sample name	Number	Pr141(MR) Conc. µg/g	RSD, %	Nd146(MR) Conc. µg/g	RSD, %	Dy163(MR) Conc. µg/g	RSD, %	Ho165(MR) Conc. µg/g	RSD, %	Er166(MR) Conc. µg/g	RSD, %	Pb208(MR) Conc. µg/g	RSD, %
18.11.2019	Loc1Sed	1	2.785169089	1.9	11.06200631	1.2	2.059479595	6	0.405075341	9.1	1.139243536	4.9	739.5392291	1.5
18.11.2019	Loc1Sed	1	2.541845679	1.3	10.11379909	1	1.849462844	4.7	0.365194786	0.9	1.003684826	9.3	664.8817254	2.5
18.11.2019	Loc1Sed	2	2.699909148	1	10.43566133	1.3	1.995932775	3.1	0.361678161	4.2	1.075847969	3	842.1934471	1.8
18.11.2019	Loc2Sed	3	2.577334729	0.7	10.17173347	4.6	2.055318847	7.6	0.441022758	3.3	1.181023322	6.9	970.7805496	1.3
18.11.2019	Loc2Sed	4	2.680238252	1.4	10.49320329	1.7	2.06073316	1.5	0.394288058	6.1	1.149903814	2.3	1044.451541	1.3
18.11.2019	Loc3Sed	5	1.367085364	1.8	5.148078124	10.1	0.653899364	10.1	0.138289444	7.1	0.368018712	7.4	33.586211	3.9
18.11.2019	Loc3Sed	5	1.462618403	2.5	5.208164551	1.5	0.65709443	6.7	0.155763247	5.5	0.365724975	12.1	34.52983535	2.3
18.11.2019	Loc3Sed	6	0.730101161	5.9	2.824892617	3.4	0.479489173	16.5	0.099795352	3.5	0.313409311	10.3	24.97225935	2.5
18.11.2019	Loc4Sed	7	2.148761837	4	8.51176919	3.3	1.409084234	6.7	0.277174417	9.3	0.740966716	8.2	102.5205861	2.4
18.11.2019	Loc4Sed	8	1.945406229	2.4	7.712862137	5	1.219701551	7.1	0.238247726	9	0.656886696	2.8	90.01851209	1.2
18.11.2019	Loc5Sed	9	4.027341047	6.1	15.57242162	1.4	2.627039821	6.7	0.546263614	3.2	1.472723571	7.1	567.7622652	1
18.11.2019	Loc5Sed	10	4.212801024	1.5	16.54521274	2.4	2.645141923	6.6	0.534843954	4.5	1.466292676	5	656.215132	2
18.11.2019	Loc5Sed	10	4.079429464	5.3	15.44155415	3	2.651228657	7.3	0.533499311	4.8	1.480794971	5.2	637.011529	2
18.11.2019	Loc6Sed	11	3.095215757	2.1	12.07536461	2.5	2.105893365	1.7	0.40003807	5.1	1.131148096	4.2	282.5217968	1.1
18.11.2019	Loc6Sed	12	3.062204752	5	11.61062141	0.7	2.125643166	3.8	0.431990471	10.3	1.223127832	3.4	272.3500929	2.5
18.11.2019	Loc7Sed	13	1.289507346	2.4	4.91520037	3.2	0.828137231	16.7	0.168622265	7.7	0.459814703	13.3	77.2585399	1.5
18.11.2019	Loc7Sed	14	1.118444923	1.3	4.41108951	2.1	0.646185748	13	0.144312013	5.6	0.385616487	15.2	83.81460811	2.9
18.11.2019	Loc8Sed	15	1.472708589	1.4	6.287404723	2.5	1.026598879	2.3	0.215905131	7.5	0.560066679	5.7	472.4120655	2
18.11.2019	Loc8Sed	16	1.411569439	4.7	5.686308886	1.6	1.356195378	4	0.224855047	8.9	0.656425108	4.2	1704.059645	4.2
18.11.2019	Loc9Sed	17	1.511483327	2.9	6.274429706	6.8	0.92716677	8.9	0.189148842	14.4	0.497816153	4.4	125.0985959	1.4
18.11.2019	Loc9Sed	18	1.404623976	5.2	5.199620269	2.5	0.817350893	5.1	0.183794806	3.5	0.554505199	14.1	101.4828385	4.5
18.11.2019	Loc10Sed	19	0.809396085	1.7	3.359601556	4.9	0.485991695	11.6	0.105955403	7.3	0.295049963	15.8	17.80435439	2
18.11.2019	Loc10Sed	20	0.80860638	1.9	2.946106381	1.2	0.492439984	12.1	0.097772461	5.8	0.303294607	10.8	18.77273867	0.4
18.11.2019	Loc11Sed	21	1.816123709	6.1	7.157461476	2.9	1.266396407	11.6	0.241145055	8.1	0.644155387	3.2	218.5576519	2.4
18.11.2019	Loc11Sed	22	0.475679455	2.5	1.836247393	2.7	0.341625435	18.5	0.055663492	14.7	0.195774938	4.5	17.9999757	2.6
18.11.2019	Loc12Sed	23	1.760936061	6.4	6.878416556	4.3	1.174221477	3.3	0.259439429	4.7	0.772054523	3.6	53.89917871	2.8
18.11.2019	Loc12Sed	24	1.087612472	0.5	4.317186275	5.6	0.883356004	6.4	0.205273128	6.6	0.543330832	10.6	28.17027467	2.2
18.11.2019	Loc9Sed	25	4.705140504	4.3	18.66287487	3.5	3.771652094	3	0.744212842	4.9	2.151308327	6.6	1653.786552	2.7
18.11.2019	Loc4Sed	7.2	2.197133527	5.5	8.45515146	6.5	1.334917071	8.4	0.250383031	4.6	0.765071469	7.5	100.1856367	2.4
18.11.2019	Loc4Sed	7.3	2.56170504	1.3	10.29006003	4	1.525658301	6	0.319396293	8.2	0.864008278	12.3	110.1337118	1.6
18.11.2019	Loc11Sed	21.2	1.69156542	7.1	6.683130643	2	1.230671381	3.8	0.21040853	11.1	0.670397203	3	201.7765512	1.5
18.11.2019	Loc11Sed	21.3	1.958294936	2.6	7.392020983	3.2	1.226304465	5	0.245805037	8.6	0.729781232	5.6	225.7355577	4.1
17.01.2020	Blank	Blank UC	0	0	0	0	0	0	0	0	0	0	0	15.1
17.01.2020	Blank	Blank UC	0	0	0	0	0	0	0	173.2	0	0	0	173.2
17.01.2020	Blank	Blank UC	0	0	0	0	0	0	0	0	0	0	0	173.2

Date	Sample name	Number	U238(MR) Conc. µg/g	RSD, %	As75(HR) Conc. µg/g	RSD, %	Zr90(HR) Conc. µg/g	RSD, %	Nb93(HR) Conc. µg/g	RSD, %	Eu153(HR) Conc. µg/g	RSD, %	Gd157(HR) Conc. µg/g	RSD, %
18.11.2019	Loc1Sed	1	1.506812088	2.1	525.7772999	4	4.289706165	8.4	0.427503047	2	0.447084694	9.3	2.075379646	7.8
18.11.2019	Loc1Sed	1	1.3464276	4.8	474.2296186	0.6	4.589272943	0.6	0.448721235	11.2	0.43120998	3.4	1.948847428	4.6
18.11.2019	Loc1Sed	2	1.374291692	3.7	383.7368457	4.4	6.316932804	11.3	0.379732034	4.8	0.423960243	16.4	1.879150014	12.8
18.11.2019	Loc2Sed	3	1.478268581	3.5	500.3242113	0.8	8.227930615	7	0.281299794	10.5	0.435260372	12.4	1.999949398	15.3
18.11.2019	Loc2Sed	4	1.370732816	3.2	489.2546314	2.1	10.92578153	5.4	0.339872276	11.4	0.421097553	17.7	1.947106534	8.5
18.11.2019	Loc3Sed	5	0.756495817	4.2	25.42190859	11.9	1.929984361	9.3	0.064796629	34.1	0.169458095	21.2	0.752129054	2.1
18.11.2019	Loc3Sed	5	0.808725129	3.3	27.7769629	7	1.674245018	4.7	0.05673011	22.3	0.183538096	10.9	0.764843966	2.8
18.11.2019	Loc3Sed	6	0.927670997	6.2	19.24952587	3.8	1.367149623	9.6	0.126591603	13.6	0.10094134	28.7	0.579981516	34.4
18.11.2019	Loc4Sed	7	1.181982935	9.9	78.42384068	1.4	3.428365595	0.8	0.07799371	17.4	0.347181123	12.4	1.395483362	17.1
18.11.2019	Loc4Sed	8	0.967187332	6.2	69.10115918	11.3	3.245792432	7.2	0.0797925	14.2	0.290669662	4	1.398224704	9.2
18.11.2019	Loc5Sed	9	1.722575694	5.8	396.7884659	4.9	10.55340013	4.4	0.264546684	10.7	0.657446627	1.2	2.446535801	10.7
18.11.2019	Loc5Sed	10	1.85691049	9	431.9385705	2.5	15.10477345	7.6	0.268481597	15.9	0.725532159	4.3	2.718991165	3.3
18.11.2019	Loc5Sed	10	1.653594409	11.4	419.1415812	4	15.85929737	5.4	0.278804366	5	0.661351422	5.5	2.892204135	8.6
18.11.2019	Loc6Sed	11	1.39340304	5.5	218.9261124	0.9	8.843279138	3.4	0.146545019	19.3	0.534460754	9.8	2.102749607	12.7
18.11.2019	Loc6Sed	12	1.518315185	11	217.3034191	2.2	8.99700797	4.6	0.209713635	18.9	0.506844409	7.5	2.281264631	13.4
18.11.2019	Loc7Sed	13	1.159055435	17	62.55209489	6.4	1.454999048	6.8	0.132645696	19.4	0.205299194	14.1	0.98568519	31.9
18.11.2019	Loc7Sed	14	1.025547113	12.7	63.37284821	2.7	1.318694153	18.2	0.175904822	21.5	0.17949482	8.6	0.702144469	27.5
18.11.2019	Loc8Sed	15	1.358565119	5.6	382.3011415	0.6	3.409753408	6.7	0.283262723	9.1	0.285081206	15	1.16472871	10.1
18.11.2019	Loc8Sed	16	1.41417401	7.7	531.200587	1.1	4.691145119	8.5	0.286028045	11.9	0.228372314	12.1	1.424854663	5.6
18.11.2019	Loc9Sed	17	1.44150317	5.8	98.12575055	7.6	2.369797981	10.6	0.137394286	2.3	0.27347655	2	0.912070206	2.8
18.11.2019	Loc9Sed	18	1.342402892	3.2	80.47575838	2.5	2.84523703	6.9	0.181112886	15.7	0.224808681	11.4	0.82043833	18.2
18.11.2019	Loc10Sed	19	1.168004143	8.8	16.45337228	22.5	1.283630927	12.5	0.081633921	15.8	0.139058719	39.1	0.579038784	26.9
18.11.2019	Loc10Sed	20	1.385286484	2	16.47790307	15.4	1.673380042	9.2	0.189290513	10.3	0.08455614	37.2	0.502572398	42
18.11.2019	Loc11Sed	21	1.578289789	7.7	140.0937944	2.3	4.049130614	2.4	0.238978734	8.5	0.232324651	9.6	1.402889072	9.7
18.11.2019	Loc11Sed	22	1.438065329	5.7	10.93901398	21.2	1.736372449	16.1	0.174326002	13.9	0.104965928	24.6	0.412106258	21.1
18.11.2019	Loc12Sed	23	1.315057647	5.8	38.6810311	8.5	2.635827905	10.2	0.125958493	49.8	0.353036646	11.4	1.13962893	18.4
18.11.2019	Loc12Sed	24	1.09140341	4.4	20.36636604	8.5	2.118494068	0.7	0.116651447	23.6	0.208658289	8.4	0.819375114	28.7
18.11.2019	Loc9Sed	25	3.223648846	0.6	753.9485427	2.4	23.2814648	11.2	0.575905151	4.7	0.817006974	4.3	3.657009647	15.5
18.11.2019	Loc4Sed	7.2	1.255947599	2	82.57114816	6.1	5.059312224	3.1	0.17294392	11.5	0.347323583	8.9	1.41701505	10.1
18.11.2019	Loc4Sed	7.3	1.213333924	3.5	101.0240703	2.1	5.639276316	15.3	0.158379322	7.5	0.439677047	10.3	1.688616862	25.8
18.11.2019	Loc11Sed	21.2	1.477513548	5.1	141.1101731	7.9	5.385688139	8.2	0.162654576	12.7	0.256495833	20.2	1.341401735	13.4
18.11.2019	Loc11Sed	21.3	1.708380316	1.3	157.9042942	2.9	6.643264223	3.4	0.137597857	12.7	0.33069758	18.6	1.502700774	17.6
17.01.2020	Blank	Blank UC	0	0	0	0	0	5	0	142	0	0	0	0
17.01.2020	Blank	Blank UC	0	0	0	0	0	14.8	0	173.2	0	173.2	0	0
17.01.2020	Blank	Blank UC	0	0	0	0	0	19.7	0	100	0	0	0	0

Hanne Brigtsen Olsen

Monitoring and Treatment of Trace Elements in Acid Mine Drainage in Trondheim

NTNU
Norwegian University of
Science and Technology